Platelet Actin Cytoskeletal Reversibility is Cyclic Nucleotide and Matrix Type Dependent

Lloyd Atkinson, MBiomedSci. (Hons) (University of Hull)

Thesis submitted for the Degree of Doctor of Philosophy (PhD)

The University of Hull and The University of York

Hull York Medical School

August 2019

Abstract

Platelets circulate in the vasculature in a quiescent state due to the presence of endothelial-derived nitric oxide (NO) and prostacyclin (PGI_2). However, this inhibition is relieved upon vascular injury due to exposed matrix proteins, which cause platelet adhesion, activation, and thrombus formation. Therefore, the interplay between the activatory extracellular proteins and the inhibitory cyclic nucleotides is critical to an effective platelet response.

This thesis shows that activated NO can reverse platelet activation in spread platelets on fibrinogen, by reversing stress fibre formation and inducing actin nodule formation. This was mediated by the NO-sGC-PKG signalling axis, resulting in RhoA inhibition, and causing a reduction in *in vitro* thrombus height. Furthermore, analysis of actin nodules indicated that after PGI2 or NO stimulation actin nodules are smaller, and more numerous. Interestingly however, by reducing the fibrinogen concentration, this not only increased actin nodule size, but also reduced cAMP levels most likely through adenylyl cyclase (AC) inhibition, inducing resistance to cyclic nucleotide signalling.

Importantly by changing the matrix protein used we also altered response of activated platelets to cyclic nucleotide signalling. Whilst spread platelets on high density fibrinogen permitted stress fibre reversal by cyclic nucleotides, collagen did not. This was mediated in a glycoprotein VI (GPVI) dependent manner, via AC inhibition, as treatment with forskolin, an AC activator, caused significant stress fibre reversal, whilst PDE3 inhibition had no effect. In agreement, PGI_2 reduced the height of formed thrombi but did not affect the underlying platelets interacting with collagen. These findings suggest that GPVI activation induces PGI_2 insensitivity in platelets, influencing thrombus formation.

These findings highlight the critical nature of the interplay between cyclic nucleotide signalling and matrix density and composition on activated platelets. They demonstrate the need to understand how changes in the vascular matrix environment alter platelet function due to resistance to cyclic nucleotide signalling.

Table of Contents

Table of Figures

List of Tables

Abbreviations

AC – Adenylyl cyclase

ADP – Adenosine monophosphate

AKAP – A kinase anchoring protein

AN – Actin nodules

Arp2/3 – Actin-related protein 2/3

A.U. – Arbitrary units

BSA – Bovine serum albumin

Btk – Bruton's tyrosine kinase

Ca^{2+} - Calcium

cAMP – Cyclic adenosine monophosphate

cGMP – Cyclic guanosine monophosphate

COX-1 – Cyclooygenase 1

COX-2 – Cyclooxygenase 2

CHD – Coronary heart disease

CRP – Collagen-related peptide

CVD – Cardiovascular disease

DAG - Diacylglycerol

DiOC6 - 3,3'-Dihexyloxacarbocyanine Iodide

ECM – Extracellular matrix

eNOS – Endothelial nitric oxide synthase

F-Actin – Filamentous actin

FAK – Focal adhesion kinase

Fc – Fragment constant

G-actin – Globular actin

GAP – GTPase activating protein

GAPDH – Glyceraldyhyde phosphate dehydrogenase

GDI – Guanine-nucleotide dissociation inhibitor

GDP – Guanosine diphosphate

GEF – Guanine-nucleotide exchange factor

GFOGER - Gly-Phe-Hyp-Gly-Glu-Arg

GFP – Green fluorescent protein

GPO – Gly-Pro-Hyp

GPVI – Glycoprotein VI

GPCR – G-protein coupled receptor

GTP – Guanosine triphosphate

iNOS – Inducible nitric oxide synthase

IP – Prostacyclin receptor

IP3 – Inositol triphosphate

ITAM – Immunoreceptor tyrosine activated motif

Mg^{2+} - Magnesium

MLC –Myosin light chain

MLCK – Myosin light chain kinase

MLCP – Myosin light chain phosphatase

NO – Nitric oxide

nNOS – Neuronal nitric oxide synthase

RhoA – Ras homolog gene family, member A

Rac1 – Ras-related C3 botulinum toxin substrate 1

RGD – Arg-gly-Asp

ROCK – Rho associated coiled-coil kinase

Cdc42 – Cell division control protein homolog 42

sGC – Soluble guanylyl cyclase

SFK – Serine family kinase

PDE - Phosphodiesterase

PGI_2 – Prostglandin I_2/prostacyclin

PGG_2 – Prostaglandin G_2

PGH_2 – Prostaglandin H_2

PGF_2 – Prostaglandin F_2

PH – Pleckstrin homology

HDF – High-density fibrinogen

LDF – Low-density fibrinogen

GSNO – S-nitrosoglutothione

DEANONOate – Dimethylamine NONOate

ODQ - *H*-[1,2,4]Oxadiazolo[4,3-*a*]quinoxalin-1-one

PBS – Phosphate buffered saline

PLC – Phospholipase C

PIP2 – Phophatidylinositol 4,5-bisphopsphate

PIP3 – Phosphatidylinositol 3,4,5-triphosphate

PKA – Protein kinase A

PKC – Protein kinase C

PKG – Protein kinase G

FITC – Fluorescin isothiocyanate

TXA_2 – Thromboxane A_2

PPACK - Phenylalanyl-Prolyl-Arginyl Chloromethyl Ketone

RBD – Rho binding domain

RGS – Regulator of G-protein signalling

Rif – Rho in filopodia

SDS-PAGE – Sodium dodecyl sulphate polyacrylamide gel electrophoresis

S.E.M. – Standard error of mean

SF – Stress fibres

SH3 – Src homology 3

TBS – Tris buffered saline

TBST – Tris buffered saline with tween

TP – Thromboxane receptor

TPO – Thrombopoeitin

vWF – Von Willebrand Factor

VASP – Vasodilator stimulated phosphoprotein

WAS – Wiskott Aldrich syndrome

WASP – Wiskott Aldrich syndrome protein

WAVE – WASP family verprolin homologous protein

Acknowledgements

This work is dedicated to my late mother, Hayley, and my late grandmother, Linda. It is very rare and fortunate to be able to research a disease that has impacted your life and family. As such, I would like to thank Simon for providing me with this opportunity and his collaborative approach towards supervision that has allowed me to explore my own avenues of interest. I will also forever be grateful for the funding provided by the British Heart Foundation that has allowed me to start a family during my training and for which completing this research would not have been possible.

I am thankful for all the initial guidance and aid with cyclic nucleotide signalling from Khalid, who was a valuable source of knowledge and expertise, and Yusuf, for his stimulating conversation surrounding our work and help in many aspects of the lab, including teaching me flow microscopy. I also give thanks to Yusra, for her help with the ELISAs performed for this work and for being a much tidier lab mate than I! I would also like to thank Roger Sturmey for his patience and understanding during the writing of this thesis. Many thanks also to Steve Thomas, Natalie Poulter and Vicky Simms at Birmingham University for their help and guidance with real time microscopy, and for being such great hosts.

I give special thanks to my wife, Sam. My shining example that I try to follow, yet rarely emulate. You're an inspiration to all upcoming female scientists and you have shown that in this day and age, being a new mother does not hinder you from excelling in your own career. Thank you also for your patience with me in writing this thesis during some difficult times. I also give a huge thanks to my son, Callan, who has been a source of great motivation and escapism.

Declaration

I confirm that this work is original and that if any passage(s) or diagrams(s) have been copied from academic papers, books, the internet or any other sources these are clearly identified by the use of quotation marks and the reference(s) is fully cited. I certify that, other than where indicated, this is my own work and does not breach the regulation of HYMS, the University of Hull or the University of York regarding plagiarism or academic conduct in examinations. I have read the HYMS Code of Practice on Academic Misconduct, and state that this piece of work is my own and does not contain any unacknowledged work from any other sources'.

Chapter 1. Introduction

1.0. Introduction

Cardiovascular disease is the leading cause of mortality worldwide (1), whilst in the UK it is the third highest cause of mortality, killing 100 000 people a year (Office for National Statistics, 2016). However, in addition it is estimated that on average, 7 million individuals live with ongoing coronary heart disease (CHD) and stroke complications at any one time, resulting in a £4.7 billion cost to the NHS per year in prescriptions, therapies and surgeries (British Heart Foundation – Heart and Circulatory Disease Statistics 2019). It is also important to recognise and tackle the social impact of CVD, which not only affects the individual, but also their family and friends (2), as family and friends may have to become carers. To curtail these expenses, several approaches must be made, including the promotion of healthy living, better detection before cardiovascular events and more cost-effective therapies. New, more cost-effective therapies can only be made through the uncovering of the biochemical and biomechanical underpinnings of thrombotic disease processes.

Myocardial infarction and ischemic stroke culminate due to the formation of a thrombus which restricts oxygen to the myocardium or brain, respectively. Taking centre stage in the initial formation of these thrombi are blood cells called platelets. Over the last few decades, anti-platelet pharmacological therapies such as aspirin have proven useful in the prevention of both primary and secondary cardiovascular events (CVEs) (3). Improved therapies and detection methods have led to a reduction of approximately 70% deaths attributable to CHD and stroke in the UK (4). However, more recent studies have questioned aspirin's validity in the primary prevention of CVEs in individuals with and without pre-existing conditions (5,6). With these recent findings considered, there is a need for a deeper understanding of the disease processes involved in the onset of a primary CVE, such as atherosclerosis, and any potential exacerbating signalling process involved, with the aim to provide further therapeutic targets. This is especially true considering the current impetus for individualised patient care within the NHS, where a patient's individual disease aetiology can be identified and treated accordingly. This may allow effective therapies in the prevention of thrombosis with diminished side effects, which currently range from nausea and minor GI bleeds, to more catastrophic events such as intracranial haemorrhage (7–9).

Platelets are small (~3μm^2) (figure 1.1.), anucleate cells which patrol the body in flowing blood and respond to breaches in the vasculature. Platelet concentrations in the plasma are extremely high, and range between 150-450 x 10^9/L in healthy individuals (10). The main purpose of the platelet is to respond to the exposure of extracellular matrix due to vascular damage by trauma or other pathological states, forming a haemostatic plug (termed a white clot) at sites of damage where extracellular matrices and/or prothrombotic molecules are present. This allows a platform for further thrombosis, mediated by coagulation factors, to take place and the eventual establishment of a compact and haemostatically inert clot in healthy individuals. This process is facilitated by the size of platelets in comparison to other cells in the blood. As they are the smallest cells in the bloodstream, platelets are pushed towards the vascular endothelium by laminar flow, thereby situating the platelets closest to any potential sites of injury (11,12). The importance of platelet number in this process is highlighted in cases of marked reduction in platelet count (thrombocytopenia), which is often accompanied by excessive bleeding and bruising (13,14). Maladies such as diabetes, cancer and dyslipidemia are known causes of dysfunctional platelet signalling, which underpins the carefully orchestrated events determining haemostasis(15–17). Accordingly, having such diseases is associated with a higher risk of CVEs (18).

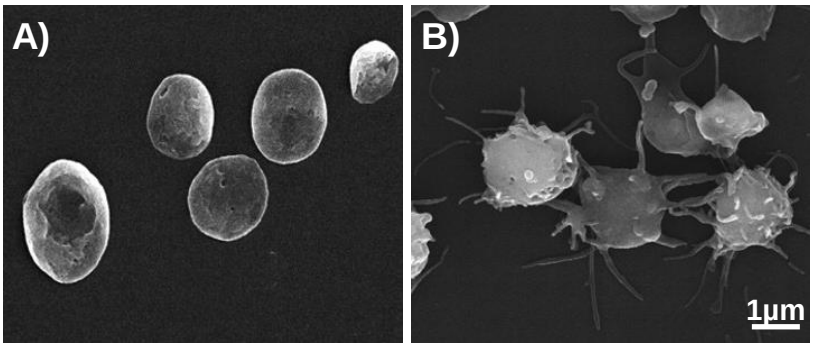

Figure 1.1. Platelet morphology in resting and active states. A) *Resting normal human platelets in their typical discoid form as seen through scanning electron microscopy.* ***B)*** *Activated human platelets in response to calcium (Ca^{2+}) ionophore treatment (A23187). Scale bars represent 1μm. (Figure adapted from Bettache et al., 2003).*

1.1 Platelet production

Platelets are produced by the megakaryocytes, which reside primarily within the bone marrow, although it has recently been found that megakaryocytes can travel through the bloodstream and seed themselves and produce platelets within the lung (20). Megakaryocytes are derived from haematopoietic stem cells (HSCs) and are committed to the myeloid lineage by exposure to growth factors and cytokines within the bone marrow and surrounding vasculature, such as thrombopoeitin (TPO). TPO is a critical determinant in megakaryocyte production from HSCs and is used clinically to generate platelets in those with severe and sustained thrombocytopenia (21,22). Once committed to megakaryopoiesis, the HSC begins to undergo endomitosis, resulting in a cell with multiple nuclei, and represents the enhanced ability for megakaryocytes to synthesise proteins for platelet production, including storage granule contents, and cytoplasmic and membrane proteins (23) Interestingly, megakaryocytes can also endocytose circulating proteins and package them into platelets (24). In addition to being polyploid, megakaryocytes form a vast network of membrane invaginations, termed the demarcation membrane system (DMS) (25). This provides sufficient plasma membrane surface area to generate platelets, which due to their small size, have a high membrane to cytoplasmic ratio.

Platelet production is dependent on cytoskeletal dynamics within the megakaryocyte (26,27). To produce platelets, they form long pseudopodia-like projections, called proplatelets, which extravasate the surrounding bone marrow tissues until a sinusoidal blood vessel is found and breached (figure 1.2.). The tips of the proplatelet processes, now exposed to shear flow of oncoming blood, begin to elongate and shed platelets into the bloodstream (26). This proplatelet elongation required for platelet production is dependent on tubulin, a cytoskeletal protein which polymerises to form microtubules (28). Another polymerised cytoskeletal protein, actin, is required for the extensive branching seen during proplatelet formation. This was found using inhibitors of actin polymerisation, which led to the formation of straight, unbranched megakaryocyte membrane protrusions (26). Along these actin and microtubule polymers, cargo for platelets is delivered to nascent platelets by the microtubule motor protein, kinesin (29). Considering these findings regarding the impact of the cytoskeleton on platelet production, one can speculate the dependence of the resulting platelets on cytoskeletal dynamics. Regulation of these

systems underlies key features associated with platelet activation and will be discussed later in this chapter.

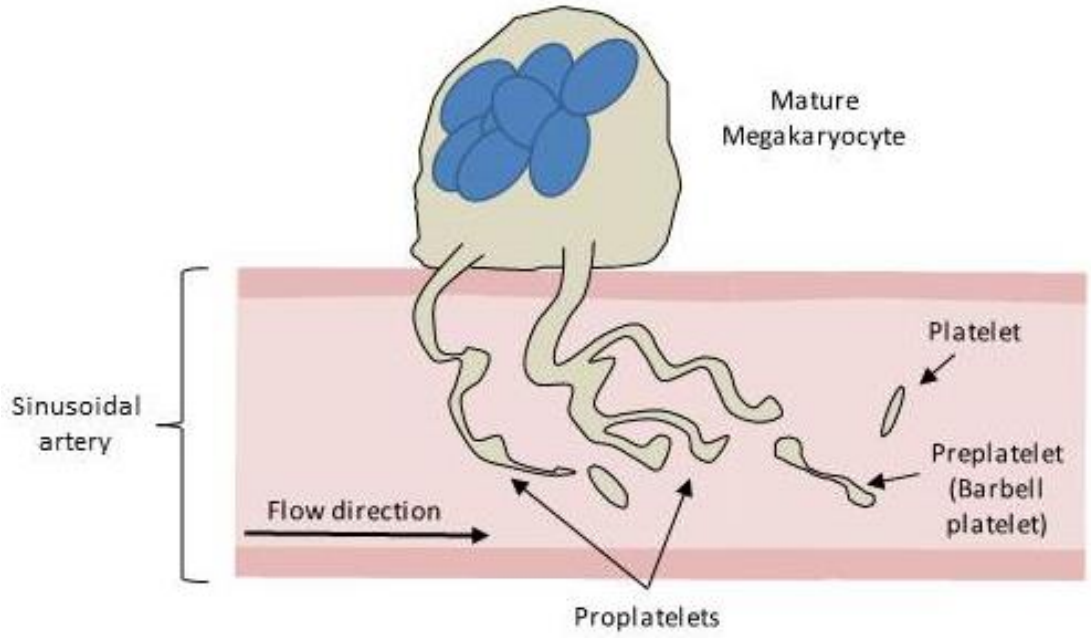

Figure 1.2. Platelet production from megakaryocytes within the bone marrow. *Mature megakaryocytes migrate from within the bone marrow to sinusoidal arteries where they project tendril-like protrusions (proplatelets) into the vasculature. Shear flow of the oncoming blood causes elongation of the proplatelet processes and detachment of platelets and preplatelets into the circulation. Sustained shear stress causes preplatet fission into further single platelets (redrawn from Machlus and Italiano, 2013).*

1.2. Platelet structure

In a resting state, platelets are in a discoid form due to an encircling microtubule coil that determines the periphery of the cell and breaks down upon platelet activation (30,31) (shown in figure 1.3). At this periphery lies the plasma membrane, which contains a multitude of receptors required for a suitable response to the platelet's extracellular environment, such as exposed subendothelial matrix proteins or soluble markers of cell damage.

The variety of receptors and ligands that the platelet expresses demonstrates their multiple purposes not only as haemostatic agents, but also as cells involved in immune response, angiogenesis and wound healing. These include $\alpha_{IIb}\beta_3$, CD36, sCD40L, CCL5 (RANTES) and platelet factor 4 (32–35). The plasma membrane of the resting platelet is not smooth, but porous in appearance due to extensive invagination of the membrane that form the open canalicular system (OCS). This structure provides extra membrane surface area during platelet spreading and a channel through which platelet granules can be secreted to ensure further activation of neighbouring platelets (36). The plasma membrane is also a vital source of lipid mediators for downstream signalling and paracrine messengers, such as phosphoinositides, which are required for the release of intracellular calcium (Ca^{2+}) stores, and arachidonic acid for thromboxane A_2 (TXA_2) production (37,38).

Below the plasma membrane lies the submembrane area, which contains the necessary tools for signal transduction into the platelet. These include intracellular integrin domains, kinases, phosphatases, receptor-linked actin binding proteins and an extensive actin filament network essential for functional integrin signalling and spatial arrangement of submembrane regions (39,40). These proteins are aided in their interactions further by adaptor and anchoring phospholipids and proteins, which can regulate the strength of the signal to downstream mediators and cause different activation patterns (41,42).

Energy requirements for activation are met chiefly by the mitochondria and granular glycogen stores that are randomly dispersed within the cytoplasm (43,44). Recently it has been shown that platelets can readily switch between glycolysis and oxidative phosphorylation depending on substrate supply, resulting in a seamless aggregatory response (45). Platelets granules are also found in the cytoplasm and are vital for haemostasis. These include lysosymes, α-granules and dense granules, which serve as storage sites for factors that result in the activation of neighbouring

platelets, activation of the coagulation cascade and recruitment of neutrophils to the developing thrombus (46–48).

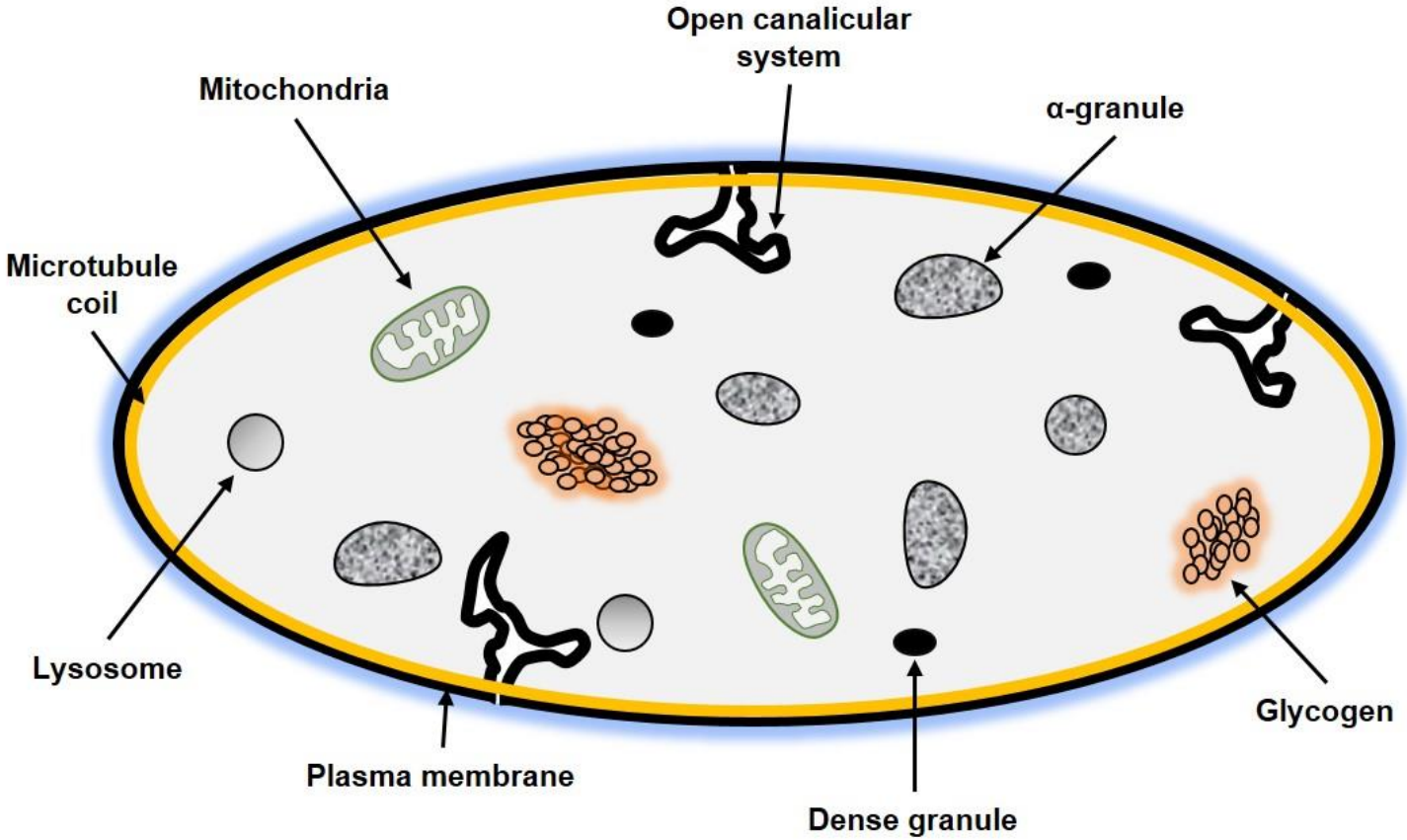

Figure 1.3. Basic structure of the resting platelet. *At rest, the platelet is encircled by a microtubule coil (yellow) established during proplatelet formation. The plasma membrane (black) contains a multitude of platelet receptors that enshroud the cell (blue), which transduce extracellular cues into the platelet, resulting in granule secretion. The platelet contains three major classes of granular organelles; α-granules, dense granules and lysosomes, which are released through the open canalicular system into the extracellular environment. Energy requirements during activation and at rest are met by a small number of mitochondria and glycogen.*

1.3. Platelet granules

When stimulated, platelets release granular contents which primarily act as an autocrine and paracrine signalling mechanism. This results in a positive feedback loop of platelet activation through additional receptor engagement, leading to further integrin activation, fibrinogen-binding capacity, Ca^{2+} flux and recruitment of leukocytes to the growing thrombus. There are two main granule species in human platelets; α- and dense-granules.

1.3.1 α granules

α-granules are by far the most prevalent granule type in platelets, with approximately 50-80 per cell (49). α-granules contain many signalling proteins, cell surface receptors and chemokines required for proper platelet function. The cell adhesion molecule, P-selectin, is a key component of these granules, and is commonly used as an experimental marker for platelet activity in flow cytometry (50,51). Expression of P-selectin during platelet activation can cause further recruitment of platelets and leukocytes through expressed P-selectin glycoprotein ligand-1 (PGSL-1), which causes the tethering of leukocytes to the thrombus and/or areas of inflammation (52,53) . α-granules are also rich in $\alpha_{IIb}\beta_3$, which is externalised to the outer plasma membrane upon α-granule secretion and represents one third of the total $\alpha_{IIb}\beta_3$ in activated human platelets (54,55). In addition to providing extra integrins to the surface of platelets, α-granules also contain several adhesion proteins, which further increase platelet adhesion and spreading to the presumed site of injury. These include fibrinogen, fibronectin, von Willebrand factor (vWF) and thrombospondin (56–58). Clotting factors are also highly abundant and contribute to the efficient activation of the coagulation cascade, the activation of thrombin and subsequent generation of fibrin, leading the formation of a stable thrombus (59,60). The overarching importance of functional α-granule release is highlighted in individuals with Gray platelet syndrome, who suffer from prolonged mild to moderate bleeding diatheses (61).

1.3.2. Dense granules

In comparison to α-granules, there are far fewer dense granules per platelet (62). Dense granules received their name due to initial electron microscopy work which found that they were electron dense and stained poorly using EPTA (63). These granules contain a high abundance of cations, nucleotides and bioactive amines. They are rich in Ca^{2+}, which is required for integrin binding and platelet activation, and ADP/ATP for energy and activation of platelet signalling pathways (64,65). The

importance of dense granule secretion is highlighted in and humans with delta platelet storage pool deficiency, where a lack of dense granule content is seen in sufferer's platelets, resulting in mild to moderate mucocutaneous bleeding (66,67). Release of serotonin from dense granules has been recently shown to modulate the immune system in response to exogenous immunocomplexes, leading to shock in mice (68), further demonstrating that platelets as more than haemostatic cells.

1.4 Thrombus formation

Central to platelet function is the ability to sense vascular injury, aggregate together and contract to form a consolidated thrombus that both prevents blood loss and ensures the flow of blood to downstream tissues. To do this, platelets must first sense the vascular damage and slow down to reach the site of injury. Damaged vascular endothelial cells release, among other factors, vWF, a high molecular weight, multimeric protein, which is expressed in an entangled native state. This conceals its binding domains for GPIb at low shear. In high-shear environments, vWF unravels and elongates which permits access for platelet GPIb and tethering of platelets towards the site of injury where subendothelial matrices are exposed (69,70). This tethering is brought about by the high on-off binding kinetics of GPIb with vWF, which causes constant engagement and disengagement from vWF peptide chains and causes rolling of the platelets to the site of injury (71). Exposed subendothelial matrices at the site of injury include collagens that signal through platelet GPVI and $\alpha_2\beta_1$, causing robust platelet activation leading to granule secretion, inside-out signalling and further integrin activation. During this period of platelet activation, flippases and scramblases responsible for the externalisation of phospholipid to the outer plasma membrane are activated (72). Exposure of negatively charged phospholipids provides a platform for the tenase complex of the coagulation cascade. This leads to the activation of FXa and the conversion of fibrinogen to fibrin; an elastic clot scaffold protein which can also interact with platelets (73,74). Inside-out integrin activation secures the binding of platelets to the site of injury through and results in a more stable thrombus. In this stable environment, platelets can then begin to spread over and around the site of injury, thus preventing further blood loss. This spreading also increases the surface area of platelets and allows more points of integrin bridging of adjacent platelets through fibrinogen and $\alpha_{IIb}\beta_3$. To increase thrombus mass and overall contractility, platelets release their α- and dense-granule contents, which both encourage the recruitment of oncoming platelets and accentuates the activity of platelets already within the

thrombus. With an aggregate of activated platelets enmeshed in a fibrin scaffold, the process of clot contraction begins. This process is highly dependent on the contractility of platelets within the thrombus (75), as a reduction of platelet contractility leads to impeded clot contraction and thrombus instability. It is of note that the processes described here are not a linear series of events. Platelets attaching to the thrombus may undergo earlier events, or may miss events such as granule secretion altogether, resulting in heterogeneous thrombus structure (Figure 1.4)

A series of papers from the Lawrence Brass laboratory in the University of Pennsylvania have demonstrated that thrombus formation is a nuanced and concerted process (76–79).Using a fluorescently labelled albumin and pulse chase experiments under *in vivo* thrombus formation assays, this group have shown that there are distinct areas of different solute transport within the thrombus. The inner-most section located close to the site of injury had the highest retention of the fluorescent albumin, indicating low plasma perfusion rates. As the thrombus grows, solute retention decreases and plasma perfusion increases. Interestingly, CD62 expression and thrombin activity was measured during this process and showed that thrombin activity clearly resided within the areas of highest solute transport, which one could speculate would be the area of highest platelet activity.

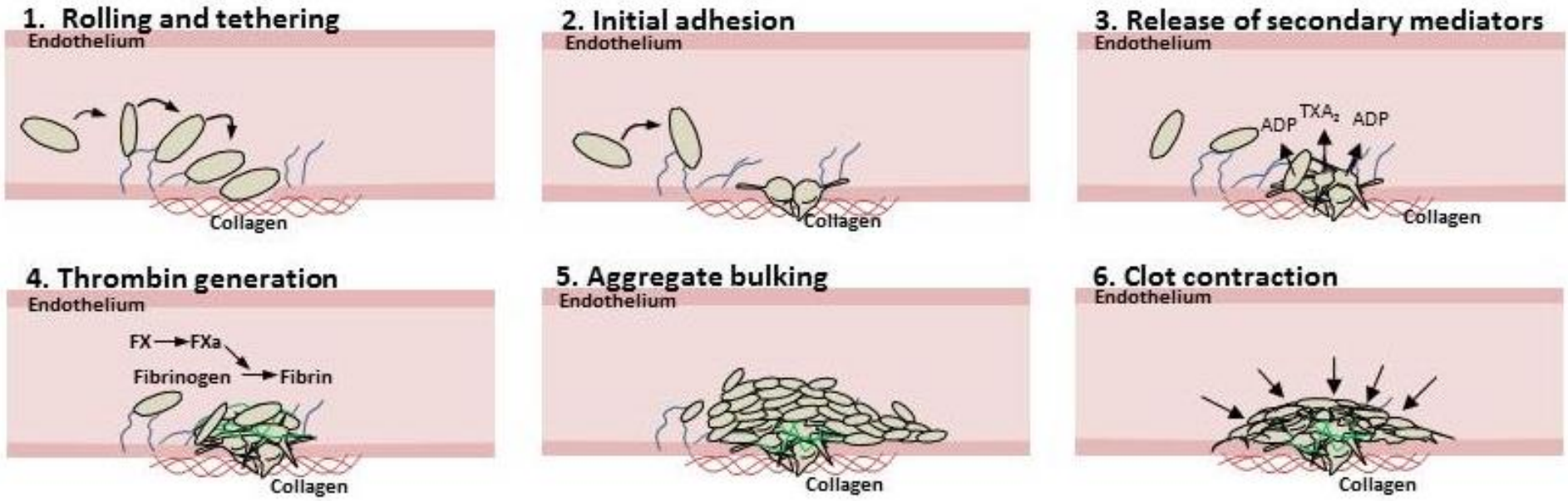

***Figure 1.4. Key aspects of thrombus formation**. **1)** Initial damage to the endothelial lining of blood vessels leads to exposure of subendothelial matrices such as collagen and the release of high molecular weight vWF (blue) from damaged endothelial cells. **2)** Rolling of platelets to the site of exposed matrices causes receptor-ligand interactions and platelet activation, where platelets begin to spread along the underlying matrix. **3)** Sufficient platelet activation causes degranulation both into the vasculature and among neighbouring platelets, both encouraging the accrual of oncoming platelets to the thrombus and heightening the response to platelets within it. **4)** Robust activation of platelets causes exposure of phosphatidylserine on the outer leaflet of the plasma membrane and leads to the generation of fibrin (green) through activated factor Xa. **5)** Further recruitment of platelets to the fibrin meshwork takes place. **6)** Sufficient intrathrombus activity and fibrin formation allows platelets to isotropically contract in synchrony, which increases the resistance of the thrombus to shear stress.*

1.5. Platelet receptors and their agonists

Platelets express a variety of receptors which provide a bespoke response to exposure of certain subendothelial matrices and/or soluble activators/inhibitors. Although distinct, these receptors often act in conjunction with each other or provide initial platelet activity to confer further activity to other receptors. Conversely, activation of one pathway can lead the inhibition of other pathways, proving more complexity to the platelet response through positive and negative feedback loops. By understanding the contribution of each receptor in haemostasis, haemorrhage or thrombosis, novel antiplatelet agents can be designed for receptor implicated disease processes.

1.5.1. Fibrinogen

The most abundant integrin in platelets, $\alpha_{IIb}\beta_3$ is a heterodimer expressed at approximately 80 000 copies per resting platelet. This integrin, along with several others, binds to Arginine-Gylcine-Aspartate (RGD) motifs located within fibrinogen, fibronectin and vWF molecules (80). Fibrinogen, the main ligand for $\alpha_{IIb}\beta_3$, is a high molecular weight (340kDa) protein which circulates through the body at high plasma concentration (approximately 1.5g/L) and is composed of three pairs of opposing polypeptide chains, Aα, Bβ and γ. These polypeptide chains are linked via disulphide bridges and coiled-coils to form a fibrinogen monomer (81,82). Within this monomer are three domains; two D-domains at both C-termini and a central E-domain which constitutes both N-termini. Within the E domain resides two pairs of fibrinopeptides, termed fibrinopeptide A and fibrinopeptide B located at the N-termini of the Aα and Bβ peptide chains, respectively. These two fibrinopeptides are cleaved through the action of thrombin, brought about by the activation of the coagulation cascade, which exposes an otherwise obscured polymerisation site. This transforms the molecule into a fibrin monomer which can polymerise through neighbouring fibrin D-domains to form large, cross-linked fibrin networks required for haemostasis (83,84). Deficiencies in $\alpha_{IIb}\beta_3$ and subsequent signalling often have bleeding phenotypes, the most notable being Glanzmann's thrombasthenia typified by quantitative and/or qualitative dysfunction in the integrin (85,86). Individuals suffering from this disease suffer mucosal bleeding episodes which, if unchecked, can be fatal and highlights the requirement for $\alpha_{IIb}\beta_3$ function in haemostasis (87). Similar with all integrin complexes, the $\alpha_{IIb}\beta_3$ integrin is composed of two subunits which form a non-covalently associated heterodimer (shown in figure 1.5). Each subunit consists of a large extracellular domain, a transmembrane region, and short

cytoplasmic tail (88). The extracellular domains are responsible for ligand-binding to RGDX motifs which are also found in other matrix proteins (89–91). Additionally, this integrin complex can also bind a KQAGDV (Lys-Gln-Ala-Gly-Asp-Val) sequence found within the carboxy terminus of the γ chain of fibrinogen (90,92), which can fully open the integrin, allowing full RGS binding. The extracellular domain of the αIIb subunit contains two calf domains, termed calf-1 and calf-2, a thigh region, and an N-terminal β-propeller, the latter of which contains ligand binding sites. There is a bending region between the outer-most calf domain and the thigh region, permitting flexibility in the integrin and gives rise to the resting and inactive state when in a 'bent' conformation. The β_3 extracellular domain is structurally distinct from αIIb. It contains an A-domain head, which possesses numerous metal ion-binding sites required for ligand-binding. These are termed the metal-ion-dependent adhesion site (MIDAS), the adjacent MIDAS (AMIDAS) and synergistic metal ion-binding site (SyMBS). Together these sites support divalent cations such as Ca^{2+} and Mg^{2+}, which are essential for integrin-mediated platelet adhesion and signalling (92,93). Below the β A-domain resides four EGF (epiderma growth factor)-like domains, which contain many cysteine residues that form several disulphide bridges which aid in maintaining an inactive state at rest. These disulphide bridges are then broken by protein disulphide isomerases (PDIs) upon platelet activation and confers and active state to the integrin, leading to functional thrombus formation (94).

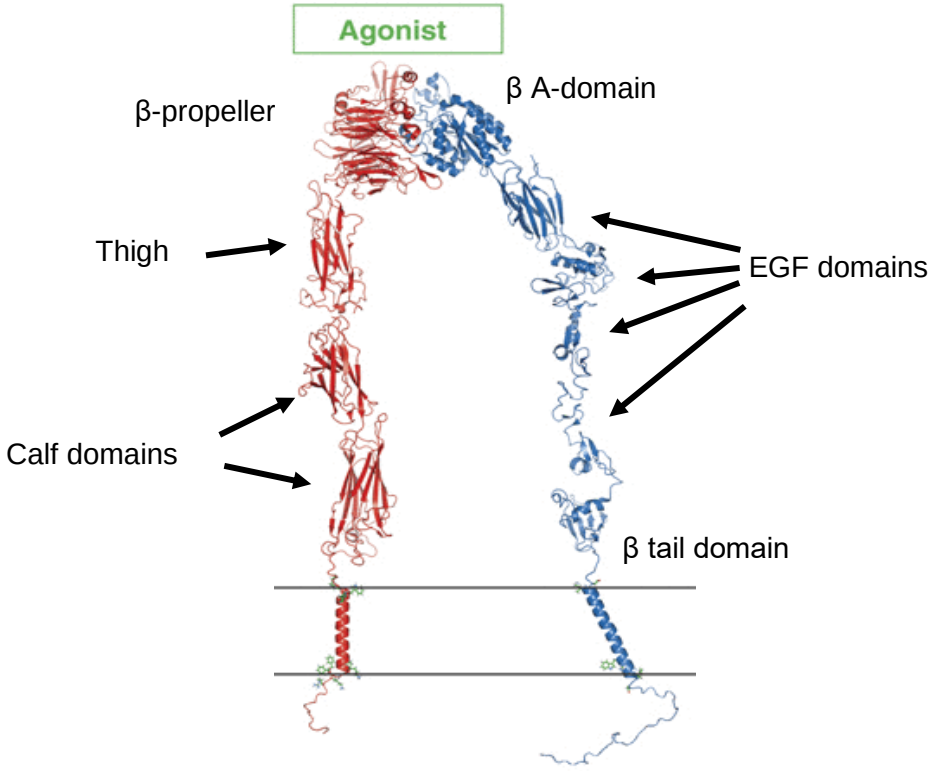

Figure 1.5. αIIbβ3 structure. *Cartoon depicting the extracellular αIIb (red) and β3 (blue) domains of the αIIbβ3 integrin complex when activated (Adapted from Lau et al., 2009)*

As $\alpha_{IIb}\beta_3$ is crucial in the formation of thrombi, part of a platelet's response to stimuli is the activation of the $\alpha_{IIb}\beta_3$ integrin. Upon activation with soluble agonists such as thrombin, ADP and thromboxane, or matrix proteins such as vWF and collagen, platelets undergo a process termed 'inside-out' signalling. This process results in both the release of platelet granules and the activation of $\alpha_{IIb}\beta_3$ from its native inactive 'bent' state to an extended state which results in high affinity ligand binding (95,96). The β_3 integrin has a number of binding partners which translate the extracellular activation signal intracellularly. Talin is a highly expressed protein in platelets and links the β_3 integrin with the actin cytoskeleton through F-actin binding (97). Upon platelet activation, talin moves from a primarily cytosolic localisation to the plasma membrane, where through F-actin binding, it can mediate inside out $\alpha_{IIb}\beta_3$ activation by 'pulling' on the β3 integrin and causing a conformational 'scissor-like' change, thereby enhancing the receptors avidity for ligands such as fibrinogen and fibrin (98). Knockout of talin in murine platelets results in early perinatal death due to haemorrhage arising from severely impacted thrombus formation (40). Platelets which are partially activated by integrins also need to further activate through granule secretion and further ligand-integrin interactions; a process called 'outside-in' signalling (figure 1.6.). During this process, increasing integrin-ligand binding causes the cross phosphorylation of adjacent β3-associated Src, leading to Syk recruitment and activation, ultimately leading to PLC activation and Ca^{2+} release (99).

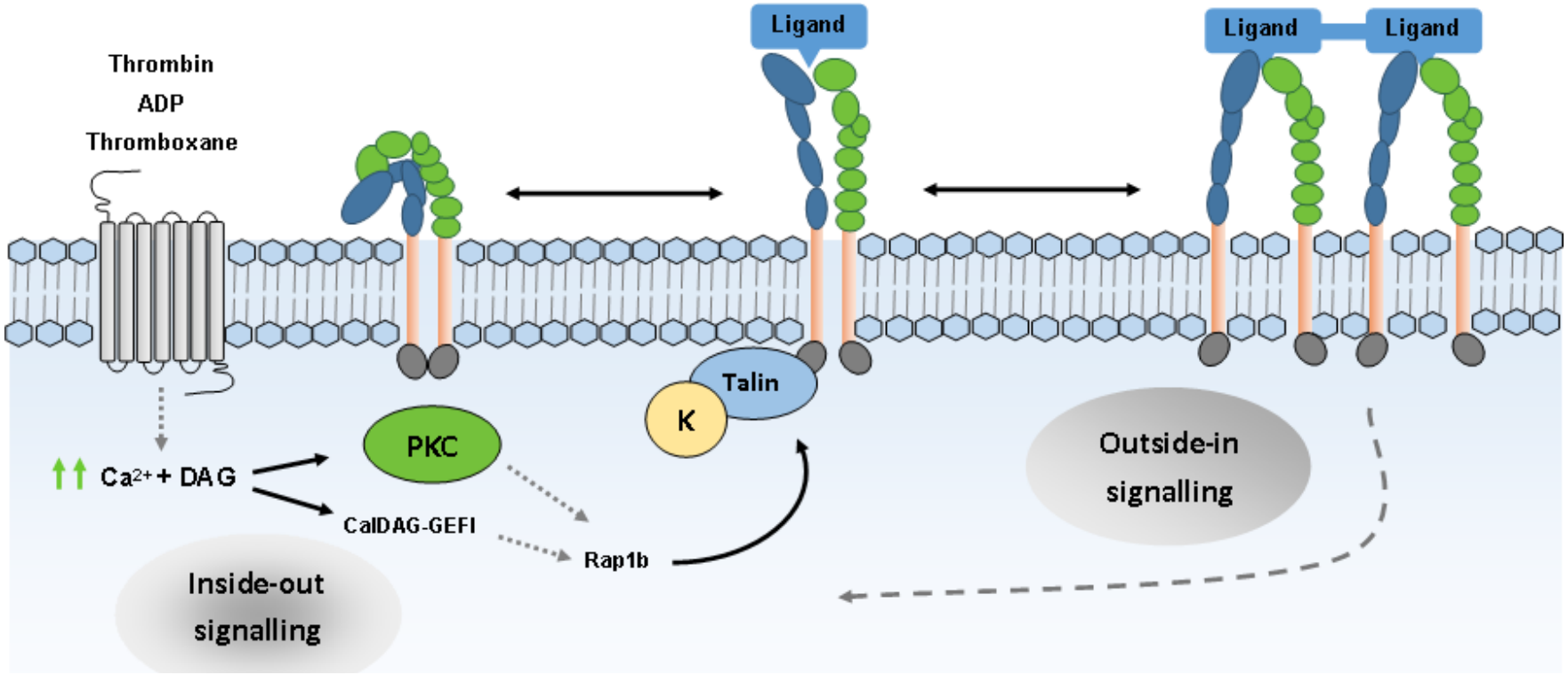

Figure 1.6. Platelet activation through inside-out and outside-in signalling. *Binding of soluble agonists to their respective GCPRs leads to an increase in* Ca^{2+} *mobilisation and DAG formation. Increasing levels of these messenger molecules causes enhanced activation of PKC isoforms and CalDAG-GEFI, leading to increased levels of GTP-bound and therefore active Rap1b. Rap1b activation leads to increased kindlin (K)-mediated talin anchoring of the cytoplasmic tails of the* $\alpha_{IIb}\beta_3$ *complex, causing a conformational switch in the cytoplasmic domains and an unbending of the extracellular domain which permits enhanced ligand binding. Further ligand binding can lead to integrin cross-linking, causing a powerful 'outside-in' signalling and amplification of platelet activation* (Adapted from Michelson, 2013).

The primary signalling event initiated upon fibrinogen-ligand binding is the phosphorylation and recruitment of Syk by Src to the β integrin cytoplasmic tail, as shown in figure 1.7. (39,100). Phosphorylation and activation of Syk then further activates PI3-kinase, which phosphorylates PIP2 to PIP3, a critical anchoring phospholipid that interacts with pleckstrin homology domains in many proteins (101). Blockade of PI3K function with inhibitors such as wortmannin inhibits platelet spreading on fibrinogen (102–104). PLCγ2 can then bind with PIP3 via its pleckstrin homology (PH) domain, localising the lipase and its adaptor proteins SLP-76 and Vav1/3 to the plasma membrane- the source of its phospholipid substrate (105,106). Also recruited is the Tec family kinase, Bruton tyrosine kinase (Btk), which has been shown to be essential for platelet spreading on fibrinogen (107). Btk phosphorylates and activates the PLC isoform to cause cleavage of PIP2 within the inner leaflet of the PM to form inositol 1,4,5-triphosphate (IP_3) and diacylglycerol (DAG) (102). IP_3 can then lead to the liberation of intracellular Ca^{2+} stores and increase the platelet's ability to form stable thrombi, such as increasing contractility through calmodulin-dependent myosin phosphorylation, causing degranulation and activating further integrins (108,109). DAG is a potent activator of PKC isoforms, which are critical in platelet spreading, thromboxane synthesis and integrin activation (110) The β3 integrin has many binding partners which are important in translating extracellular matrix cues into appropriate actin cytoskeletal responses. These will be discussed later in this chapter.

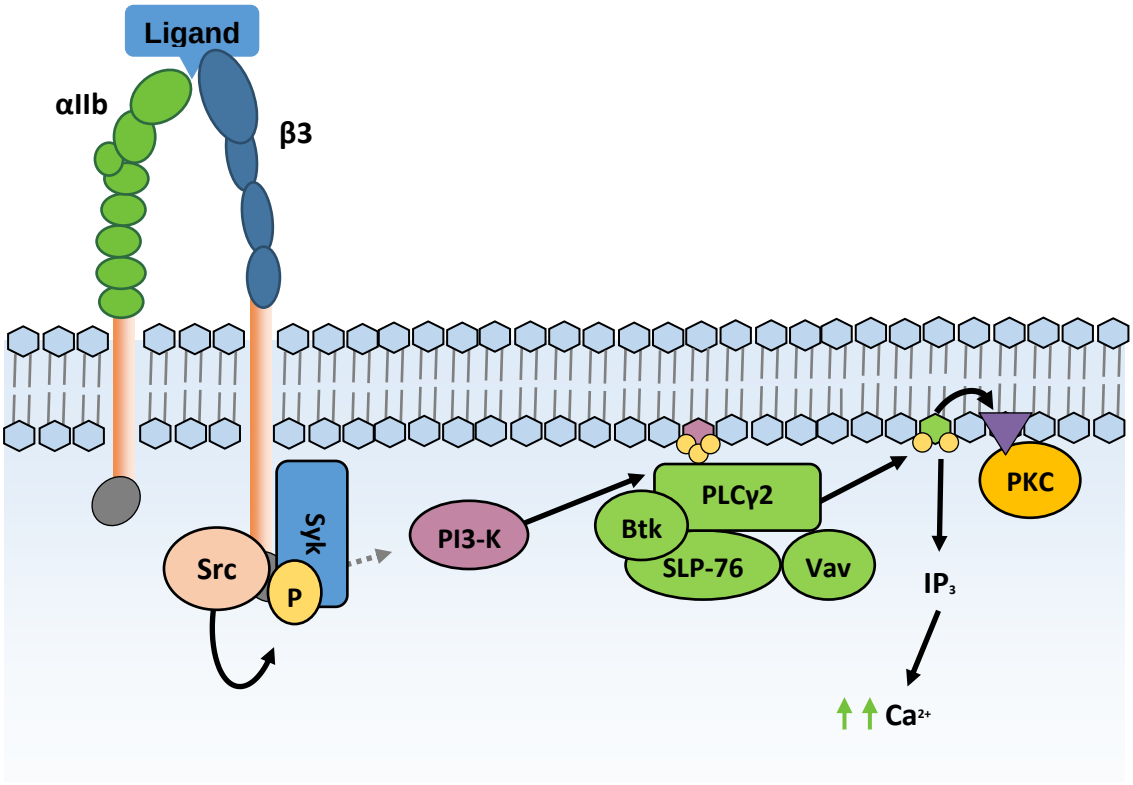

Figure 1.7. Signalling initiated by activation of $\alpha_{IIb}\beta_3$ in platelets. *Binding of $\alpha_{IIb}\beta_3$ with its ligand(s) results in the recruitment and phosphorylation of Syk by β_3-associated Src. Syk activation causes downstream activation of PI3-kinase, which phosphorylates PIP2 and forms PIP3- a key anchoring lipid required for the localisation of protein complexes to the plasma membrane. PIP3 causes the recruitment of PLC and the formation of the PLCγ2 signalosome, which cleaves IP3 from PIP2 (green) and results in DAG formation (yellow triangle). Increasing levels of IP_3 causes enhanced Ca^{2+} flux within the platelet and subsequent activation of downstream pro-activatory platelet signalling cascades. DAG acts as both and activator and anchor for PKC isoforms, leading to platelet granule release and cell spreading.*

1.5.2. Collagen

The vascular wall requires many matrix proteins to ensure structural integrity and elasticity, as well as anchorage for the formation of a uniform endothelium that prevents unwanted platelet activation. Arterial wall thickening due to collagen-mediated fibrosis and atherosclerosis is linked with an increased risk of cardiac events (111,112). Conversely, arterial wall thinning due to mutations within collagen-related genes can lead to vessel aneurysm, rupture and severe bleeding (113,114). Therefore, collagens play an important role in haemostasis, and perturbations in collagen deposition in disease can have catastrophic consequences.

Collagens are a widely expressed protein family consisting of approximately 28 members in mammals. Within the vasculature, only 4 of these members are expressed at readily detectable levels in humans- collagens I, III, IV, VI (van Zanten *et al.*, 1994). All collagens form homo/heterotrimeric helices. Within this triple helix structure, collagens share a common GPO domain consisting of glycine-proline-hydroxyproline repeats which are brought about in close proximity by the secondary structure of the peptide (figure 1.8.) (116,117). This is a specific site for one of the collagen receptors on platelets, GPVI (116). GFOGER sequences are also present in collagens and are the ligand for another collagen receptor in platelets; the integrin α2β1 (118).

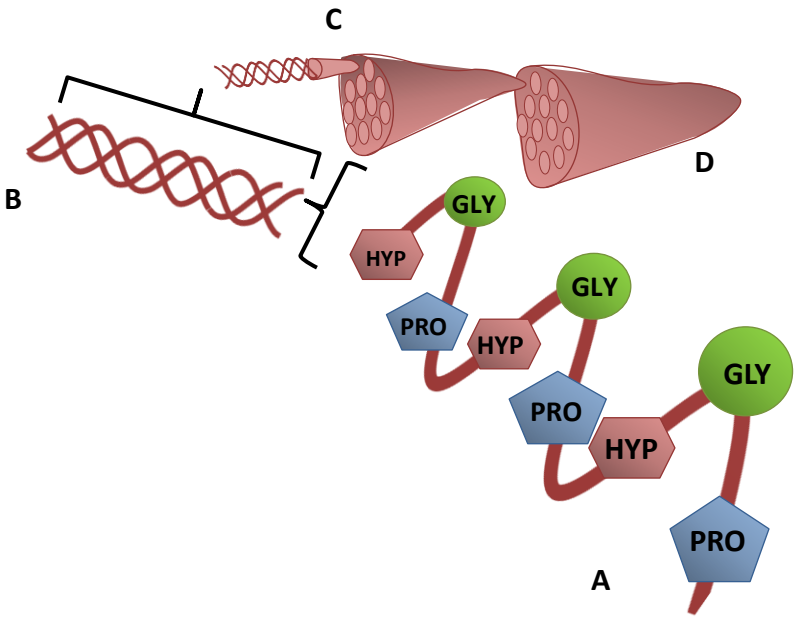

Figure 1.8. Basic structure of collagen. A) *Secondary structure of a collagen peptide relating to glycine-proline-hydroxyproline sequences, called protocollagen, that bind with platelet GPVI. Residues between this sequence have not been shown.* ***B)*** *Each collagen monomer forms a trimeric helical structure through hydrogen bonding, termed tropocollagen.* ***C)*** *Tropocollagen can arrange into protofibrils, which then form* ***D)*** *greater collagen fibres that constitute basement membranes, tendons and cartilage (Adapted from Buehler, 2006).*

1.5.2.1. GPVI

The GPVI platelet receptor is critical for full interaction and activation with collagens (120–123). This low affinity receptor consists of two extracellular immunoglobulin domains, termed D1 and D2, linked with a glycated mucin domain and a singular peptide transmembrane strand (124). There is a small cytosolic tail which contains a proline-rich motif that permits binding of proteins via Src homology 3 (SH3) domains. Using these domains, two SFK members, Fyn and Lyn, are associated with the cytosolic tail of GPVI and mediate downstream signalling (shown in figure 1.9.) (125,126). GPVI is mostly expressed in monomeric form at platelet rest and is dimerised upon activation with a number of agonists, where the two D1 immunoglobulin heads on either GPVI monomer bind GPO-containing ligands and generate robust downstream signals (127,128).

GPVI interacts with Fc-gamma chain on platelets (129). This interaction is dependent on an aspartate-arginine salt bridge in the transmembrane region, which physically associates the two proteins together (130). The importance of the association of GPVI with FcγR has been demonstrated in mice, where it was found that a lack of FcR-gamma chain prevented collagen-induced aggregation and proper expression of GPVI (131). The FC gamma chain is a homodimer which contains an immunoreceptor tyrosine activated motif (ITAM), which is made up of two YXXL amino acid repeats. The SFKs, Fyn and Lyn, phosphorylate these ITAMs on the FCγR homodimer, providing an activatory platform for Syk to activate PLCγ2 through the formation of the LAT-mediated signalosome (132,133), causing robust downstream signalling and platelet activation. The importance of Syk in GPVI-induced signalling was highlighted using Syk-deficient mice, which resulted in significantly reduced serotonin and arachidonic acid release, platelet aggregation and global tyrosine phosphorylation (134). The PLCγ2 signalosome is comprised of the adaptor protein LAT, SLP-76, Btk/Tec and Vav1/3 and others and is assembled upon ITAM phosphorylation by Syk (135). Deficiency in these components results in a drastic reduction in downstream signalling, leading to inhibition of aggregation and stable 3D thrombus formation under arterial shear, thus indicating that a fully assembled signalosome is vital for GPVI signalling (130,136–138).

Targeting the GPVI-collagen interaction is an attractive target for antiplatelet therapy. In a phase I clinical trial with the drug Revacept, healthy donors receiving this treatment did not suffer any major side effects; however, as expected, their

aggregation response to GPVI stimulation *ex vivo* was markedly reduced (139). This drug works by adsorbing exposed GPO repeats within the vascular walls, and thus prevents any issues with directly targeting GPVI, such as increased platelet clearance or dysfunctional platelet production. Currently, this drug is in phase II clinical trials and as of yet, there are no reports of the trial's findings.

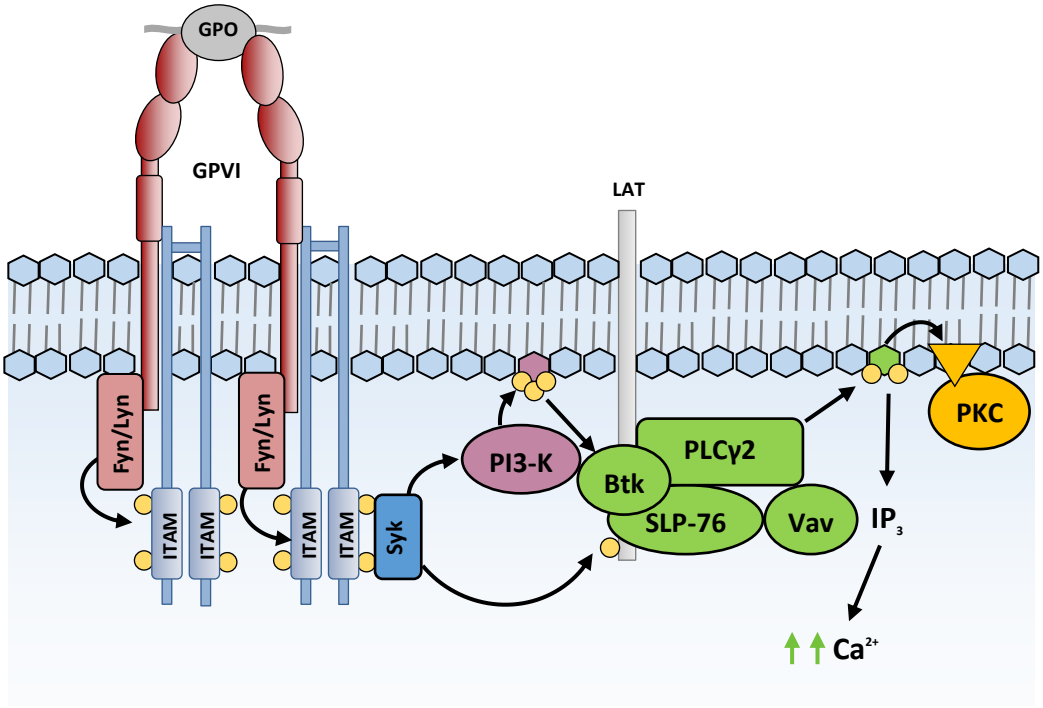

Figure 1.9. GPVI mediated signalling in response to GPO-containing proteins. *GPVI is a monomeric immunoreceptor which is expressed as a monomer associated with FcγRIIa. Activation through GPO-containing peptides causes GPVI clustering which causes SFK-mediated (Fyn and Lyn) phosphorylation of ITAM on the FcγRIIa chain. ITAM phosphorylation leads to the recruitment of Syk, which causes the activation of PI3-kinase and formation of PIP3. Additionally, Syk phosphorylates the adaptor protein, LAT, which leads to the recruitment of the PLCγ2 signalosome. Within this signalosome, Btk/Tec kinases, activated though PIP3, activate PLCγ2 and subsequent hydrolysis of PIP2 to IP3 and DAG (yellow triangle). This leads to an increase in cytosolic Ca^{2+} flux and PKC activity, respectively (Adapted from Michelson, 2013; Rayes, Watson and Nieswandt, 2019).*

1.5.2.2. α2β1

Initially thought to play only a supporting role in platelet activation on collagen, α2β1 is expressed in relatively low numbers on the surface of platelets (141). Unlike GPVI, where variation in expression between individuals is minimal, α2β1 expression has been shown to vary by as much as 40%, which has been correlated with an increase in platelet activation in response to collagen (142). As illustrated in figure 1.10., this integrin consists of two heterodimeric subunits, α2 and β1, which are in an inactive state when platelets are at rest (143). The α2 subunit contains a short cytoplasmic and transmembrane region linked to a large extracellular complex of β-sheet domains followed by a β-propeller domain. Attached to this is a domain responsible for collagen binding, the I-domain, which possesses a site for Mg^{2+}/Mn^{2+}-mediated collagen binding (144). In partnership is the β1 integrin subunit, which also contains a short cytoplasmic and transmembrane region. This is followed by a cysteine-rich region, which keeps the integrin in an inactive conformation through extensive disulphide bridging within this subunit. Platelet activation and subsequent PDI activity, like with the β3 integrin, breaks these bonds and allows the β1 subunit to elongate into a more active, ligand-binding state (145,146).

The importance of α2β1 in thrombus formation was previously theorised as an accessory receptor which further activates platelets in support of the more robust GPVI signalling. However, there have been a number of conflicting reports as to the importance of α2β1 *in vivo*. Initial investigations using β1 knockout mice found no significant change in bleeding time, aggregation to collagen and other agonists, or thrombus coverage to collagen in an *in vitro* thrombus formation assay (147). Conversely, loss of α2 through inhibitory antibodies or mutational knockouts in mice cause a slightly diminished thrombotic response to collagen under higher shear and a slight reduction in aggregation to soluble collagen (148,149). Therefore, it seems that initial GPVI activation and downstream signalling is required to activate α2β1 through inside out signalling, along with other secondary mediators such as ADP and thromboxane, which then strengthens the formed clot against increasing shear.

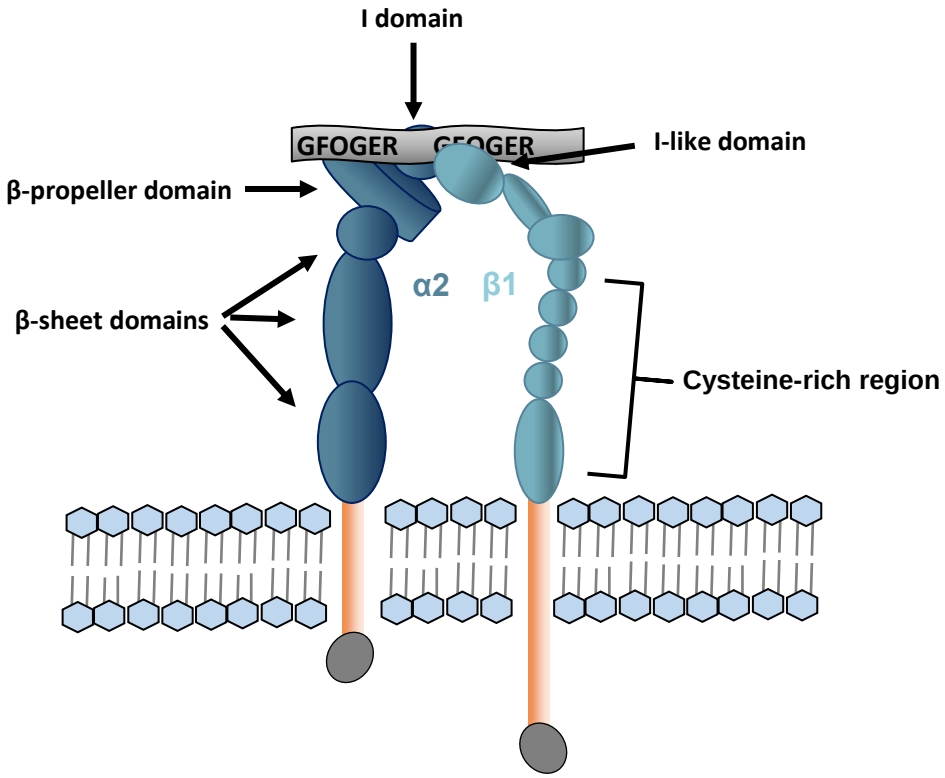

Figure 1.10. Structure of the activated α2β1 integrin complex. *The α2β1 integrin consists of two heterodimer subunits α2 and β1which are expressed together on the plasma membrane. Each subunit has a small (diagram not to scale) cytoplasmic and transmembrane region through which the integrin can signal downstream and receive inside out signals to undergo conformational change. The α2 subunit has large β-sheet domains which link to an N-terminal β-propellar domain, on which resides a so-called I-domain. The I-domain contains to binding site for GFOGER sequences on collagen. The β1 integrin has an expansive region rich in cysteine residues, permitting multiple disulphide bridges that, when unstimulated, keep the β1 integrin in a 'bent' conformation. The N-terminus contains an I-like domain which is structurally similar to the I-domain within α2. The I-like domain also contains a binding site for GFOGER sequences.*

1.5.3. Laminin

Laminins are among the most abundantly expressed proteins in subendothelial matrices. Platelets have been shown to bind with laminin under both static and arterial shear conditions primarily through the α6β1 integrin complex, causing the subsequent activation of GPVI (150). The α6β1-laminin interaction has since been directly implicated in thrombus formation *in vivo* using a platelet-specific $\alpha6^{-/-}$ mouse model (151). This study identified an interdependence of α6β1 and the GPIb complex in stable adhesion under flow. Lack of the α6 subunit completely abrogates any adhesive response to laminin. In the presence of α6, platelets also require GPIb binding to roll on the laminin matrix, where further α6β1 and GPVI activation can take place. This dependence of several integrins and glycoproteins is becoming more typical in platelet signalling and adds further complexity to thrombus formation.

1.5.4. Fibronectin

Fibronectin plays an ancillary role in thrombus assembly. Soluble fibronectin bound to platelets provide structural rigidity to the thrombus through cross-linking with collagen at the site of injury. This was shown using plasma fibronectin-depleted mice, which under intravital video-microscopy showed that fibronectin depletion prevented the establishment of stable thrombi, with significant platelet embolisation (152). Further research has corroborated these findings, but show that fibronectin is insufficient for stable platelet adhesion, where the importance of the vWF-GP1b interaction becomes apparent (153).

1.5.5. GPIb-IX-V complex

Vascular endothelial damage upon injury causes release of vWF from Wiebel-Palade bodies within the damaged and surrounding endothelial cells. vWF in low shear environments natively entwines within itself and obscures its primary sites from binding. However, when exposed to arterial shear during injury, this protein unravels and exposes its binding site for its primary platelet receptor, the GPIb-IX-V complex (69,70). The high on-off binding rate of this complex with vWF causes the tethering and rolling of platelets to the site of injury (71). Absence or deficiency of the GPIb-IX-V complex is seen in individuals with Bernard Soulier syndrome, who have severe bleeding episodes (154). Changes to the length of vWF multimers is linked with risk of thrombosis, for example familial thrombotic thrombocytopenic pupura. In this disease, a loss of function or expression of ADAMTS13, a metalloproteinase responsible for the cleavage of vWF from the endothelium, results in reduced cleavage rate of vWF and increasing the length of vWF peptides (155).

These HMW multimers extensively unravel at high shear and can cause thrombosis through enhanced platelet recruitment (156).

1.5.6. G-coupled protein receptors (GCPRs)

1.5.6.1. PAR1/4 and thrombin

GCPRs are a group of seven transmembrane receptors that are coupled to cytosolic G-proteins. G-proteins are heterotrimers consisting of an α, β and γ subunit. The α subunit is responsible for GDP/GTP binding, which determines the activation status of the G-protein and is the basis of G-protein nomenclature. Lack of GPCR agonism keeps the G-protein in an inactive state through continued GDP binding. When activated by a soluble agonist, there occurs a conformational change that frees the βγ complex, which then permits the release of GDP in the α subunit and subsequent replacement with GTP, thereby activating the G-protein and initiating downstream signalling.

There are several GPCRs expressed in the platelet membrane. Thrombin is a serine protease and a potent platelet agonist which activates human platelets by cleaving the extracellular domains of protease activated receptors 1 and 4 (PAR1/PAR4), which provides an autoligand for the receptor (157). Thrombin is formed from prothrombin via activation of the coagulation cascade by factor X. This process is expedited by platelets at the site of injury, where they provide negatively charged phospholipids as a surface for the enzyme complex required for factor X activity (158). This also ensures localisation of thrombin synthesis, which prevents systemic thrombin generation. Cleavage of the N-terminal extracellular domains of PAR1 and PAR4 causes a conformational change within the receptors, liberating G_q and/or G_{13}, resulting in robust downstream signals that increase platelet contractility, Ca^{2+} flux and granule secretion. G_{13} activates the small GTPase, RhoA, by activating p115RhoGEF, a guanine exchange factor that activates RhoA through the substitution of GDP to GTP (159). G_q activates PLCβ and causes liberation of IP_3 which leads to Ca^{2+} mobilisation through binding to IP3R on the endoplasmic reticulum (160,161). Additionally, PLCβ also causes the formation of DAG and the downstream activation of PKC isoforms and subsequent granule secretion. Not only does PAR1/4 activation cause activation of proaggregatory pathways, it can also mediate cAMP breakdown through the activation of cAMP-hydrolysing phosphodiesterases, thereby lowering intracellular cAMP and reducing the opposing inhibitory signal for full platelets activation (162).

The importance of PAR agonism is demonstrated by loss of PAR4 in murine platelets, which causes diminished *in vivo* thrombus formation and P-selectin exposure in a ferric chloride injury model (163). Additionally, although not directly targeting PAR receptors, the anti-FXa drug, dabigatran, has been shown to reduce thrombin-induced human platelet aggregation in a dose-dependent manner (164).

1.5.6.2. P2Y12, P2Y1 and ADP

ADP is another agonist for GPCRs and binds to two GPCRs, P2Y12 and P2Y1, which leads to relatively weak downstream signalling. A major contributor to the platelet response is the inhibition of inhibitory signalling in platelets through the action of P2Y12-mediated Gi activation (165). When active, Gi can form an inhibitory complex that interacts with AC, reducing its cAMP output (166). The role of ADP signalling in thrombus formation has been highlighted using mice deficient in the P2Y12 receptor and individuals with mutations in the *P2RY12* gene. Deficient mice have increase haemorrhage risk, with an underlying inability to aggregate to ADP and a slightly diminished response to PAR4 agonism (167). As expected, cAMP production upon ADP stimulation of $P2Y12^{-/-}$ platelets was unaffected, whereas WT platelet cAMP levels were significantly reduced. Individuals with mutated P2Y12 are also associated with bleeding episodes and have a lack of secretory and aggregatory response to ADP (168,169). P2Y12 antagonism has proven an effective antiplatelet therapy and dampens the platelet response to agonists dependent on secondary mediators for full activation. However, significant subsets of recipients develop major bleeding complications in response to therapy (170), indicating more nuanced and individualised therapies would be preferable.

1.5.6.3. Thromboxane A_2 and TP

Thromboxane A_2 (TXA_2) is an eicosanoid lipid that is synthesised from arachidonic acid by the enzyme thromboxane synthase (171). TXA_2 synthesis is activated upon platelet activation and is released as an auto/paracrine signal alongside ADP release from dense granules. It binds to the thromboxane receptor (TP) expressed on the plasma membrane and activates its accompanying G-proteins, G_q and G_{13} (159,172). Inhibition of TXA_2 synthesis with low dose aspirin has been used as a cost-effective means of lowering risk of cardiovascular events (173). Aspirin works by inhibiting the cyclooxygenase-2 enzyme within the platelet, reducing the amount of the TXA_2 precursor PGH_2. More recently, Rothwell *et al* have assessed clinical trial data using low and high dose aspirin and found that patients above 70kg has

no lower risk of CVEs than control counterparts, indicating that the 'one size fits all' approach to aspirin is ineffective (174).

1.6. Cyclic nucleotide signalling in platelets

Increased platelet reactivity is implicated in multiple thrombotic diseases, including MI, ischaemic stroke and peripheral vascular disease. Without a system in place to maintain platelet quiescence, platelets could preactivate and form pathological thrombi. Cyclic nucleotides (CN) generated within the platelets address this issue, which results in the inhibitory phosphorylation of several key pathways in platelet activation. The initial signal to cause this increase in CNs is released primarily through the vascular endothelium in the form of nitric oxide (NO) and prostacyclin (PGI_2), which essentially 'bathe' oncoming platelets in inhibitory signals. This process is overcome by potent activation of the platelets through release of prothrombotic matrices and soluble factors when vascular damage occurs.

1.6.1. Nitric oxide

Previously termed endothelial-derived relaxation factor (EDRF), nitric oxide (NO) was originally discovered to cause vasodilation of carefully prepared rabbit aorta (175). Later EDRF was determined to be NO by the Moncada lab, who showed identical aortic vasodilation in response to EDRF-inducing bradykinin and NO (176). Importantly, the effect of EDRF and NO were abolished in the presence of haemoglobin, which binds to and neutralises the effects of NO. This group further went on to demonstrate that endothelial-derived NO is a potent inhibitor of platelet aggregation and adhesion to vascular endothelium (177); These seminal findings have led to an explosion of research over the last three decades, resulting in a comprehensive knowledge of NO, its intracellular actions and bodily consequences.

As indicated from previous work, the vascular endothelium releases NO into the bloodstream. This is enabled through the actions of nitric oxide synthases (NOS), of which there are three broad isotypes; inducible NOS (iNOS), neuronal NOS (nNOS) and endothelial NOS (eNOS). These enzymes utilise L-arginine to produce L-citrulline and NO. eNOS appears to be a main contributor to the maintenance of platelet quiescence, as knockout of eNOS in mice causes decreased clotting times in *in vivo* thrombus formation assays (178). However, further studies thereafter questioned this notion and showed that eNOS plays only a minor role in platelet inhibition (179), which could be a result of the opposing phenotypes observed with lack of NO for platelet inhibition and lack of vWF release from $eNOS^{-/-}$ mice upon

injury (180). Individuals with polymorphisms in *NOS3*, the gene that codes eNOS, are correlated with an increase in cardiovascular events (CVEs), which corroborates initial findings from Freedman *et al*.

Conflicting research has led to debate on whether platelets themselves express NOS isoforms, with some labs identifying eNOS at both a protein and gene level, and others not. One possible cause of this discrepancy could be contamination of leukocytes in platelet preparations, which express eNOS (181). Freedman *et al* reported the production of NO from platelets but did not report the identification of NOS isoforms (182). Using real-time videomicroscopy and a NO reporter probe, Cozzi *et al* have visualised the production of NO in platelets in real-time in WT and $eNOS^{-/-}$ platelets (184). Platelet-dependent NO was significantly lower in knockout mice than WT counterparts in response to collagen, which resulted in an increase in *ex vivo* thrombus formation. Oddly, the NOS isoform presence within platelets was not reported and suggests that it was non-detectable in either mouse. As of yet, there have only been a few reports of eNOS detection at a protein level in platelets (185,186). It appears that NO is being produced in platelets in a NOS-independent manner, which would explain the discrepancies among research groups. Perhaps the presence of nitrosylated proteins may provide a reservoir for NO, which may then be liberated given specific signalling cues. S-nitrosoglutothione reductase (GSNOR) is an alternative method of NO availability in the cell but has yet to be investigated in platelets (187). PDIs have also been implicated as the determining factor in the platelet specific actions of GSNO and may represent another mechanism of autoinhibition (188).

1.6.1.2. NO signalling in platelets

In platelets, NO can freely diffuse across the plasma membrane and bind to its only known receptor in platelets, soluble guanylyl cyclase (sGC) (189). This enzyme forms the signalling molecule cyclic guanosine monophosphate (cGMP) from GTP. sGC consists of homologous α and β subunits, the latter of which contains an N-terminal haem moiety for NO binding. Binding of NO causes a conformational change in sGC structure and the exposure of the enzymes two cyclase homology domains, which when dimerised produce cGMP. sGC activity can be artificially enhanced through binding to a ‘pseudosymmetric’ site used for regulatory ligands. Compounds such as YC-1 bind to this site and cause constitutive sGC function and cGMP synthesis (190). Upon sGC activation and cGMP production, cGMP can bind

to and activate protein kinase G Iβ (PKGIβ) (191). Activated PKG has a number of targets involved in critical signalling pathways that regulate platelet activity.

Phosphodiesterase 5 is responsible for hydrolysis of cGMP levels and thus reducing the activity of PKG in platelets. Loss of PDE5 function results in unchecked cGMP accrual and strong inhibition of platelet activation. Sildenafil is a potent inhibitor of PDE5 which works in the nanomolar range and was originally created as a vasodilator and antiplatelet drug (192). As a PDE5 inhibitor, sildenafil potentiates the effects of NO in platelets and vascular smooth muscle cells (VSMCs). Interestingly, PKG itself phosphorylates and stimulated PDE5 activity, creating a negative feedback loop that self-regulates cGMP levels at specific areas within the cell (193). The role of PDE distribution in cells is a key area of cyclic nucleotide regulation that requires further investigation.

1.6.1.3. Targets of PKG in platelets

There are several targets of PKG in the human platelet, phosphorylation of which by PKA causes global platelet inhibition (figure 1.11.). The movement of Ca^{2+} within activated platelets has been extensively investigated and is critical for platelet function. Addition of the Ca^{2+} chelating agent BATPA-AM, causes complete inhibition of platelet aggregation, spreading and thrombus formation *in vitro* (194–196). PKG has been shown to inhibit this movement of intraplatelet Ca^{2+} by binding and phosphorylating the inositol-1,4,5-trisphosphate receptor-associated cGMP kinase substrate (IRAG) at Ser664, which prevents the release of Ca^{2+} stores from the endoplasmic reticulum through binding with the IP3 receptor. Loss of this IRAG-IP3R interaction diminishes the inhibitory effect of NO on platelet fibrinogen binding, aggregation and *in vitro* thrombus formation (197).

Platelet activation leads to inside out signalling and the externalisation of further integrins and their activation through talin and actin interactions. This is dependent the activation of the GTPase Rap1b. Loss of Rap1b drastically increases tail bleeding times and aggregation responses to multiple agonists (198). A key regulator of Rap1b function, Rap1GAP2, is phosphorylated in platelets at ser7, leading to enhanced activity of the GAP and thus diminished activity of Rap1b through and increase in intrinsic Rap1b GTPase function.

PKG can regulate also the actin cytoskeleton, which is required for platelet shape change during aggregation and maintain contractility in thrombus formation. RhoA is the major contributor to cellular contractility and its activation leads to an increase

in MLC phosphorylation and the association of myosin II with actin filaments. PKG has recently been shown to phosphorylate RhoA at Ser188 in platelets, leading to a reduction in platelet shape change through reduced ROCK activity, leading to uninhibited MLC dephosphorylation via MLCP (199).

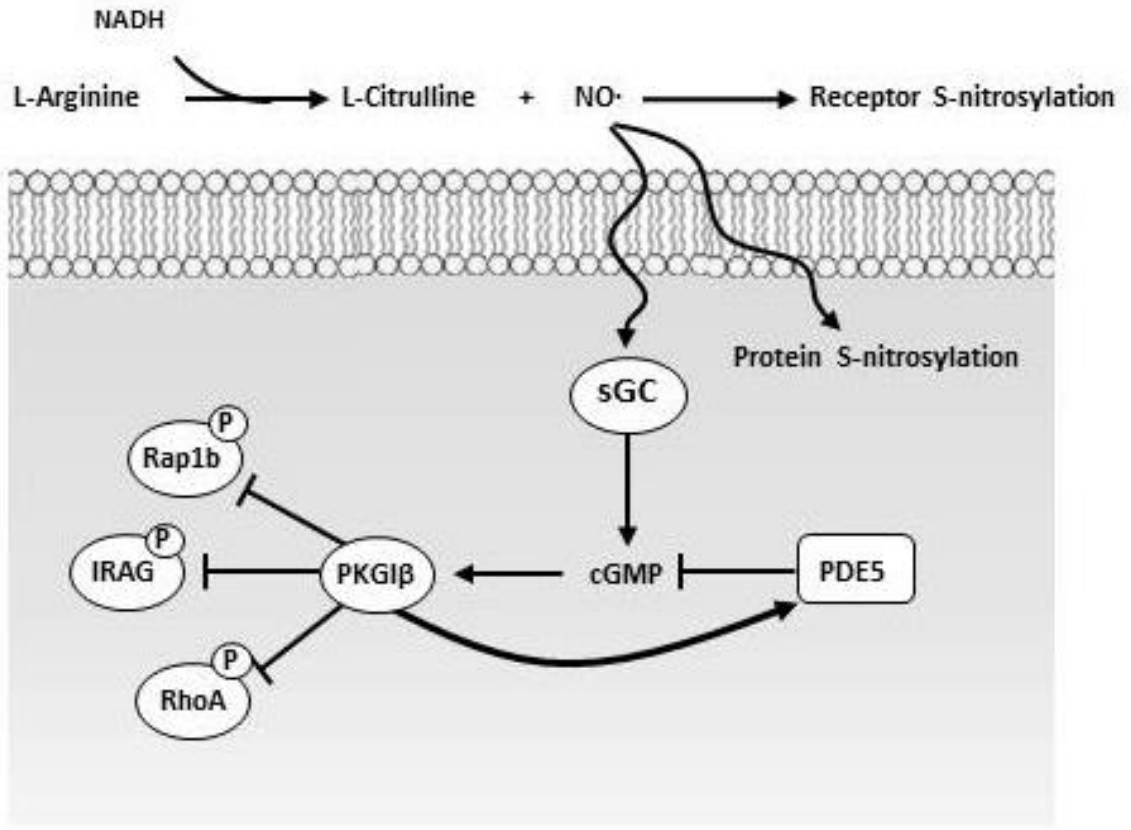

Figure 1.11. NO signalling in platelets. *Nitric oxide is synthesised through eNOS which uses L-arginine and $NADH_2$ as a cofactor. Experimentally high levels of NO lead to measurable intracellular and extracellular protein s-nitrosylation. NO freely diffuses through the plasma membrane and binds to and activates its receptor, sGC. sGC then synthesises cGMP, which can activate PKGIβ. cGMP levels are mediated by PDE5 activity, which among other mechanisms, is activated by downstream PKG and creates a negative feedback loop of PKG activity. Activated PKG can phosphorylate several targets involved in platelet activation, namely Rap1b, IRAG and RhoA, which activate integrin externalisation,* Ca^{2+} *flux and actin cytoskeletal dynamics, respectively.*

1.6.1.4. Impact of dysfunctional NO signalling *in vivo*

The effect of NO signalling in platelets is highlighted through both the use of knockout mouse models and humans with polymorphisms within the cGMP-sGC-PKG signalling axis. Loss of PKGIβ in murine platelets causes increased fibrinogen binding and increased platelet adhesion to arterial walls (191). Similarly, loss of upstream sGC in mouse platelets results in decreased tail bleeding times and no inhibition of aggregation in response to NO treatment (Dangel *et al*, 2010). In humans, mutations within the gene encoding the alpha 1a subunit of sGC, GUCY1A3, are linked with a higher risk of myocardial infarction, highlighting the role of NO in the prevention of unwarranted thrombosis (200).

1.6.2. PKA and prostacyclin

1.6.2.1. PKA signalling in platelets

Platelet activation, aggregation and thrombus formation is a highly concerted process with the convergence of numerous signalling processes often acting in a feed-forward nature to encourage further platelet activity. Therefore, without a system of inhibition, platelets could become pathologically active. PGI_2 in part addresses this issue by causing the inhibitory phosphorylation of many proteins involved in platelet activation.

PGI2 causes inhibition of platelet function, via increasing the activity to AC leading to elevation in cAMP concentration. This in turn activates Protein Kinase A (PKA) leading to phosphorylation of multiple proteins, causing platelet inhbition. PKA is a heterotetramer consisting of two regulatory subunits and two catalytic subunits. There are three regulatory isoforms; RIα, RIβ and RIIβ, and two catalytic isoforms; Cα and Cβ. Together, these isoforms combine to create two individual PKA enzymes in platelets, PKAI and PKAII (201). As a holoenzyme, PKA is inactive when unbound to cAMP due to withholding of the catalytic subunits from their respective substrates by the regulatory subunits. A conformational change occurs upon cAMP binding to the regulatory subunits, causing release of the catalytic subunits and activation of the PKA enzyme (202) (figure 1.12.).

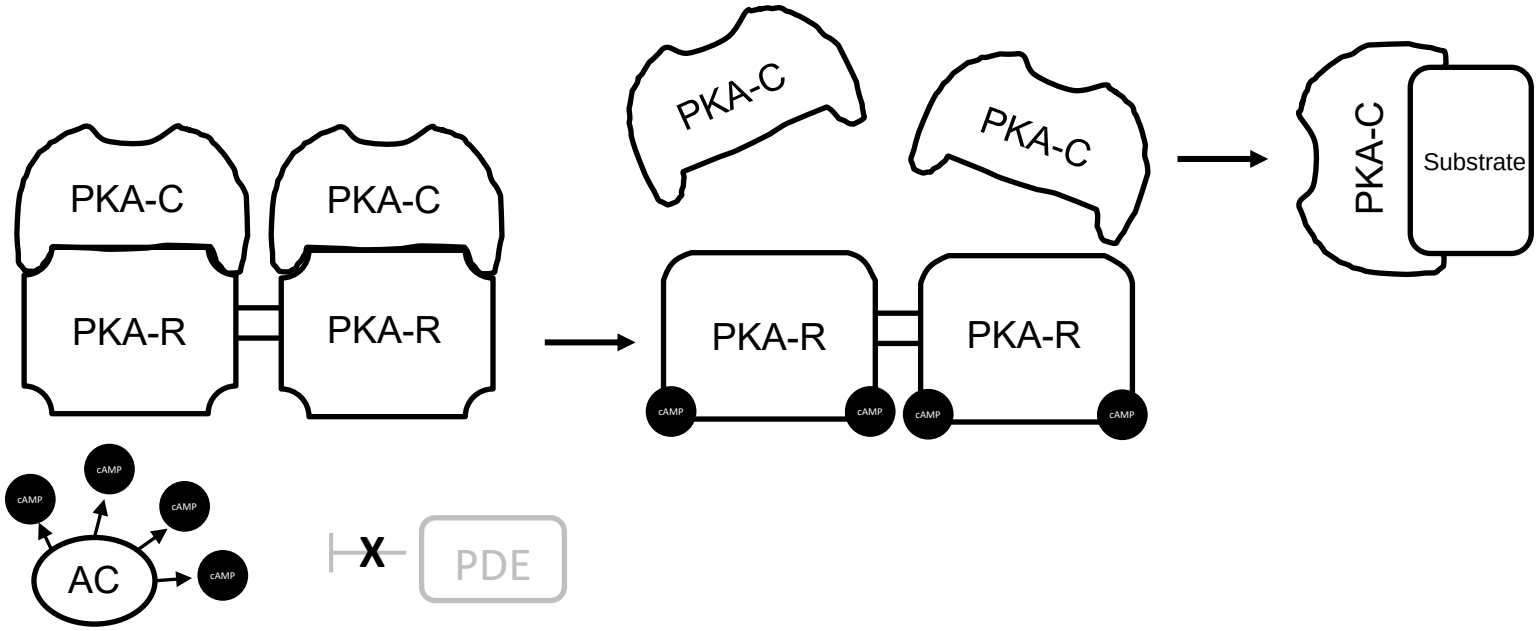

Figure 1.12. Regulation of PKA through cAMP binding. In its native state, the PKA holoenzyme consists of two regulatory (R) and two catalytic (C) subunits. *Binding of PKA-R with PKA-C obscures the catalytic cleft in PKA-C and keeping the enzyme inhibited. Increasing cAMP levels, caused by either increased activity of AC or inhibition of PDE function, causes cAMP binding to PKA-R subunits, which have two cyclic nucleotide binding sites termed cyclic nucleotide binding domains (CBD). cAMP-PKA-R binding causes a conformational change in the regulatory subunit and release of PKA-C, which is then permitted to phosphorylate multiple downstream targets (Adapted from Johnston, Lehnart and Burgoyne, 2015).*

PKA is a highly promiscuous kinase, which binds to protein targets containing a consensus RRXS sequence of amino acids (204). This sequence is a useful tool when investigating possible PKA regulation of protein function; however, this sequence does not necessarily indicate that the protein of interest is phosphorylated by PKA. Perhaps the most well characterised target of PKA in platelets is the serine-157 residue of VASP and is used as a marker of PKA and PKG activity in platelets (205). There appears to be little effect of PKA-mediated VASP phosphorylation in platelet function. Recently, Benz *et al.* (2016) highlighted a lack of VASP binding with a Rap1b-activating adaptor protein, Crkl. The effect of this disruption unfortunately was not investigated or reported.

PKA can also inhibit Ca^{2+} mobilisation and influx in platelets as shown by El-Daher *et al*, where PGI_2 treatment led to IP-3 receptor phosphorylation of an unknown site. This receptor has two consensus RRXS PKA binding sequences at serine-1598 and serine-1774 (https://www.uniprot.org/uniprot/Q14643). Accordingly, PKA-mediated phosphorylation of two nearby serine residues has been shown to occur in HEK293 cells; however, the occurrence of this has yet to be confirmed in platelets. The transient receptor potential channel 6 is a membrane bound Ca^{2+} flux channel expressed in platelets which imports Ca^{2+} into the cytosol in response to stimuli (207). TRPC6 phosphorylation by PKA has been shown in platelets, but this did not reduce the transporting of cations through the channel (208). Further discussion around the role of PKA-mediated inhibition of platelets will be discussed later in this chapter.

1.6.2.2. Prostacyclin (PGI_2)

PGI_2 is a prostanoid signalling molecule synthesised by the metabolic action of multiple enzymes on arachidonic acid (209). COX-2 metabolism of AA leads to the formation of PGG_2 and then PGH_2 through biphasic cyclooxygenation and peroxidation. Finally, PGI_2 synthesis is completed by prostacyclin synthase, giving rise to a potent platelet inhibitor and vasodilator (figure 1.13.). Upon binding to its membrane-bound receptor, PGI_2 activates downstream signalling cascades within platelets that inhibit a number of processes involved in platelet activation.

Within the vasculature, the cellular origin of PGI_2 has been shown to be from the vascular endothelium lining the blood vessels by Sir John Vane, Salvador Moncada and others. This seminal work involved the generation of microsomes from rabbit and pig aorta which converted PGG_2 and PGH_2 into an unknown substance which

causes inhibition of platelet aggregation (210). It was then quickly discovered that PGG_2 and PGH_2 are converted to PGI_2 by prostacyclin synthase within the vascular endothelium (211). PGI_2 has a short half-life of 42 seconds, making both determination of physiological concentration and experimental work difficult. PGI_2 is readily degraded into a weaker platelet inhibitor, 6-keto-PGF, which circulates through the vasculature and is excreted, along with further metabolites in the urine (212). Extensive efforts have been made to determine both blood and urinary concentration so to confer PGI_2 levels, with initial investigators concluding that PGI_2 was unlikely to act as a platelet antagonist *in vivo* due to a lack of effect *ex vivo* from healthy subjects infused with intravenous PGI_2 (213,214). This was however likely an artefact owing to prostacyclin's very short half-life or was reflective of the inducible nature of PGI_2 synthesis in response to arterial wall shear stress, as shown by a number of groups (215,216). Therapeutic inhibition of COX-2 function and PGI_2 synthesis with rofecoxib, a non-steroidal anti-inflammatory drug (NSAID), was linked with a 2.24 relative risk of MI in a meta-analysis by Jüni *et al.* (2004), thus highlighting the importance of sufficient prostanoid synthesis in the prevention of thrombus formation.

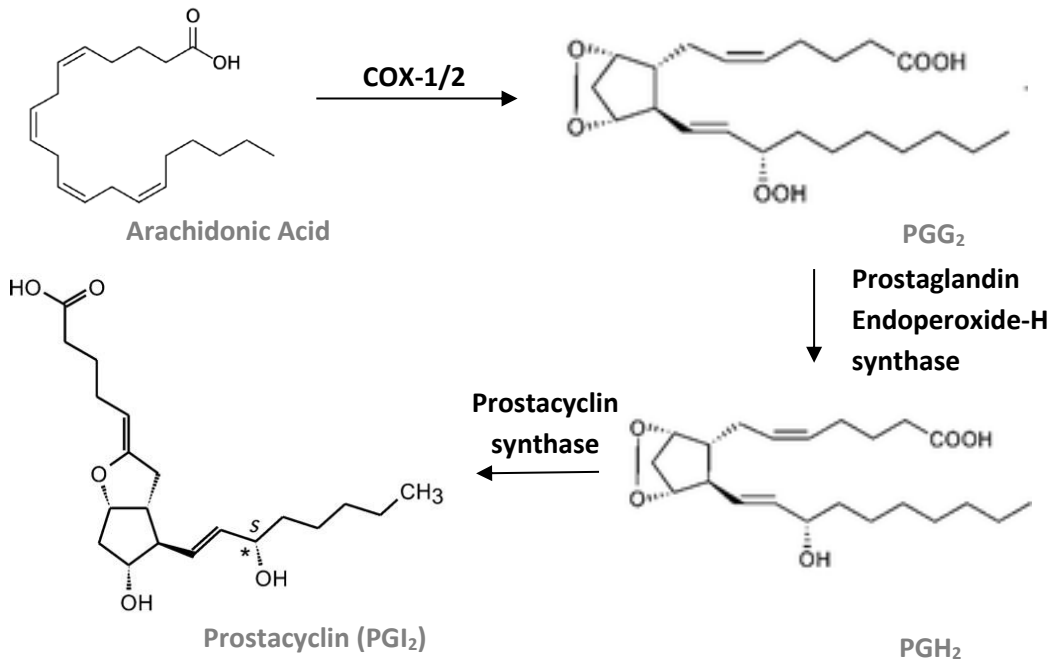

Figure 1.13. Prostacyclin synthesis through cyclooxygenases within the endothelium. *Arachidonic acid is converted to PGG_2 by cyclooxygenase 1/2. This is then converted to PGH_2 and then prostacyclin through prostaglandin endoperoxide-H synthase and prostacyclin synthase, respectively.*

1.6.2.3. cAMP synthesis through adenylyl cyclase

Platelets readily express the extracellular receptor for prostacyclin, termed the IP receptor (I prostanoid receptor). Upon PGI_2 binding, the membrane-bound IP receptor activates its coupled G-protein, leading to dissociation of the G_s subunit and downstream activation of membrane-bound adenylyl cyclase (AC) through Gs binding (218) (figure 1.14.). Activated AC then synthesises cyclic adenosine monophosphate (cAMP) through the hydrolysis of a pyrophosphate group from ATP to form cAMP to translate the extracellular signal into an intracellular one. There are three detectable AC isoforms in human platelets- AC3, AC5 and AC6 (219,220), which unfortunately are also expressed in other tissues in the body and preclude the targeted inhibition of platelet function through direct platelet AC activation (221). The expression of three AC isoforms in platelets suggests they may have distinct roles. Currently, there is little research into the spatiotemporal regulation of AC isoforms in platelets and their specific role in platelet physiology. This subject requires investigation, as there could potentially be platelet-specific AC binding partners that could serve as potent targets for antithrombotic therapies. AC5 and AC6 are highly expressed in the mammalian heart, which upon activation/overexpression has been shown to induce hypertrophy, fibrosis and arrhythmia due to the critical role of cAMP in myocardium contractility and membrane depolarisation (222).

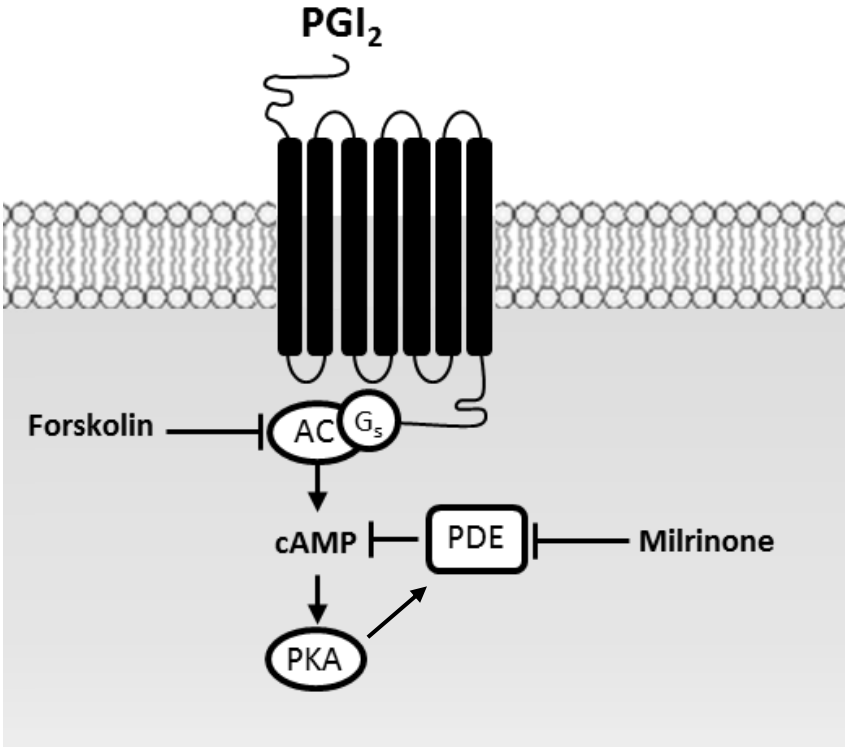

Figure 1.14. cAMP formation and PKA activation in response to IPR-PGI_2 binding. *PGI_2 within the vasculature binds to IPR, a GPCR linked with G_s, leading to its liberation for the G protein complex. G_s activation or treatment with the direct Ac activator, forskolin, causes the activation of AC which then synthesises cAMP from ATP. To ensure controlled levels of cAMP, PDEs degrade this increase in cAMP signal to maintain platelet response to stronger platelet agonists. This can be inhibited experimentally by using milrinone, which prevents cAMP breakdown and leads to a continual increase in cAMP content. cAMP binds to and activates PKA, which can phosphorylate a number of downstream targets involved in platelet activation. Additionally, activated PKA can phosphorylate and thereby activated upstream PDE3A, thus forming a negative feedback loop to keep cAMP concentrations in check.*

1.6.2.4. Phosphodiesterases: composers of cAMP signalling

cAMP accrual within the cell may have deleterious effects if not diminished or localised. Some downstream targets of cAMP signalling appear to be more receptive than others, which highlights the need for localisation of pools of cAMP within the cell. Phosphodiesterases (PDEs) are responsible for the hydrolysis and reduction of cAMP. There are 9 known PDE families which are differentially expressed throughout the body, with 3 isoforms of these being readily detected in platelets- PDE2A, PDE3A and PDE5A (162,223,224). PDE2A can hydrolyse both cAMP and cGMP to a similar extent (224). PDE3A has a higher capacity for cAMP breakdown, with a much lower ability to break down cGMP. Under these conditions, PDE3A can be inhibited by high levels of cGMP, which competitively resides within the catalytic cleft of PDE3A, preventing cAMP hydrolysis at comparatively lower

concentrations (225). PDE activity in resting platelets is low and provides sufficient levels of cAMP and PKA activity within the cell to keep platelets quiescent (226). Activation of platelets with thrombin leads to PDE3A phosphorylation and activation by Akt, leading to enhanced PDE3A activity and cAMP hydrolysis and permits increased platelet activation (162).

1.6.2.5. A kinase anchoring proteins (AKAPs): Distribution of PKA activity

A-kinase anchoring proteins (AKAPs) are a diverse group of proteins which facilitate the compartmentalisation of PKA, other kinases and phosphatases and respective substrates and regulators throughout the cell (227). Raslan *et al* have demonstrated that the PKA-I holoenzyme is anchored to lipid rafts within platelets, leading to the inhibition of vWF signalling through GPIbβ phosphorylation(228). Here, the use of lipid raft disruptors led to a reduction in PKA-mediated GPIbβ phosphorylation. Further investigations into the identification and impact of AKAPs in the control of PKA signalling are required. As seen with PDE activity, cAMP pools are localised tightly throughout the cell and so are their downstream consequences. Perhaps novel AKAP isoforms in platelets may also localise the effect of PKA in different areas of the platelet, leading to high PKA activity in one area, and low in another.

1.7. The actin cytoskeleton

Platelets are the first responders to signs of vascular damage. As such, they need to elicit a swift response to these signs to stem the loss of blood. To do this, platelets use extracellular cues in the form of exposed matrices, soluble agonists and shear stress, which orchestrate the platelet's spatiotemporal response. The platelet actin cytoskeleton is crucial in this response and leads to the formation of distinct structures within the cell during platelet adhesion, spreading and thrombus formation. This results in the generation of a smooth, contractile and non-occlusive thrombus in healthy individuals that stems blood loss whilst maintaining blood flow downstream of the site of injury. Although there have been many investigations into the role of the actin cytoskeleton in platelets, there still remains many areas that require further insight. For example, the formal identification, description and hypothesised purpose of small punctate patterns of actin in cells, termed actin nodules, has only been reported relatively recently but seems critical in determining thrombus stability (103,229).

1.7.1 Actin structure and function

Monomeric, globular actin (G-actin) is a 42kDa protein and represents the most basic building block for the actin cytoskeleton. Highlighting the importance of actin in platelets is the finding that actin is by far the most highly expressed protein in the cell, contributing almost 20% of the total protein content (230). These monomers can be of three main isoforms, α, β and γ. α-actin is mostly expressed in muscle cells, whereas β- and γ-actin are more widely expressed throughout the body. Platelets express the β- and γ-isoforms, which are rapidly polymerised and depolymerised, resulting in controlled granule secretion and a dynamic change of platelet shape upon platelet activation (230–232). G-actin is 375 amino acid polypeptide chain that is folded into two distinct α- and β-domains. Between these domains is a central site responsible for nucleotide binding. In its unbound form, G-actin holds and ADP in this site. This is swapped for ATP by the actin binding protein, profilin, which then permits G-actin addition to the growing F-actin chain. G-actin associates with the barbed end of the actin filament, where this weak intrinsic ATPase activity of the actin monomer causes the slow hydrolysis of ATP to ADP. This degradation of ATP to ADP is crucial for actin dynamics and allows the liberation of G-actin from the filament, allowing the monomer to form new filaments elsewhere. During ATP binding, the association of G-actin in the filament is stable and provides structural rigidity. ATP to ADP hydrolysis in actin added earlier to the filament causes pointed end destabilisation and depolymerisation. This is useful, as there is only a finite amount of actin in one area of the platelet at a given time. This concomitant polymerisation and depolymerisation of F-actin causes a phenomenon known as ‘treadmilling’, where addition of G-actin to the barbed end and subtraction at the pointed end are equal (233). F-actin depolymerisation is performed by cofilin, which binds to ADP-bound actin, causing filament instability and disassembly (234). Free ADP G-actin can then bind again with profilin and join another growing filament, or bind to another ABP, β-thymosin, which sequesters ADP-bound G-actin (235,236). This sequestration is important for two reasons; 1) it lowers ADP G-actin concentrations, thereby allowing cofilin to more readily sense and liberate ADP-bound G-actin in filaments, and 2) it prevents full and unwarranted polymerisation of all of the G-actin in a given area.

Further complexity in the regulation of actin dynamics is provided by other methods of filament severing, branching and *de novo* nucleation. Filament branching is brought about by the nucleation of filaments on the sides of existing ones by the

Arp2/3 complex (237). This complex attaches the minus end of G-actin monomers to the side of existing filaments at a 70^{o} angle. On a larger scale, enhanced Arp2/3 action leads to lamellipodia formation, sheet-like protrusions which are thought to be essential for platelet function and thrombus formation (238,239). Another form of filament nucleation is through the formin family of actin nucleators. Formins are dimeric proteins which associates with G-actin and causes polymerisation by 'capturing' free G-actin monomers and profiling-GTP-actin complexes and allowing them to join the filament. Formin complexes remain at the growing barbed end and facilitate in further actin polymerisation (240,241). Severing of existing filaments is performed by members of the gelsolin actin severing protein family, which can bind to side of F-actin and cause potent ATP-independent filament severing on a large scale and providing further barbed ends for actin polymerisation (242). Additionally, this protein can also act as an actin capping protein (ACP) and prevent further filament growth. CapZ is another ACP, which has been shown in resting platelets to be readily bound to actin. Upon platelet stimulation, a proportion of CapZ dissociates with actin and permits filament elongation (242,243).

1.7.2. Cdc42/Rif and filopodia

During early platelet spreading, finger-like protrusions appear from the platelet body across the underlying matrix, termed filopodia. These structures consist of parallel bundles of actin, which grow forward from the leading edge of the plasma membrane and push it forward. This is due formin activity, which as discussed, associates and stays with the barbed plus ends whilst polymerising the filament. This process, along with platelet rounding, is thought to contribute to the typical shape change seen in aggregation traces.

Cdc42 is considered the primary mediator of platelet filopodia formation. In its GTP-bound activated state cdc42 activates p21-activated kinase (PAK), WASP, Arp2/3, and formins, resulting in the formation of expansive parallel actin bundles (244,245). Knock-out of cdc42 in mouse models has resulted in contradictory findings, with the formation of filopodia in response to fibrinogen in one, but not the other (245,246). This may be a result of the different knock-out strategies used, or the differing concentrations of fibrinogen used in both experiments, which has been shown to influence platelet signalling and activity (247). Possibly these conflicting findings are a result of redundancy in filopodia formation. Rif, a more recently discovered GTPase, has been shown to cause filopodia formation via interaction with formins and is independent of cdc42 activity (248–250), however this was subsequently

found to be dispensable for platelet filopodia formation (251). Knock-out of both cdc42 and Rif could further clarify the possible redundancy evidenced by current research.

1.7.3. Rac1 and lamellipodial spreading

Rac1 is a ubiquitously expressed GTPase which is associated with lamellipodial spreading in platelets. There are other Rac isoforms expressed in the body, Rac1 and Rac2, however platelets only appear to express Rac1 (239). Activated Rac1 is linked with branched, sheet-like networks of actin filaments that drive forward the leading edge of the plasma membrane. Differential Rac1 activity at the leading edge of the plasma membrane is associated with differential Rac1 activity (252). Rac1 activity has also been implicated in platelet secretion, where inhibition of Rac1 with the inhibitor NSC23766 significantly reduced ATP production, P-selectin exposure and aggregation to a number of agonists (253,254). Knockout of Rac1 in mouse megakaryocytes has highlighted its importance in platelet spreading and the formation of lamellipodia on immobilised matrix proteins. Knockout platelets have an inability to spread effectively, demonstrated by a significantly reduced surface area when compared to wildtype counterparts (239). These platelets were unable to form stable thrombi under arterial shear rate both *in vitro* and *in vivo.* Upstream regulation of Rac1 is mediated through GEFs and GAPS, like RhoA. There are over 20 different GEFs associated with Rac1 activity within biological systems which facilitate the exchange of ADP for ATP within the GTPase (255). T cell lymphoma invasion and metastasis-inducing protein 1 (TIAM1) is a RhoGEF that can activate Rac1. Aslan *et al* have shown that TIAM1 complexes with ribosome S6 kinase (S6K1) and the mammalian target of rapamycin (mTOR), which when complexed together cause activation of Rac1 at the lamellipodial edge of spreading platelets (256). More recently, another Rac1-specific GEF, P-Rex1 was implicated in Rac1 activity in platelets (257).

Here, deletion of P-Rex1 in mice increased tail bleeding time, consistent with earlier findings of decreased thrombus stability in Rac1^{-}deficient mice (McCarty *et al*, 2005). Also consistent was the reduction in ATP secretion and reversible platelet aggregation to a number of agonists at submaximal concentrations, suggesting an inhibition of granule secretion.

The regulation of Rac1 and its respective upstream GEFs in platelets is poorly understood. There are however several key aspects of platelet activation that must be in place to activate Rac1. These include Ca^{2+} mobilisation and upstream $G_{\alpha q}$ activity. Inhibition of Ca^{2+} in platelets completely prevents lamellipodial spreading on all matrices (258,259).This is consistent with Ca^{2+} being a critical method of platelet activation and its requirement for Rac1-mediated spreading. Gratacap *et al* found that $G\alpha_q$-deficient mouse platelets fail to form lamellipodia in response to thrombin and TXA_2 (260). Ca^{2+} chelation in this study also demonstrated a return to basal Rac1 activity in response to thromboxane mimetic in WT platelets and therefore corroborated previous data. Further investigations should be undertaken to uncover the missing link(s) between Ca^{2+} and $G\alpha_q$ and the activity of Rac1 and its GEFs.

Activated Rac1 causes the assembly of Arp2/3, a multimeric complex of proteins, via activation of its cofactors WASP/ WAVE, which then move to the plasma membrane and aid in Arp2/3 membrane association (261,262) (figure 1.15.). Loss of WASP, a protein constrained to the haematopoietic lineage, leads to Wiskott-Aldrich syndrome (WAS), for which the protein was named. These individuals, among other afflictions, suffer haemorrhage due to thrombocytopenia and platelet dysfunction (57,263). WASP is also critical for the formation of F-actin-rich podosome-like structures, termed actin nodules (229)

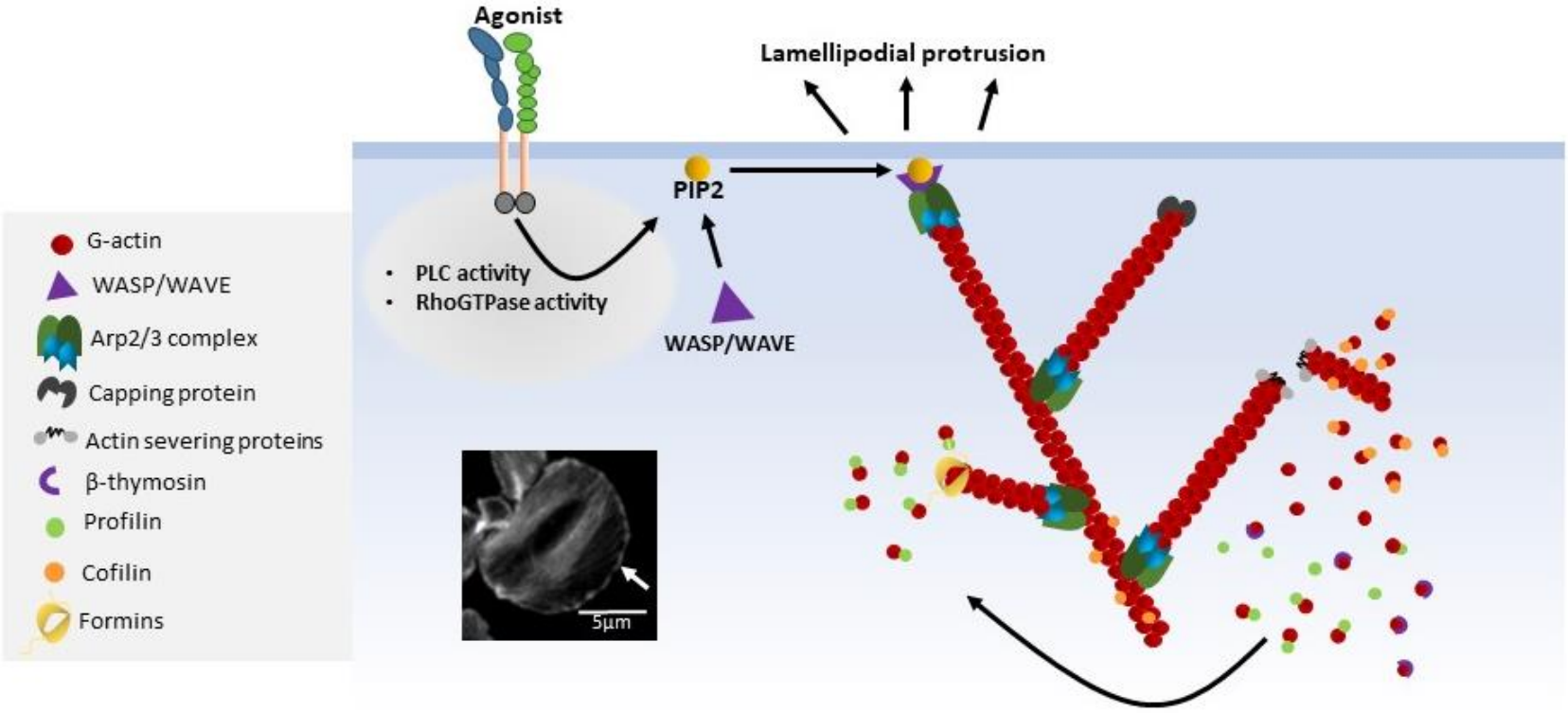

Figure 1.15. Basic platelet actin dynamics resulting in lamellipodia formation. *Receptor stimulation in platelets leads to increased PLC isoform activity and resultant generation of PIP2, which provides an anchorage point for WASP/WAVE docking through their PH domains. This represents a cofactor for Arp2/3 complex assembly, which can then nucleate actin filaments. Filament polymerisation is inhibited by capping proteins, which obscure the growing barbed ends from further actin monomers. Formins can associate with the free barbed ends of F-actin and facilitate in the addition of further monomers. Actin severing proteins can dismantle large actin oligomers. Cofilin binds to aged, ADP-bound actin monomers and causes their liberation from the filament. Conversely, profilin facilitates in ADP-ATP switching and the addition to the filament barbed end via nucleators such as formins. β-thymosin sequesters surplus ADP actin, preventing unwarranted actin polymerisation (adapted from Isogai et al., 2015).*

1.7.4. RhoA and platelet contractility through stress fibre formation

Platelet contractility primarily results from the interaction of actin with myosin IIa (195,264). This interaction is brought about by the phosphorylation of myosin light chain (MLC) by MLC kinase (MLCK). Opposing the kinase action of MLCK is MLC phosphatase (MLCP), which dephosphorylates MLC and reduces platelet contractility by limiting actin-myosin binding (265). RhoA is the upstream regulator of MLCP function, which is further regulated upstream by activated G-proteins, more specifically $G\alpha_{13}$ (172,266). In addition to actin-myosin interactions, RhoA causes the activation of the formin, mDai1, and LIM kinase, the latter of which phosphorylates and inhibits the filament destabiliser, cofilin. Together, these two processes allow the formation of long F-actin filaments (240,241). These filaments are bundled together by α-adducin, which is also activated by ROCK. This bundling of long actin filaments linked with non-muscle myosin leads to the establishment of stress fibres (figure 1.16.).

The importance of RhoA has been uncovered in multiple studies. Using a RhoA knock-out mouse model, Pleines *et al.* (2012) discovered RhoA null mice are macrothrombocytopenic, in part due to a reduction in platelet life span, and perhaps owing to the importance of proper actin regulation in the release of platelets within the vascular niche. This is supported by an observed increase in megakaryocyte number and ploidy in $RhoA^{-/-}$ mice compared to wildtypes, suggesting dysfunctional platelet production from terminal-staged megakaryocytes. Interestingly, lack of RhoA in these platelets did not drastically affect their ability to spread on immobilised fibrinogen, nor did it affect their ability to form filamentous actin structures, such as stress fibres. This suggests little to no deleterious effect on actin-myosin interactions, however, a reduced capacity for clot retraction was observed; an actin-myosin-dependent process (264,268). Although it appeared that these platelets were forming stress fibres, it is likely that they were not coupled properly with myosin, and thus did not provide sufficient contractility for full clot contraction and stability. Calaminus *et al* have shown that platelets require myosin IIa contractility in order to sustain thrombus stability through the use of inhibitors, Y-27632 and blebbistatin, which inhibit ROCK and myosin, respectively (103). Upstream regulation of RhoA is controlled by p115RhoGEF in platelets and was shown using G_{13} analogous peptides, which bound to this GEF and blocked its activity and subsequent activity of the RhoA pathway (269). p190RhoGAP is a contributor to the inhibition of RhoA through typical activation of the intrinsic GTPase function of RhoA

(270), however this has not been reported in platelets and requires investigation. This GAP has been isolated and studied in myeloid progenitors such as neutrophils and so may also be expressed in platelets (271).

Phosphorylation of serine-188 is a well-characterised method of RhoA inhibition, which has also been identified in platelets (272,273). Phosphorylation at this site by PKA results in a greater affinity for GDP-bound RhoA with guanine dissociation inhibitors (GDI) which sequesters and maintains inactive RhoA (274). The resulting inhibition leads to reduced RhoA membrane binding and activity, reduced ROCK-mediated inhibition of MLCP, and decreased downstream MLC phosphorylation due to the opposing actions of activated MLCP and MLCK (272,273). Similarly, high dose NO has also been shown to phosphorylate RhoA at serine-188 via cGMP-PKG-dependent signalling, causing a dose dependent reduction in platelet shape change upon thrombin stimulation (199)

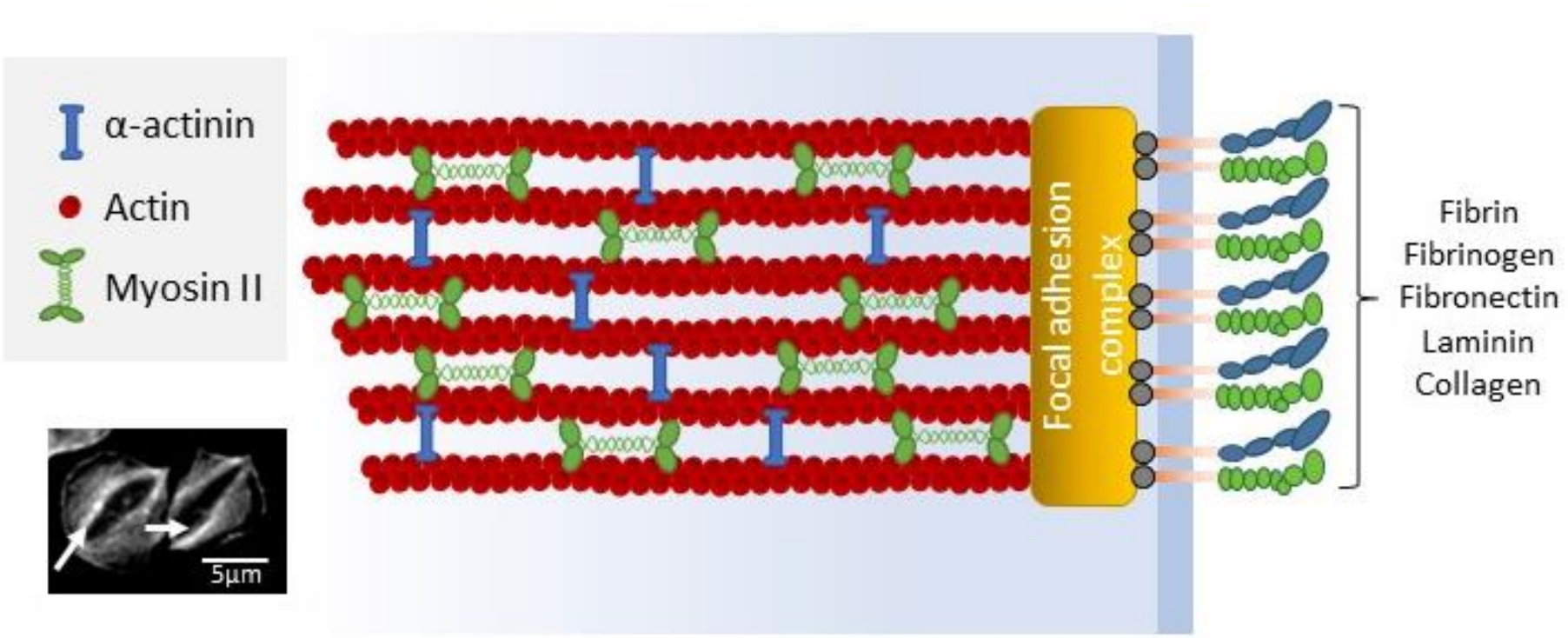

Figure 1.16. Basic structure of platelet stress fibres observed during spreading. *Numerous matrix proteins can cause stress fibre formation in platelets during spreading. Integrin clustering causes the formation of focal adhesion complexes, which anchor parallel α-actinin bundled actin filaments to the plasma membrane. These bundled filaments are associated with myosin II, which imparts the contractile nature of stress fibres and their ability to maintain platelets in situ during thrombus formation.*

1.7.5. The actin nodule

During the early stages of platelet spreading, punctate patterns of F-actin can be observed when staining with phalloidin. These were termed actin nodules by Calaminus *et al*, who originally characterised this structure, which shares similarities with podosomes (103). Interestingly, actin nodules were reciprocally associated with stress fibres, and appeared to be a prerequisite for stress fibre formation. It was found that nodules form on several matrices, including fibrinogen, laminin and vWF+botrocetin. This was dependent on Src activity and actin polymerisation, as the Src inhibitor, PD0173952, or the inhibitor of actin polymerisation, latrunculin A, completely abolished actin nodule formation on fibrinogen. These structures also colocalised with Rac1 and Arp2/3, suggesting that they require high levels of filament branching to form. An important finding was the absence of ROCK1, myosin II or Src within this structure, which distinguishes nodules from podosomes and suggests that they have different purposes.

More recently, Poulter *et al* further characterised the actin nodules through super resolution stochastic optical reconstruction microscopy (STORM)(229). In this study, actin nodules were found to be encircled by integrins and the mechanosensing protein vinculin, suggesting a role in matrix density and shear stress detection. Staining for phosphotyrosine, a marker of SFK activity, showed that nodules are areas of distinct phosphorylation, consistent with previous findings showing Src dependence for nodule formation. Also consistent with the previous findings from Calaminus *et al* regarding Rac1 and Arp2/3 within nodules, was that the Arp2/3 cofactor, WASP, strongly colocalised to the nodule (figure 1.17.). The importance of WASP in nodule formation was solidified using platelets form WAS donors. Platelets from these donors failed to form actin nodules on several matrices and were unable to establish or maintain stable 3D thrombi under arterial shear, which recapitulates clinical findings in these individuals. Although of limited knowledge, it is apparent that actin nodules are critical in functional thrombus formation.

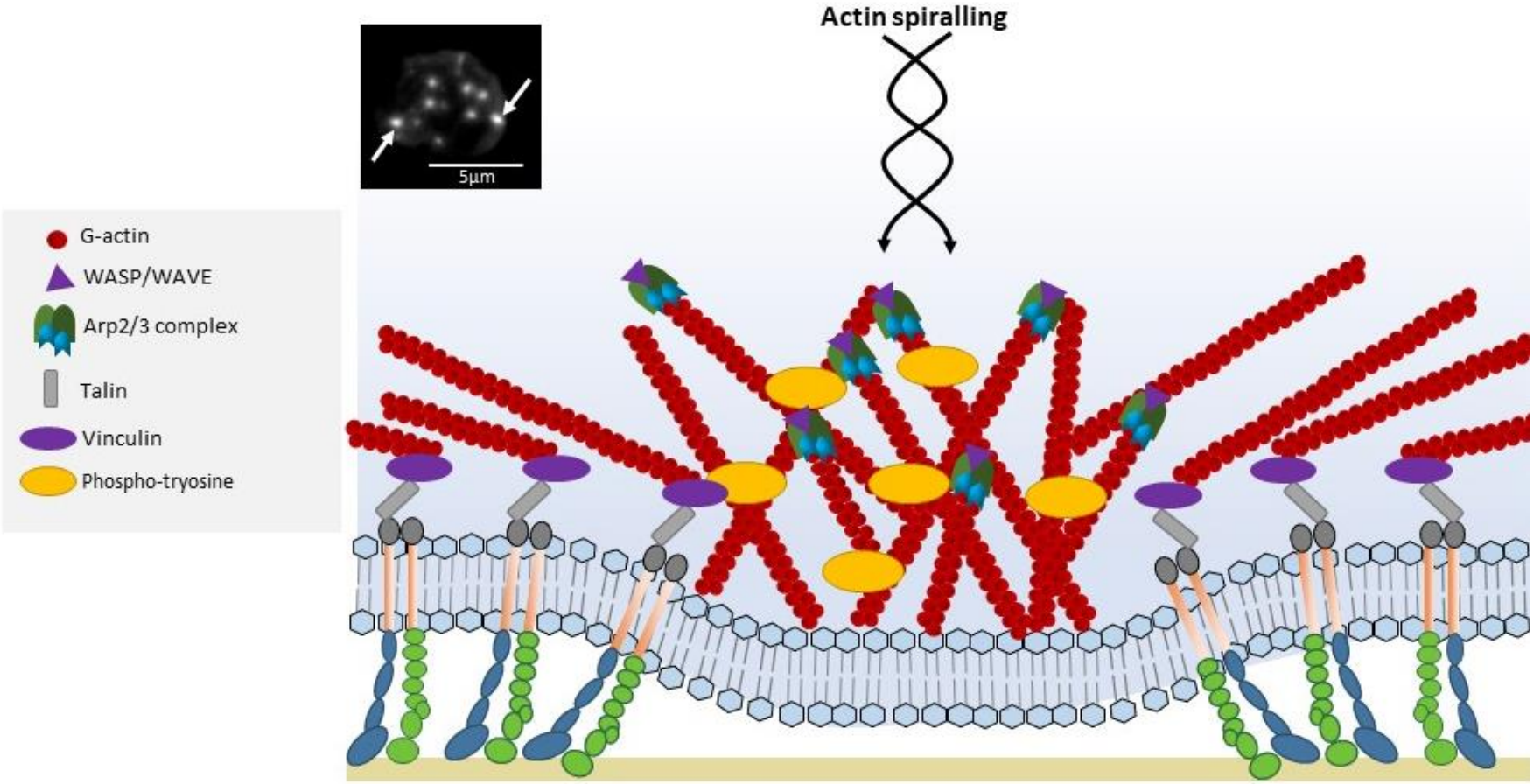

Figure 1.17. Currently known structure of the platelet actin nodule. *During the early stages of platelet spreading, punctate patters of F-actin can be observed (upper left insert). F-Actin spiralling, likely a result of Arp2/3 and WASP/WAVE activity, probes the underlying matrix. These nodules are encircled by integrins and their respective binding partners, talin and vinculin. There is a high abundance of tyrosine phosphorylation within the nodule, which may suggest the nodule's role as a signalling hub during spreading (Adapted from Poulter et al, 2015).*

1.8. Aims of this study

Platelet activation and spreading are critical for haemostasis. However, in disease this process can be exacerbated and cause thrombosis, leading to MI and stroke. The body uses NO and PGI_2 to keep platelets in a quiescent state until required and this is requested by the vasculature through exposure of subendothelial matrices and soluble factors. During platelet spreading, drastic changes in the actin cytoskeleton occur; a tightly regulated process. Although the effect of NO and PGI_2 has been investigated previously, their role in regulating platelets that have already spread has not. Recently, our group has uncovered the ability for PGI_2-cAMP-PKA signalling to cause reversal of platelet spreading.

The work presented in this thesis was designed to understand the impact of NO and PGI_2 on the spread platelet actin cytoskeleton and the role of different matrices on this effect. This work was separated into three following aims:

1. Determine the role of NO in the regulation of the spread platelet actin cytoskeleton.
2. Uncover why the spread platelet actin cytoskeleton is resistant to the effects of PGI_2 treatment.
3. Determine the role of fibrinogen matrix concentration on the sensitivity of the spread platelet actin cytoskeleton to PGI_2 and its effect on actin nodule dynamics.

Chapter 2. Methods

Table 2.1. Antibodies used in this thesis, their respective suppliers and dilutions

Antibody	Supplier/catalogue no.	Dilution factor
pVASPser157 (rabbit)	Cell Signaling Technology (#3111)	1:1000
pVASPser239 (rabbit)	Cell Signaling Technology (#3114)	1:1000
GAPDH (mouse)	Millipore (AB2302)	1:5000
pRhoAser188 (rabbit)	Santa Cruz Biotechnology (sc-32954)	1:500
RhoA (rabbit)	Cell Signaling Technology (#2117)	1:1000
pPKA substrate (rabbit)	Cell Signaling Technology (#9624)	1:1000

Table 2.2. Inhibitors used in this thesis, their suppliers and final concentrations

Compound	Supplier/catalogue no.	Final working concentration
S-nitrosoglutothione	Enzo Life sciences (ALX-420-002-M025)	1µM unless otherwise stated
Diethylamine NONOate	Enzo Life Sciences (ALX-430-034-M010)	10µM
8-pCPT-PET-CGMP	Biolog Life Science Institute (C 045)	10µM
Prostacyclin (Na^{2+} salt)	Cayman Chemicals (18220)	10nM unless otherwise stated
Y27632 dihydrochloride	Enzo Life Sciences (ALX-270-333-M001)	10µM
Forskolin	Enzo Life Sciences (BML-CN100-0010)	10µM
Milrinone	Enzo Life Sciences (ALX-270-083-M005)	10µM
Apyrase	Sigma Aldrich (A6535)	2U/ml
Indomethacin	Sigma Aldrich (I7378)	10µM

Table 2.3. Matrix proteins, suppliers and concentrations used

Matrix protein/peptide	Supplier/catalogue no.	Adsorption concentration
Fibrinogen	Enzyme Research Laboratories (FIB 3)	3 - 100µg/ml
Collagen (Horm)	Takeda	25-100µg/ml
CRP	University of Cambridge	1µg/ml
GFOGER	University of Cambridge	10µg/ml

Fibronectin	Sigma Aldrich (F1141)	50µg/ml

2.1. Platelet isolation via the pH method

Whole blood was added to acid citrate dextrose (113.8mM D-glucose, 29.9mM tri-Na citrate, 72.6mM NaCl, 2.9mM citric acid) and platelets were isolated by centrifugation at 90 x g for 10 minutes, where the initial platelet rich plasma (PRP) was obtained. A second spin of 120 x g was performed for a further 10 minutes to obtain a second fraction of PRP which was combined with the previous fraction and mixed with 0.3M citric acid (20µl per mL of plasma to make 6mM) to reduce plasma pH and maintain platelets in a quiescent state. This PRP was then centrifuged at 800 x g for 12 minutes to sediment the platelets, where platelet poor plasma (PPP) was discarded and the platelet pellet was resuspended in platelet wash buffer (36mM citric acid, 10mM EDTA, 5mM D-glucose, 5mM KCl, 90mM NaCl). This was then centrifuged at 800g for 10mins. Platelets were resuspended in modified Tyrode's buffer (20mM HEPES, 134mM NaCl, 2mM KCl, 0.34mM Na_2HPO_4, 12mM $NaHCO_3$, 1mM $MgCl_2$) at the concentrations stated and allowed to rest for 40 minutes before use. Whole blood was obtained from healthy volunteers in accordance with relevant health and safety guidelines under the ethical permission granted by the Hull York Medical School ethical committee for 'The study of platelet activation, signalling and metabolism.'

2.2. Platelet spreading

Matrix proteins were adsorbed on to 13mm^2 coverslips for either one hour at room temperature, or overnight at 4^oC prior to washing twice in PBS to remove any unbound protein. Platelets (2x10^7/ml) were allowed to spread on either fibrinogen, fibronectin, collagen, GFOGER or CRP matrices for varying time points before being washed with PBS and then treated with inhibitors in modified Tyrode's buffer for the specified times (post-treatment). Alternatively, as shown in figure 2.1., platelets (2x10^7/ml) were incubated with inhibitors or vehicle and then spread for a specified amount of time (pre-treatment). The samples were fixed in 4% paraformaldehyde solution for 10 minutes, permeabilised in 0.1% Triton X-100 for 5 minutes before being stained for actin via FITC-phalloidin incubation for 1 hour at room temperature. Slides were then washed in PBS and mounted onto

glass slides using ProLong Diamond antifade mountant (Invitrogen - Fisher Scientific, Massachusetts, USA) and imaged after overnight curing on the Zeiss Axio Imager fluorescence microscope (Cambridge, United Kingdom) at x63 (1.4NA) magnification through the Zen Pro software package. Platelet adhesion, actin nodule: stress fibre ratios and surface area measurements were analysed through Fiji (275) by manual counting and circling, respectively. An actin nodule positive phenotype was defined as two or more actin nodules in the absence of stress fibres. A stress fibre positive phenotype was recorded if a platelet had distinct parallel bundling of F-actin. Platelets which had no discernible actin nodules or stress fibres were recorded as 'unclassifiable'. Five random fields of view were imaged per condition, with all platelets within the field being manually counted for adhesion and actin structures. 100 platelets were analysed per condition for surface area using the freehand circling function in Fiji and their means were expressed as μm^2.

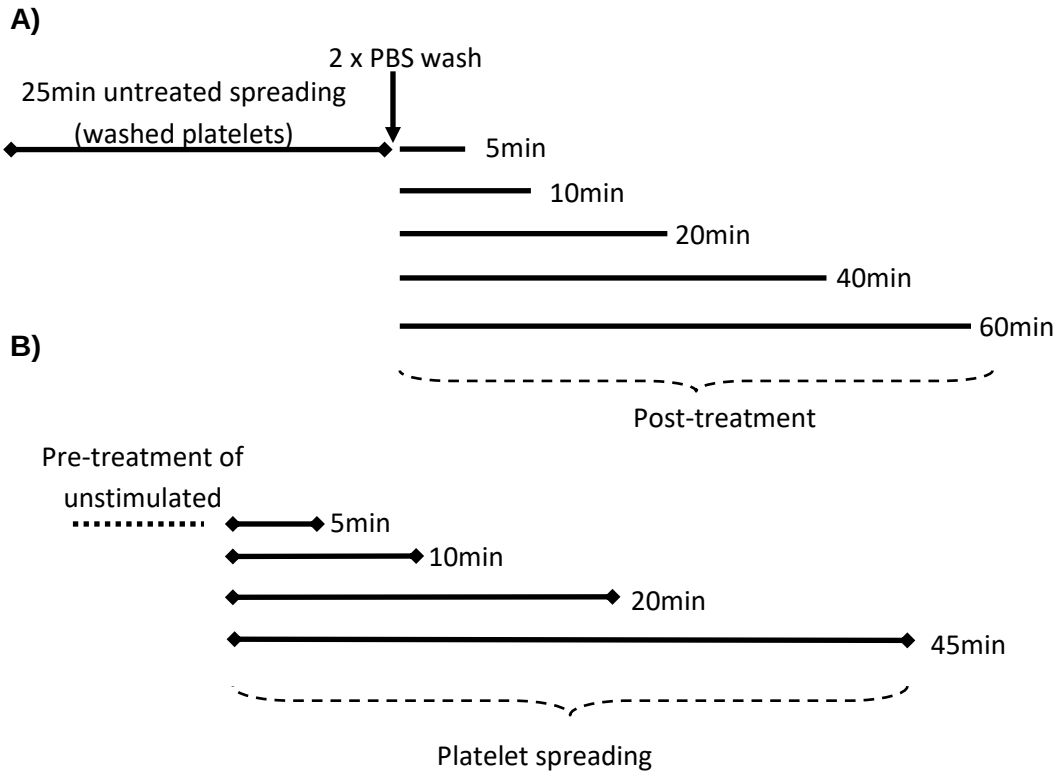

Figure 2.1. Different platelet spreading approaches used within this thesis. A) Post-treatment spreading. *Untreated washed platelets ($2x10^7$ for spreading or $2x10^8$ for lysate preparation) were allowed to spread on matrices of choice for 25 minutes prior to being washed in PBS twice. Adhered platelets were then treated with various compounds and their respective vehicle controls for the times indicated. The diagram provided exemplifies a post-treatment time course. B) Pre-treatment spreading. Platelets ($2x10^7$ for spreading or $2x10^8$ for lysate preparation) were incubated with various compounds prior to being spread on matrices of choice. The diagram exemplifies a pre-treatment time course of spreading, with a fixed incubation time prior to spreading.*

2.3. Protein quantitation via the Precision Red assay

Platelet lysates were generated by using 2x lysis buffer (100mM Tris pH6.8, 4% SDS, 10% glycerol, 2% 2-mercaptoethanol, 10mM EDTA pH8.0, protease inhibitor cocktail (1:100), phosphatase inhibitor (1:100)) on spread platelets and platelets in suspension ($2x10^8$/ml). Protein was quantified immediately using a small sample of the lysates and the remaining lysates were stored at -20^{o}C for later use. Protein quantification was performed using the Precision Red assay kit from Cytoskeleton Inc (Denver, USA). 3µl per lysate were loaded in triplicate onto a 96 well plate and 300µl of Precision Red reagent was added. After allowing the colorimetric reaction to take place, the plate was read at 600nm absorbance on the Tecan M200 plate reader using the i-control software program. To determine the final protein concentration and content in the lysate, the following formula was used according to the manufacturer's guidelines:

Protein concentration (µg/ml) = mean value of triplicates x 125 x100

2.4. SDS-PAGE/Immunoblotting

Platelets ($2x10^8$) were spread according to experimental requirements, lysed and protein quantified as stated above. Lysates were diluted in 4x Laemmli buffer (40% w/v glycerol, 240mM Tris-HCl, 8% SDS, 0.04% bromophenol blue, 5% β-mercaptoethanol, pH6.8) to generate equal protein concentrations among samples and denatured at 95^{o}C for 5 minutes. Samples were then run on a 10% SDS-polyacrylamide gel (table 2.4) at 120v for 90 minutes. Gels were transferred onto PVDF via the Trans-blot turbo blot system with kit-specific blotting buffer (Bio-Rad, Hertfordshire, UK) (2.5A, 25v) for 10 minutes. After transfer, PVDF membranes were allowed to dry for one hour before being reactivated in methanol and blocked for 1 hour in 5% milk in tris buffered saline with 0.1% tween (TBST). Blocked membranes were then incubated with primary antibody overnight in 0.1% TBST (Anti-phospho-VASP (Ser239) rabbit polyclonal 1:1000, Cell Signaling Technology, MA, USA; anti-GAPDH mouse monoclonal 1:6000, Calbiochem (Merck Millipore), Watford, UK; anti-phospho-RhoA (Ser188) rabbit polyclonal, Santa Cruz Biotechnology, Heidelberg, Germany; anti-RhoA mouse monoclonal 1:500, Denver, USA). Membranes were then washed in 0.1% TBST and infra-red secondary antibodies (IRDye 680RD goat anti-rabbit IgG or IRDye

800CW goat anti-mouse IgG (both 1:15000)) were added for one hour with 2% non-fat milk in 0.1% TBST. Membranes were then washed three times in 0.1% TBST for 10 minutes and imaged on the Odyssey-CLx imaging system at either 680nm for rabbit primary-anti-rabbit secondary antibodies or 800nm for mouse primary-anti-mouse secondary antibodies (LI-COR laboratories, Cambridge, UK). Densitometric analysis of banding patterns was automatically performed through the Image Studio Lite software package (ver 5.2).

Table 2.4. Protocol for preparation of 10% SDS polyacrylamide gels

10% Resolving gel	**3% Stacking gel**
6.4mL dH_2O	4.87mL dH_2O
5.3mL bis/acrylamide (20%)	1.87mL bis/acrylamide (20%)
4mL Buffer 1	1.87mL Buffer 2
75µl ammonium persulfate (10%)	75µl ammonium persulfate (10%)
5.3µl TEMED	10µl TEMED

2.5. RhoA activation pull down assay

Knowledge in the protein structure of RhoGTPases and their respective binding partners can be exploited to determine the activation status of the RhoGTPases in response to differing conditions. Among these exploits is their GTP- vs GDP-binding status which determines their activation or inhibition, respectively. GTP binding increases the RhoGTPase's affinity for its binding partners, leading to downstream signalling events, such as increased ROCK activity and stress fibre formation in platelets upon RhoA activation. This increased affinity for binding partners has been used to generate robust purification assays for a number of RhoGTPases, including the detection of GTP-loaded (activated) RhoA (272,276). This assay involves the usage of a highly-specific RhoA substrate, Rhotekin, which preferentially binds with GTP-bound RhoA through its Rho-binding domain (RBD). Immobilisation of rhotekin-RBD onto glutathione agarose beads allows the 'pulling down' of the GTP-RhoA:Rhotekin-RBD:glutathione agarose bead

complex, while leaving unbound GDP-loaded (thus inactivated) RhoA in suspension.

Platelets were allowed to spread on fibrinogen-coated (100µg/ml) 10cm dishes as per the platelet spreading post-treatment protocol and treated with either vehicle, S-nitrosoglutothione (1µM) with and without 1H-[1,2,4]oxadiazolo[4,3-a]quinoxaline-1-one (2µM) for 20 minutes. Adhered platelets were then lysed in kit-specific cell lysis buffer supplemented with protease inhibitor cocktail and snap frozen in liquid nitrogen. Protein quantitation was performed via Precision Red reagent (Cytoskeleton Inc., Denver, USA) with a 96-well plate reader. 50µg of rhotekin-RBD beads (Cytoskeleton Inc., Denver, USA) were loaded with 200µg of protein and agitated for 90 minutes at 4^{o}C. Samples were centrifuged for 1min at 4^{o}C. The resulting supernatant was then discarded and the pellet of beads was resuspended in 400µl kit-specific wash buffer (25mM Tris pH7.5, 30mM $MgCl_2$, 40mM NaCl) and centrifuged again for 3mins at 4^{o}C to remove any unbound GDP-RhoA. The resulting supernatant was discarded and 20µl of 2x laemmli buffer (20% w/v glycerol, 120mM Tris-HCl, 4% SDS, 0.02% bromophenol blue, 2.5% β-mercaptoethanol, pH6.8) was added to the pellets before heating the samples for 5min at 95^{o}C. Samples were run with their respective total RhoA controls (whole cell lysate) though SDS-PAGE and immunoblotting.

2.6. cAMP concentration measurement through ELISA assay

10cm dishes were coated in the matrix protein of choice (100µg/ml and 3µg/ml fibrinogen) overnight at 4^{0}C. These dishes were then washed twice with PBS and blocked using 5µg/ml bovine serum albumin. Platelets ($2x10^8$/ml) were spread for 25 minutes prior to the addition of PGI_2, milrinone, forskolin or vehicle control for either a further 2 or 20 minutes prior to being lysed in 200µl of kit-specific lysis buffer. To compare cAMP levels in platelets in suspension, unstimulated and PGI_2, milrinone and forskolin-treated platelets in suspension ($8x10^8$/ml) were also lysed. After protein quantification to ensure equal loading, cAMP content in platelet lysates was analysed using a cAMP ELISA kit (GE Healthcare - Amersham cAMP Biotrak EIA system). 100µl of lysates from all conditions and the standards provided were transferred into the supplied 96 well plate. A further 100µl of kit-specific antiserum was added to each sample well, gently agitated and incubated at 4^{0}C for 2 hours. 50µl of cAMP-peroxidase conjugate was then

added for a further 60 minutes in the dark at 4^0C. After incubation, each well was completely aspirated and washed four times with kit-specific wash buffer. 150µl of enzyme substrate was then added to each well and incubated for a further hour at room temperature, at which the reaction was terminated using 0.1M sulphuric acid. Plates were then read at 450nm wavelength using the Tecan M200 plate reader and i-control software program. Each sample was read in triplicate and three independent biological repeats were performed to generate mean cAMP content. Sample cAMP concentrations were determined using a calibration curve of standards provided in the kit and expressed as fmol/mg protein.

2.7. In vitro flow microscopy

In vitro flow studies were performed on multichannel microfluidic capillary systems (Vena8 fluoro+, Cellix Ltd, Dublin, Ireland) which had been coated in 300µg/ml fibrinogen or 25µg/ml Horm (equine tendon type I and III) collagen and blocked in 5mg/ml BSA. Whole blood from healthy donors was obtained in PPACK (50µM) and platelets were fluorescently labelled with 3,3'-Dihexyloxacarbocyanine Iodide (10µM) prior to being flowed for 2 minutes at a shear rate of $1000s^{-1}$ (37^oC). Following this initial flow to adhere platelets and form thrombi, buffer only or GSNO (100nM or 1µM) were post-flowed over the adhered platelets for a further 20 minutes prior to fixation with 4% paraformaldehyde. Fixed adhered platelets were permeabilised in 0.1% Triton X-100 and stained with FITC-phalloidin for epifluorescence imaging on the Zeiss Axio Observer (x63 oil immersion objective, 1.4 NA (Zeiss, Cambridge, UK)) via the Zen Pro software package on the same day. Acquired images were analysed using Fiji (275) through Z-stacking for measurement of thrombus height by taking at least 50 0.5µm slices and ensuring that no platelets remain in the upper or lower levels of the acquired stack. Platelet adhesion on fibrinogen-coated channels was manually counted for $50\mu m^2$ per field of view in the upper left-hand corner of each image. Within this quadrant, 25 platelets were circled through the freehand circling function in Fiji. For each condition, 5 images were taken at random.

2.8. Real-time platelet spreading and F-actin visualisation in LifeAct© mice

As platelets have no nucleus and cannot readily be cultured from proliferating megakaryocytes, there is a limited ability for the real-time visualisation of actin

dynamics within the platelet. Although there have been recent advances in actin-binding probes that claim to allow this, they have had only limited success, especially considering the small size of platelets and the need for high resolving probes. To address this, a novel 17-amino-acid peptide called LifeAct has been generated, which specifically labels actin in its filamentous form without dramatically affecting actin dynamics (277). This lack of disruption of actin dynamics is key for its real time visualisation. Typically, phalloidin conjugates are used for F-actin staining, however these 'lock' the actin cytoskeleton in place. The LifeAct peptide can be expressed in mice through transfection, resulting in GFP fluorescence of F-actin in cells and macro-level tissues.

Real-time recordings of F-actin dynamics allows analysis of intensity, movement and occurrence of F-actin events within the platelet. To accomplish this, analysis of video-microscopy recordings of spread LifeAct platelets treated with or without PGI_2 was undertaken. These platelets were first isolated from CO_2 terminally anaesthetised 9- to 12-week old mice through the vena cava and added to 100µl of acid-citrate-dextrose (113.8mM D-glucose, 29.9mM tri-Na citrate, 72.6mM NaCl, 2.9mM citric acid). This was performed by a trained and Home Office licenced member of staff at the University of Birmingham in accordance with UK animal research laws (Animal Act 1986 (Scientific procedures)) and approval through local ethics committee (Birmingham Animal Welfare and Ethical Review Board). PRP was obtained through centrifugation at 200 x g for 6 minutes, upon which 100ng/ml prostacyclin was added and the PRP centrifuged at 1000 x g for a further 6 minutes to obtain a platelet pellet. Pellets were resuspended in modified Tyrodes buffer at $2x10^7$. To obtain a fibrinogen matrix for these platelets to spread on, 100µg/ml fibrinogen was coated onto 35mm glass-bottomed dishes (Mattek, Massachusetts, USA) for 1 hour prior to washing in PBS twice and blocking in 5mg/ml BSA (boiled and filtered). Dishes were then washed twice again in PBS for later use. For the visualisation of platelet spreading, mouse platelets were added to the prepared dishes and imaged in real time using Köhler illuminated Nomarski differential interference contrast optics with a 63x oil immersion lens (1.4NA) on a Zeiss Axiovert 200M microscope (Zeiss, Cambridge, UK). Digital images were captured by a Hamamatsu Orca 285 cooled digital camera (Cairn Research, Kent, UK) using Slidebook 4.0 (Intelligent Imaging Innovations, Inc., Denver, CO, USA).

Platelet suspensions were allowed to interact with the slide until at least one platelet adhered to the field of view for the initiation of autofocus for video clarity. Platelets were allowed to spread in the dishes for 25 minutes prior to treatment with PGI_2 for a further 20 minutes. Due to the disturbance in the dish during addition of the PGI_2 or vehicle control, another field of view had to be recorded as a separate file. Videos obtained from platelet spreading and PGI_2 treatment consisted of repeating 5 second intervals between static images and videos were therefore recorded at 0.2 frames per second framerate.

After video capture, acquired movies were analysed through the Trackmate plugin in the Fiji software package. Blob diameter gating was obtained through earlier nodule analysis in human platelets. To reduce background noise and false positive acquisitions in the analysis, images were thresholded for maximal intensity and quality of fluorescence. Linking distance between video frames was set at 100nm to ensure that movement of nodules between the 5 second image acquisitions was linked and recorded as one nodule and accounted for any possible drifting of the field of view. Nodule characteristics were exported into Excel and reported as nodule lifetime (s) and nodule number over time.

2.9. Statistical analysis

Data obtained was analysed via one- or two-way ANOVA in the Prism6 software package, with statistical significance defined as $p<0.05$. Statistical analysis of two conditions with only one variable were analysed using an unpaired student t test. Post-hoc analysis of data was obtained using Tukey's analysis to determine significance among experimental conditions. For percentage data, arcsine transformation was performed to create standardly distributed data sets which could then be analysed through ANOVA.

Chapter 3.
Effect of nitric oxide on the actin cytoskeleton of spread platelets

3.0. Summary

In *in vitro* conditions, platelets spread on multiple extracellular matrix proteins, including collagens, fibronectins, laminin, fibrin and fibrinogen (74,195,278,279). During this spreading process, platelets drastically reorganise and redistribute actin into actin nodules, filopodia, lamellipodia and stress fibres, which have been shown to be critical for effective platelet function and thrombus formation (103,195,229,239,280). NO has previously been shown to regulate RhoA activity and actin dynamics prior to platelet activation (199). Our group has recently uncovered a role of PGI_2 in reversal of platelet spreading and stress fibres at low concentrations of PGI_2 (273), however as of yet, there has been no reports of the effects of NO on the spread platelet and formed thrombus. Therefore, the aim of this chapter was to investigate the mechanisms by which NO might affect activated spread platelets and how these changes might affect thrombus stability under flow conditions. This work led to the discovery that spread platelets, are susceptible reversal of platelet activation upon NO treatment and that this could underlie the reduction in thrombus formation after treatment with NO.

3.1. Introduction

It has long been established that platelets are inhibited by endogenously derived NO and PGI_2 through activation of PKG and PKA, respectively (199,260,281,282). These activated protein kinases are thought to target similar proteins and generally have the same purpose, possibly acting in a synergistic manner, (201). However, their role during and after thrombus formation is not well understood. It recently been shown that platelets form a thrombus with defined areas of signalling, resulting in greater solute retention within the inner core, whilst the outer shell is more permeable to flowing plasma (76). This indicates that the outer core would be potentially susceptible to inhibition via cyclic nucleotides. In agreement with this, we have previously shown that PGI_2 can reduce thrombus coverage (273). Furthermore, whilst sGC knockout mice have no spontaneous thrombosis, which suggests that NO signalling may not be required for platelet inhibition before thrombus formation (189), sGC knockout platelets produce occlusive thrombi upon vascular damage. This suggest NO is able to regulate the shell of the thrombus limiting thrombus size and aid in its consolidation and/or thrombolysis via inhibition of platelets in the thrombus shell.

A possible mechanism by which NO could inhibit the thrombus shell is via control of the actin cytoskeleton. As platelets encounter subendothelial matrix or adsorbed fibrinogen they rearrange their actin cytoskeleton to help withstand the shear forces within the vasculature. Initially they form finger-like actin projections, termed filopodia. As the platelet spread, punctate patterns of f-actin (actin nodules) form, followed by lamellipodia and finally stress fibres. Actin nodules, lamellipodia and stress fibres have all been implicated in thrombus stability, partly due to the importance of platelet contractility in thrombus formation (195,229,239,283).

Previous research has highlighted that NO can regulate the actin cytoskeleton in several ways, more recently through the regulation of MLC phosphorylation status via inhibition of RhoA (199). The ability for the platelet to regulate its actin dynamics in response to a number of activatory and inhibitory stimuli is essential to platelet function and overall haemostasis. For example, platelets from Wiskott-Aldrich syndrome patients, which lack WASp, are unable to form actin nodules and resultingly are unable to stably adhere, spread and resist even low arterial shear stress (229).

The aim of this project was to determine, if NO can modulate the actin cytoskeleton of spread platelets and if so, by which mechanism(s). This was studied through the use of static platelet spreading assays to identify changes in the actin cytoskeleton, immunoblotting of spread platelet lysates to correlate phenotypic findings, activated GTPase assays to measure the level of activated RhoA, and flow microscopy to identify the effect of NO perfusion on preformed thrombi at arterial shear rate. Through these techniques, I have found that platelets spread on fibrinogen are susceptible to NO-mediated stress fibre reversal through, unlike PGI_2, phosphorylation-independent inhibition of RhoA. This was found to be cGMP-dependent and synergised with low picomolar doses of PGI_2 to further reverse stress fibres and inhibit platelet spreading. The reversal of stress fibres was shown to reduce the height of preformed thrombi under flow conditions, suggesting a role akin to PGI_2 for NO in thrombus consolidation.

3.2. Results

3.2.1. Time-dependency of platelet spreading

To investigate the effect of NO on the spread platelet, an optimal time point for platelet spreading and stress fibre formation had to be determined. This was investigated by allowing platelets to spread for 10, 25, 40 and 60 minutes on immobilised fibrinogen (100µg/ml). Previous research in our lab has identified that the platelets require approximately 25 minutes to maximally spread and form stress fibres (284). As shown in figure 3.1., platelets readily adhere to fibrinogen in a time-dependent manner. Additionally, in agreement with our previous findings, maximal platelet spreading appeared to be reached at the 25 minute time point, with no increase in spread surface area at later times. Also in agreement was the formation of stress fibres, which was most prevalent at the 25-minute time point compared to any other time. Therefore 25 minutes was chosen as the spreading time for further experiments.

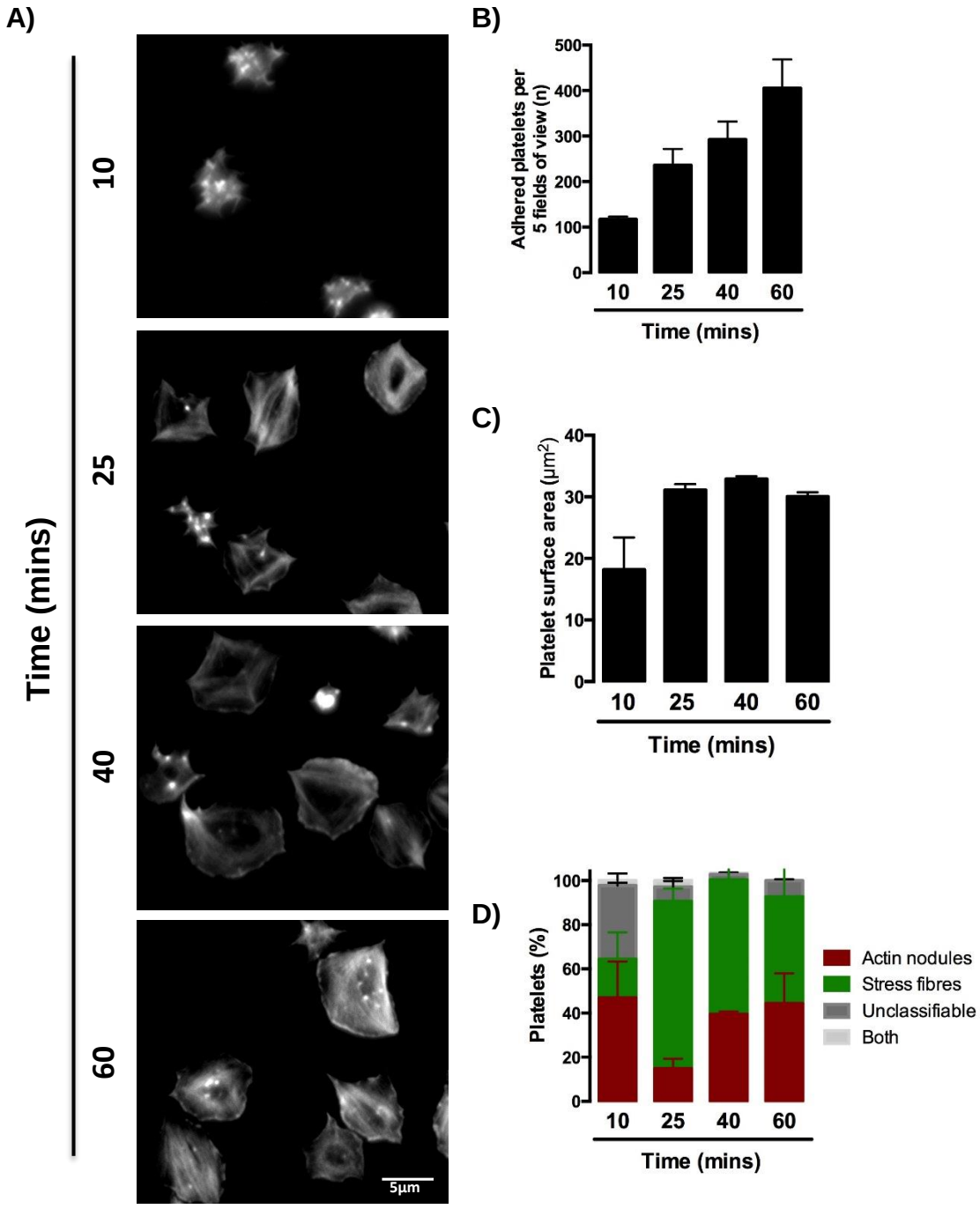

Figure 3.1. Time course of platelet spreading on fibrinogen. *Platelets ($2x10^7$) were allowed to spread on fibrinogen-coated coverslips (100µg/ml) for the indicated times.* ***A)*** *Representative images.* ***B)*** *Platelet adhesion per 5 fields of view.* ***C)*** *Spread platelet surface area of 100 platelets per condition.* ***D)*** *Actin stress fibre and nodule percentages of all platelets within 5 fields of view. Data is representative of two independent repeats, with error bars representing standard deviation. Scale bar represents 5µm.*

3.2.1. Effect of varying concentrations of NO treatment on spread platelets

A platelet's ability to maintain its structural integrity through the actin cytoskeleton is paramount for functional haemostasis. As our group has previously shown that treatment of already spread platelets with PGI_2 leads to a reversal of surface area and actin stress fibres to actin nodules (a reversal to an earlier spreading phenotype) (273), we hypothesised that NO may perform a similar role. We therefore designed a spreading experiment to determine the maximal effect, if any, that NO may have on the spread platelet and its actin cytoskeleton using an F-actin-binding fluorescent dye (FITC/Rhodamine B phalloidin). Initially, platelets were spread for 25 minutes prior to treatment with varying indicated GSNO doses for a further 20 minutes. As demonstrated in figure 3.2., GSNO has no effect on either platelet adhesion or average platelet surface area at any of the concentrations tested. Platelets treated with 0.01 and 0.1µM GSNO did not significantly increase their actin nodule percentages than control platelets, with the levels of actin nodules remaining similar. However, upon treatment of spread platelets with 1 and 10µM GSNO, platelets had a significantly higher percentage of actin nodules. Importantly, there was no statistically significant difference between actin dynamics, surface area or platelet adhesion between treatment with 1µM and 10µM GSNO (p = 0.98), therefore suggesting that 1µM was the maximal dose for future use.

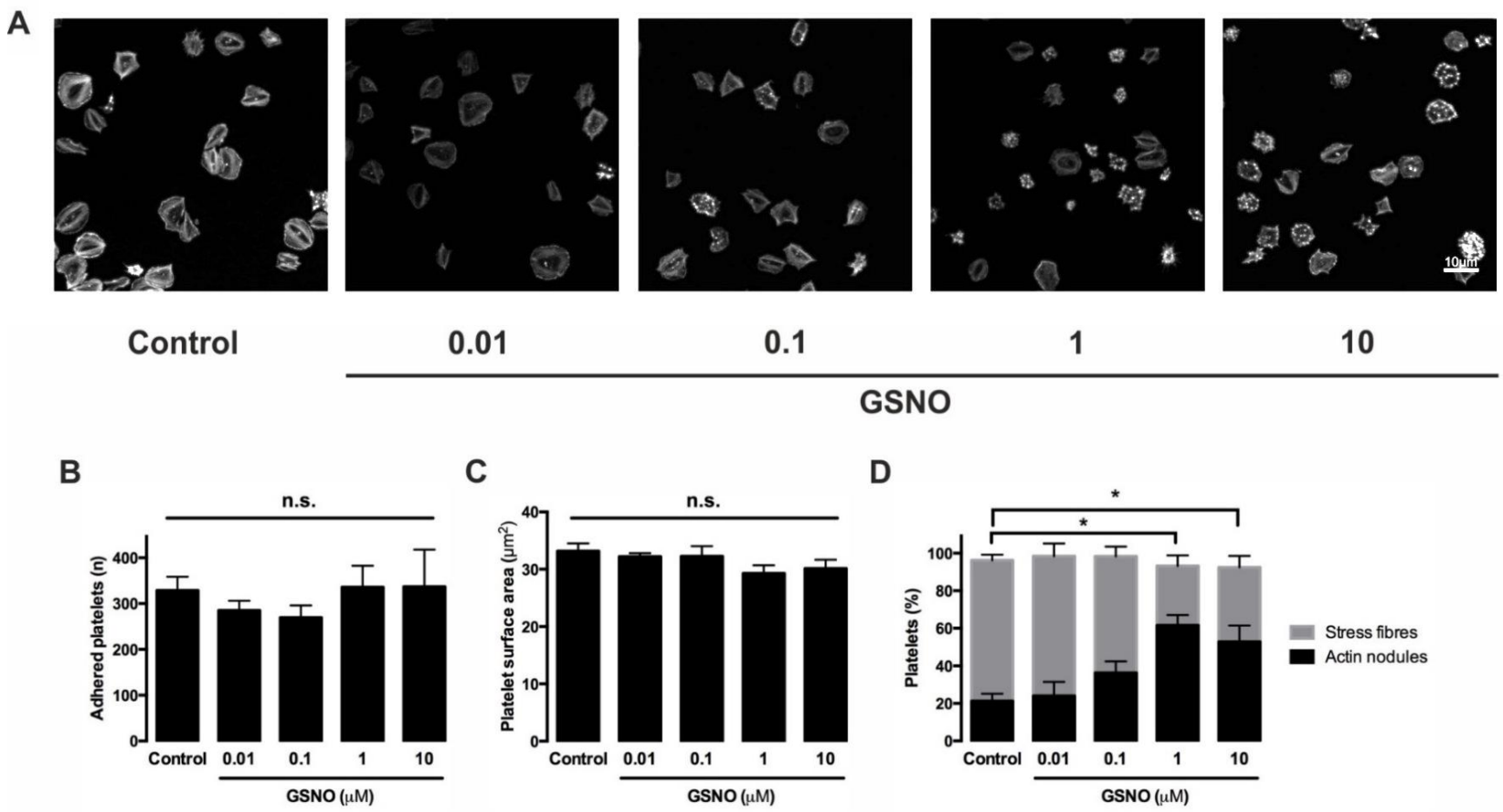

Figure 3.2. Dose-response effect of GSNO on spread platelets. *Platelets were spread on 100µg/ml fibrinogen for 25 minutes prior to treatment with varying concentrations of GSNO (0.01µM, 0.1µM, 1µM and 10µM) for 20 minutes. A) Representative images. B) Number of adhered platelets per five fields of view. C) Average platelet surface area. D) Percentage of platelet positive for stress fibres or actin nodules. Data is representative of three independent repeats with significance defined as p≤0.05. Scale bar represents 10µm.*

3.2.2. Time-dependent effect of NO treatment on spread platelets

After identifying the maximal effect of treatment of GSNO on spread platelets, we next sought to determine its peak temporal effect. The time by which NO has its effect on platelets may indicate its possible utilisation *in vivo* before, during and after thrombus formation. Classically, NO has been viewed as a mild inhibitor which keeps platelets in their quiescent state while flowing in the blood and increases the activation threshold for platelets to overcome in order to initiate thrombosis. Peak time of effect of GSNO on was determined by the treatment of platelets spread for 25 minutes with 1µM GSNO for a further 2-60 minutes. As indicated in figures 3.3. and 3.4., both platelet stress fibres and actin nodules remain at similar percentages in control and GSNO-treated conditions at earlier timepoints. This effect appears to diverge as GSNO exposure time continues, with a significant reduction in platelet stress fibres at 10 minutes and actin nodules at 20 minutes. Due to this discrepancy between actin nodules and stress fibres at these time points, it was decided that a 20-minute GSNO treatment window would be sufficient to show optimal effect for further experiments regarding actin structures. To a similar effect, later treatment timepoints were not chosen for further experiments due to the increased variation in the balance of actin nodules and stress fibres in control conditions.

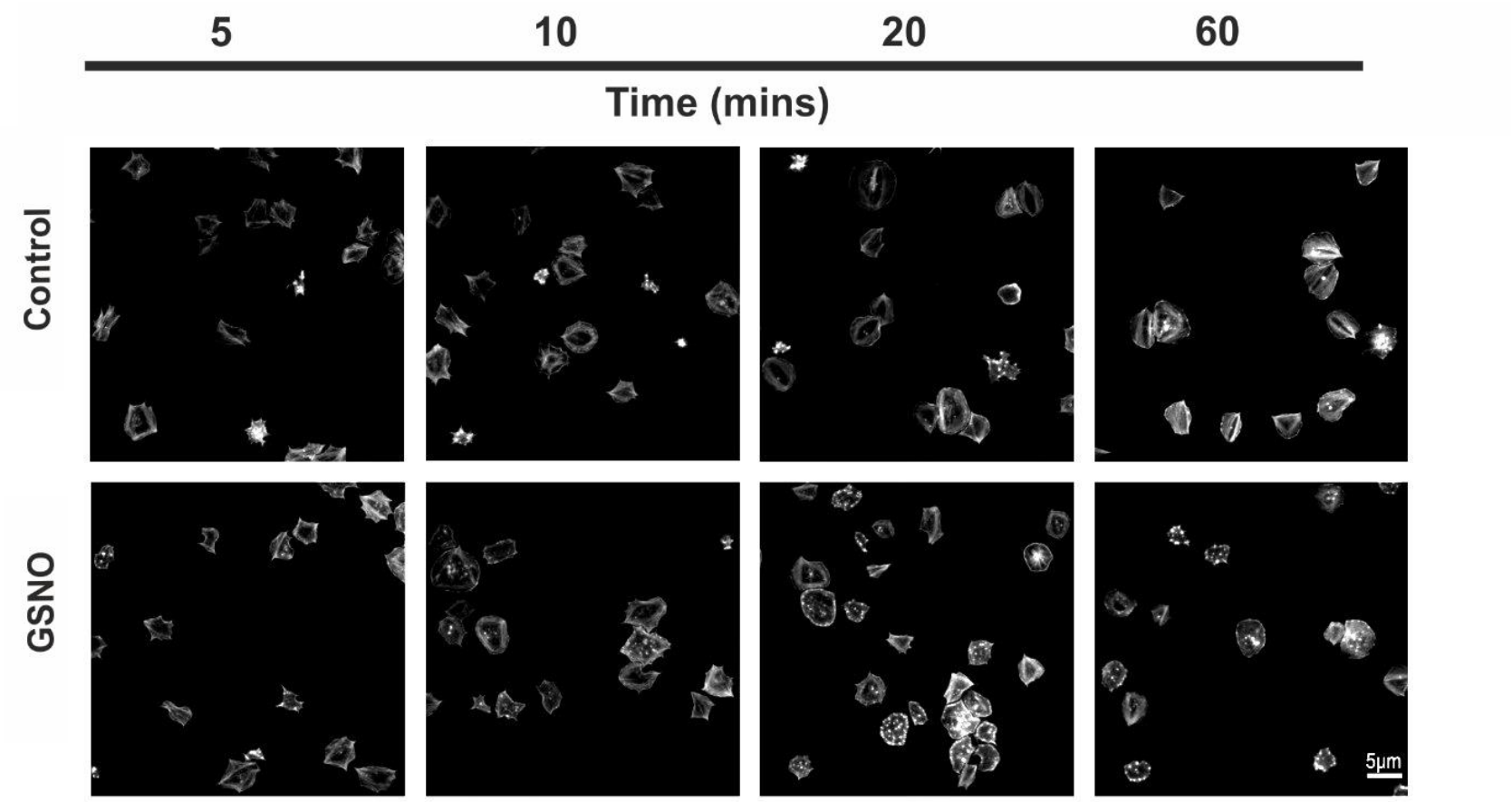

Figure 3.3. Time-dependent effect of GSNO treatment of spread platelets. *Platelets ($2x10^7$) were spread on 100µg/ml fibrinogen coated coverslips for 25 minutes prior to treatment with 10µM GSNO or a vehicle control (Modified Tyrode's buffer) for the times indicated. Platelets were then fixed, permeabilised and stained for F-actin with FITC-phalloidin. Representative images acquired at x63 magnification. Scale bar represents 5µm.*

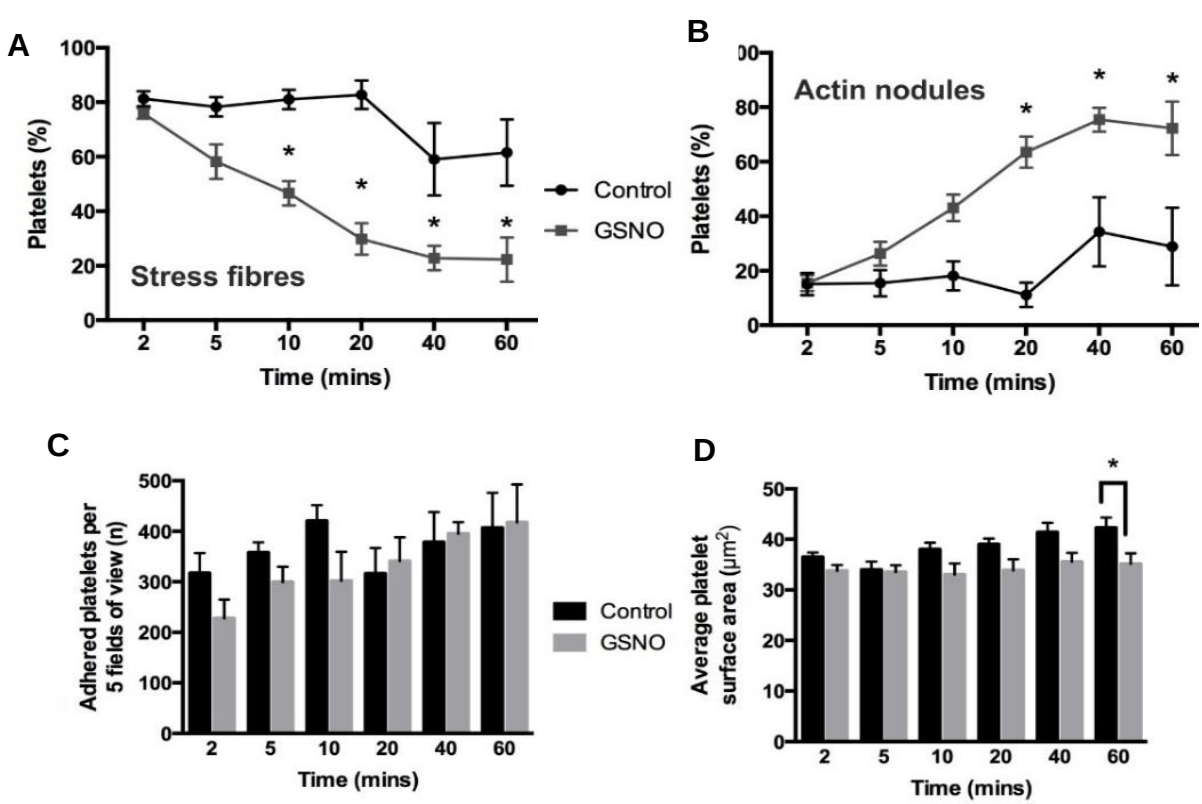

Figure 3.4. Analysis of the time-dependent effect of GSNO treatment on fibrinogen spread platelets. *A) Percentage of platelets positive for stress fibres. B) Percentage of platelets positive for actin nodules. C) Number of platelets adhered per five fields of view. D) Average surface area of 100 platelets per repeat, per experiment. Data is representative of at least 3 individual experiments with significance defined as p ≤ 0.05 (* ≤ 0.05, ** ≤ 0.01, *** ≤ 0.001, **** ≤ 0.0001).*

3.2.3. Platelet reversibility upon treatment with another NO donor (DEANONOate)

Upon demonstrating the ability for GSNO to reverse platelet actin dynamics, the identification if this effect was NO- or GSNO-dependent needed to be undertaken. If this effect was only seen upon GSNO treatment, it would likely be due to the glutathione residue acting via an unknown mechanism, rather than through NO signalling. With this in mind, a similar experiment was performed using an alternative NO donor, DEANONOate (DEANO). Upon treatment of spread platelets with 10µM DEANO for the same 20 minute treatment window as GSNO, platelets reversed their stress fibres and formed actin nodules (figure 3.5). This effect appeared to be stronger than GSNO at maximal dose and also significantly reduced platelet surface area. Like GSNO at all time points and concentrations, DEANO treatment did not lead to a significant reduction in platelet adhesion. These findings suggest that the effect of GSNO on the platelet actin cytoskeleton is linked with NO signalling.

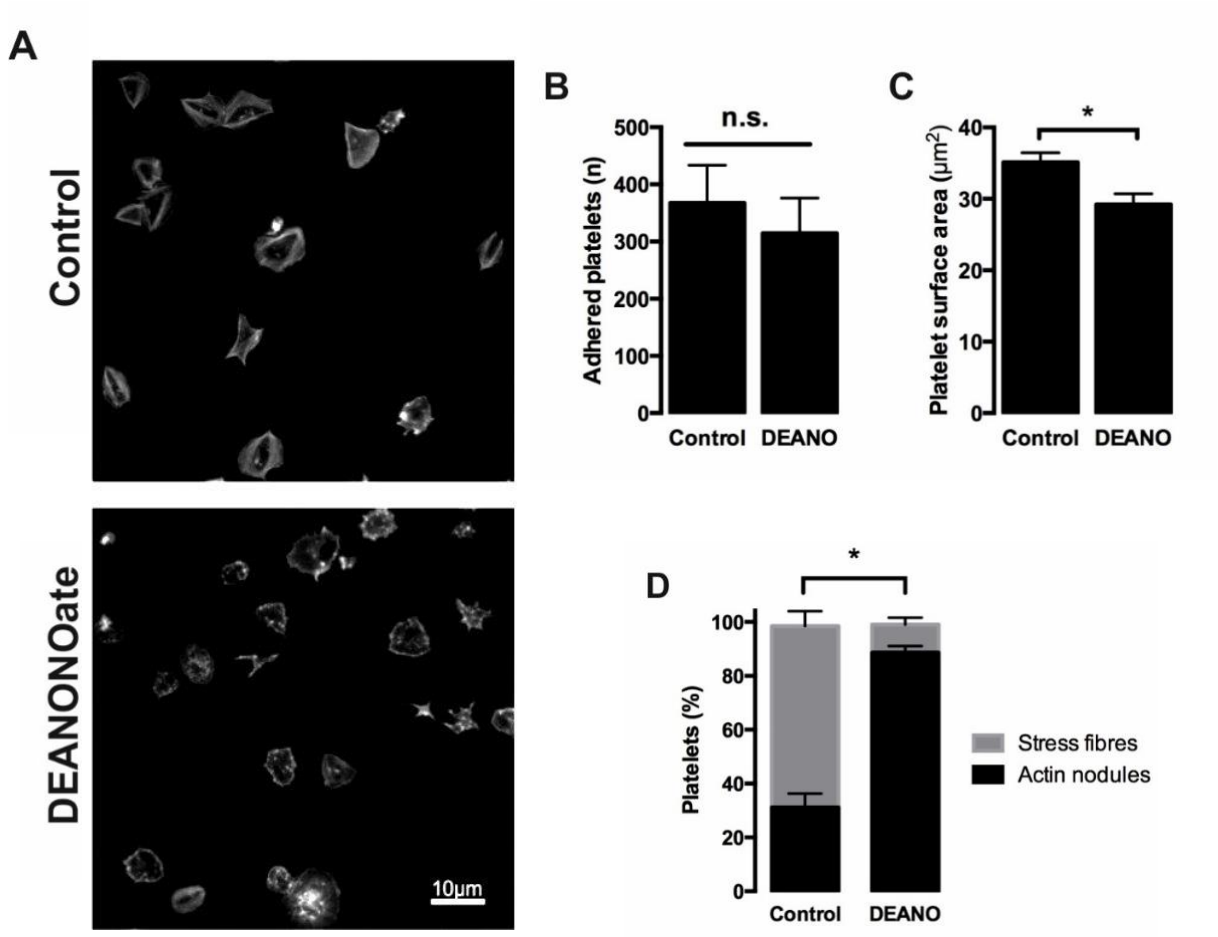

***Figure 3.5. Effect of a second NO donor, DEANONOate, on fibrinogen spread platelets**. **A)** Representative images. **B)** Platelet adhesion per five fields of view. **C)** Average platelet surface area. **D)** Percentage of platelets positive for stress fibres and actin nodules. Data is representative of at least 3 individual experiments with significance defined as $p \leq 0.05$. Scale bar represents 5µm.*

3.2.4. Effect of a PKG-activating cGMP analogue on spread platelets

After identifying the temporal and dose-dependent effects of GSNO and recapitulating the effects with the use of another NO donor, it was necessary to identify the mechanisms by which GSNO acts upon platelets. It was hypothesised that GSNO functions through canonical NO signalling involving activation of sGC, production of cGMP and subsequent activation of PKG. In order to begin to understand the process by which GSNO affects the platelet actin cytoskeleton, a PDE-resistant cGMP analogue, 8-pCPT-PET-cGMP (8-pCPT), was used. Upon treatment of spread platelets with 10µM 8-pCPT for 10 minutes, platelets switched their actin structures from stress fibres to actin nodules (figure 3.6.), as previously observed with GSNO and DEANO. Analogue treatment also led to a proportion of platelets that were unclassifiable in structure and were not included in the actin structure analysis, but were counted for adhesion and surface area measurements. Unlike GSNO but like DEANO, the use of 8-pCPT led to a significant reduction in spread platelet surface area. Similarly, with both donors, 8-pCPT did not lead to a reduction in platelet adhesion. This data indicates that the observed effect of NO donors on the platelet actin cytoskeleton is through cGMP signalling.

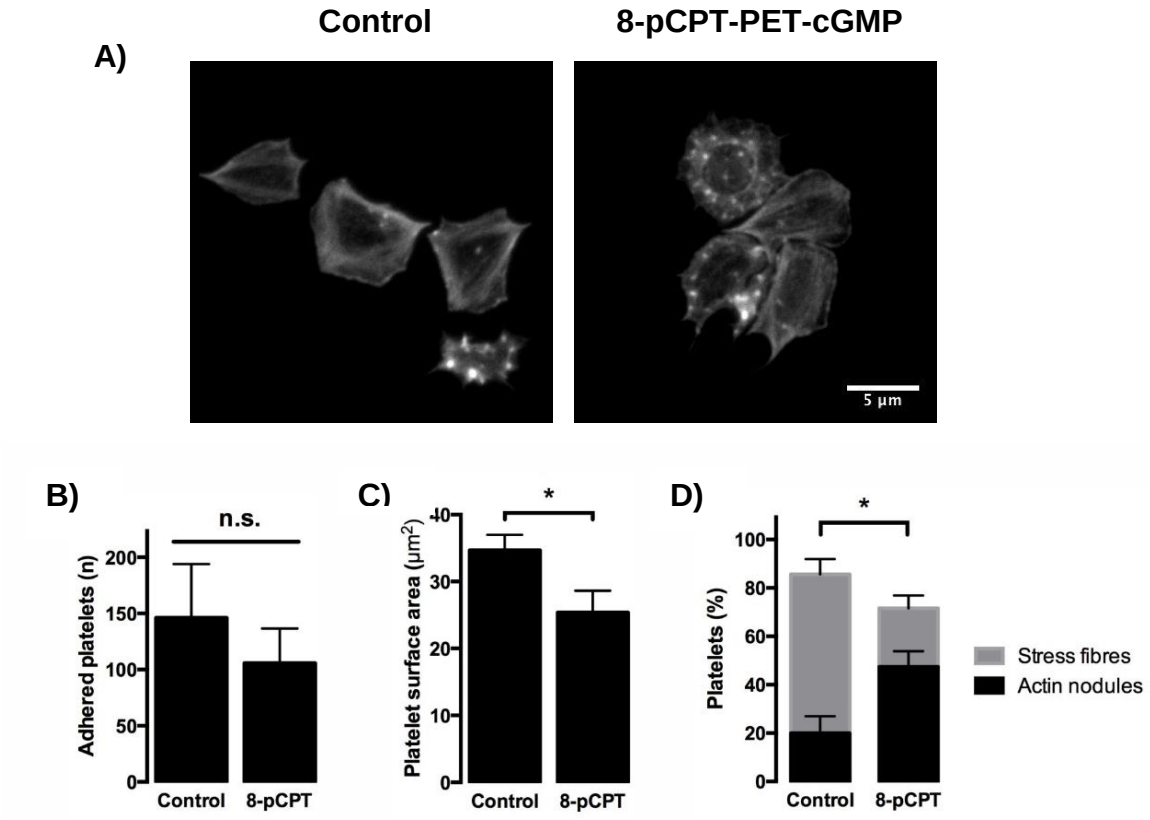

Figure3.6. Effect of PKG activation through a cGMP analogue on spread platelets. *Platelets (2x10^7/ml) were spread for 25 minutes prior to treatment with 10µM 8p-CPT-PET-cGMP or a DMSO control (0.1%) for a further 20 minutes.* ***A)*** *Representative images* ***B)*** *Platelet adhesion per five fields of view.* ***C)*** *Average platelet surface area.* ***D)*** *Percentage of platelets positive for stress fibres and actin nodules. Data is representative of at least 3 individual experiments with significance defined as p ≤ 0.05. Scale bar represents 5µm.*

3.2.5. Investigation into the role of secondary mediators ADP and TXA_2 on NO-mediated stress fibre reversal

Upon platelet activation, platelets release their granule contents as an auto- and paracrine signalling mechanism in order to bolster their activation and attract other platelets to join the growing thrombus. Among these granule contents is ADP and TXA_2. Antagonism of TXA_2 and ADP through cyclooxygenase and $P2Y_{12}$ receptor inhibition via aspirin and purinergic receptor inhibitors such as Ticagrelor, respectively, has been a boon for antithrombotic therapy over the last few decades (285,286). As ADP and TXA_2 increase the activation status of platelets, it was required to identify the effect of NO on ADP- and TXA_2-mediated signalling. If inhibition of these signalling processes led to a similar phenotype as seen with NO, then perhaps NO affects the cytoskeleton in a more indirect mechanism by merely decreasing the activation status of the platelet, allowing it to return to an earlier spreading point. To investigate the role of ADP and TXA_2 signalling and their inhibition of platelets, the ADP-catalysing enzyme, apyrase, and the COX-1 inhibitor, indomethacin, were used. Upon preincubation and post-treatment with 2U/mL ADP and 10µM indomethacin, platelets were significantly inhibited in their adhesion to the fibrinogen matrix when compared to control platelets or those post-treated with GSNO (Figures 3.7. and 3.8.) This inhibition was maintained, but importantly not compounded in the additional presence of 1µM GSNO, with similar platelet adhesion among all samples treated with apyrase and/or indomethacin. Like previous experiments, platelet surface area in response to GSNO treatment alone did not significantly reduce platelet surface area. This lack of inhibition of surface area was also seen in platelets treated with apyrase and/or indomethacin. Interestingly, combined treatment with apyrase and GSNO led to a significant reduction in platelet surface area. This reduction was also maintained upon addition of indomethacin. Independently or in combination with GSNO, indomethacin did not induce a significant reduction in surface area. Platelet actin structures in response to GSNO showed the typical increase in actin nodules and a concomitant decrease in stress fibres. This effect was maintained even in the presence of apyrase, indomethacin or both, with a strikingly similar phenotype to platelets treated with GSNO alone. This data indicates that the modulation of the platelet actin cytoskeleton in response to GSNO is not dependent on secondary mediator signalling.

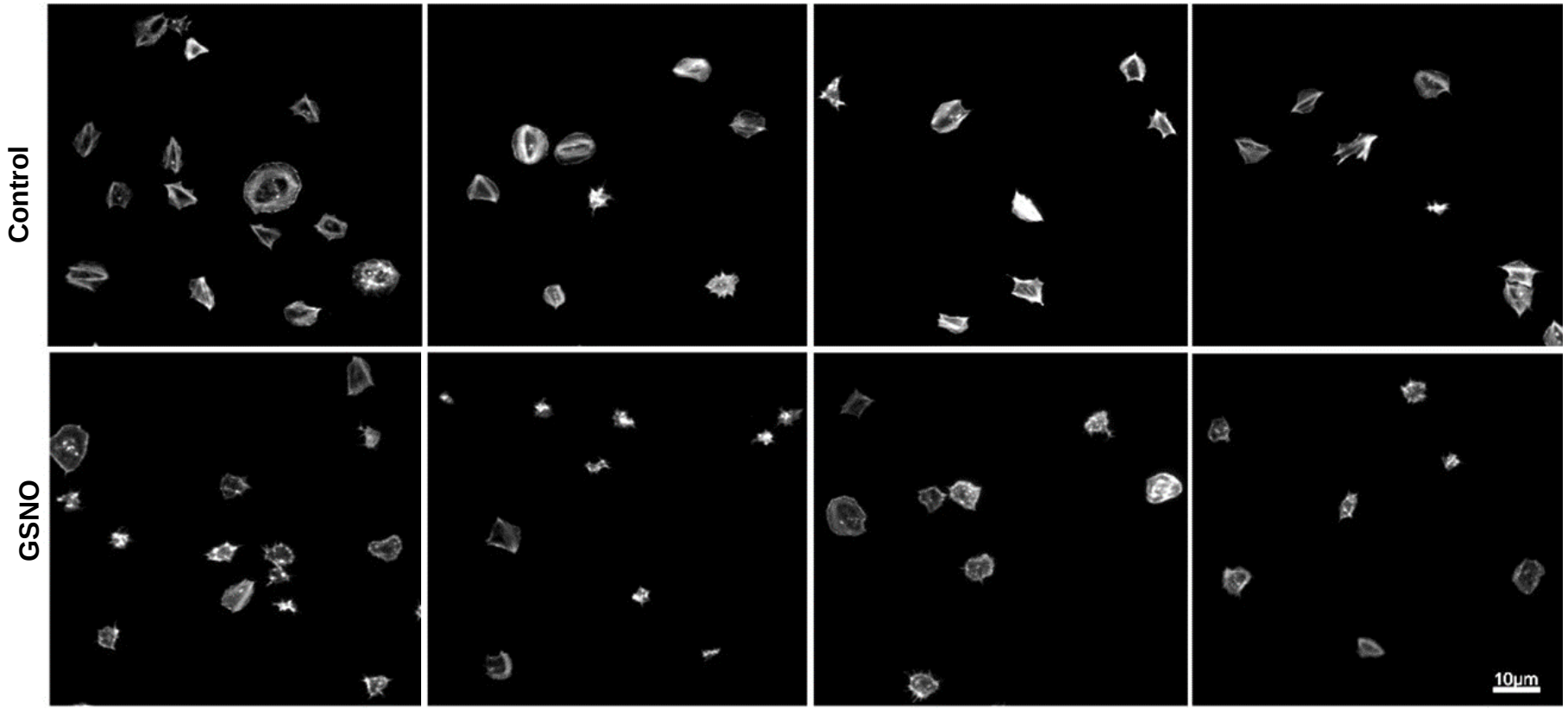

Figure 3.7. Representative images demonstrating the effect of secondary mediator inhibition on NO-induced stress fibre reversal in spread platelets. *Platelets were preincubated with apyrase (2U/ml), indomethacin (10µM), Both, or control (0.1% DMSO) for 10 minutes prior to being spread on 100µg/ml fibrinogen for 25 minutes, where control buffer or GSNO (1µM) was added in the presence or absence of further apyrase, indomethacin or both at the same previous concentrations. Platelets were then fixed, permeabilised and stained for F-actin with FITC-phalloidin. Representative images acquired at x63 magnification. Scale bar represents 10µm.*

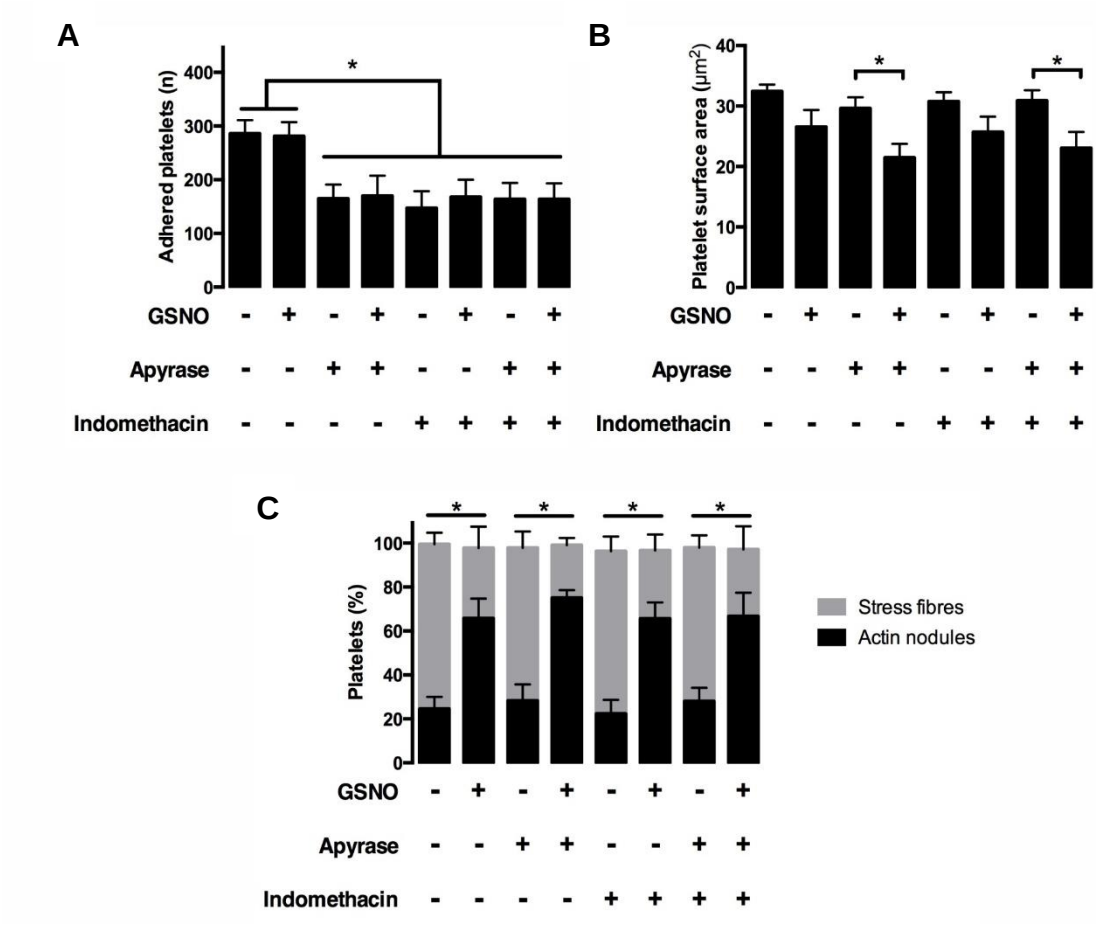

Figure 3.8. Analysis of the effect of secondary mediator inhibition on NO-induced stress fibre reversal in spread platelets. A) *Number of platelets adhered per five fields of view.* ***B)*** *Average platelet surface area.* ***C)*** *Percentage of platelets positive for stress fibres and actin nodules. Data is representative of 4 independent experimental repeats, with significance defined as p≤0.05.*

3.2.6. Effect of sGC inhibition on NO-treated spread platelets

In previous experiments, the effect of a cGMP analogue led to a similar phenotype of spread platelets treated with GNSO. This suggested that the reversal of the actin cytoskeleton is linked with cGMP signalling. As cGMP production in platelets is dependent on sGC activation, an experiment was designed to identify the phenotypic and signalling effects of sGC inhibition on spread platelets. This was done by utilising the small molecular inhibitor of sGC, ODQ. As can be seen in figure 3.9., treatment of platelets with 2µM ODQ led to an inhibition of GNSO-mediated cytoskeletal regulation. Platelets treated with GSNO alone demonstrated the typical stress fibre to actin nodule switch, however upon co-treatment with ODQ, this effect was completely abolished. Importantly, treatment of spread platelets with ODQ alone did not affect platelet adhesion, spreading or actin structures. Under these conditions, platelets treated with GSNO have significantly higher levels of phosphorylated $VASP^{ser239}$, a marker of PKG activation, than control platelets (figure 3.10.). In accordance with the spreading data, platelets treated with both GSNO and ODQ had similar $pVASP^{ser239}$ levels to control platelets, indicating that the effect of GSNO had been prevented/abolished. These data indicate that the effect of NO on the spread platelet actin cytoskeleton is sGC-dependent and results in robust PKG activation.

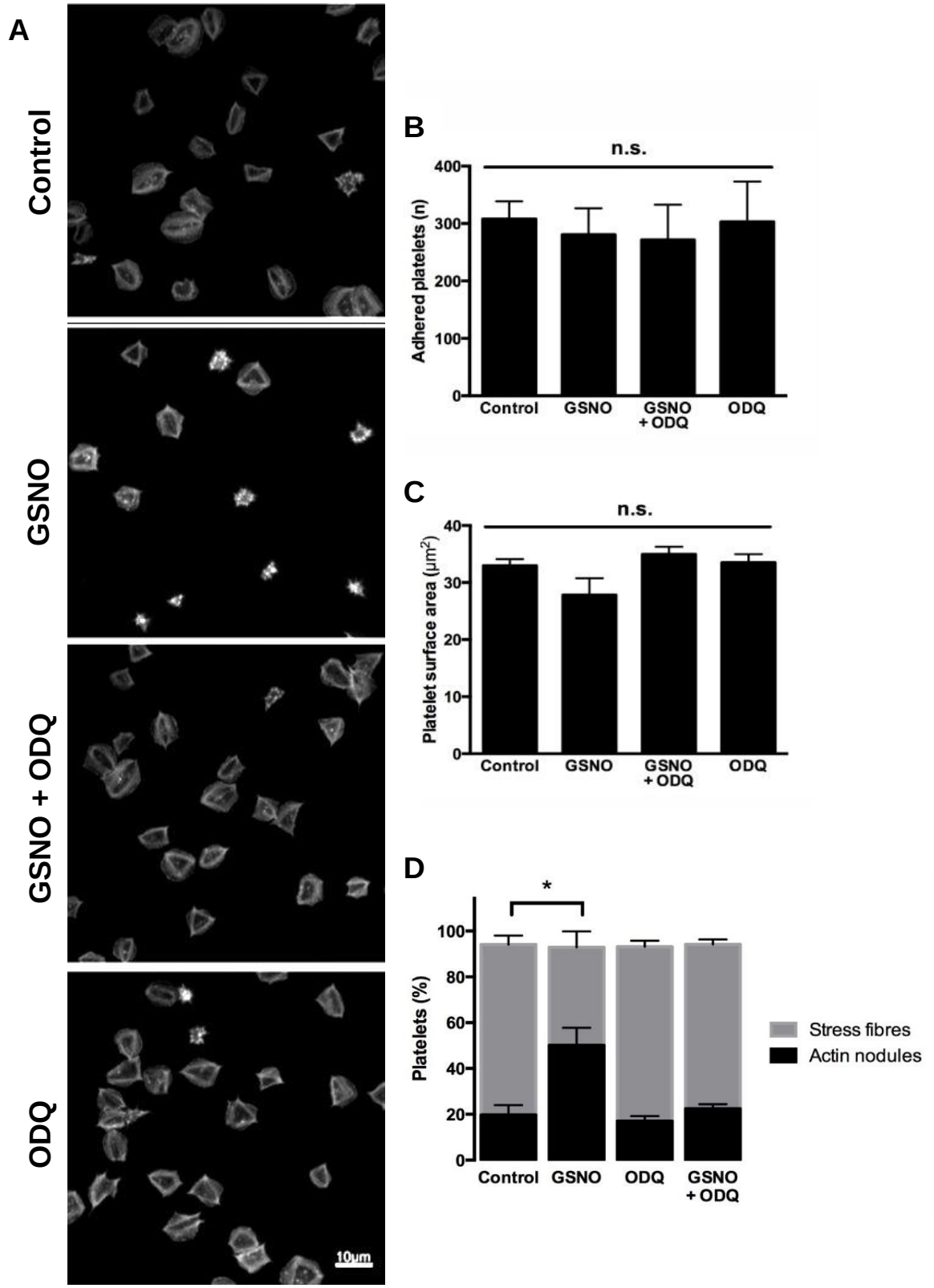

Figure 3.9. Effect of sGC inhibition on GSNO-mediated platelet stress fibre reversal. *Platelets were spread for 25 minutes on 100µg/ml fibrinogen prior to treatment with vehicle (0.1% DMSO) or GSNO (1µM) in the presence or absence of ODQ (2µM) for a further 20 minutes.* ***A)*** *Representative images.* ***B)*** *Platelet adhesion per five fields of view.* ***C)*** *Percentage of platelets positive for stress fibres or actin nodules. Data is representative of three independent repeats, with significance defined at p≤0.05. Scale bar represents 10µm.*

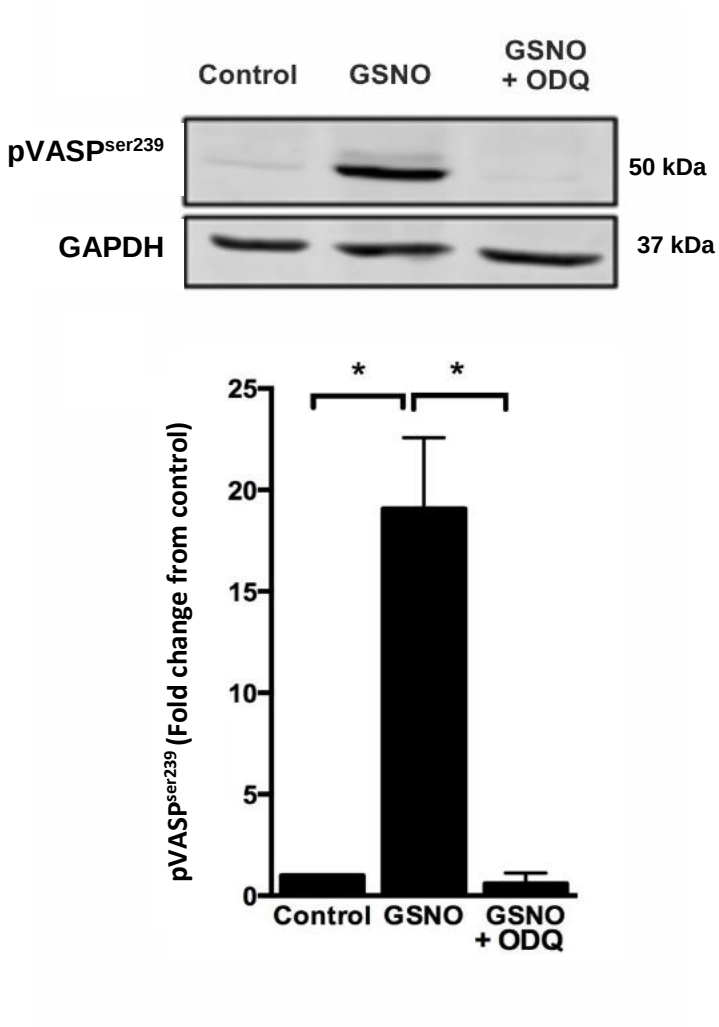

Figure 3.10. VASPser239 phosphorylation in response to GSNO treatment in the presence or absence of a sGC inhibitor. *Platelets were spread on 100µg/ml fibrinogen adsorbed 10cm dishes for 25 minutes prior to the addition of GSNO (1µM) in the presence or absence of the sGC inhibitor, ODQ (2µM) for a further 20 minutes before lysis. Lysates were equally loaded onto SDS polyacrylamide gels and probed for $pVASP_{ser239}$ and GAPDH.* ***A)*** *Representative immunoblot of $pVASP^{ser239}$ with GAPDH used as a loading control.* ***B)*** *Cumulative data obtained from immunoblotting. Data is representative of 3 independent repeat experiments, with significance defined as $p \leq 0.05$.*

3.2.7. Signalling mechanisms involved in NO-mediated spread platelet inhibition

After identifying that NO modulates the platelet actin cytoskeleton through a sGC:cGMP:PKG mechanism, the mechanism(s) by which PKG can cause this effect were investigated. Considering that our group has previously shown that PKA can reverse platelet stress fibres through phosphorylation and inhibition of RhoA, it was hypothesised that NO was targeting this pathway also. RhoA inhibition leads to a reduction in ROCK activation, which would otherwise phosphorylate and inhibit MLCP (272) as MLCP is left constitutively active, it can dephosphorylate MLC at will and thus limit the potential for actin-myosin interactions, leading to limited platelet contractility. To test this hypothesis, spread platelets were treated with the ROCK inhibitor, Y-27632. Upon treatment with Y-27632, platelets significantly reversed their stress fibres into actin nodules, as observed with treatment of NO donors or PKG-elevating agents. Shown in figure 3.11., like GSNO, Y-27632 did not induce a reduction in platelet adhesion, nor did it affect mean platelet surface area. This data suggested that the effect of NO signalling on the platelet actin cytoskeleton likely was through inhibition of the RhoA pathway.

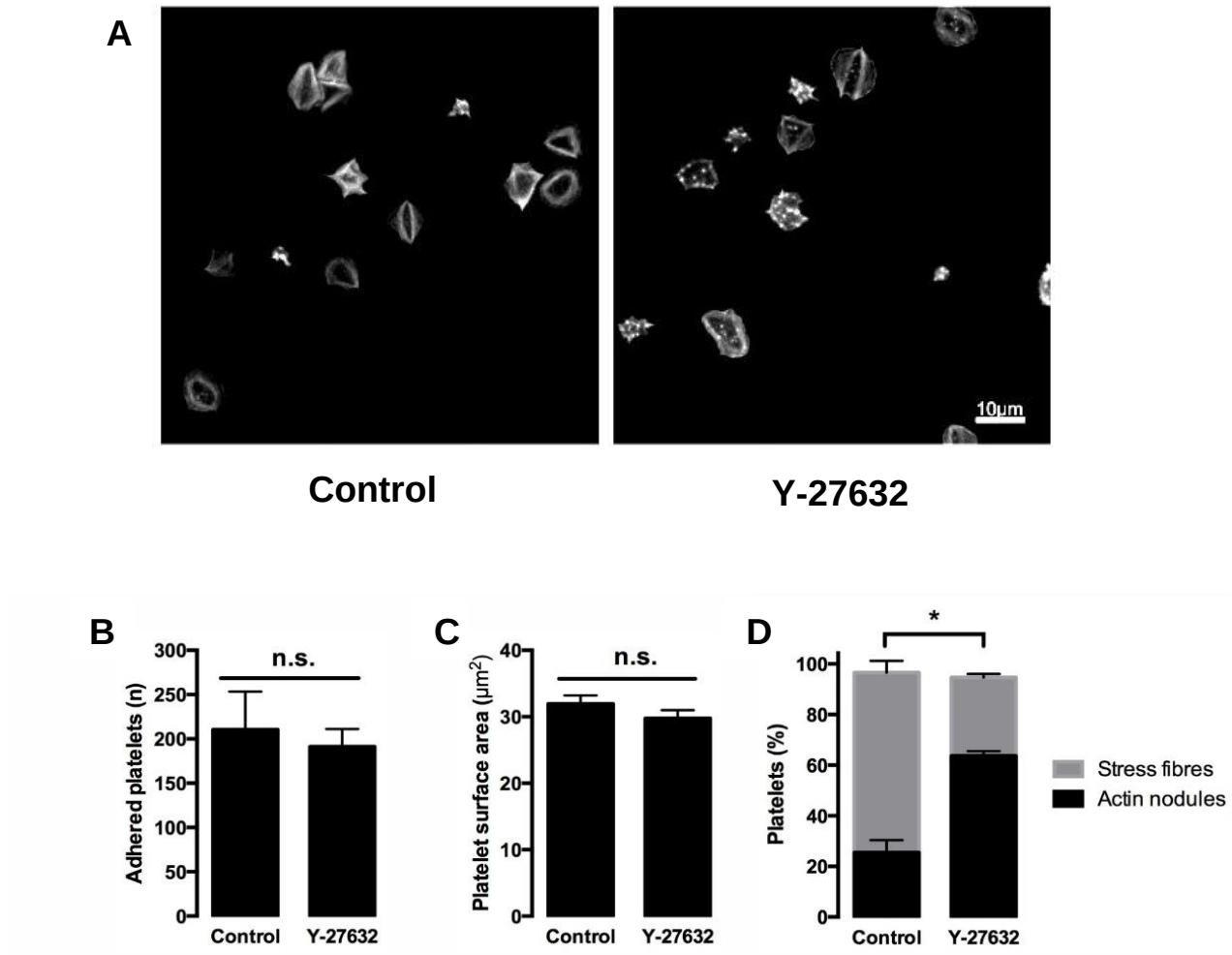

Figure 3.11. Effect of ROCK inhibition in spread platelets. *Platelets were spread on 100µg/ml fibrinogen for 25 minutes before being treated with vehicle (0.1% DMSO) or 10µM Y-27632 for 20 minutes.* ***A)*** *Representative images.* ***B)*** *Platelet adhesion observed from five fields of view per experimental condition, per experiment.* ***C)*** *Average platelet surface area.* ***D)*** *Percentage of platelets positive for stress fibres and actin nodules. Scale bar represents 10µm. Images and data are representative of three independent repeat experiments. Significance was defined as p≤0.05. Scale bar represents 10µm.*

The Y-27632 spreading data suggested that NO may be exerting its effects through the inhibition of the RhoA pathway. To further investigate this, spread platelet lysates were made from platelets in suspension (basal), platelets spread on fibrinogen (control), and platelets spread on fibrinogen ± GSNO and ODQ. These samples were then analysed for activated RhoA via a pulldown assay, which purifies GTP-loaded and thus activated RhoA. As shown in figure 3.12., basal platelets in suspension have little activated RhoA compared to spread platelets (control), which have approximately three-fold higher RhoA levels. Upon treatment of spread platelets with GSNO for 20 minutes, GTP-RhoA levels significantly drop to levels seen in basal platelets. Importantly, treatment of platelets with ODQ and GSNO results in similar GTP-RhoA levels, thus corroborating previous findings. This data indicates that GNSO inhibits RhoA activity in spread platelets and that this is dependent on sGC activity. As PGI_2 has previously been shown to phosphorylate RhoA and thus reduce its activity, it was hypothesised that NO would also phosphorylate RhoA at serine188. Using spread platelet lysates with the indicated conditions, there was a clear lack of $pRhoA^{ser188}$ in response to GSNO treatment compared to PGI_2 treatment (figure 3.13.). This was unexpected, and to validate these findings, PGI_2 treatment of spread platelets was also used as a positive control. As can be seen, under the same experimental conditions, using the same antibody, there was significant $RhoA^{ser188}$ phosphorylation in platelets treated with PGI_2, but not in GSNO-treated platelets. Together, these data suggest that GSNO causes a reduction in spread platelet RhoA levels, however this is independent of $pRhoA^{ser188}$ status.

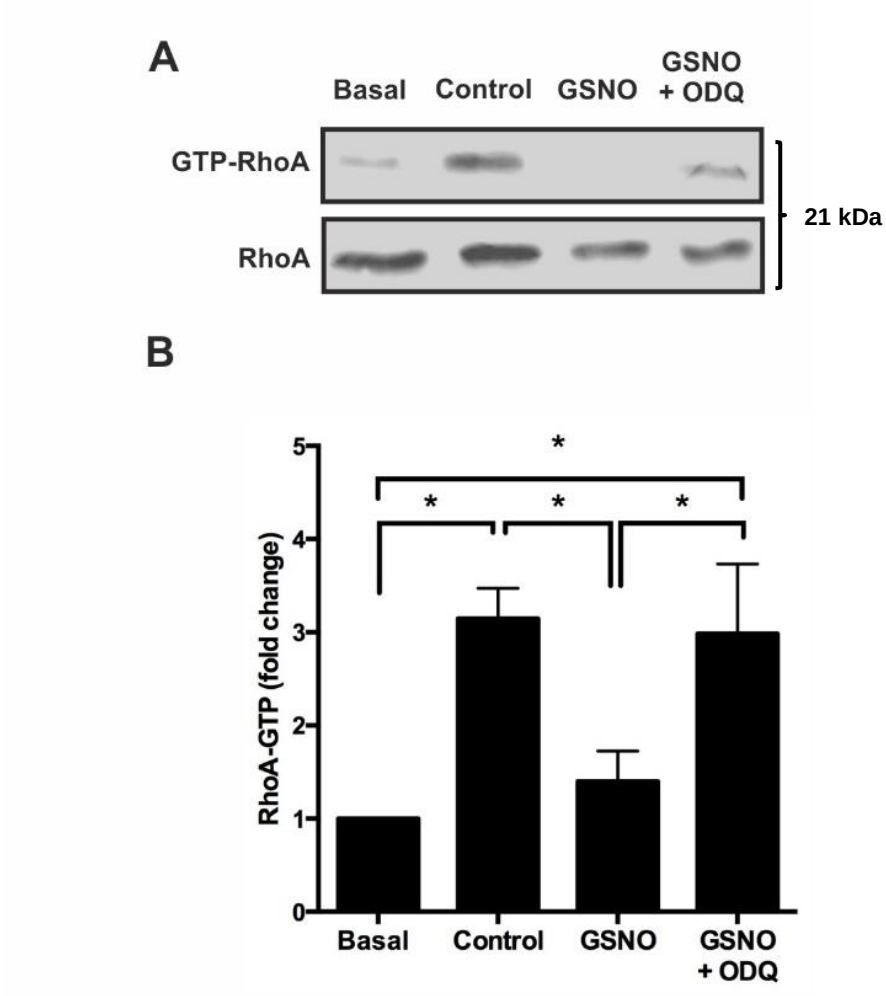

Figure 3.12. GTP-RhoA levels in platelets treated with or without GSNO in the presence or absence of a sGC inhibitor. *Platelets were spread on 100µg/ml fibrinogen adsorbed 10cm dishes for 25 minutes prior to treatment with vehicle (control (0.05% DMSO)) or GSNO (1µM) in the presence or absence of 2µM ODQ for a further 20 minutes. Lysates were collected and a Rhotekin lure was used to isolate the fraction of activated RhoA in each condition. Isolated GTP-RhoA was the ran under standard SDS-PAGE and probed for total RhoA. Whole cell lysate was used as a loading control.* ***A)*** *Representative immunoblot.* ***B)*** *Densitometric analysis of banding obtained, with data represented as fold change over basal. Data is expressed as mean with S.E.M and is representative of 4 independent repeats with significance defined as p≤0.05.*

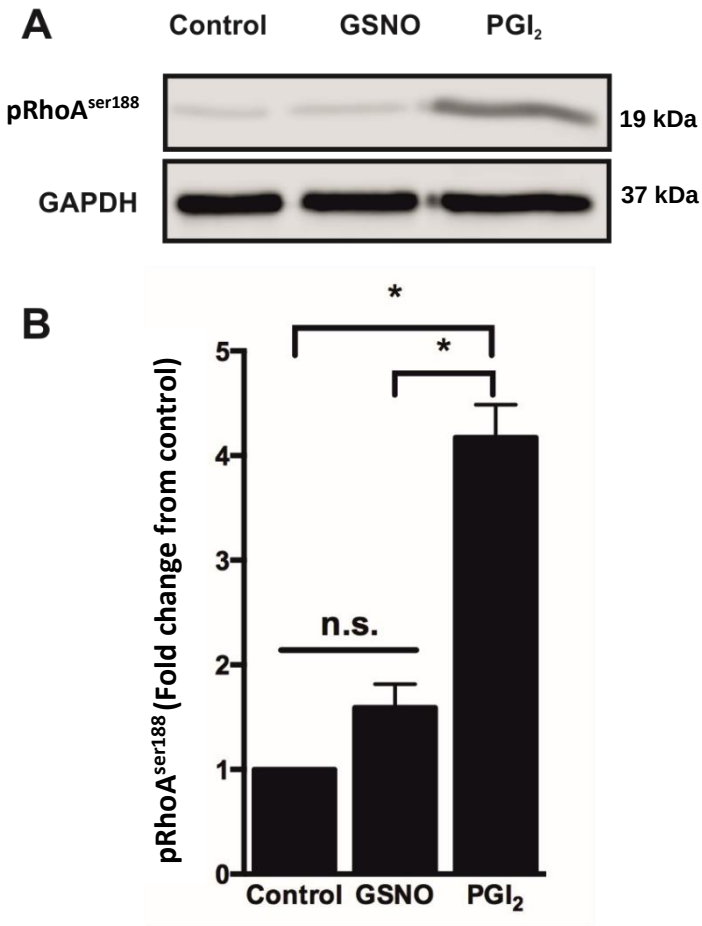

Figure 3.13. Phosphorylation of RhoA at serine 188 in response to NO and PGI_2 treatment of spread platelets. *Platelets were spread on 10cm dishes adsorbed with 100µg/ml fibrinogen for 25 minutes before treatment with a vehicle control (0.005% PGI_2). NO (1µM) or PGI_2 (10nM). Platelets were then lysed, ran under SDS-PAGE and immunoblotted for pRhoAser188.* ***A)*** *Representative immunoblot.* ***B)*** *Densitometric analysis of banding obtained, with data represented as fold change over basal. Data is representative of four independent repeats with significance defined as p≤0.05.*

3.2.8. Synergism of NO and PGI_2 on the spread platelet actin cytoskeleton

Previous literature has shown that PGI_2 and NO can synergise at very low concentrations (287). The data highlighted in figures 3.16. and 3.17., as well as previous work from our lab indicated that platelet actin can be modulated through phosphorylation of RhoA upon treatment with PGI_2, but RhoA can be reduced by $pRhoA^{ser188}$-independent mechanisms in platelets treated with NO (273). Therefore, it was hypothesised that NO and PGI_2 synergistically act on the RhoA pathway through different mechanisms. To investigate this, spread platelets were treated with very low physiologically appropriate concentrations of NO and/or PGI_2. As shown in figure 3.14., control platelets spread on fibrinogen, like previously, formed stress fibres, with a minority of actin nodule-positive platelets. This was a similar finding with treatment of platelets with 10nM NO or 300pM PGI_2. Similarly, platelet surface area was also unchanged between control, NO-treated and PGI_2-treated platelets. Strikingly, co-treatment with the same concentrations of NO and PGI_2 resulted in a significant increase in the percentage of platelets positive for actin nodules, and a significant decrease in the number of stress fibres, indicating that these platelets had reversed their actin structures to an earlier spreading phenotype. Additionally, platelets treated with this combination significantly reduce in surface area. Importantly, the effect of co-treatment with NO and PGI_2 on actin structures and surface area was not only significant compared to control platelets, but also singular NO or PGI_2 treatments. This data indicates that NO and PGI_2 synergise to regulate the spread platelet actin cytoskeleton and spreading dynamics.

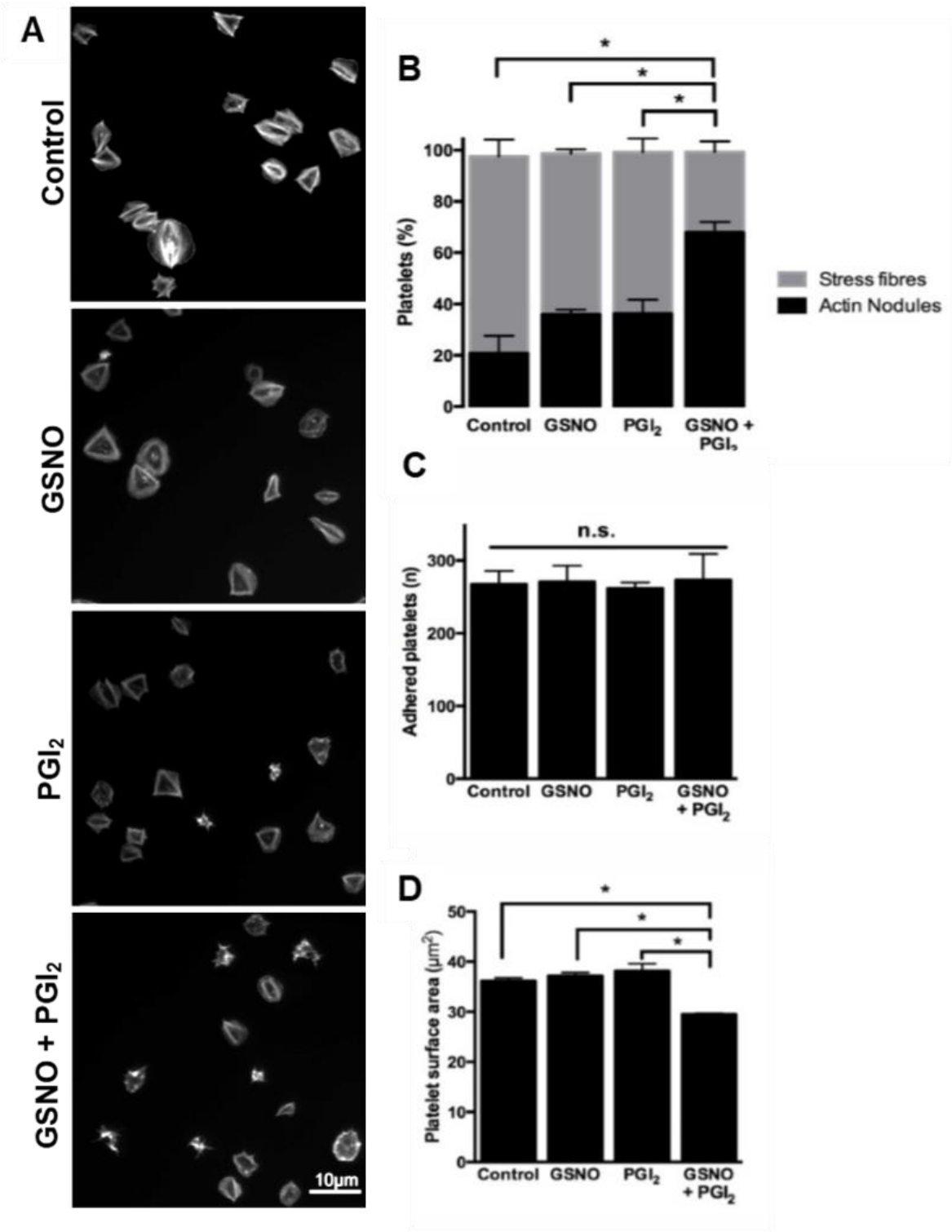

Figure 3.14. Synergism between GSNO and PGI_2 on the spread platelet actin cytoskeleton. *Platelets were spread on 100µg/ml fibrinogen for 25 minutes prior to treatment under control conditions, 10nM GSNO, 300pM PGI_2 or both GSNO and PGI_2 for a further 20 minutes.* ***A)*** *Representative images taken at 630x magnification.* ***B)*** *Percentage of platelets positive for stress fibres and actin nodules.* ***C)*** *Number of adhered platelets per five fields of view obtained.* ***D)*** *Average platelet surface area. Data is representative of 3 independent repeats, with significance defined as p≤0.05. Scale bar represents 10µm.*

3.2.9. Effect of GSNO on thrombus sustenance under flow

Platelets must be able to withstand shear stress within the vasculature during thrombus formation. This, in part, is provided by the actin cytoskeleton by linking activated integrins with F-actin and actin-myosin interactions. As previous experiments have helped identify that NO signalling can reduce intraplatelet RhoA activity, it was hypothesised that platelets within a preformed thrombus would be unable to withstand arterial shear upon exposure to NO. Therefore, anticoagulated whole blood was flowed over collagen-coated microfluidic channels to form thrombi for 2 minutes, after which GSNO or buffer + vehicle was perfused through the thrombi at the same arterial shear rate. Initially, 1µM GSNO was only used, as this had been the concentration used in previous spreading experiments. However, due to the addition of shear stress into the experimental conditions, a lower concentration of 100nM GSNO was also used, as the act of flow may exacerbate any effects on the thrombus stability. As shown in figure 3.15., platelets readily form thrombi on collagen matrix at $1000s^{-1}$ shear. Upon treatment with buffer + vehicle (PBS), thrombi that are formed have a height of 17.4 ± 0.94µm and a surface coverage of 17.9 ± 1.29%, thus indicating that the platelets are forming three-dimensional thrombi. Upon post-perfusion of preformed thrombi with GSNO at both 1µM and 100nM for 20 minutes, thrombus height was significantly reduced compared to control conditions. Interestingly, there was no difference in thrombus height between GSNO-treated thrombi at these two different concentrations. Although thrombus height was reduced upon GSNO treatment, the underlying thrombus foundations, in the form of platelet surface coverage, remained unaffected in all conditions. It is of note that the thrombus structure in platelets treated with GSNO at both concentrations appeared phenotypically different compared to control thrombi. Thrombi treated with GSNO showed a streakier appearance in alignment with the direction of flow. This data indicates that GSNO can reduce the height of preformed thrombi on collagen *in vitro*.

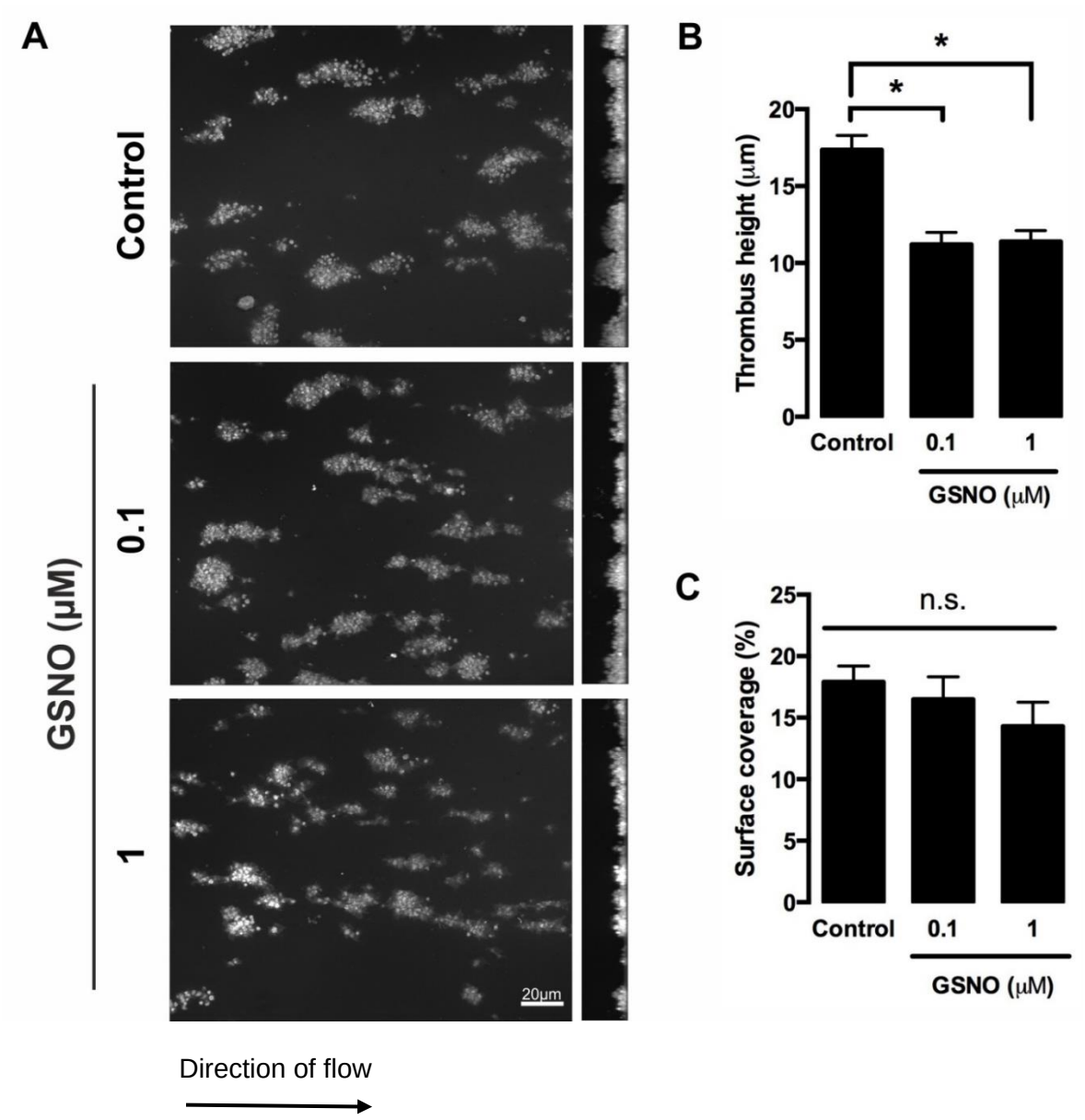

Figure 3.15. Effect of GSNO post-perfusion on established thrombi formed on collagen. *Whole PPACK anticoagulated blood stained with $DiOC_6$ was perfused through Collagen (50μg/ml) coated microfluidic channels for 2 minutes before being treated with a vehicle control or GSNO (100nM or 1μM) for 20 minutes. Thrombi were then fixed in 4% paraformaldehyde and restained in $DiOC_6$ before being visualised under epifluorescence microscopy (including z-stacking).* ***A)*** *Representative images of DiOC6 (membrane) stained platelets.* ***B)*** *Thrombus height measured via z-stacking.* ***C)*** *Percentage surface coverage per five fields of view. Images obtained at x63 magnification. Data is representative of three independent repeats and expressed as mean with S.E.M, with significance defined as p≤0.05. Scale bar represents 20μm.*

3.2.10. Effect of NO on fibrinogen adhered and spread platelets under flow

After discovering a possible role for NO on formed thrombus stability on collagen, it was next queried how this removal of platelets from the thrombus occurs. Platelets adhering on collagen under flow can form large multi-layered thrombi through the abridgment of neighbouring platelets through plasma fibrinogen interactions with their $\alpha II_b\beta_3$ integrins (288,289). Therefore, we hypothesised that platelets adhered to fibrinogen would be markedly affected by post flow of GSNO.To identify if this was the case, anticoagulated whole blood was flowed over fibrinogen-coated (300µg/ml) microfluidic channels for 2 minutes to allow platelets to successfully adhere and spread. GSNO (100nM) or buffer + vehicle (PBS) was then perfused over the platelets at the same shear rate for 20 minutes. As can be seen in figure 3.16., under control conditions, the majority of platelets adhering to the underlying fibrinogen fully spread, with a minority of platelets still in their rounded, pre-spread form. Surface coverage of platelets in control conditions was 40.78 ± 1.89% coverage of the underlying fibrinogen matrix. Upon GSNO treatment, platelets have a significantly reduced surface coverage (24.96± 4.68%). Individual platelet adhesion between both conditions were similar, suggesting that the reduction in surface area coverage was due to reversal of platelet spreading. This was confirmed through measurement of individual platelet surface area, with GSNO-treated platelets having a significantly reduced surface area compared to control platelets. It was hypothesised that, in accordance with the static spreading data, these platelets that had reduced in surface area would have had their stress fibres reversed also. To determine this, the same flow experiment was performed, however platelets were then stained with Rhodamine-B phalloidin to visualise actin structures in these platelets. F-actin staining confirmed this hypothesis; upon GSNO treatment platelets had undergone a similar reversal of stress fibres. Due to resolving issues in these much smaller platelets and the fact that they were imaged in a 3D format using epifluorescence, actin nodule formation, as analysed in static platelets, could not be confidently achieved. However, as shown in figure 3.16.E**,** platelets under flow can form actin nodules. Together, this data demonstrates that NO can cause stress fibre reversal on fibrinogen under flow, which is linked with a reduction in platelet surface area and overall matrix coverage.

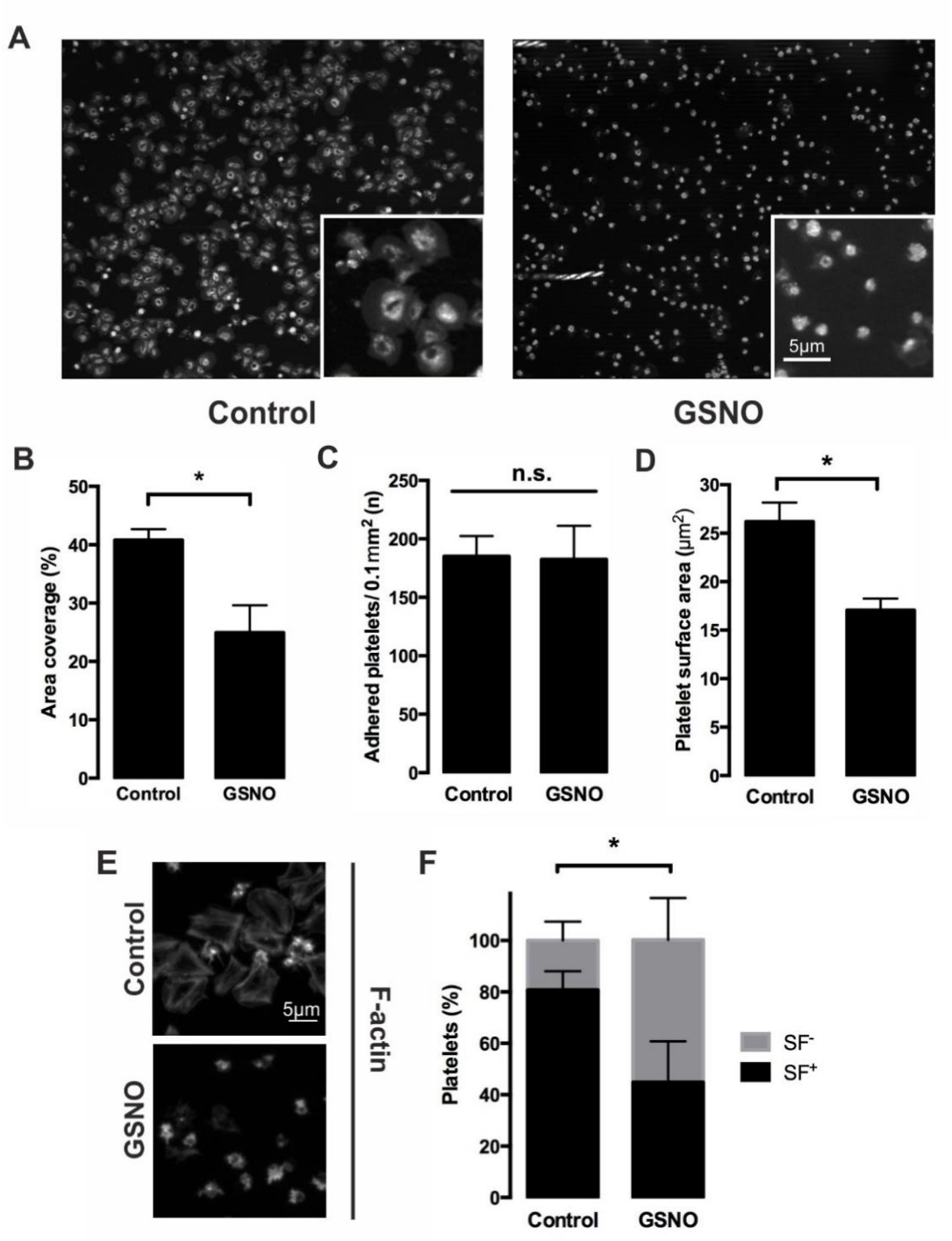

Figure 3.16. Effect of GSNO treatment on fibrinogen spread platelets under flow. *Whole PPACK anticoagulated blood stained with $DiOC_6$ was perfused through fibrinogen (300µg/ml) coated microfluidic channels for 2 minutes before being treated with a vehicle control or 100nM GSNO for 20 minutes. Channels were fixed in 4% paraformaldehyde after each run, permeabilised and stained with Rhodamine-B phalloidin before being visualised under epifluorescence microscopy.* ***A)*** *Representative images of $DiOC_6$ (membrane) stained platelets.* ***B)*** *Percentage area coverage.* ***C)*** *Number of adhered platelets per $0.1mm^2$.* ***D)*** *Average platelet surface area.* ***E)*** *F-actin staining of spread platelets under flow following treatment with a vehicle control or GSNO (1µM).* ***F)*** *Percentage of platelets positive (SF+) or negative (SF-) for stress fibres. Images obtained at 630x magnification. Data is representative of three independent repeats, with significance defined as $p \leq 0.05$. Scale bar represents 5µm.*

3.3. Discussion

Historically, platelets have been considered terminal in their activation status. The effect of cyclic nucleotide signalling on platelets has had a similar dogma, with PGI_2 and NO merely being considered as weights in the balance of platelet activation status within the circulating blood, whereby activated platelets overcome this threshold to then fully activate and form a thrombus. This present work has challenged both notions by demonstrating that platelets are plastic in their activation and cytoskeletal dynamics in response to NO-mediated signalling. This effect was determined using two separate NO donor molecules, GSNO and DEANONOate, which showed similar effects on the spread platelet actin cytoskeleton, leading to reversal of formed stress fibres into actin nodules. This effect was determined to be through the activation of the only receptor for NO in platelets, sGC, using the selective inhibitor, ODQ. In agreement with this finding of presumed cGMP-mediated stress fibre reversal, the non-hydrolysable cGMP analog, 5-cPT-PET-cGMP, led to a similar significant increase in stress fibre reversal and actin nodule formation. Previously, our group has uncovered a role for PGI_2 in potent reversal of stress fibres in platelets, effected through an inhibition of the RhoA pathway through phosphorylation of RhoA (273)Unlike PGI_2, NO treatment did not lead to a significant increase in $pRhoA^{ser188}$, however, there was a significant reduction in GTP-bound (activated) RhoA, which was then reversed in the presence of ODQ, suggesting that the reduction in RhoA activity observed upon GSNO treatment was via a phosphorylation-independent mechanism.

It is of importance to note that the level of stress fibre reversal observed in GSNO treated platelets was lower than those treated with DEANONOate. This may be a result of an increase in rate of spontaneous NO release by DEANONOate, which has been shown to follow first order kinetic release (290), but may due to the dual NO groups attached to this complex, thereby leading to double NO release per mole compared to GSNO. Additionally, GSNO has been shown to be enzymatically metabolised on the cell surface, with NO liberation dependent on a protein disulphide isomerase (188), which may be a rate-limiting step in the generation of NO and subsequent activation of the PKG pathway. Conversely, here the use of a cGMP analog led to a similar reversal of stress fibres as GSNO, therefore it may be more likely that either the rate of NO release from DEANONOate may cause non cGMP mediated effects, such as S-nitrosylation of extracellular and/or cytosolic proteins. Although there was a greater reversal of stress fibres observed with

DEANONOate treatment, GSNO was used for further experimentation, as it was a more physiologically relevant source of NO, which has been identified within the body and proposed as storage pool for NO.

Due to the labile nature of NO and PGI_2, studies investigating their concentrations have used more stable metabolites, which although easier to measure, are often utilised or produced by other pathways. This is especially true of the determination of NO in the plasma. NO concentration has been inferred using its more stable oxidation products, nitrate and nitrite, which were shown to be approximately 70μM (291). The validity of these measurements however is limited, as these metabolites, although more stable than NO, accumulate over time and are also present in the diet and is hard to control for in human subjects (292). To measure accurate vascular endothelial release of NO, a more direct approach must be made. Using a catheterised NO sensor, Neishi *et al.* found that the NO concentration in the coronary artery increased from almost non-detectable levels to 3-10nM, depending on the dose of acetylcholine injected into participants (293). Currently, there has been no consensus reached for the resting plasma concentration for NO, and this is an obvious area of further research.

Estimation of plasma PGI_2 concentration has been performed and indicates a low nanomolar range. Early studies from Fitzgerald *et al*. used the stable PGI_2 metabolite variants of 6-keto-PGF1α excreted in the urine to estimate PGI_2 plasma concentrations upon infusion of PGI_2 into healthy subjects (294). This study surprisingly estimated PGI_2 plasma concentrations much lower than was expected, at 3.4pg/ml (9.64nM). More recently, the levels of excreted PGI_2 metabolites was corroborated by Cavalca *et al*. using an identical chromatographic approach, which further suggested that plasma PGI_2 concentrations are in the low nanomolar range (295).

Radomski *et al.* have previously shown a synergistic relationship between NO and PGI_2 at nanomolar and picomolar concentration, respectively, leading to increased inhibition of aggregation to collagen (287). It was therefore hypothesised that both endogenous inhibitors would be synergistic partners in reversal of stress fibres in our spreading assays. Accordingly, fibrinogen spread platelets treated with 10nM NO and 300pM PGI_2 led to a significant reduction in formed stress fibres when compared to NO or PGI_2 alone (figure 3.14.). This finding is consistent with those previously published by the Moncada group (287), and further supports the

phosphorylation-independent inhibition of RhoA that was observed upon NO treatment, as it is likely that RhoA was being inhibited by two distinct mechanisms in spread platelets due to the synergism observed. Nagy *et al*. have reported the phosphorylation of a GEF and GAP, ARHGEF17 and ARHGAP6, respectively, through PKA and PKG leading to a reduction in Rac1 activity (296). Investigation of the effects of NO on these inhibitors and activators of RhoGTPases should be further undertaken on regulators responsible for RhoA regulation. Currently, there is no reported mechanism of phosphorylation-independent inhibition of RhoA by PKG, which may suggest the combined data shown in figures 3.16. and 3.17. represent a novel, unreported mechanism, potentially involving regulation of upstream RhoGEFs and RhoGAPs. Alternatively, the insignificant phosphorylation increase in GNSO-treated spread platelets may require further experimental repeats to reach significance. However, it is clear that at a GSNO concentration required for maximal stress fibre reversal, pRhoAser^{188} levels are significantly lower than when treated with low dose PGI_2, may reflect the comparatively weaker inhibitory capacity of NO signalling in platelets.

More recently, a synergistic relationship between PKG and PKA has been shown in HEK293 cells, whereby active PKG can positively regulate PKA function through phosphorylation of the PKA regulatory subunit at ser101 (297). This was seen with PKG1α however, and there are no current reports of this effect with the platelet-expressed β isoform. Due to the similarity between the α and β isoforms in their catalytic domains, this effect should also be investigated in platelets. This may uncover the possible enhancement of PKA sensitivity to cAMP in response to PKG activation, thus increased RhoA inhibition and stress fibre reversal in spread platelets.

Platelet contractility, in part through the formation of stress fibres, allows secure binding to sites of vascular injury. Accordingly, PF4-Cre RhoA knockout mice have a reduction in stress fibre and thrombus formation *in vitro* and *in vivo*, with those platelets forming more unstable thrombi (280). Consistent with this, our findings involving RhoA inhibition correlated with a significant reduction in the height of preformed thrombi on collagen. This reduction in thrombus height was not accompanied by a reduction in surface coverage, indicating that the upper layers of the thrombus had embolised away upon GSNO treatment. It was hypothesised that the upper layers of platelets within the thrombus were predominantly abridged by

fibrinogen monomers. In agreement, platelets spread under shear significantly reverse in their stress fibres in response to GSNO, suggesting that the reduction in thrombus height may be attributable to a loss in platelet contractility in the form of stress fibre disassembly. Previous research has also demonstrated inhibition of platelet contractility using blebbistatin, a myosin II inhibitor, or Y27632, a ROCK inhibitor, led to the formation of unstable thrombi on collagen with enhanced embolisation events (195).

Collagen-mediated thrombi height was significantly reduced with 1μM GSNO perfusion; the dose that was found to be maximal for stress fibre reversal under static conditions (figure 3.3). Surprisingly, a lower perfusion dose of 100nM caused a similar reduction in thrombus height also. At the time of experimentation and publishing there were no published research regarding flow-induced NO sensitivity in platelets. Recently, Wen *et al*. have reported dose-dependent shear-induced NO sensitivity in murine platelets using an expressed fluorescent intracellular cGMP biosensor (298). It was also found that cGMP levels were most abundant in the 'shell' of the thrombus and resulted in the controlled consolidation of the thrombus over time. Importantly embolization events were significantly lower in sGC knockout mice, indicating that this was primarily through cGMP synthesis.

3.4. Conclusion

With the findings outlined in this chapter and previous research highlighting the critical role of platelet contractility in thrombus formation, it appears that NO can lead to the reduction of preformed thrombus mass through controlled embolisation of the upper layers of the thrombus. These findings require further investigation, including the quantification of platelet contractility in response to GSNO and potential upstream targets of NO which regulate RhoA function.

Chapter 4.
Collagen mediated PGI_2 resistance in spread platelets

4.0. Summary

During thrombus formation, platelets interact with the subendothelium exposed through endothelial damage. Within the basal lamina lie a vast array of matrix proteins which have historically been demonstrated to activate platelets in several different ways, either using overlapping or distinct signalling pathways depending on the matrix protein concerned (96). The utilisation of different signalling pathways has also been shown to result in different phenotypic effects on platelets, with different matrices and or soluble agonists, and their concentrations causing different actin and spreading dynamics (103,247,299,300). Our lab has previously found that platelets spread on collagen do not reverse their stress fibres or reduce in spread surface area in response to PGI_2. The aim of this chapter was to determine which mechanism(s) are involved in PGI_2 resistance in spread platelets.

4.1. Introduction

Previous findings within our group have shown that when interacting with fibrinogen, platelets are readily reversed by treatment with PGI_2 or NO and other PKA- and PKG-elevating agents, respectively (273,301). Other groups have also shown elevated PKA activity and cGMP accumulation in developing thrombi, further indicating that PKA and cGMP signalling may be required for more than platelet quiescence prior to thrombus formation (298,302)This has highlighted the possibility of PGI_2 and/or NO to not only prevent thrombosis, but also coordinate it through the ongoing reversibility of platelet activity within and around the thrombus. Given findings from the Brass group at the University of Pennsylvania, showing that the thrombus environment heavily relies on platelet packing and that thrombi have distinct areas, platelet contractility provided by stress fibre formation is likely key in maintaining thrombus integrity (76,78,79). This, coupled with our stress fibre reversal findings, suggests that a thrombus can be kept from excessive growth by the ever-present challenge of inhibitory signals provided by PGI_2 and NO, not only preventing platelet attachment, but also potentially causing controlled platelet embolisation. Additionally, overall thrombus architecture may be determined by the activation and phenotype of platelets due to the varying effects of PGI_2. For example, platelets interacting with fibrinogen are readily reversed by PGI_2, leading to loss of stress fibres and a presumed reduction in contractility. This may then cause fibrinogen-activated platelets to embolise from the thrombus, giving the ‘tail’ to the thrombus that is regularly seen in *in vivo* thrombus formation assays (78,302).

Platelets interacting with other proteins, likely deeper within the thrombus may be less sensitive to the effects of PGI_2 and will therefore retain their contractility and remain bound to the body of the thrombus. This has been observed previously by our group, where it was found that collagen spread platelets did not respond to PGI_2, whereas those spread on fibrinogen fully reversed their stress fibres (unpublished data).

Thrombi are highly heterogeneous, likely owing to several factors such as local shear rate of flowing blood, atheromatous plaques, presence of oxidised LDL, and types and stiffness of matrix proteins exposed and incorporated upon vascular injury (17,303–305). As our group has shown reversal of formed stress fibres in platelets spread on fibrinogen but not collagen, we sought to investigate why collagen-spread platelets do not respond to PGI_2 and the potential role of this lack of effect on thrombus formation. There is surprisingly little published data on the effects of PGI_2 on collagen spread platelets. There is a report of PGI_2 causing an inhibition of platelet adhesion and spreading on collagen, however this has yet to be corroborated by other groups (228). One group has negated the use of PGI_2 in preference of the cAMP activator, forskolin, during collagen spreading, which caused an inhibition of platelet adhesion (306). With the data currently at hand, it was hypothesised that either GPVI or α2β1 signalling was responsible for the lack of response to PGI_2 that our group had previously observed.

4.2. Results

4.2.1. Platelet spreading on collagen matrices in the presence or absence of PGI_2

Platelet spreading analysis was performed on platelets spread on collagen for 5, 15, 30 and 45 minutes with or without PGI_2 to validate scarce findings previously published (228). Platelets were incubated with 10nM PGI_2 for two minutes prior to being spread on 100µg/ml collagen for the allotted times. As shown in figures 4.1. and 4.2., platelets interacting with collagen adhere in a time-dependent manner, with platelets significantly increasing in their adhesion at 30 and 45 minutes when compared to platelets spread for 5 minutes. Spread platelet surface area was also time-dependent, with maximal surface area being reached at 45 minutes. There was a concomitant increase in platelet spreading and stress fibre formation, with lesser spread platelets at 5 minutes having fewer stress fibres than those spread for 45 minutes. Unlike platelets spread on fibrinogen, actin stress fibres on collagen do not appear to be preceded by actin nodules, which was in agreement with previous data (284). In place of actin nodules, platelets initially spreading on collagen have varying non-descript actin structures which were deemed unclassifiable. These unclassifiable platelets were inversely correlated with stress fibre formation and had the highest incidence at 5 minutes and disappeared in a time-dependent manner. Irrespective of PGI_2 treatment, both adhesion and platelet spreading was unaffected in comparison to control conditions. Surprisingly, this lack of effect was observed in the formation of stress fibres in these platelets also, suggesting that collagen spread platelets are resistant to PGI_2.

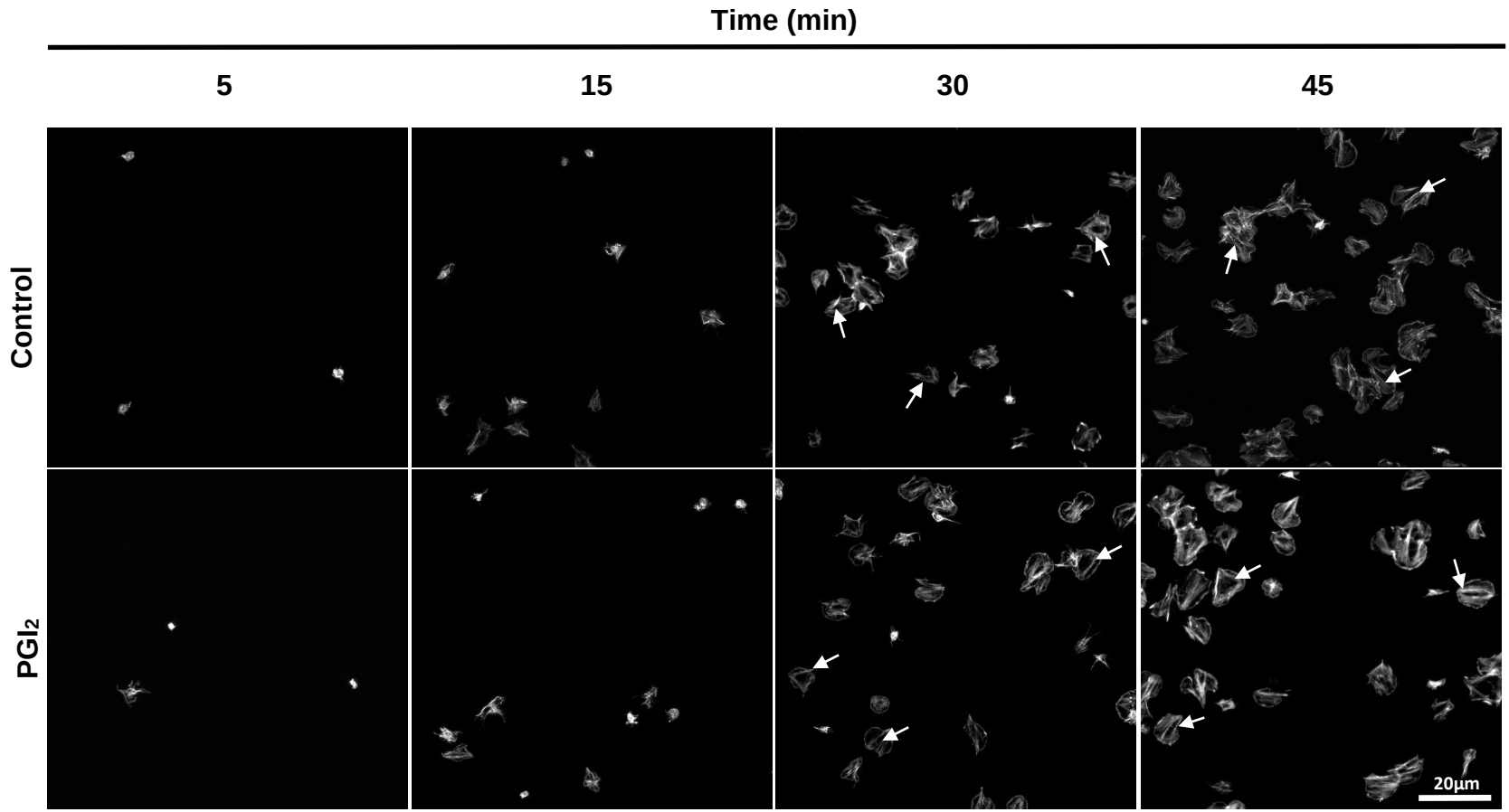

Figure 4.1. Platelet spreading on collagen in the presence or absence of PGI_2. *Platelets ($2x10^7$/ml) were incubated with PGI_2 (10nM) 2 minutes prior to being spread on collagen immobilised coverslips (100µg/ml) for the indicated times. Platelets were then fixed in 4% formaldehyde and permeabilised in 0.1% Triton x-100 before being stained in rhodamine-B phalloidin. Examples of stress fibres are indicated with white arrows. Scale bar represents 20µm.*

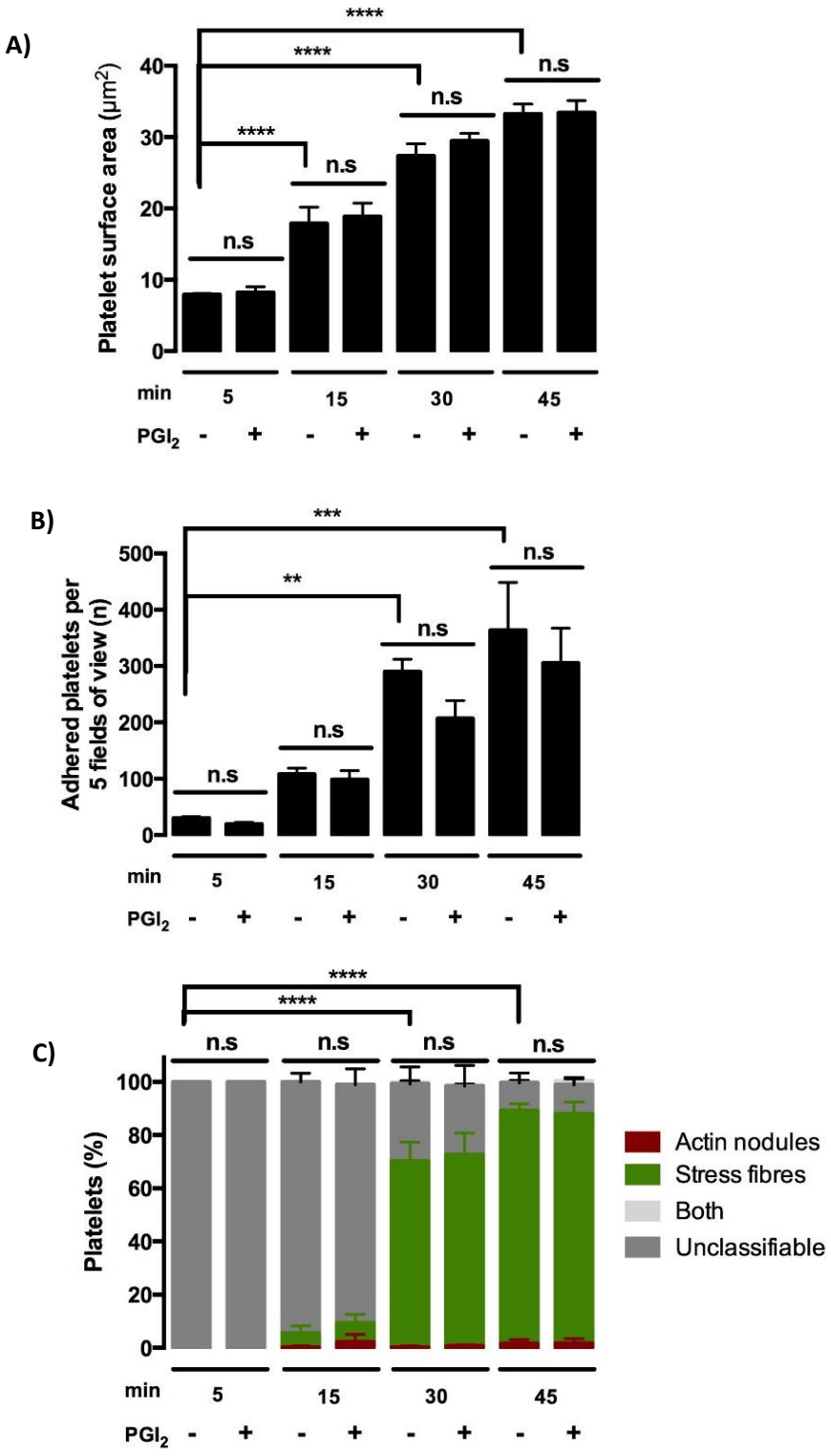

Figure 4.2. Analysis of platelet spreading on collagen in the presence or absence of PGI_2. A) *Platelet adhesion per 5 fields of view.* ***B)*** *Spread platelet surface area.* ***C)*** *Percentage of platelets positive for actin nodules, Stress fibres, both or unclassifiable. Data represents the means ± SD of three independent experiments, with significance defined as $p \geq 0.05$ (* ≤ 0.05, ** ≤ 0.01, *** ≤ 0.001, **** ≤ 0.0001).*

4.2.2. Collagen spread platelets are resistant to PGI_2-mediated cytoskeletal reversal independently of secondary mediator signalling

Having established that platelets preincubated with a physiologically-relevant PGI_2 concentration are uninhibited when interacting with collagen, we next sought to investigate the effect of PGI_2 on platelet reversal when spread on collagen. Our group has previously demonstrated that fibrinogen-spread platelets are sensitive to low dose PGI_2, therefore any differences in sensitivity to PGI_2 on these two matrices may demonstrate the underlying mechanics of thrombus formation.

Platelets were incubated in the presence or absence of apyrase and indomethacin for 10 minutes and were spread on collagen-immobilised coverslips for 25 minutes prior to treatment with 10nM PGI_2, apyrase (2U/ml) and indomethacin (10µM), PGI_2 + apyrase and indomethacin or vehicle (0.1% DMSO) for a further 20 minutes. As demonstrated in figure 4.3., platelets pre-treated with apyrase and indomethacin appear to have reduced adhesion when interacting with collagen, however this did not reach statistical significance when using a one way ANOVA with Tukey analysis and therefore would require more experimental repeats. Interestingly, when treated with PGI_2, irrespective of apyrase and indomethacin, collagen spread platelets were completely resistant to the effects of PGI_2, with no differences in platelet adhesion, spread surface area, or actin structures. This data suggests that unlike fibrinogen-spread platelets, platelets spread on collagen are resistant to PGI_2. Additionally, the independence of this resistance to inhibition of secondary mediators indicates that there is no effect of ADP or TXA_2 on PGI_2 sensitivity in these platelets.

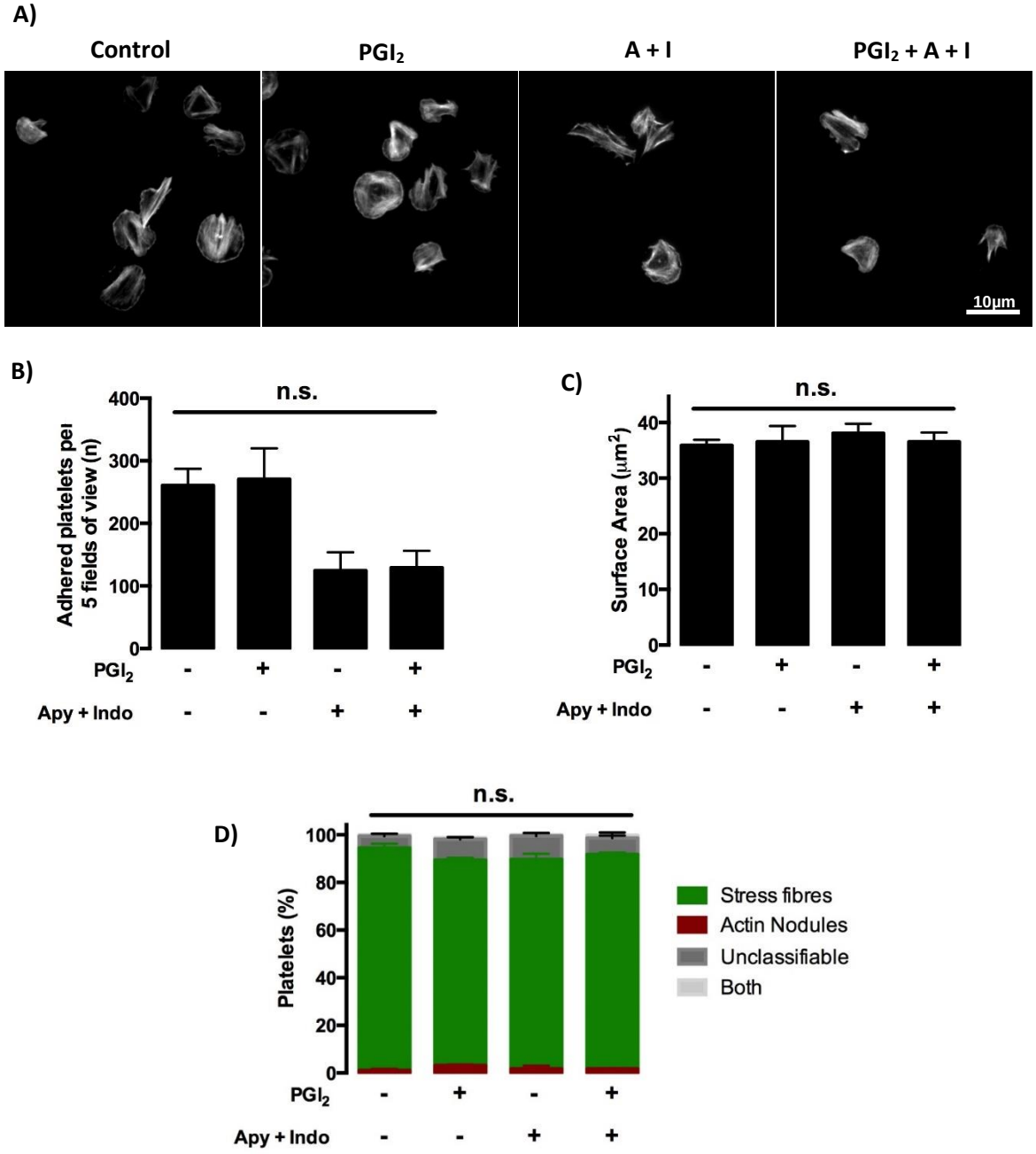

Figure 4.3. Analysis of platelet spreading on collagen in the presence or absence of PGI_2 with or without secondary mediator inhibition. *Platelets ($2x10^7$/ml) were incubated with apyrase (2U/ml) and indomethacin (10µM) or vehicle alone (0.1% DMSO) for 10 minutes prior to being spread on collagen coated coverslips (100µg/ml) for 25 minutes. Spread platelets were then treated with vehicle, PGI_2 (10nM), apyrase (2U/ml) and indomethacin (10µM), or a combination of PGI_2 and apyrase and indomethacin for a further 20 minutes. Platelets were then fixed in 4% formaldehyde and permeabilised in 0.1% Triton x-100 before being stained in rhodamine-B phalloidin.* ***A)*** *Representative images.* ***B)*** *Platelet adhesion per 5 fields of view.* ***C)*** *Spread platelet surface area.* ***D)*** *Percentage of platelets positive for stress fibres, actin nodules, both or unclassifiable. Data represents the means ± SEM of three independent experiments, with significance defined as $p \geq 0.05$. Scale bar represents 10µm).*

4.2.3. Validation of PKA elevating agents in platelets spreading on collagen

Due to lack of sensitivity to PGI_2-mediated cytoskeletal reversal in platelets spread on collagen, it was then decided that an underlying mechanism of this lack of effect should be investigated. This was initially investigated using inhibitors targeting the generation of cAMP formation in response to PGI_2. To inhibit degradation of cAMP, milrinone was used to inhibit PDE3, the chief effector of cAMP hydrolysis. To establish the role of AC in the generation of cAMP in collagen spread platelets, the AC activator, forskolin, was used. The reversal of formed stress fibres in collagen spread platelets with either of these inhibitors would suggest that the mechanism of PGI_2 insensitivity is related to the target of the inhibitor. If there was no response from either inhibitor, this would suggest that there may be direct PKA inhibition, or another cAMP:PKA mechanism at play, likely the inhibition of an effector protein that would be a target for PKA-mediated phosphorylation.

To ensure that both milrinone and forskolin were effective at the doses chosen from the literature, they were incubated with platelets prior to spreading on fibrinogen for 45 minutes. Fibrinogen was chosen as the matrix as our group has previously shown reversal of stress fibres upon incubation with either molecule. As shown in figure 4.4., platelets allowed to spread on fibrinogen for 45 minutes readily adhere , spread and form stress fibres. Consistent with the inverse relationship between actin nodules and stress fibres, the number of actin nodule positive platelets was relatively low in control conditions. Upon PDE3 inhibition with milrinone, platelet adhesion was significantly reduced when compared to control conditions, as was spread platelet surface area. Direct AC activation by forskolin treatment in platelets resulted in a similar effect as milrinone, also with significantly reduced platelet adhesion and surface area. As with PGI_2 treatment in platelets, there was an inhibition of platelet stress fibre formation in both milrinone and forskolin. Actin nodule formation was drastically increased in platelets treated with milrinone or forskolin. This data suggests that at the doses chosen, milrinone and forskolin have a significant effect on platelet activity and is therefore suitable to use in collagen spread platelets to investigate the mechanisms of PGI_2 insensitivity.

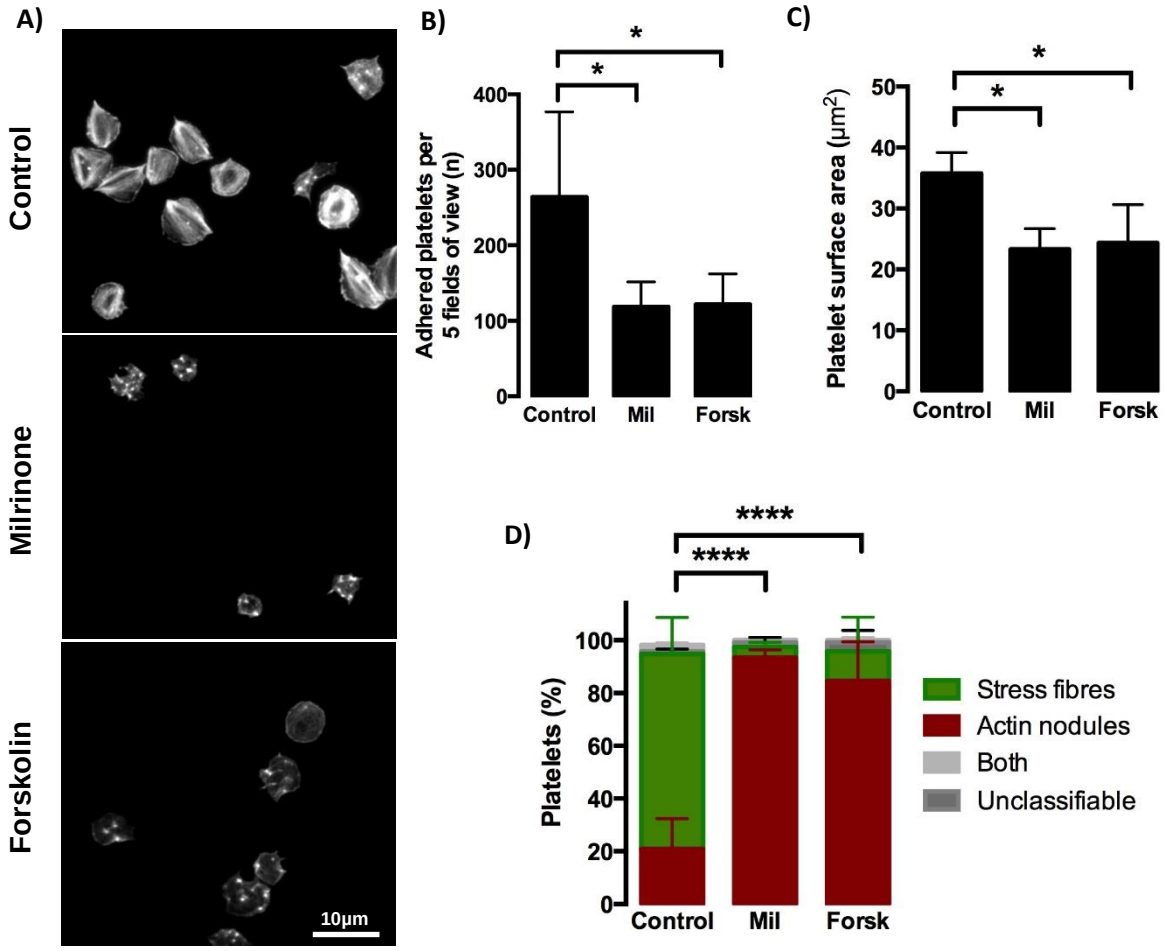

Figure 4.4. Platelet adhesion and spreading in response to pre-treatment with molecules which increase cAMP production. *Platelets ($2x10^7$) were incubated with vehicle (0.1% DMSO), milrinone (10µM) or forskolin (1µM) for 10 minutes prior to being spread on 100µg/ml fibrinogen for 45 minutes. Platelets were then fixed in 4% formaldehyde and permeabilised in 0.1% Triton x-100 before being stained in rhodamine-B phalloidin.* ***A)*** *Representative images.* ***B)*** *Platelet adhesion per 5 fields of view.* ***C)*** *Spread platelet surface area.* ***D)*** *Percentage of platelets positive for stress fibres, actin nodules, both or unclassifiable. Data represents the means ± SEM of four independent experiments, with significance defined as $p \geq 0.05$. Scale bar represents 10µm.*

4.2.4. PGI_2 insensitivity in collagen spread platelets is likely through the inhibition of adenylyl cyclase

Due to lack of sensitivity to PGI_2-mediated cytoskeletal reversal in platelets spread on collagen, it was then decided that an underlying mechanism of this lack of effect should be investigated. This was initially investigated using inhibitors targeting the generation of cAMP formation in response to PGI_2. To inhibit degradation of cAMP, milrinone was used to inhibit PDE3, the chief effector of cAMP hydrolysis. To establish the role of adenylyl cyclase in the generation of cAMP in collagen spread platelets, the AC activator, forskolin, was used. The reversal of formed stress fibres in collagen spread platelets with either of these inhibitors would suggest that the mechanism of PGI_2 insensitivity is related to the target of the inhibitor. If there was no response from either inhibitor, this would suggest that there may be direct PKA inhibition, or another cAMP:PKA mechanism at play, likely the inhibition of an effector protein that would be a target for PKA-mediated phosphorylation.

As can be shown in figure 4.5., platelets spread on collagen remain resistant to PGI_2 with regards to adhesion, surface area and stress fibre sustenance. This lack of reversal was also maintained in platelets treated with milrinone, indicating that PGI_2 resistance in collagen spread platelets is not through modulation of PDE3 function. Interestingly, when platelets were treated with the AC activator, forskolin, collagen spread platelets readily formed actin nodules, suggesting that they had reversed their formed stress fibres, indicated by a reduction in stress fibre sustenance. Because of this stress fibre reversal, platelet surface area in response to forskolin treatment was significantly reduced also.

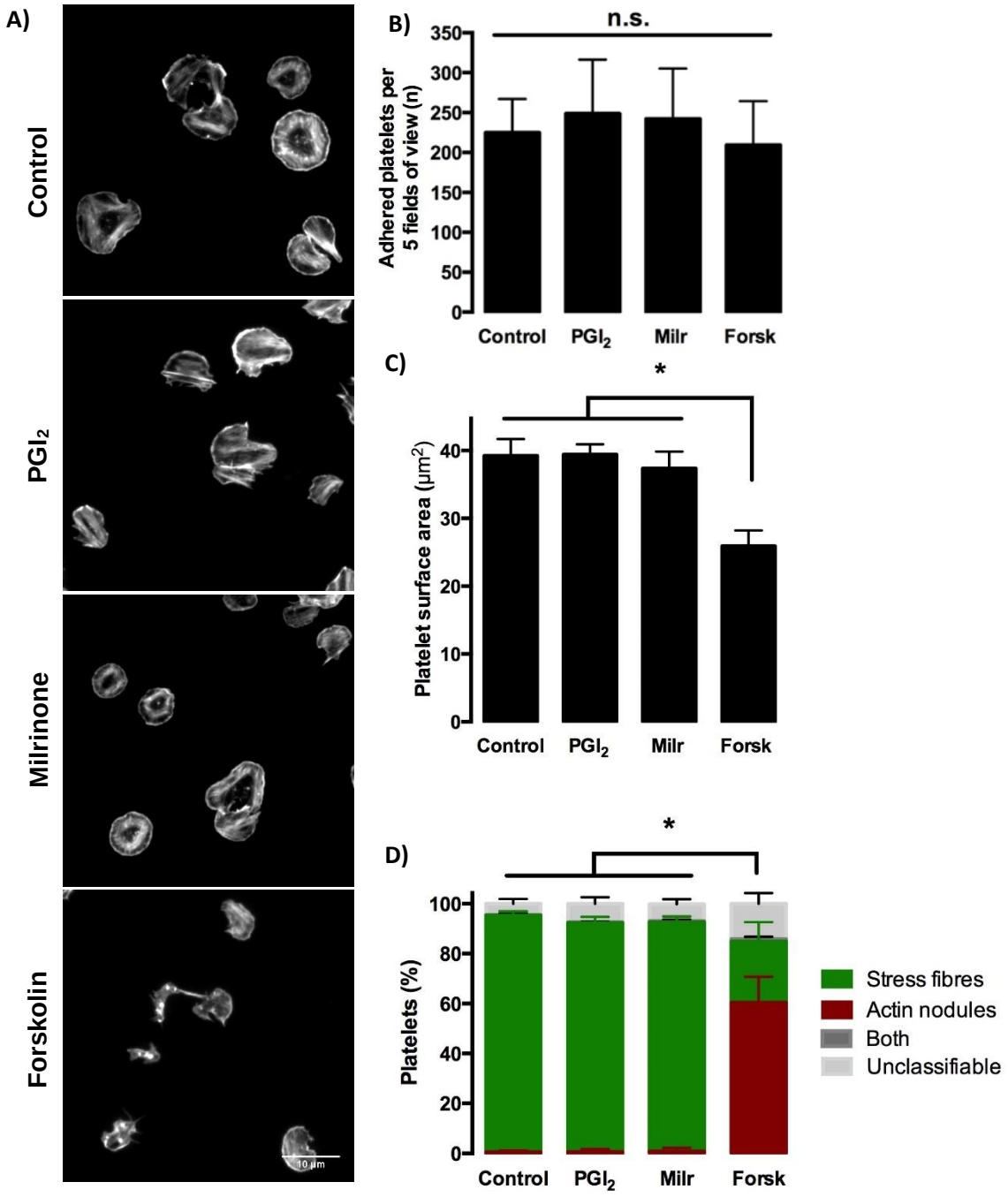

Figure 4.5. Effect of inhibition of PDE3 and activation of AC in platelets spread on collagen. *Platelets ($2x10^7$) were spread on 100µg/ml collagen for 25 minutes prior to treatment with vehicle (0.1% DMSO), PGI_2 (10nM), milrinone (10µM) or forskolin (10µM) for a further 20 minutes. Platelets were then fixed in 4% formaldehyde and permeabilised in 0.1% Triton x-100 before being stained in rhodamine-B phalloidin.* ***A)*** *Representative images.* ***B)*** *Platelet adhesion per 5 fields of view.* ***C)*** *Spread platelet surface area.* ***D)*** *Percentage of platelets positive for stress fibres, actin nodules, both or unclassifiable. Data represents the means ± SD of at least three independent experiments, with significance defined as p ≥ 0.05. * = p ≥ 0.05. Scale bar represents 10µm.*

4.2.5. Investigation of collagen-specific receptors in platelet PGI_2 insensitivity

The finding that collagen spread platelets are resistant to PGI_2 and that this is seemingly dependent on the inhibition of AC posed the question as to which receptor was the cause of this effect. To understand this mechanism further, platelet spreading was performed on two collagen-specific peptides which independently activate the two main collagen receptors in platelets, GFOGER and CRP, which activate $\alpha_2\beta_1$ and GPVI, respectively. To investigate which receptor-ligand interaction may be causing PGI_2 insensitivity in platelet spread on collagen, platelets were spread on GFOGER or CRP at doses widely used in the literature in the presence or absence of PGI_2. In addition, platelets were also spread on fibrinogen as a positive control to ensure the PGI_2 had been appropriately administered. Platelets were also spread on collagen to demonstrate insensitivity to PGI_2 in the donor per experiment, so that sensitivity in either GFOGER or CRP was attributable to the peptide and not due to other variables such as platelet preparation or donor variation.

As shown in figures 4.6. and 4.7., platelets spread on fibrinogen are highly sensitive to PGI_2-mediated stress fibre reversal, with a significant reduction in stress fibres and an increase in the number of platelets positive for actin nodules. As previously demonstrated, collagen spread platelets are resistant to PGI_2, with no significant differences in platelet adhesion, average platelet surface area, or changes in actin structures. Interestingly, platelets spread on GFOGER peptide were significantly sensitive to PGI_2-mediated stress fibre reversal and readily formed actin nodules in response to treatment. This was however not coupled with a reduction in spread platelet surface area, likely due to high variation among donors. There appeared to be a noticeable reduction in platelet adhesion in GFOGER-stimulated platelets after PGI_2 treatment, however this was not statistically significant with the number of repeats performed.

Overall, platelet adhesion on GFOGER was quite low, and may be a result of the relatively low expression of $\alpha_2\beta_1$ in platelets (141).Conversely, platelets spread on CRP peptide are completely resistant to the effects of PGI_2, maintaining formed stress fibres, spread platelet surface area and adhesion. Interestingly, sensitivity of stress fibre reversal was significantly different between fibrinogen spread platelets compared to platelets spread on GFOGER. These findings indicate that the

insensitivity to PGI_2 in platelets spread on collagen is likely due to the activation of GPVI and its signalling.

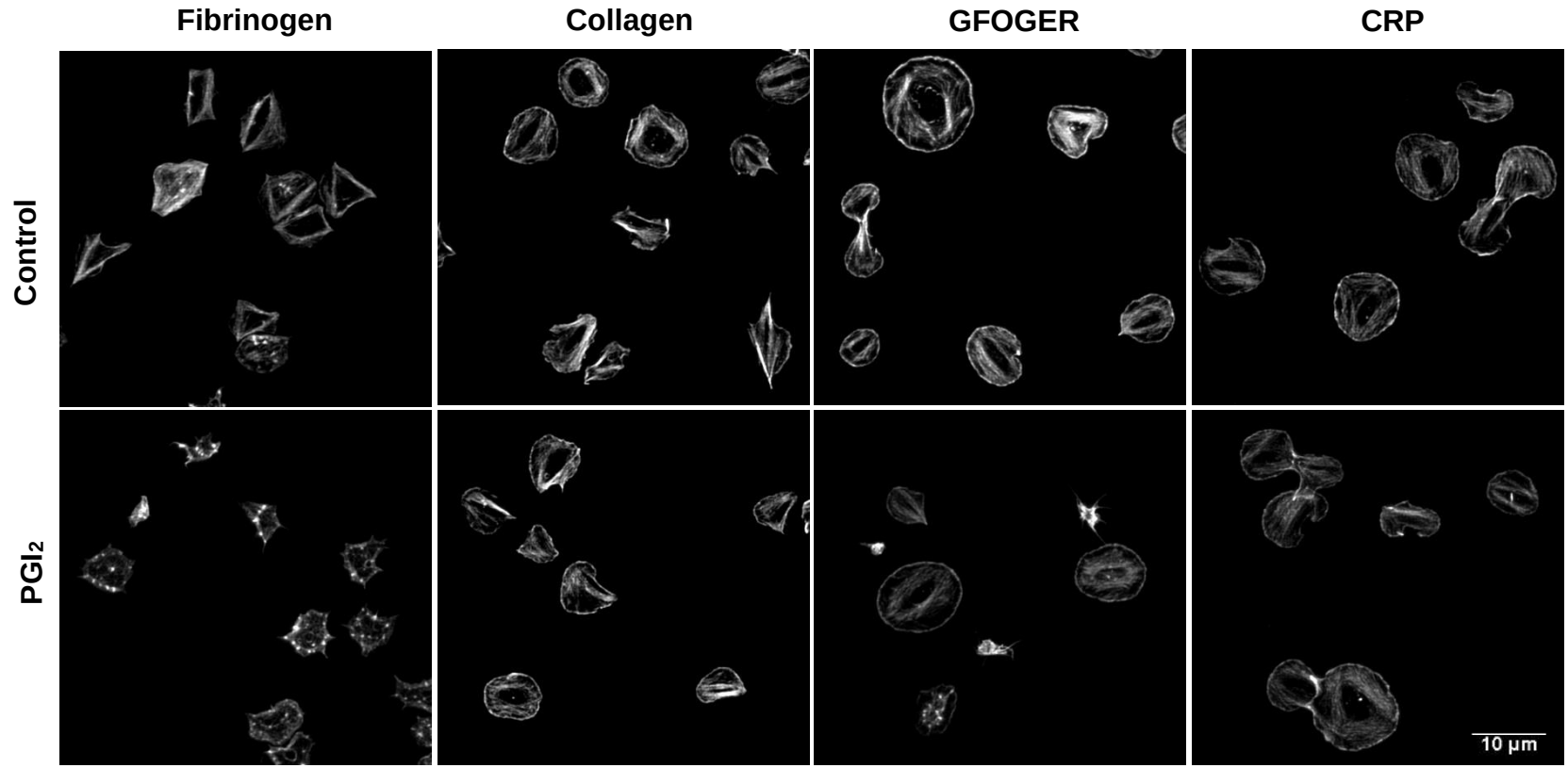

Figure 4.6. Effect of PGI_2 on platelets spread on collagen peptides GFOGER and CRP. *Platelets ($2x10^7$/ml) were spread on fibrinogen (100µg/ml), collagen (100µg/ml), GFOGER (10µg/ml) or CRP (3µg/ml) for 25 minutes prior to treatment with vehicle (0.1% DMSO) or PGI_2 (10nM) for a further 20 minutes. Platelets were then fixed in 4% formaldehyde and permeabilised in 0.1% Triton x-100 before being stained in rhodamine-B phalloidin. Images are representative of at least 3 independent experiments. Scale bar represents 10µm.*

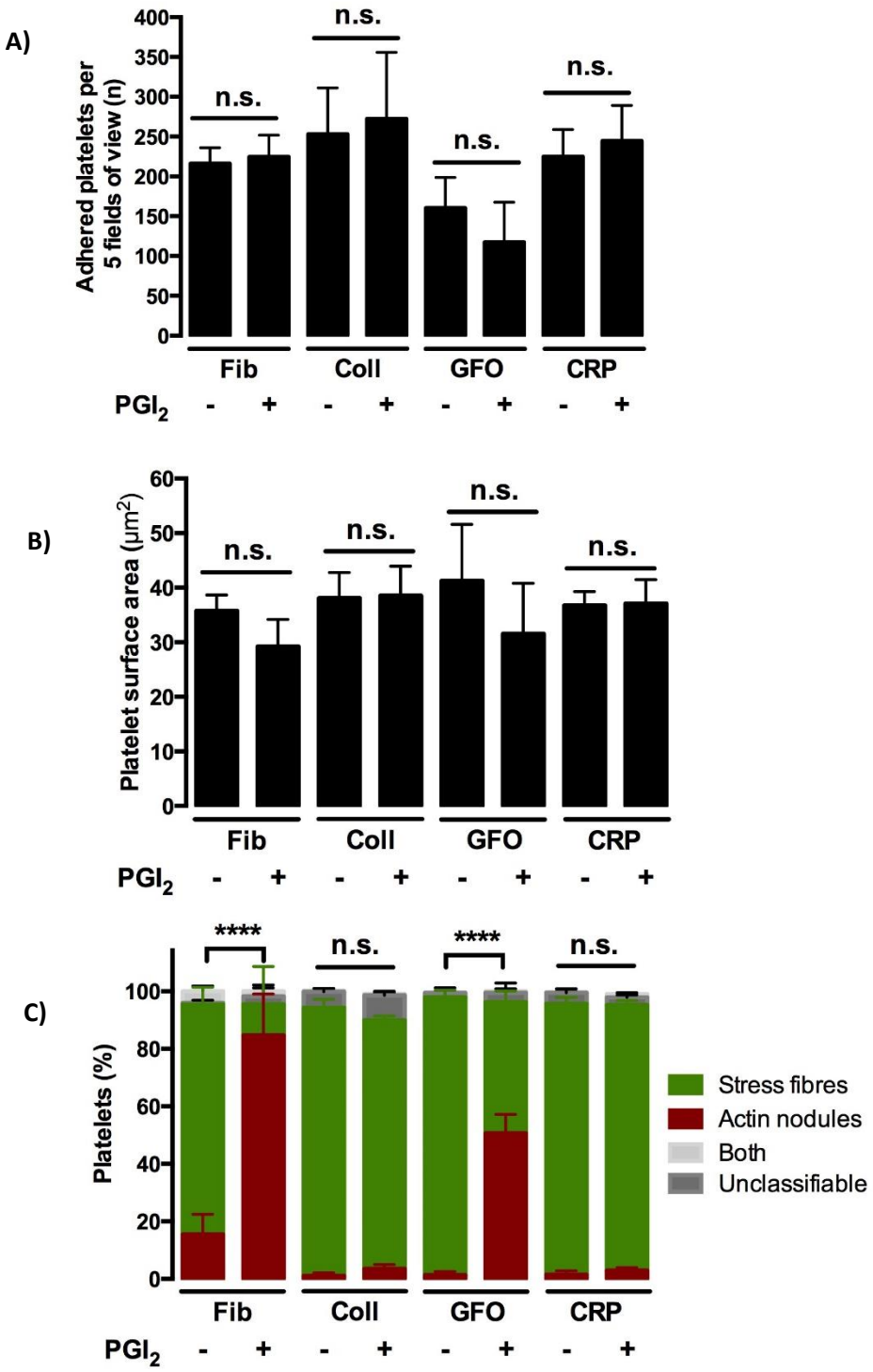

Figure 4.7. Analysis of the effect of PGI_2 on platelets spread on collagen peptides GFOGER and CRP. *Platelets ($2x10^7$/ml) were spread on fibrinogen (100µg/ml), collagen (100µg/ml), GFOGER (10µg/ml) or CRP (3µg/ml) for 25 minutes prior to treatment with vehicle (0.005% ethanol) or PGI_2 (10nM)* ***A)*** *Platelet adhesion per 5 fields of view.* ***B)*** *Spread platelet surface area.* ***C)*** *Percentage of platelets positive for stress fibres, actin nodules, both or unclassifiable. Data represents the means ± SD of at least three independent experiments, with significance defined as p ≥ 0.05 (* ≤ 0.05, ** ≤ 0.01, *** ≤ 0.001, **** ≤ 0.0001).*

4.2.6. Activation of adenylyl cyclase causes stress fibre reversal in platelets spread on GPO-containing collagen related peptide

The finding that platelets are sensitive to PGI_2-mediated stress fibre reversal when spread on GFOGER peptide, but not CRP suggests that PGI_2 insensitivity on collagen is related to the activation of the GPVI receptor. Like with collagen, the next experiment was designed to identify the mechanism by which PGI_2 insensitivity was mediated in platelets spread on collagen peptides. Platelets were spread on GFOGER or CRP for 25 minutes and then treated with the PDE3 inhibitor, milrinone, or the AC activator, forskolin, for a further 20 minutes. Given the reversal of stress fibres seen in collagen spread platelets with forskolin, it was hypothesised that platelets spread on either GFOGER or CRP would also reverse their formed stress fibres in response to forskolin, as their respective receptors, $\alpha_2\beta_1$ and GPVI, are the main two receptors for collagen. Potentially, there may be some process in play when platelets are activated via GPVI that can override PGI_2 sensitivity.

Platelets were also spread on fibrinogen and treated with milrinone and forskolin at the same time points for positive control, as platelets spread on this matrix have been previously shown to significantly reversed their formed stress fibres and form actin nodules in response to either drug (273). As shown in figures 4.8. and 4.9., treatment with either milrinone or forskolin, platelets readily reverse their stress fibres and form actin nodules, indicating that the treatments were successful. Changes in actin nodule formation between platelets in either treatment were statistically insignificant, however the incidence of sustained stress fibres between the two groups was significant. Platelets spread on GFOGER or CRP do not reverse their formed stress fibres in response to PDE3 inhibition with milrinone. Along with this lack of cytoskeletal response, differences in platelet adhesion and surface area were found not to be statistically significant with the number of repeats performed. Like in fibrinogen spread platelets, platelets spread GFOGER and CRP significantly reverse formed stress fibres in response to forskolin. This response was significantly different between platelets spread on these peptides, indicating that platelets activated through α2β1 are more susceptible to AC activation and its downstream effects than platelets activated through GPVI. Platelet adhesion in response to either milrinone or forskolin treatment on any matrix remained unchanged, consistent with previous findings in platelets spread on collagen. Taken together, these findings suggest that platelets activated through either immobilised GFOGER or CRP are resistant to the effects of PDE3 inhibition when compared to fibrinogen spread

platelets. Importantly, platelets spread on both matrices significantly reverse their formed stress fibres and form actin nodules in response to AC activation, however this response was significantly different between all three matrices tested, indicating that the potential for platelet reversibility may be different according to the signalling pathways activated during spreading.

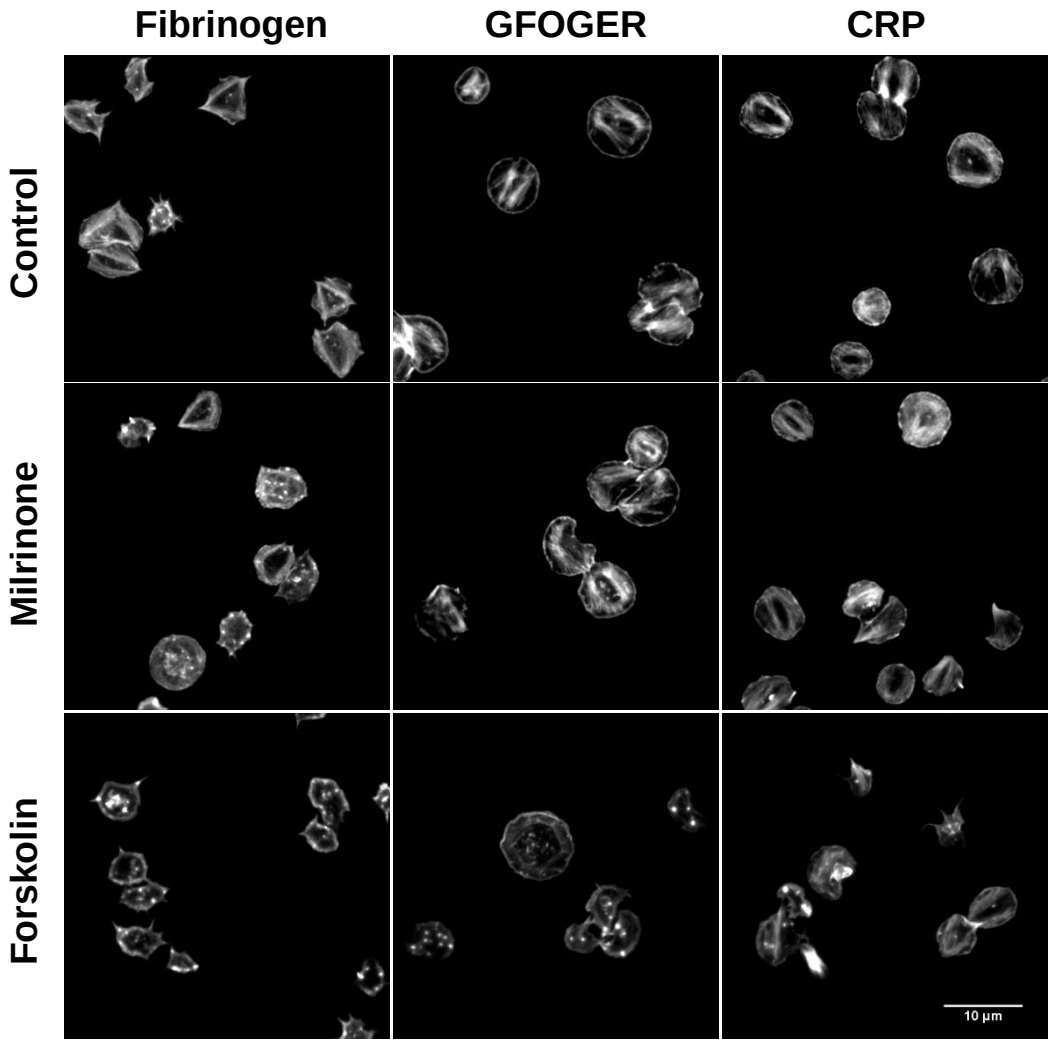

Figure 4.8. ***Effect of cAMP elevating agents on platelets spread on collagen peptides.*** *Platelets ($2x10^7$/ml) were spread on fibrinogen (100µg/ml), GFOGER (10µg/ml) or CRP (3µg/ml) for 25 minutes prior to treatment with vehicle (0.1% DMSO), milrinone (10µM) or forskolin (1µM) for a further 20 minutes. Platelets were then fixed in 4% formaldehyde and permeabilised in 0.1% Triton x-100 before being stained in rhodamine-B phalloidin. Images are representative of 3 independent experiments. Scale bar represents 10µm.*

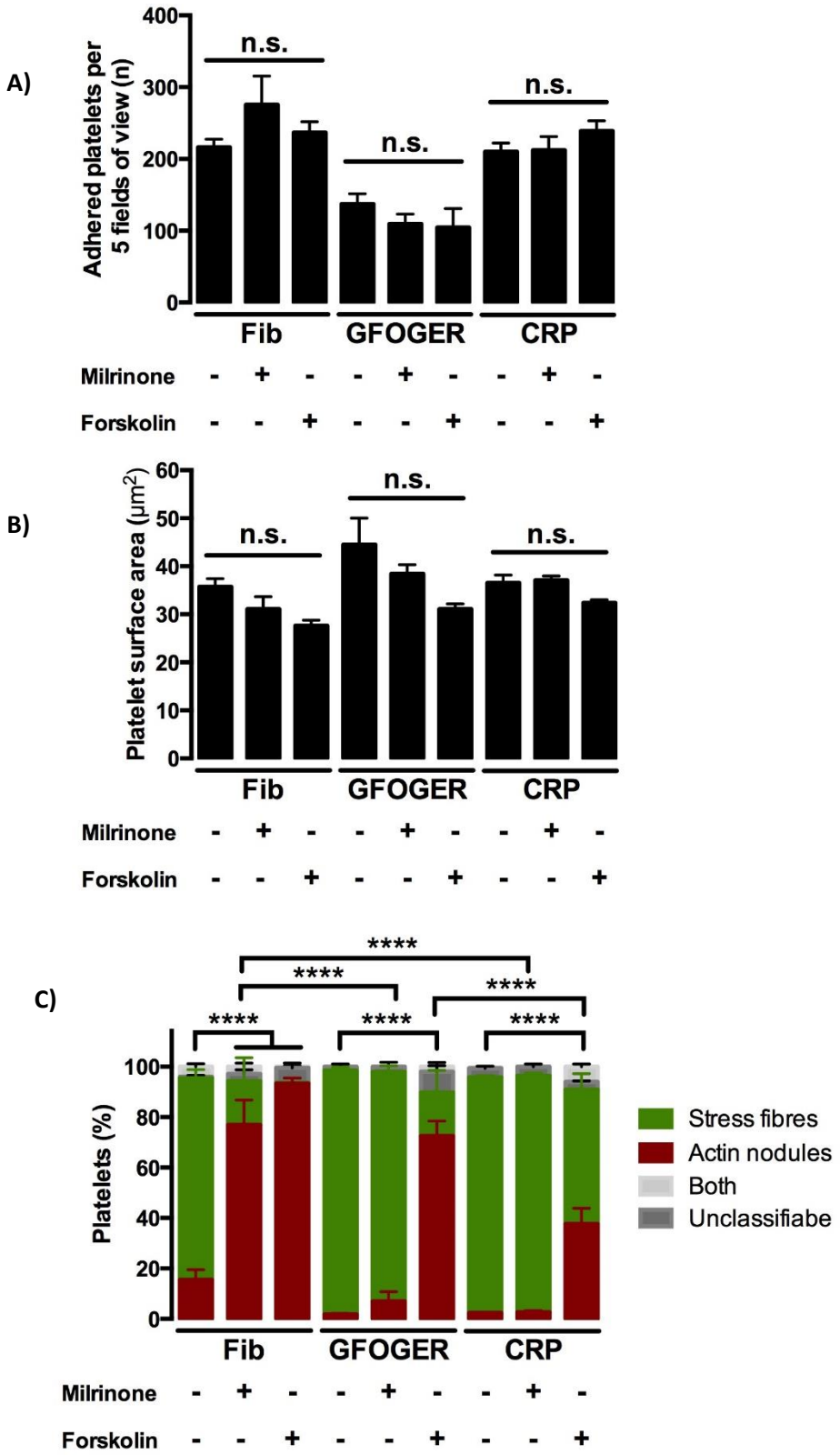

Figure 4.9. Analysis of the effect of cAMP elevating agents on platelets spread on collagen peptides. *Platelets (2x10^7/ml) were spread on fibrinogen (100μg/ml), GFOGER (10μg/ml) or CRP (3μg/ml) for 25 minutes prior to treatment with vehicle (0.1% DMSO), milrinone (10μM) or forskolin (1μM) for a further 20 minutes.* ***A)*** *Platelet adhesion per 5 fields of view.* ***B)*** *Spread platelet surface area.* ***C)*** *Percentage of platelets positive for stress fibres, actin nodules, both or unclassifiable. Data represents the means ± SEM of at least three independent experiments, with significance defined as p ≥ 0.05 (* ≤ 0.05, ** ≤ 0.01, *** ≤ 0.001, **** ≤ 0.0001).*

4.2.7. Investigation of the effect of PGI_2 and other PKA elevating agents in platelets spread on fibronectin

To investigate if the reversal seen on fibrinogen, and lack of reversal on collagen, were exclusive to these matrices, another matrix protein, fibronectin, was investigated. Platelets were spread on 50µg/ml fibronectin for 25 minutes prior to treatment with either vehicle control (0.1% DMSO + 0.005% ethanol), 10nM PGI_2, 10µM milrinone or 1µM forskolin for a further 20 minutes.

Shown in figures 4.10., platelets readily spread on fibronectin, covering an average area of 45.92µm^2 ± 1.96 and almost exclusively forming stress fibres. In response to PGI_2, these platelets significantly reverse their formed stress fibres into actin nodules. Alongside this, platelet surface area in PGI_2 treated platelets appeared to be reduced, however this was not statistically significant with the number of repeats performed. Upon treatment with milrinone, platelets also significantly reverse their formed stress fibres into actin nodules. Like with PGI_2 treatment, platelets treated with milrinone did not significantly reduce their platelet spreading. Forskolin treatment again led to a significant reduction in stress fibres, and a significant increase in platelets positive for actin nodules. Platelet surface area was non-significantly reduced. These findings suggest that platelet reversibility is not constrained to platelets spread on fibrinogen, and that the disparity of effect between fibrinogen and collagen is likely due to collagen/GPVI signalling.

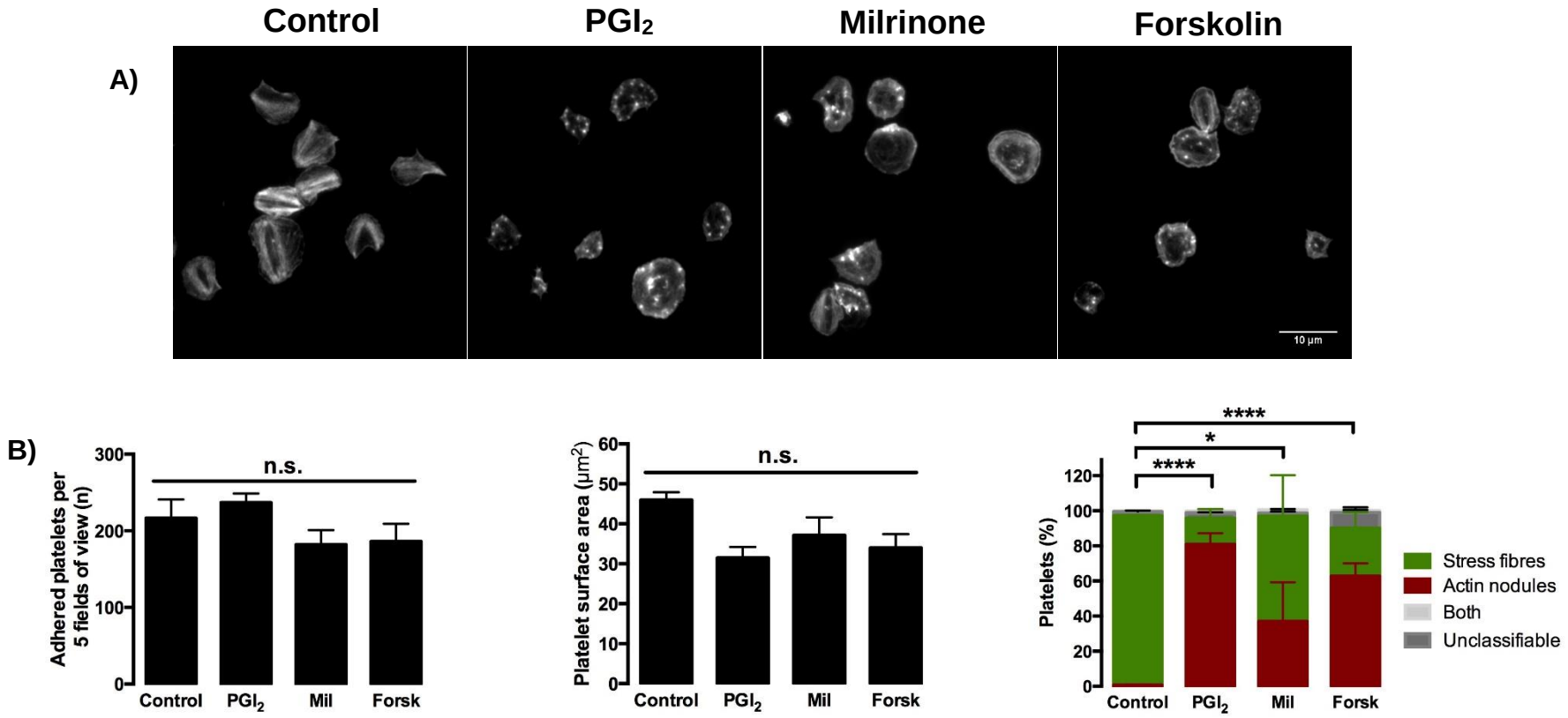

Figure 4.10. **Effect of PKA elevating agents on platelets spread on fibronectin.** Platelets ($2x10^7$/ml) were spread on fibronectin (50µg/ml) for 25 minutes prior to treatment with vehicle (0.005% ethanol), PGI_2 (10nM), milrinone (10µM) or forskolin (1µM) for a further 20 minutes. Platelets were then fixed in 4% formaldehyde and permeabilised in 0.1% Triton x-100 before being stained in rhodamine-B phalloidin. **A)** Representative images. **B)** Platelet adhesion. **C)** Mean platelet surface area. **D)** Percentage of platelets positive for stress fibres, actin nodule or both. Additionally, platelets that were unidentifiable were classified as unclassifiable. Data is representative of 3 independent experiments with significance defined as $p<0.05$ (* ≤ 0.05, ** ≤ 0.01, *** ≤ 0.001, **** ≤ 0.0001). Scale bare represents 10µm.

4.2.8. Investigation of markers of PKA activity in platelets spread on different matrices

The finding that platelets spread on collagen are resistant, whereas platelets are sensitive, to PGI_2 in an AC-dependent manner, suggests that levels of intraplatelet cAMP and thus PKA activity downstream is different among these matrices. Therefore, markers of downstream PKA activity were investigated. This was initially done due to the high cost of quantifying cAMP levels via ELISA methodology. If a difference in downstream PKA signalling was identified, cAMP analysis would then be performed. Conversely, if there was no discernible difference in PKA activity among platelets spread on different matrices, then cAMP analysis would not be investigated.

Possibly the most widely used marker for PKA activity has been the focal adhesion-binding protein, VASP. $pVASP^{ser157}$ and $pVASP^{ser239}$ have been used extensively to demonstrate PKA and PKG activity in many cell types, respectively (272,273,307). To investigate this marker of PKA activation, platelets were spread on fibrinogen, collagen, GFOGER or CRP for 25 minutes prior to treatment with 10nM PGI_2 for a further 20 minutes. Platelets were then lysed and probed for the presence of $pVASP^{ser157}$. As shown in figure 4.11., platelets spread on fibrinogen have very little $pVASP^{ser157}$, whereas upon treatment with PGI_2, phosphorylation increases. Strikingly, platelets spread on either collagen or CRP have very high levels of $pVASP^{ser157}$which are comparable to those seen in fibrinogen spread platelets treated with PGI_2. The addition of PGI_2 did not significantly increase levels of $pVASP^{ser157}$, most likely due to maximal phosphorylation of its serine residues irrespective of treatment. This surprising data suggests that platelets spread on collagen or CRP (and therefore GPVI activation) results in drastically different PKA signalling when compared to fibrinogen or GFO (and therefore $\alpha_2\beta_1$activated) spread platelets.

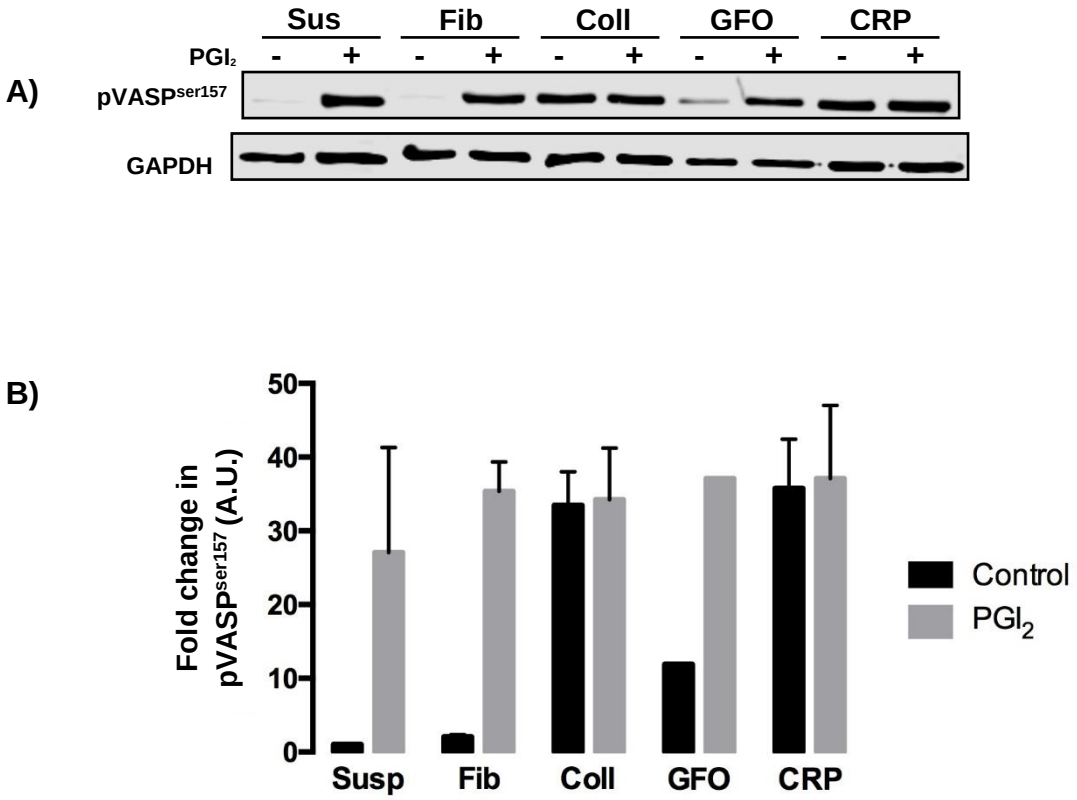

Figure 4.11. Phosphorylation of VASPser157 in response to PGI_2 treatment in platelets spread on different matrices. *Platelets ($2x10^8$/ml) were spread on either fibrinogen (100µg/ml), collagen (100µg/ml), GFOGER (10µg/ml) or CRP (3µg/ml) for 25 minutes prior to treatment with vehicle control (0.005% ethanol) or PGI_2 (10nM). In addition, platelets in suspension ($1x10^9$/ml) were treated with either vehicle (0.005% ethanol) or PGI_2 (100nM) for 2 minutes. After treatment platelets were lysed in 2x cell lysis buffer and protein quantified using a colorimetric assay. Protein was equally loaded onto a 10% gel, ran under electrophoresis, blotted and probed for pVASPser157. GAPDH was also probed as a loading control.* ***A)*** *Representative immunoblot demonstrating banding of pVASPser157 (top) and GAPDH (bottom).* ***B)*** *Relative densities of $pVASP^{ser157}$. All densities were normalised to their GAPDH loading control and expressed as fold change over basal (untreated suspension) platelets. Bands and densities are representative of two independent repeats, however the GFO group consist of one repeat due to technical issues with platelet spreading.*

The surprising finding that platelets spread on collagen or CRP have high levels of pVASP^{ser157} phosphorylation, but stress fibres can form and remain sustained irrespective of PGI_2 treatment, suggested that these platelets have become disengaged from typical inhibitory PKA signalling. To ensure these platelets were activating PKA and not some other kinase that causes and increase in pVASP^{ser157} levels, platelets were spread and treated identically to the previous pVASPser157 blots and probed for the presence of phosphorylated substrates of PKA. It was decided that the GOFGER peptide was not investigated due to previous issues with platelet spreading.

As shown in figure 4.12., platelets spread on fibrinogen have a small number of phosphorylated substrates notably at ~120 and ~45kDa, indicating minimal PKA substrate phosphorylation and therefore PKA activity in these platelets. Upon treatment PGI_2, multiple bands of varying intensity can be seen, indicating that PKA was activated and was phosphorylating more target substrates than control platelets. These changes in phosphorylation include the appearance of likely two high molecular weight bands over 120kDa, and two bands at ~90kDa and ~50kDa. Interestingly, the band at ~45kDa in control fibrinogen spread platelets decreases in response to PGI_2 treatment. Strikingly, PKA substrate phosphorylation in platelet spread on collagen was drastically increased when compared to fibrinogen-spread platelets, indicating that PKA was highly activated when spread on collagen. Most notably, there was a highly saturated band at ~45kDa, suggesting that there is a substrate within collagen and fibrinogen spread platelets that is robustly phosphorylated in control conditions. This robust phosphorylation of the ~45kDa protein remained unchanged when collagen spread platelet were treated with PGI_2, however there were several changes in the substrate profile, most notably the appearance of one or two high molecular weight bands at >120kDa, as seen in fibrinogen spread platelets treated with PGI_2, and another at ~50kDa. However, this increase in intensity of the ~50kDa band is variable among donors, with no band showing in others. The lack of difference in band intensity at ~45kDa suggests control spread platelet have fully saturated PKA-mediated phosphorylation of this substrate and cannot be phosphorylated in further detectable quantities. Similar to collagen spread platelets, platelets spread on 3µg/ml CRP demonstrated a similar phosphorylation profile, with minimal response to PGI_2, further suggesting that GPVI is likely the receptor mediating the lack of effect of PGI_2 on the spread platelet actin cytoskeleton. Collectively, the findings that fibrinogen spread platelets have a

drastically different PKA substrate phosphorylation profile to platelets spread on either collagen or CRP suggests that platelets spread on fibrinogen are more responsive to PGI_2. This disappearance of the ~45kDa band in PGI_2 treated platelet spread on fibrinogen, but not on collagen or CRP, suggests that this substrate may play an integral part in the cytoskeletal response.

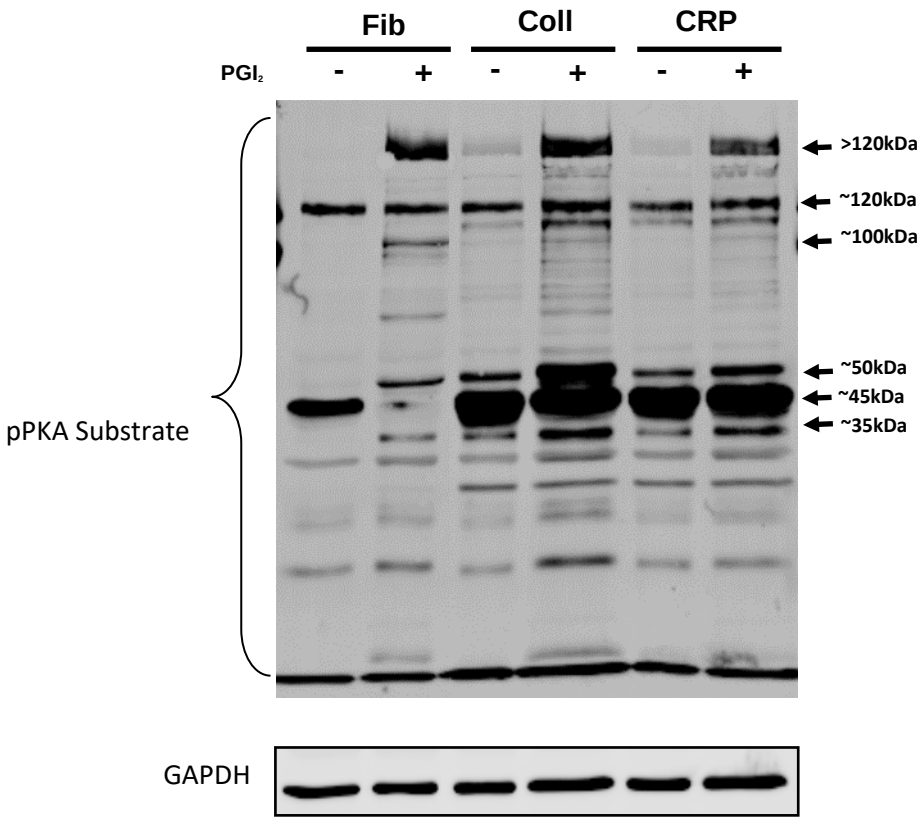

Figure 4.12. Effect of PGI_2 treatment on PKA substrate phosphorylation in platelets spread on different matrices. *Representative immunoblot demonstrating banding of pPKA substrate (top) and GAPDH (bottom). Platelets ($2x10^8$) were spread on either fibrinogen (100µg/ml), collagen (100µg/ml) or CRP (3µg/ml) for 25 minutes prior to treatment with vehicle control (0.005% ethanol) or PGI_2 (10nM). After treatment platelets were lysed in 2x cell lysis buffer and protein quantified using a colorimetric assay. Protein was equally loaded onto a 10% gel, ran under electrophoresis, blotted and probed for pPKA substrate abundance. GAPDH was also probed as a loading control. Blots are representative of three independent repeat experiments.*

4.2.9. Effect of PGI_2 and forskolin on collagen-established thrombi

The findings surrounding stress fibre reversal in response to PGI_2 indicated that platelets more readily respond to PGI_2 when spread on fibrinogen and fibronectin or activated through $\alpha_2\beta_1$. It was theorised that platelets on the outside of the thrombus predominantly interact with fibrinogen, which bridges platelets together and therefore would respond to PGI_2 treatment, whereas platelets interacting with collagen would be resistant. To investigate this, anticoagulated whole blood was flowed over microfluidic flow channels for 2 minutes at 1000^{s-1} prior to being perfused with either vehicle control, PGI_2 or forskolin for a further 20 minutes at the same shear rate. Due to technical issues, thrombi could not be recorded in real time. Taking this into account, thrombi were fixed in formaldehyde and stained once more using $DiOC_6$ and imaged under epifluorescence.

Upon perfusion of whole blood for 2 minutes and treatment with the vehicle control for 20 minutes, platelets readily adhere, spread and form microthrombi (shown in figure 4.13.). Thrombus surface coverage was measured as 50.87% ± 2.91 of the flow channel. Thrombus height was measured as 12.57µm ± 1.23, indicating that platelet had stacked to form microthrombi. Upon post perfusion of thrombi with PGI_2, there was an observable reduction in thrombus height, however surface coverage of the channel remained similar as with control conditions. Thrombus height in response to AC activation via forskolin perfusion resulted in a diminished thrombus height. Interestingly, surface coverage of platelets treated with forskolin was reduced and may reflect the reduced spreading of the basal layers of platelets interacting with collagen. This seems likely, given the findings from the static platelet spread assays on collagen, where PGI_2 had no effect on spreading or stress fibre reversal, whereas forskolin treatment led to a significant reduction in surface area and stress fibres (shown in figures 4.8. and 4.9.). These findings suggest that platelets interacting with collagen under flow do not respond to PGI_2 in an AC dependent manner, however platelets in the upper layers of the thrombus, likely interacting with fibrinogen, are embolised.

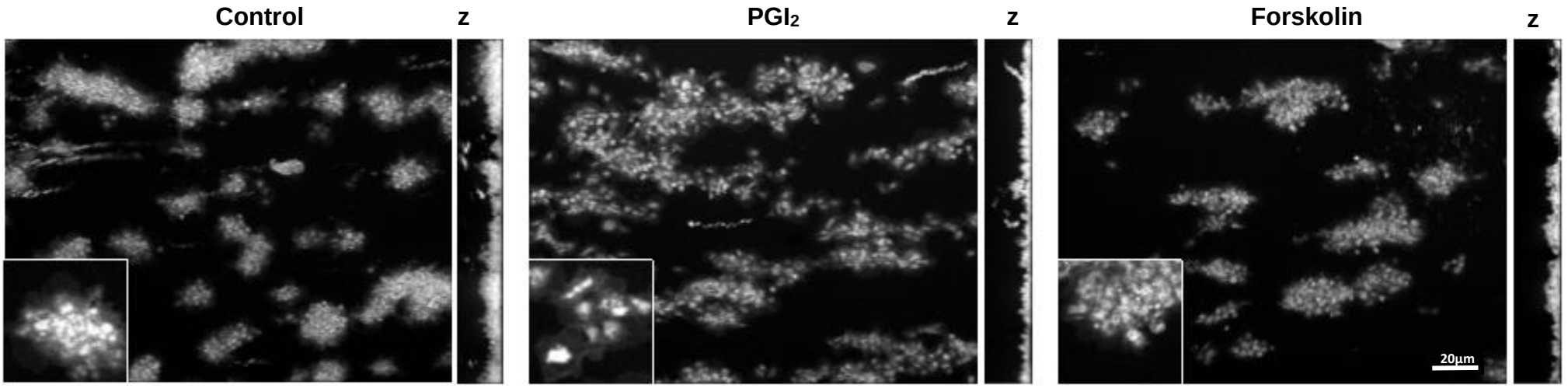

Figure 4.13. Effect of post-perfusion of PGI_2 and forskolin on thrombi formed on collagen. *Whole blood anticoagulated with PPACK (50µM) and stained with $DiOC_6$ (10µM) was flowed over collagen coated (25µg/ml) microfluidic channels for 2 minutes at 1000^{s-1} shear rate. Formed thrombi were then perfused with control (0.01% DMSO, 0.005% ethanol), PGI_2 (100nM) or forskolin (1µM) for a further 20 minutes. Thrombi were fixed in 4% formaldehyde and stained once more with $DiOC_6$ before being imaged and Z-stacked via epifluorescence. Main panels represent the xy plane, with lower left inserts demonstrating basal platelet layer spreading. Z = z stack demonstrating thrombus height. Images are representative of 2 independent repeats. Scale bar represents 20µm.*

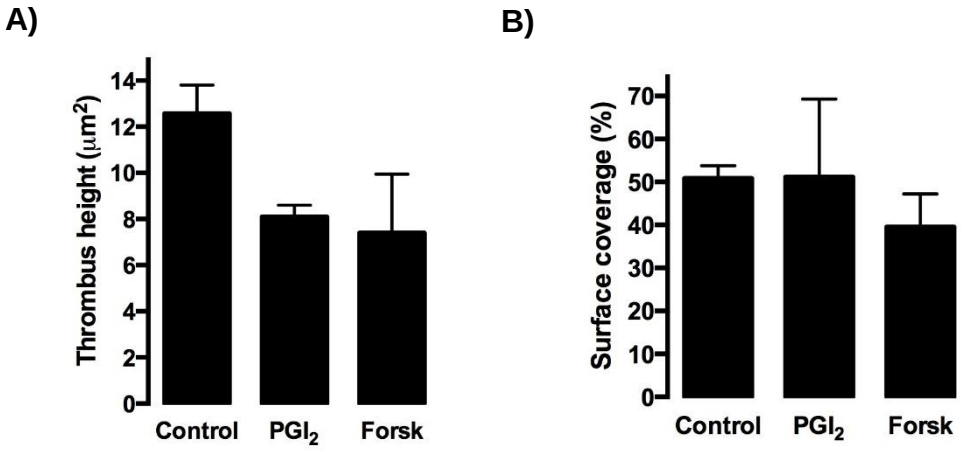

Figure 4.14. Analysis of the effect of post-perfusion of PGI_2 and forskolin on thrombi formed on collagen. A) *Thrombus height as measured through z-stacking of tested microfluidic channels,* ***B)*** *Percentage coverage of the channels by thrombi. Data representative of two independent repeats, with data representing the mean and error bars representing SD.*

4.2.10. Effect of PGI_2 on platelets flowed over fibrinogen

As preliminary results showed that platelets within a collagen-activated thrombus have differential responses to PGI_2, with those interacting with the basal collagen layer being resistant to PGI_2, and those in the upper layers embolising away, it was decided that the platelet response to PGI_2 when flowed over fibrinogen would be investigated. Anticoagulated whole blood was flowed over fibrinogen coated microfluidic channels for 2 minutes at 1000^{s-1} shear rate prior to perfusion of PGI_2 or vehicle control for a further 20 minutes. Platelets were then fixed in formaldehyde, permeabilised with 0.1% triton x-100 and stained for both actin and the platelet membrane with rhodamine-B phalloidin and $DiOC_6$, respectively.

As shown in figure 4.15. and analysed in figure 4.16., platelets readily adhere and spread on fibrinogen and treated with buffer and 0.005% ethanol. Platelet adhesion (B) was measured as 915 ± 154 platelets per $0.5\mu m^2$ of the flow channel. These platelets were mostly positive for actin stress fibres, with a small proportion of platelets being positive for actin nodules. Individual platelet surface area in control platelets was $27.33\mu m^2$ ± 3.62 and overall surface coverage of the flow channel was 65.45% ± 2.44. In response to PGI_2 perfusion, platelet adhesion remained unchanged, indicating that when flowed and spread on fibrinogen, platelets remain adhered regardless of PGI_2 treatment. There was a stark reduction in platelet stress fibre in response to PGI_2, with no stress fibres being visible in any images taken. There was a massive increase in the proportion of platelets positive for actin nodules, and in line with this reduction of stress fibres and formation of actin nodules, individual platelet surface area and overall surface coverage of the channel was reduced. These findings indicate that platelet flowed and spread on fibrinogen readily form stress fibres and that these stress fibres can be reversed by PGI_2 treatment.

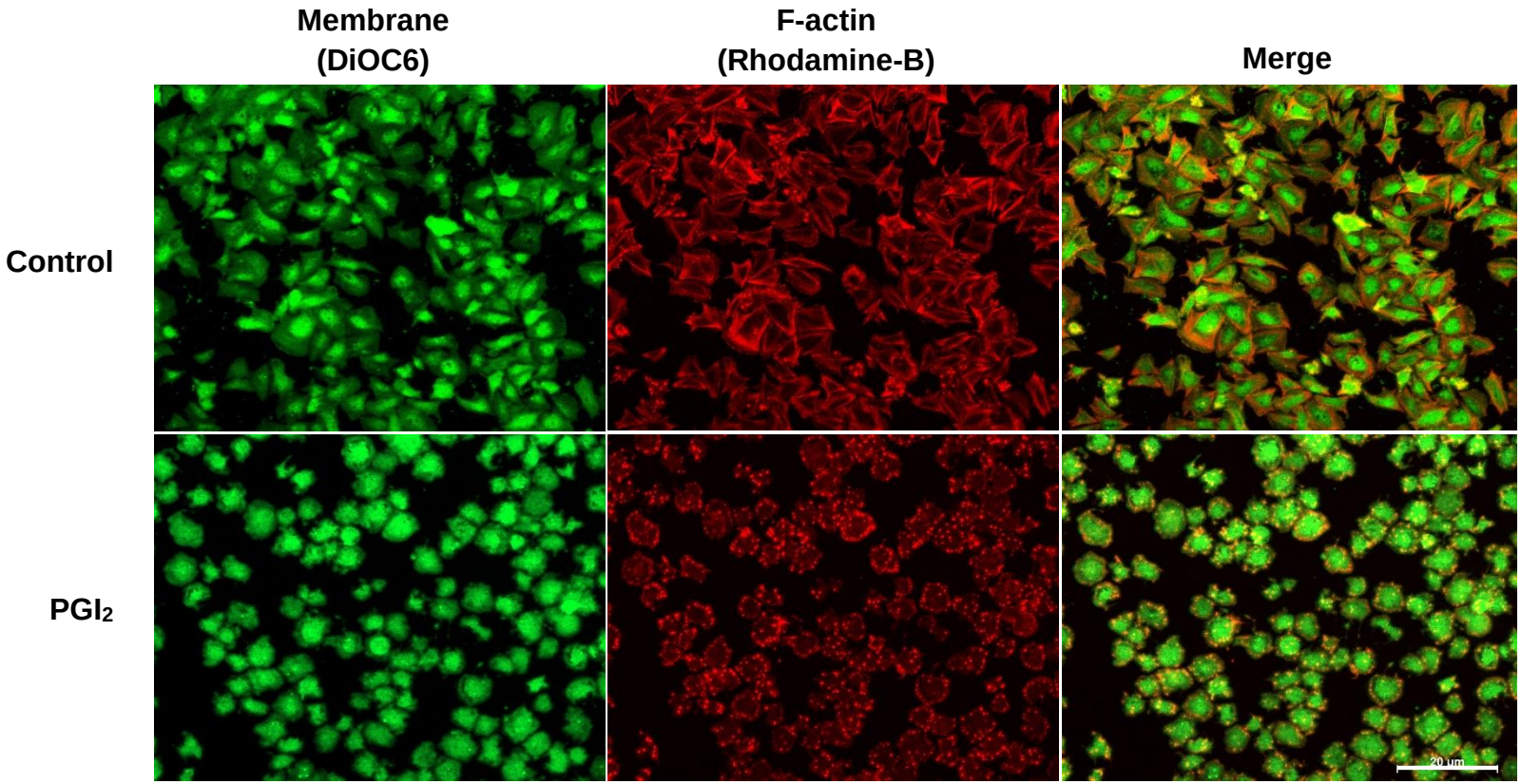

Figure 4.15. Effect of PGI_2 on platelets flowed, adhered and spread over fibrinogen. *Whole blood anticoagulated with PPACK (50µM) and stained with DiOC6 (10µM) was flowed over fibrinogen coated (300µg/ml) microfluidic channels for 2 minutes at 1000^{s-1} shear rate. Formed thrombi were then perfused with control buffer (0.005% ethanol) or PGI_2 (100nM) for a further 20 minutes. Thrombi were then fixed with 4% formaldehyde and permeabilised with 0.1% triton x-100 before being stained again with DiOC6 and the f-actin stain, rhodamine-B phalloidin. Images were acquired via epifluorescence microscopy. Images are representative of two independent repeats. Scale bar represents 20µm.*

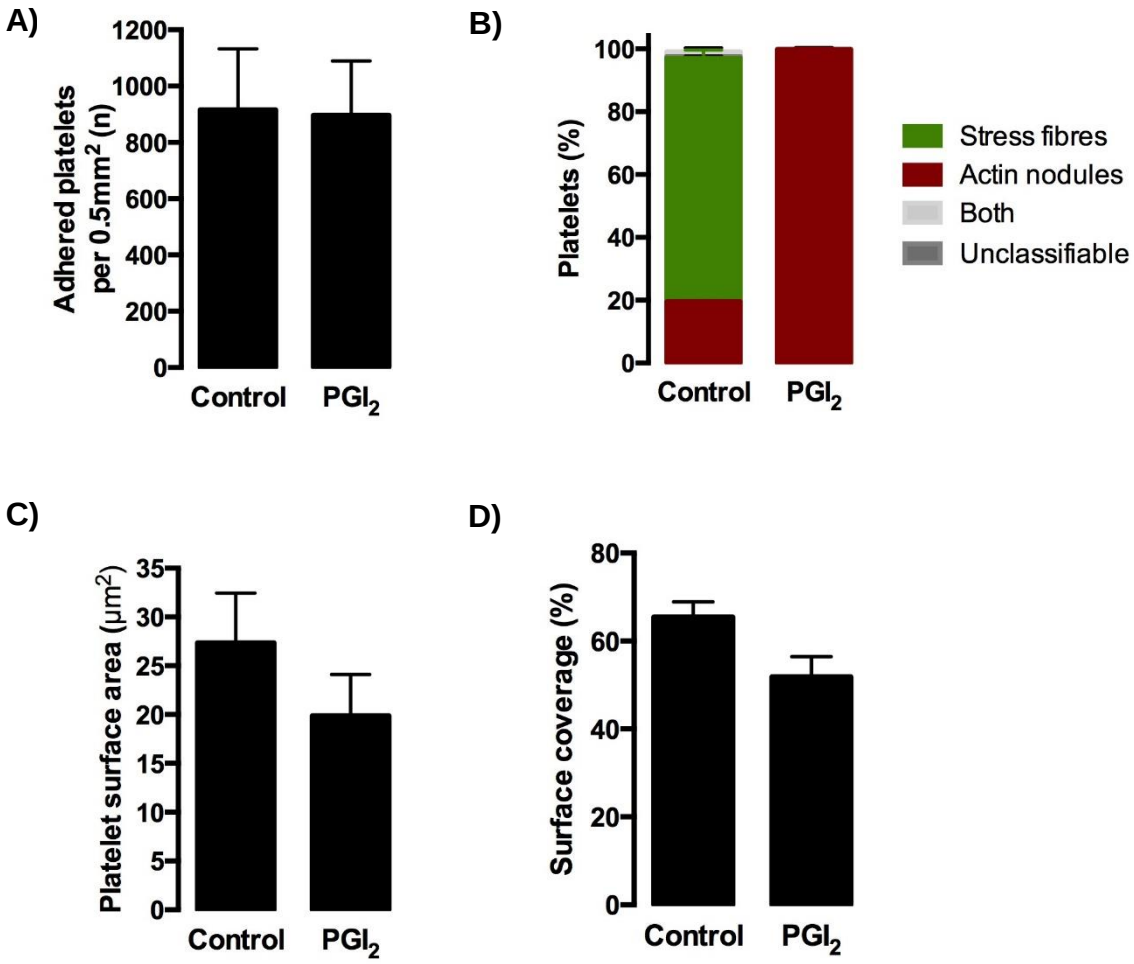

Figure 4.16. Analysis of the Effect of PGI_2 on platelets flowed, adhered and spread over fibrinogen. A) *Number of platelets adhered to the flow channel per 0.5mm^2.* ***B)*** *Percentage of platelets positive for actin structures.* ***C)*** *Mean individual platelet surface area.* ***D)*** *Overall thrombi surface coverage of the flow channel. Data representative of two independent repeats, with data representing the mean and error bars representing SD.*

4.3. Discussion

The aim of this chapters was to determine the effect of PGI_2 on collagen spread platelets. Previously our group had demonstrated that platelets become resistant to PGI_2-mediated stress fibre reversal in response to PGI_2, unlike fibrinogen spread platelets that readily reverse their stress fibres (273). A series of experiments were designed to uncover the mechanism(s) by which collagen induces this resistance. Firstly, platelets were preincubated with PGI_2 and spread on a collagen-coated matrix (100µg/ml) for varying times to determine the temporal effect of PGI_2 on platelet spreading. Surprisingly, it was found that PGI_2 at 10nM had no effect on platelet adhesion or spreading, including the number of platelets positive for stress fibres. This was in complete contrast to fibrinogen spread platelets, which completely reversed their stress fibres and formed actin nodules. Although PGI_2 has been shown to inhibit platelet spreading and adhesion in platelet spreading on collagen, this was seen using higher concentrations of PGI_2 than used here (228)

Considering the surprising lack of effect of PGI_2 preincubation on platelets spreading, the effect of PGI_2 on platelets which were already spread on collagen was explored. Additionally, in this experiment, the role of the secondary mediators of platelet activation, ADP and TXA_2, was investigated using apyrase and indomethacin, respectively. The impact of these was probed due to that ability for P2Y12 to inhibit AC and TXA_2 to activate p115RhoGEF and thus the RhoA pathway, possibly leading to stress fibre formation (172,308,309). Similarly, with preincubation, spread platelets treated with PGI_2 were unaffected. Formed stress fibres remained and there were few platelets positive for actin nodules and there was no difference in platelet adhesion. In the presence of apyrase and indomethacin there was no effect on stress fibre formation, however there appeared to be a large decrease in the number of platelets adhering to the matrix. Although this was statistically insignificant, another repeat of the experiment could clarify this finding. These findings indicate that; a) collagen spread platelets are completely resistant to PGI_2; and b) this lack of effect is not due to activation of secondary mediator signalling and must be a result of some other mechanism.

Having found that the lack PGI_2 response in collagen spread platelets was not due to secondary mediator signalling, the role of cAMP synthesis and breakdown was next investigated. This was undertaken using both an activator of AC, forskolin, and the PDE3 inhibitor, milrinone. Firstly, these two compounds were validated for

efficacy by pre-treating platelets before being spread on fibrinogen. This was done to ensure that the compounds were working properly and that they showed the same results as our group have previously reported. As expected, treatment with either milrinone or forskolin led to a significant reduction in the numbers of platelet adhesion, platelet spreading and the number of platelets positive for stress fibres when interacting with fibrinogen. These findings indicated that these compounds were working as expected and could then be confidently used in collagen spread platelets. Collagen spread platelets were found not to reverse their stress fibres in the presence of milrinone, indicating that PDE3 activity was not causing resistance. Interestingly, forskolin caused a significant reversal of stress fibres in platelets, suggesting that the lack of response seen with PGI_2 treatment was due to inhibition of AC. However, forskolin did not cause complete stress fibre reversal, which was found in fibrinogen spread platelets by our lab previously (273). This suggested that there might be a strong inhibition of AC, which even pharmacological activation cannot fully reverse.

As collagen has two main receptors in human platelets, GPVI and $\alpha_2\beta_1$, an experiment was designed to determine the receptor responsible for PGI_2 resistance. Platelets were spread on fibrinogen, collagen, CRP and GFOGER, the latter two of which specifically activate GPVI and $\alpha_2\beta_1$, respectively. Consistent with previous findings, fibrinogen spread platelets significantly reverse their stress fibres and form actin nodules, whereas collagen-spread platelets are completely resistant. Platelets spread on GFOGER significantly reversed their actin nodules and formed stress fibres, whereas CRP-spread platelets did not. This finding suggested that the resistance in collagen-spread platelets to PGI_2 was largely due GPVI signalling. However, the incomplete response to PGI_2 seen in GFOGER-spread platelets suggested that there may be some residual resistance to PGI_2 and required further investigation. This was done through the use of milrinone and forskolin in GFOGER- and CRP-spread platelets. Here it was found that platelets spread on GFOGER or CRP peptides did not reverse their stress fibres in response to milrinone treatment, but did so in response to forskolin, which indicated that either matrix may have altered the activity of AC. Interestingly, when compared to each other, forskolin-mediated reversal of stress fibres was significantly higher in platelets spread on CRP than GFOGER. These findings suggested that GPVI may be the key player in PGI_2 resistance in collagen-spread platelet, however some resistance may be contributed to by $\alpha_2\beta_1$ activation.

As there was significant PGI_2 resistance in both GFOGER- and CRP-spread platelets, it posed the question if it was in fact $\alpha_{II}\beta_3$ that was the cause of the difference in PGI_2 response. In that instance, fibrinogen would be imparting increased sensitivity. To address this, another matrix protein, fibronectin, was used to spread platelets prior to treatment with PGI_2, milrinone and forskolin. This led to a significant reduction in the percentage of platelets positive for stress fibres and an increase in the number of those positive for actin nodules in response to PGI_2, milrinone and forskolin. This indicated that fibronectin, like fibrinogen, was sensitive to PGI_2 and further supported the hypothesis that collagen spread platelets are uniquely resistant.

With the evidence that collagen specifically causes PGI_2 insensitivity in spread platelets, which was likely due to AC inhibition through GPVI activation, the signalling involved in this process was investigated. A major marker in the study into PKA activation is the presence of $pVASP^{ser157}$ and was used here on platelet lysates which were formed by spreading platelets on fibrinogen, collagen, GFOGER and CRP and subsequent treatment with PGI_2. Additionally, platelets in suspension were treated with or without PGI_2 as controls to demonstrate $pVASP^{ser157}$ levels irrespective of matrix binding as a point of reference. In complete contrast to the hypothesised findings, platelets spread on collagen or CRP had higher levels of $pVASP^{ser157}$ compared to PGI_2-treated fibrinogen-spread platelets or those in suspension. Importantly, platelets that had spread on GFOGER appeared to have lower $pVASP^{ser157}$ levels when untreated than those on collagen or CRP and had basal $pVASP^{ser157}$ levels more akin to fibrinogen-spread platelets. The origin of the increase in collagen/CRP-spread platelets is unknown and there have been no reports of this previously. Wentworth *et al.* have previously reported the phosphorylation of $VASP^{ser157}$ in response to thrombin, which was dependent on both PKC and ROCK. This could mean that enhanced RhoA or ROCK activity in GPVI activated platelets was causing VASP phosphorylation (310). This also demonstrates that although often presented as a PKA-specific marker, the presence or pVASPser157 may not be completely exclusive with PKA activity.

In parallel with the $pVASP^{ser157}$ probing, lysates were also used to probe for the abundance of phosphorylated PKA substrate residues. Unfortunately, there was no GFOGER lysate left for testing. With the remaining fibrinogen, collagen and

CRP lysates, it was found that pPKA substrate abundance, irrespective or PGI_2 treatment was much higher than that found in control fibrinogen spread platelets. Again, this was a surprising finding and may, along with the $pVASP^{ser157}$ findings, suggest that PKA was being activated, possibly in a cAMP-independent manner. This concept is not new to biology and there have been several reports surrounding cAMP-independent activation of both type I and II PKA in other cell lines (311,312). Perhaps more interesting is how PKA could remain active in collagen- and CRP-spread platelets, but not cause stress fibre reversal seen with those on fibrinogen. This may be a result of some form of disengagement between PKA and the actin cytoskeleton, which would otherwise be allowed to interact in fibrinogen and fibronectin-spread platelets and lead to stress fibre reversal. This may demonstrate a proactivatory nature of PKA signalling in platelets, which has been a controversial topic for several years (313). Such findings suggest that PKA activation in platelets leads to bleb formation, procoagulant microparticle release and phosphatidylserine exposure. Interestingly, long-standing research has demonstrated that collagen but not fibrinogen surfaces induce similar effects (314), and given our findings, suggests that PKA signalling in collagen spread platelets is intact and activated in a cAMP independent manner, leading to enhanced platelet activation. Hiratsuka *et al* (2017) have recently reported the development of a PKA probe for *in vivo* detection of PKA levels. In agreement with the reduction of thrombus height in response to PGI_2 treatment, the outer shell of the thrombus in their study was rich in PKA activity. Importantly, as too was the inner core that was interacting with the subendothelial matrix. Therefore, it seems that PKA in platelets may contribute to their activation and supports the theory from the Xiaoping Du lab that cyclic nucleotide signalling also plays a role in platelet activation (Li et al., 2003). This could be initially investigated by incubating platelets with inhibitors of PKA such as Rp-cAMPS and KT-5720, which have been used successfully in platelets in previous studies, and then spreading these platelets on collagen. If this hypothesis is correct, platelet spreading on collagen would be markedly reduced.

In response to GPVI stimulation, this work has determined that collagen spread platelets are resistant to PGI_2, yet counterintuitively, markers of PKA activity are elevated. These findings suggest that as AC function is inhibited, PKA activity is increased. There are currently no reports of this effect in platelets, which suggests that this finding is novel. However, the signalling responsible for this needs to be investigated further. A potential cause of collagen-mediated PGI_2 resistance is the

intermediate of sphingolipid metabolism, sphingosine, which has been shown to cause cAMP-independent activation of PKA in COS cells (315). Platelets contain a sphingosine-1-phosphate receptor, a GPCR than signals through the AC-inhibiting G_i protein (316). Sphingosine-1-phosphate (S1P) has been shown to cause platelet shape change, suggesting that the pathway used by sphingosine-1-phosphate may converge on the regulation of contractility, such as RhoA (317). If this is the case, S1P may be contributing to shape change through activation of RhoA and the inhibition of MLCP, causing increased actin-myosin interactions and contractility. As there is a basal level of AC function in platelets, S1P may be causing inhibition of AC function through activation of Gi, much like ADP signalling. This agrees with the lack of PGI_2 sensitivity in response to ADP signalling inhibition shown in figure 4.3, as it may be S1P that is causing the Gi activation required for AC inhibition in collagen spread platelets. This could be partly addressed by using inhibitors of Gi during platelet spreading on collagen. If S1P signalling is the cause of PGI_2 resistance in GPVI-activated platelets, then inhibition of the resulting signalling may reinstate sensitivity, resulting in stress fibre dissolution in response to PGI_2. To further this work, the S1P receptor modulator, Fingolimod, could be used in similar spreading assays to directly associate S1P with PGI_2 resistance. Additionally, the interplay between sphingosine and its phosphorylation into S1P during platelet activation on collagen should also be uncovered as sphingosine and S1P may be concomitantly activating PKA whilst lowering cAMP, respectively.

There are three AC isoforms detectable in platelets, AC3, AC5 and AC6. There has been limited work into uncovering their regulation in platelets function. The data presented in this chapter indicates that this should be studied further, as their regulation on different matrices may be a fundamental step in the regulation of platelet contractility, thrombus formation and consolidation. AC5/6 have been shown in many different cell types to be potently inhibited by high Ca^{2+} calcium concentration (318–320). Our current understanding of cAMP and Ca^{2+} in platelets is based on reports of PKA inhibiting Ca^{2+} release from intracellular stores and import through TRPC6 (208,321). However, if like in other cell types, Ca^{2+} can be shown to inhibit AC activity, which would indicate a reciprocal inhibitory relationship between the two in platelets that warrants detailed spatiotemporal investigation. GPVI stimulation has been shown to cause a large and sustained increase in Ca^{2+} flux in platelets, which suggests that it may cause inhibition of AC5/6 (322). Importantly, fibrinogen spread platelets have little Ca^{2+} release and the majority of

platelets show no release at all (247), which agrees with the increase in PGI_2 sensitivity in these platelets in previous work and this chapter (273)Ca^{2+} release in GFOGER and $a_2\beta_1$ is also somewhat sustained (323), which again agrees with the data shown in this chapter, where platelets spread on GFOGER were partially resistant to PGI_2 and readily reversed their formed stress fibres when treated with forskolin (figures 4.7. and 4.9., respectively).

As figures 4.1.-4.12. were performed under static conditions and therefore did not address the shear stress that platelets are exposed to within a thrombus, the role of PGI_2 on platelets and thrombi under flow was investigated. Whole anticoagulated blood was flowed over collagen-coated microfluidic flow channels for 2 minutes to establish microthrombi. PGI_2 or forskolin was then perfused over the microthrombi for a further 20 minutes, a timepoint used in the previous static platelet spreading assays. Control thrombi perfused with vehicle remained columnar in nature, brought about by the stacking of many platelets. In contrast to this, thrombi perfused with either PGI_2 or forskolin were almost 2D and had much lower thrombus heights in response to treatment. Interestingly, the basal layers of platelets which were interacting with the collagen matrix appeared to form lamellipodia in control conditions. This was also seen in PGI_2-treated thrombi, again suggesting that these platelets were resistant to PGI_2, but the other upper layers of the thrombus had embolised away, presumably because they were abridged by fibrinogen and thus were sensitive to PGI_2. The underlying platelets in forskolin-perfused thrombi also appeared to have reduced lamellipodia, which agreed with previous static adhesion findings and indicated that under flow conditions, activation of AC in collagen-interacting platelets is sufficient to cause reversal of platelet spreading.

The effect of PGI_2 on platelets flowed over fibrinogen was next investigated as the upper layers of collagen-formed thrombi embolised in response to PGI_2 post-perfusion. It was hypothesised that, in line with the reversal of stress fibres in statics spreading assays, that platelets flowed and spread on fibrinogen would reverse their stress fibres in response to PGI_2. In agreement with this hypothesis, these platelets completely reversed their stress fibres and formed actin nodules. This finding is further suggestive of platelet embolisation from thrombi through the act of PGI_2 under flow through loss of stress fibre-mediated contractility.

4.4. Conclusion

In this chapter, the role of collagen in the resistance of platelets to PGI_2 has been investigated. Collagen can impart complete resistance in platelets to PGI_2 likely through GPVI-dependent inhibition of AC and may be a requirement for functional thrombus formation. This adds yet another layer in the complexity of thrombus formation and demonstrates how different receptor activity can establish the blueprint for thrombus structure, with collagen and GPVI taking centre stage. This process requires further investigation to highlight the signalling involved and may provide novel targets for antithrombotic therapy.

Chapter 5.

Matrix density determines prostacyclin sensitivity and actin nodule characteristics in platelets

5.0 Summary

Cells require machinery and processes for initial binding to matrices to allow for further, more secure binding through actin cytoskeletal rearrangement (324). It has previously been shown that platelets form actin-rich structures, termed actin nodules when initially adhering and spreading on fibrinogen, fibronectin, laminin and vWF (103) and that the actin nodules is critical for adhesion under high shear (229). Interestingly, collagen spread platelets do not form actin nodules, and as I have demonstrated in chapter IV, most likely due to GPVI signalling. It is also clear that different matrices elicit varying actin cytoskeletal responses to cyclic nucleotide signalling, potentially through regulation of AC isoforms or activation of PDEs. Following on from these findings, the aim of this chapter is to uncover the effect of varying fibrinogen matrix concentrations on platelet actin nodule formation and the overall number and dimensions of nodules.

5.1 Introduction

Upon platelet activation on fibrinogen, platelets undergo rapid shape change and begin spreading. At this time, punctate actin-rich structures termed actin nodules form diffusely within the platelet. The actin nodule, is a podosome-like structure consisting of a central bundle of filamentous actin and actin-binding proteins such as WASp and the Arp2/3 complex (103,229). These structures are rich in WASp and tyrosine phosphorylated proteins, the former of which are of unknown purpose, but is thought to result in extrasensory signalling cues from the underlying matrices which transmit downstream, leading to a nuanced platelet response. The importance of WASp in nodules has been demonstrated, with platelets from individuals with WAS being incapable of forming nodules and stable thrombi under shear stress *ex vivo* (229). Surrounding the nodule are integrins, such as $\alpha_{IIb}\beta_3$ for fibrinogen binding, and integrin binding partners, including talin and the mechanosensing protein, vinculin. It has been hypothesised that these integrins surrounding the nodule are pushed away by the ensuing bundles of actin, rather than an integral part of the nodule structure. Therefore, it appears that platelet actin nodules are closely related to podosomes seen in cells including megakaryocytes. Although related, these structures are not homologous, as nodules have been shown to be considerably smaller and shorter lived than podosomes (325).

Although the function of actin nodules in platelets has not been fully explained, these nodules appear to give way to the formation of actin stress fibres, which are

required for resistance to shear stress within the vasculature during thrombus formation. Therefore, the actin nodules is believed to be an in intermediate adhesion complex which further facilitates secure binding through increased actin-myosin interactions, leading to stress fibre formation, and a signalling 'hub' which transmit extracellular matrix cues through enhanced tyrosine phosphorylation. With a focus on the latter, seminal findings from Jirouskova *et al* and supporting evidence from Qui *et al*. show a clear effect of underlying matrix concentration on platelet activation, adhesion and spreading (247,326). Platelets spread on low-density fibrinogen (LDF (3µg/ml)) have a higher surface area and increased tyrosine phosphorylation that those spread on high-density fibrinogen (HDF (100µg/ml)). Although no clear physiological relevance has been linked with these findings, there have been research demonstrating distinct areas within the thrombus, with differing levels of platelet activation throughout. As we have previously shown that formed thrombi begin to embolise upon PGI_2 treatment, it was hypothesised that nodule formation would be impacted by the density of underlying matrix protein, and that this would further be differentially regulated by treatment with PGI_2. The importance of this hypothesised effect could lead to further understanding of the regulation of thrombus formation in both health and disease.

In this chapter I have demonstrated that fibrinogen matrix density affects actin nodule formation in either the presence or absence of PGI_2. Platelets spread on LDF are more resistant to the inhibitory effects of PGI_2 than those spread on HDF, resulting in lower numbers of platelets positive for actin nodules. Using milrinone, a potent PDE3 inhibitor, and forskolin, a potent AC activator, it was found that the resistance to PGI_2 observed in LDF spread platelets was likely due to decreased AC activity, much like those activated on collagen/GPVI. In addition, real time visualisation of actin nodule formation showed that platelets spread on fibrinogen are more numerous and smaller, with a shorter duration than nodules forming in spread platelets without PGI_2 treatment. Therefore, I speculate that actin nodule formation is primarily driven by activation of integrins, with higher numbers of activated integrins leading to more numerous and smaller nodules upon PGI_2 treatment. Furthermore, these smaller nodules are likely to be a result of increased nodule turnover, likely through blockage of an unknown process involved in tethering actin to the plasma membrane in order to form a mature, matrix sensing nodule.

5.2 Results

5.2.1. Effect of PGI_2 on fibrinogen spread platelets

Washed human platelets were spread on fibrinogen (100µg/ml) for 25 minutes prior to washing and treatment with 10nM PGI_2 or a vehicle (0.005% ethanol) control for a further 20 minutes. Platelets were then fixed and permeabilised before being stained with rhodamine-B phalloidin. As previously identified, PGI_2 treatment did not significantly affect platelet adhesion when compared to control conditions (figure 5.1.). However, PGI_2-treatment significantly reduced the average spread platelet area in comparison to control platelets. Furthermore, platelets treated with PGI_2 had reversed their stress fibre formation and formed actin nodules more readily than in control conditions. Interestingly, there appeared to be a difference in nodule size and number in response to PGI_2 treatment. To investigate this, nodular actin staining was manually counted per nodule-positive platelet for 50 platelets per condition, per repeat. Manual measurements of surface area were also taken by freehand drawing around nodules through the Fiji software package. Nodule number in response to PGI_2 was significantly higher than control nodule positive platelets. Additionally, PGI_2 treatment led to a reduction in nodule size. These data indicated that PGI_2 treatment affects nodule size and number in fibrinogen spread platelets.

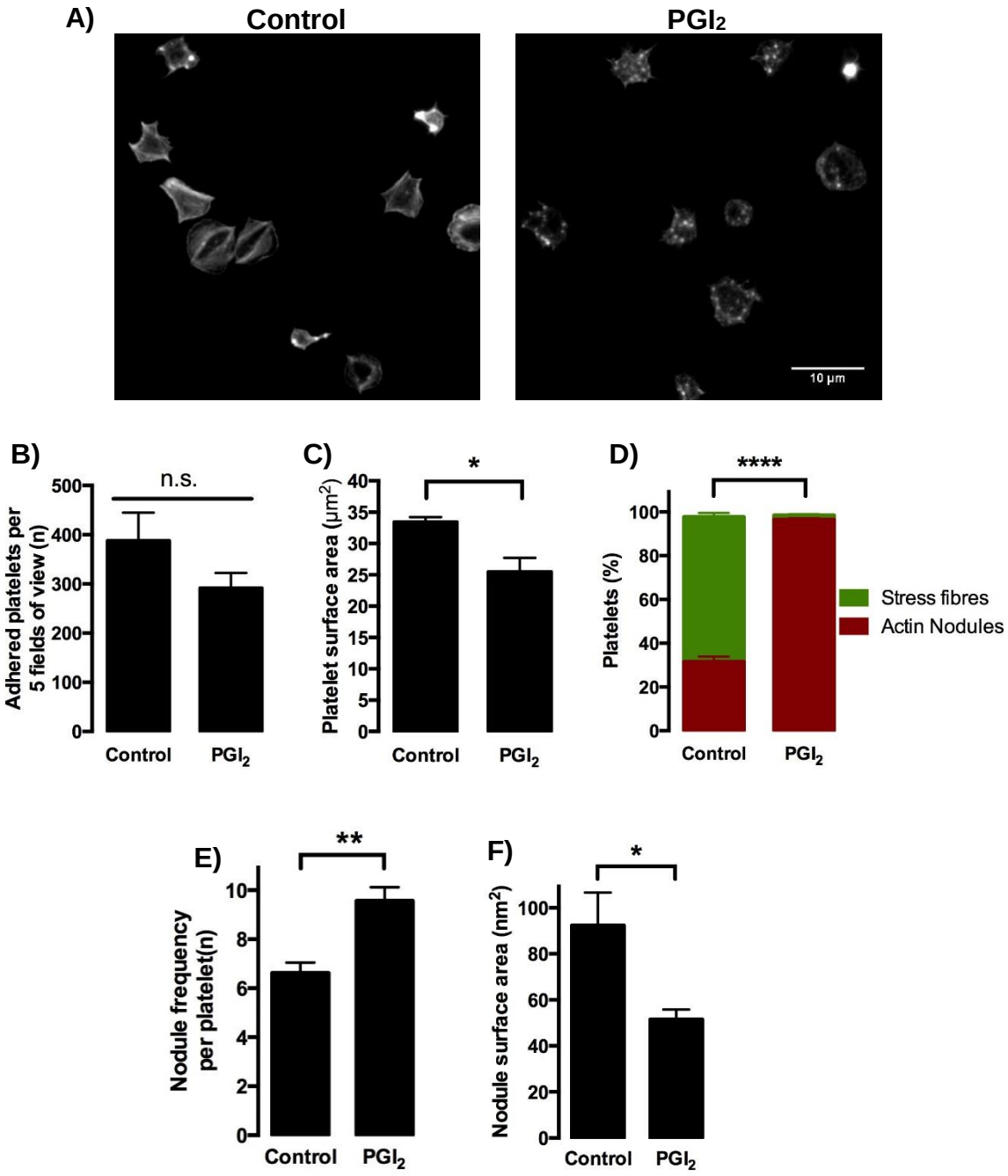

Figure 5.1. Effect of PGI_2 on spread platelets and actin nodule dynamics. *Washed platelets ($2x10^7$/ml) were spread on 100µg/ml fibrinogen for 25 minutes prior to treatment with 10nM PGI_2 or 0.005% ethanol (control) for a further 20 minutes. Platelets were then fixed, permeabilised and stained for F-actin with Rhodamine-B phalloidin.* ***A)*** *Representative images acquired at x63 magnification.* ***B)*** *Average number of platelets adhered per 5 field of view.* ***C)*** *Average platelet surface area.* ***D)*** *Percentage of platelets positive for stress fibres or actin nodules.* ***E)*** *Number of nodules per nodule positive platelet in each condition (50 platelets per condition, per repeat).* ***F)*** *Actin nodule surface area (100 nodules per condition, per repeat). Data is representative of at least 3 independent experiments with significance defined as p ≤ 0.05 (* ≤ 0.05, ** ≤ 0.01, *** ≤ 0.001, **** ≤ 0.0001). Scale bar represents 10µm.*

5.2.2. Effect of NO on nodule size and number in platelets spread on fibrinogen

Having initially demonstrated that PGI_2 treatment leads to an increase in nodule formation and a decrease in their size, we next sought to investigate if this was a phenomenon exclusive to PGI_2, or if this effect was also observed with NO treatment. Images obtained in chapter III (from figure 3.1.) were analysed for nodule number and size. Similar to PGI_2 treatment, NO treatment of spread platelets causes altered actin nodule characteristics (figure 5.2.). Nodule numbers in nodule-positive platelets were increased with GSNO treatment compared to control conditions. Nodule surface area was decreased upon GSNO treatment also. These data indicated that NO, like PGI_2 can also affect nodule size and number in fibrinogen spread platelets.

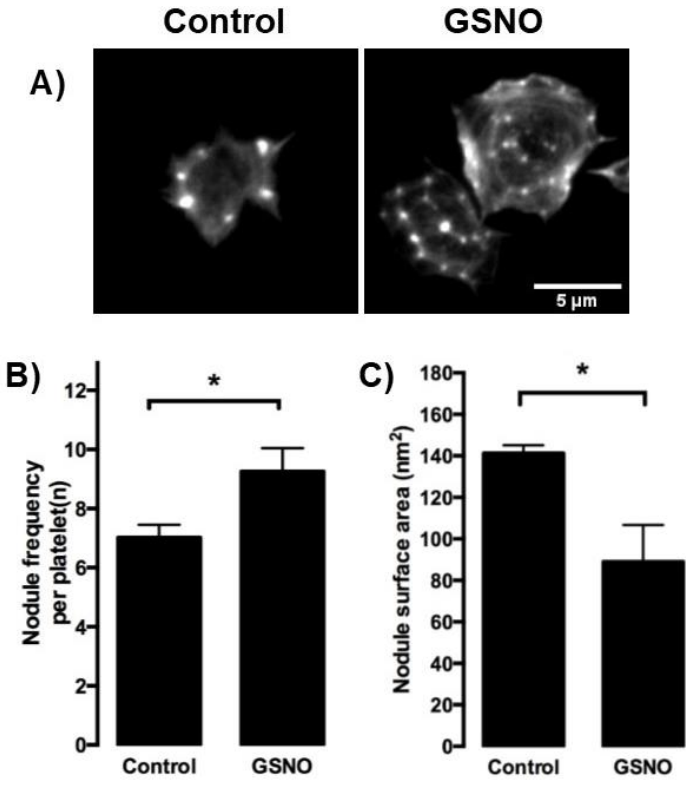

Figure 5.2. Nodule characteristics in spread platelets treated with GSNO. *Platelets ($2x10^7$ were spread on on 100µg/ml fibrinogen for 25 minutes prior to treatment with GSNO (1µM) for a further 20 minutes.* ***A)*** *Representative images.* ***B)*** *Average nodule number per platelet deemed nodule positive. 50 individual platelets per condition and repeat were randomly selected for nodule counting.* ***C)*** *Average nodule surface area. 100 nodules per condition, per repeat were measured manually through the Fiji software package. Data is representative of three independent repeat experiments, with significance defined as p≤0.05.Scale bar represents 5µm.*

5.2.3. Real-time visualisation of actin nodule formation in mouse platelets in repose to PGI_2

The findings uncovered in figure 5.1 (E and F) suggested a change in nodule dynamics upon PGI_2 treatment. To investigate this, real time epifluorescence imaging was performed on platelets isolated from LifeAct-GFP mice. The platelets ($2x10^7$/ml) were spread for 25 minutes in the presence of 0.01U/ml thrombin prior to being treated with or without 100nM PGI_2 for a further 20 minutes. The time series captured was then analysed via the TrackMate plugin in the Fiji software package to determine the number of nodules and their lifetimes and movements within the platelets with 5 platelets per experimental condition, per repeat to be analysed. As mouse platelets do not readily form stress fibres on fibrinogen matrices, thrombin was used prior to the platelet spreading assay so to encourage stress fibre formation and illustrate any real-time reversal. Additionally, due to the use of thrombin in these platelets, initial actin nodule analysis during spreading could not be performed in the same experiment due to a complete lack of nodule formation, with platelets initially spreading with a more amoeboid, lamellipodia-rich phenotype. Therefore, PGI_2 post-treated platelets were compared to non-treated counterparts, which didn't go on to form stress fibres and formed 'wild type' actin nodules, as previously described.

As shown in figure 5.3, lifetimes of nodules in PGI_2 treated platelets were similar to control conditions. This lack of significant difference between both conditions was true when nodule lifetimes were expressed as either means. However, total cumulative nodule formation over the 20-minute time course was significantly higher in PGI_2-treated platelets.

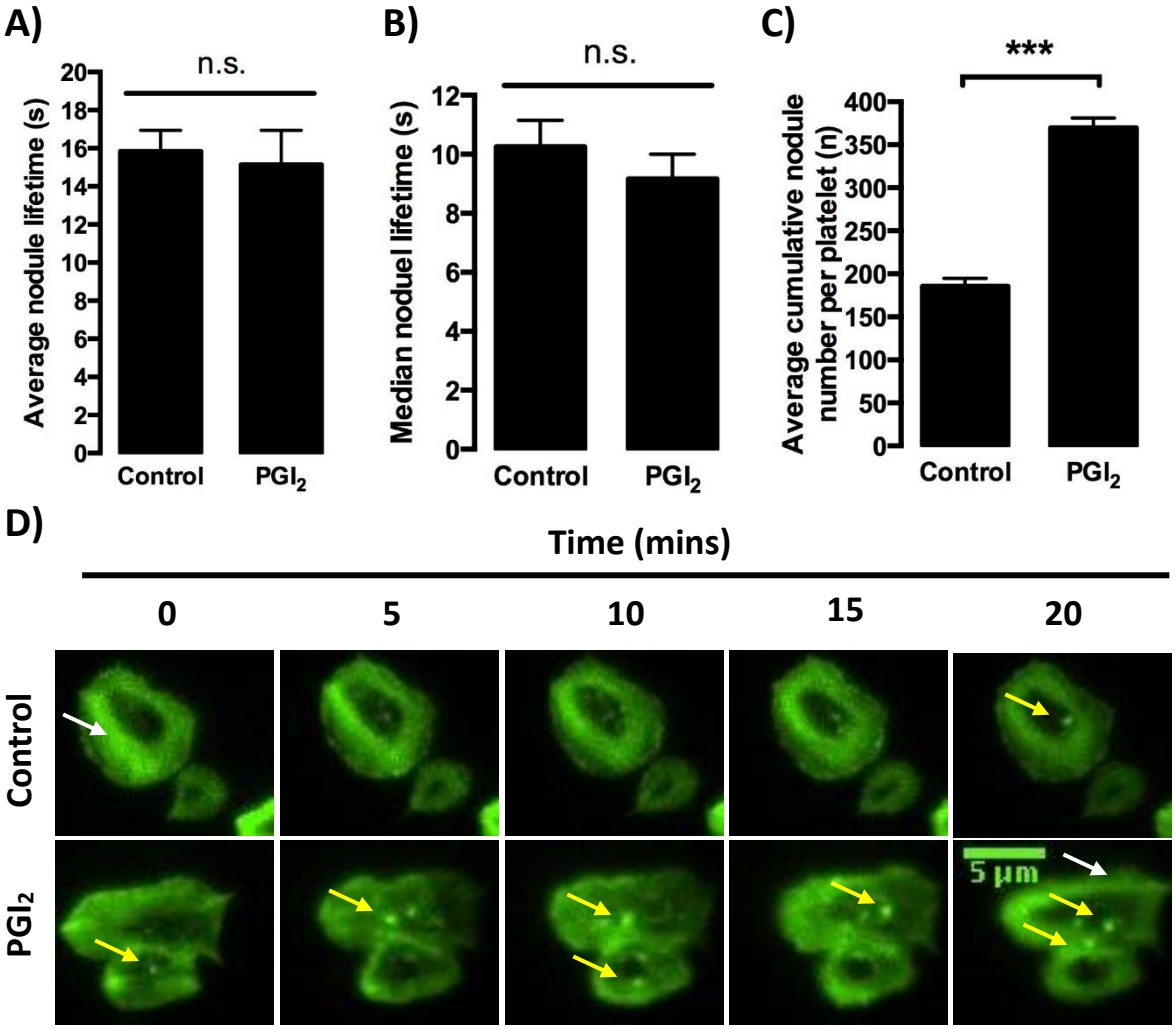

Figure 5.3. Real-time actin nodule dynamics in LifeAct mouse platelets treated with PGI_2. *Platelets (2 x10^7/ml) isolated from LifeAct-GFP mice were allowed to spread on 100µg/ml fibrinogen coated glass bottom petri dishes in the presence of 0.01U/ml thrombin for 25 minutes. Upon spreading, platelets were then treated with either 100nM PGI_2 or 0.005% ethanol (vehicle) for a further 20 minutes and continually imaged every 5 seconds at 480nm. Analysis of nodule number and lifetimes was performed using the TrackMate plugin for Fiji.* ***A)*** *Average and* ***B)*** *median nodule lifetimes of 10 individual nodule positive platelets (per experimental repeat) in spreading platelets vs spread platelets treated with PGI_2.* ***C)*** *The cumulative incidence of nodular fluorescence.* ***D)*** *Representative image of spread platelets treated with or without PGI_2 for 20 minutes. Data is representative of three independent repeats, with significance defined as p≤0.05. White arrows indicate stress fibres. Yellow arrows indicated actin nodules. Scale bar represents 5µm. *** = p ≤ 0.001.*

5.2.4. Validation of low-density and high-density fibrinogen coatings

Although the findings shown in 5.2.1 recapitulate previous observations (273), we next sought to observe the effect of different fibrinogen densities on PGI_2 regulation of the actin cytoskeleton. As different fibrinogen densities were shown to induce different intraplatelet signalling, it was hypothesised that PGI_2 would have different actin cytoskeletal effects. Firstly, in house validation of fibrinogen coatings was performed using the high and low coating concentration of fibrinogen used by Jirouskova *et al* (247).This was for two reasons; a) materials used for spreading were from different manufacturers, therefore binding rates of fibrinogen to the glass coverslip may be altered, and b) the spreading protocol used in this study was different, so results between studies cannot reliably be compared. To validate concentration-dependent binding of fibrinogen coverslips, coverslips were coated in 3µg/ml and 100µg/ml AF488-fibrinogen for 1 hour prior to mounting on a glass slide. To ensure limited autofluorescence of the coverslip itself, a plain coverslip was also mounted using the same mounting media. Coverslips were imaged using immunofluorescence microscopy at 488nm wavelength and mean fluorescence intensity was obtained for each coverslip.

As demonstrated in figure 5.4, fold change in mean fluorescence intensity in coatings using a concentration of 3µg/ml was significantly lower than in coatings using 100µg/ml, indicating that the quantity of fibrinogen immobilised onto the coverslips was significantly higher in the 100µg/ml coated condition. Interestingly, fold change in MFI in the 3µg/ml coating was not significantly different from slides lacking fluorescent fibrinogen, indicating that this concentration leads to minimal coating of the coverslip with fibrinogen. This could be clarified with further experimental repeats. Like with 3µg/ml coatings, MFI of coverslips with no coating was significantly lower than 100µg/ml.

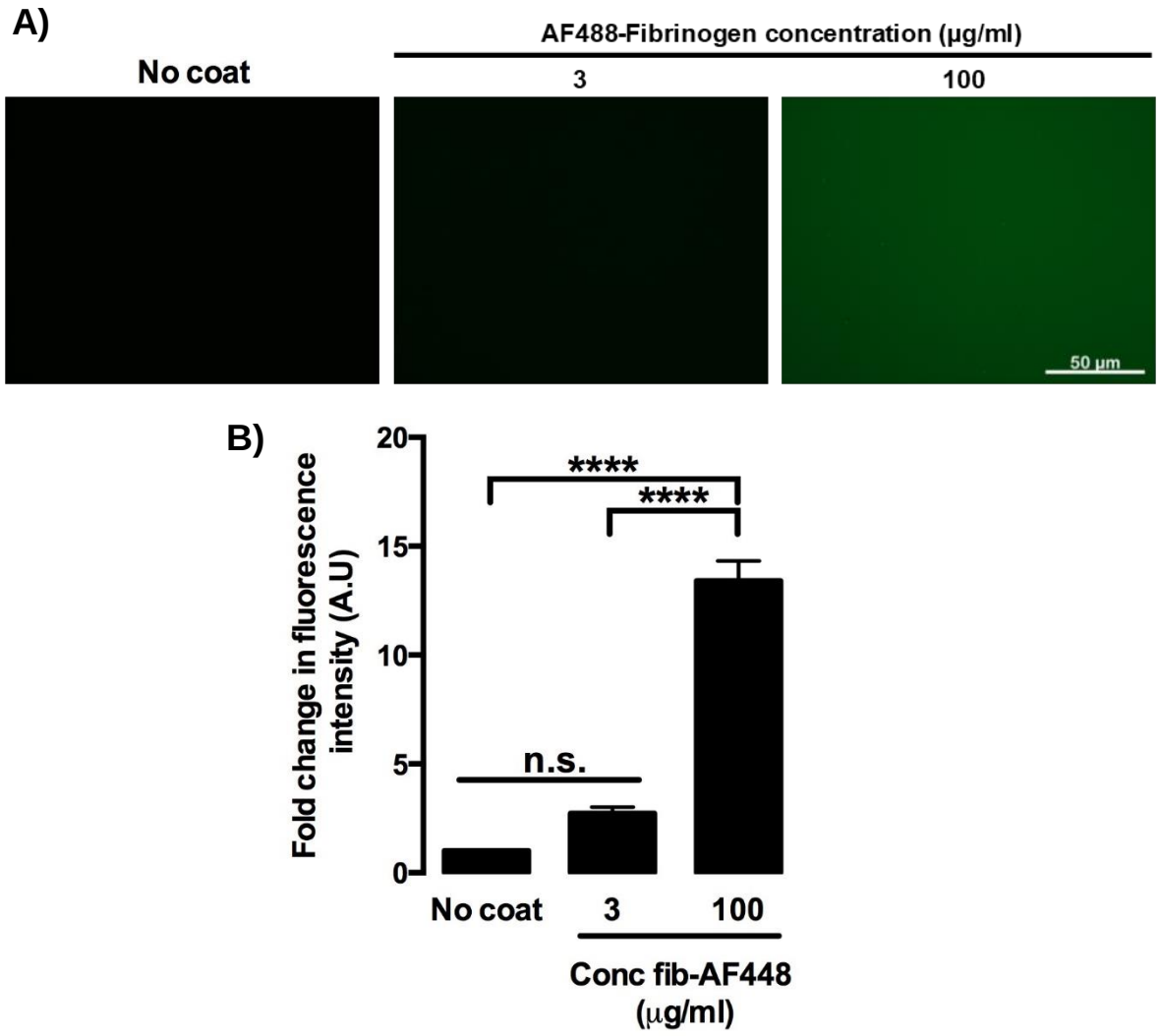

Figure 5.4. Relative mean fluorescence intensities of low- and high-density fibrinogen coatings on glass coverslips. *13mm glass coverslips were coated using 3µg/ml or 100µg/ml Alexa Fluor-488 conjugated fibrinogen for 1 hour prior to washing in PBS. Slides were also coated in PBS alone (no coat) for 1 hour prior to mounting. Slides were mounted using an anti-fade mounting media and imaged on an inverted epifluorescence microscope. 3 fields of view were taken per condition at x63 magnification and mean fluorescence intensity of each image was measured through Fiji.* ***A)*** *Representative images of fields of view obtained.* ***B)*** *Mean change in fluorescence intensity from the control (no coat/BSA only). Data is representative of 3 independent repeats, with significance defined as p<0.05 (***≤0.001, ****≤0.0001). Scale bar represents 50µm.*

5.2.5. Fibrinogen concentration determines spread platelet sensitivity to PGI_2-mediated reversal of stress fibres

Having identified the different level of coating of fibrinogen on the glass coverslips, we next sort to determine how platelets spread on these different surfaces. Considering previous findings by Jirouskova et al, it was hypothesised that platelets spread on LDF would initially spread more, however due to the likelihood of reduced number of integrins binding to fibrinogen, platelets would more readily reverse their stress fibres in response to PGI_2. Platelets ($2x10^8$/ml) were spread on varying concentration coatings of fibrinogen (3µg/ml, 10µg/ml and 30µg/ml) for 25 minutes prior to treatment with 10nM PGI_2 for a further 20 minutes. Consistent with findings from Jirouskova *et al* and Qiu *et al,* platelets spread on 3µg/ml spread further than platelets spread on higher densities with a significant reduction in surface area at 30ug/ml and 100ug/ml fibrinogen (figures 5.5.and 5.6.) (247,326). Interestingly, platelets spread on lower densities of fibrinogen had almost no platelets positive for nodules in control conditions. There appeared to be a reduction in platelet adhesion in platelets adhering and spreading on 3µg/ml compared to higher density coatings, however this was not statistically significant and requires further experimental repeats to clarify. Upon PGI_2 treatment, platelets spread on LDF were surprisingly more resistant to PGI_2-mediated stress fibre reversal when compared to higher density coatings. This stress fibre reversal was accompanied by actin nodule formation, indicating that platelets had reversed their stress fibres and subsequently formed actin nodules. These findings indicated that fibrinogen matrix density determines PGI_2-mediated effects on the actin cytoskeleton.

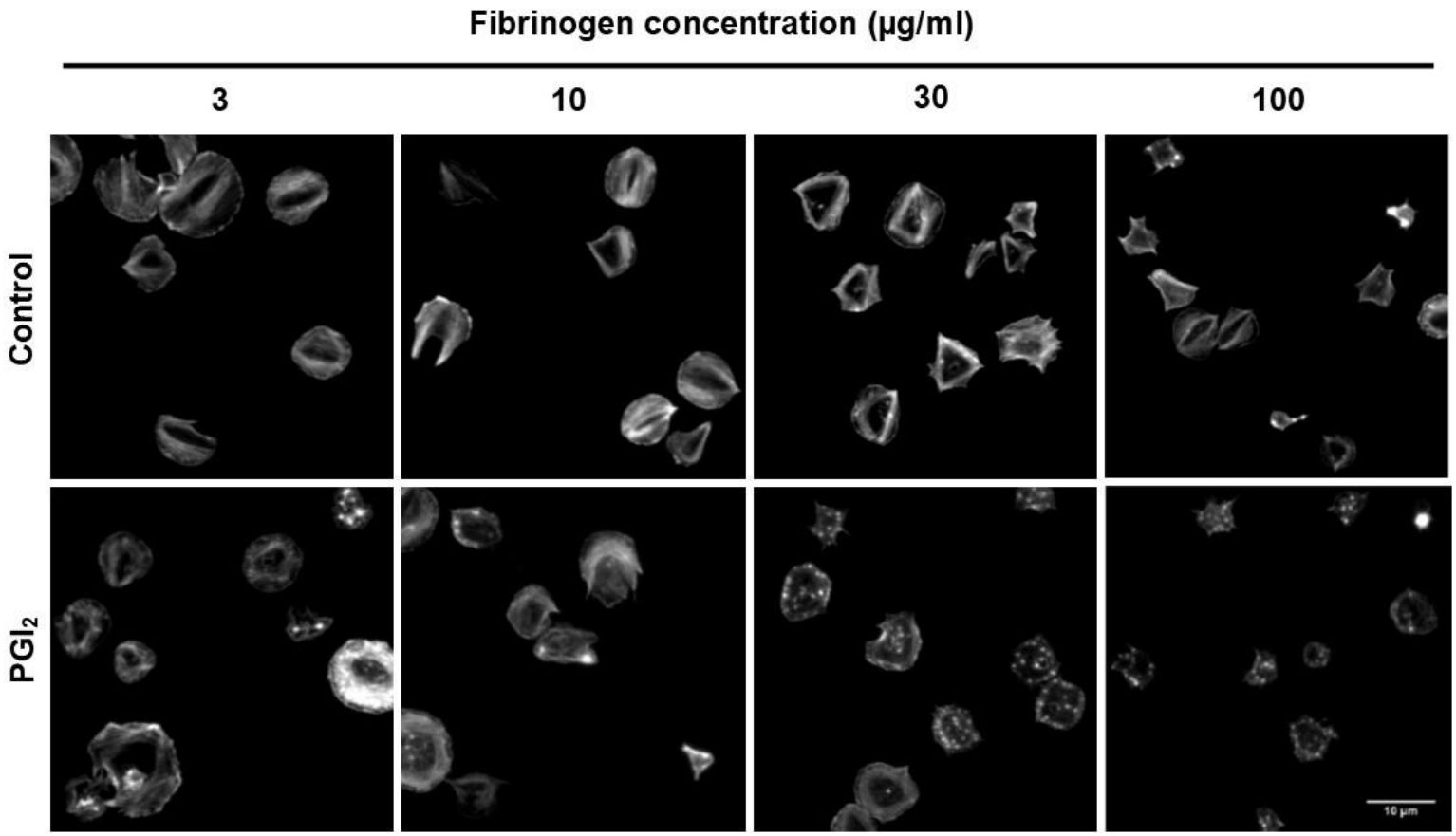

Figure 5.5. Effect of varying immobilised fibrinogen densities on PGI_2 sensitivity in spread platelets. *Platelets ($2x10^7$) were spread for 25 minutes on 3, 10, 30 or 100µg/ml fibrinogen-coated coverslips prior to treatment with 10nM PGI_2 for 20 minutes. . Platelets were then fixed in 4% formaldehyde and permeabilised in 0.1% Triton x-100 before being stained in rhodamine-B phalloidin. Images are representative of 3 individual experiments. Scale bar represents 10µm.*

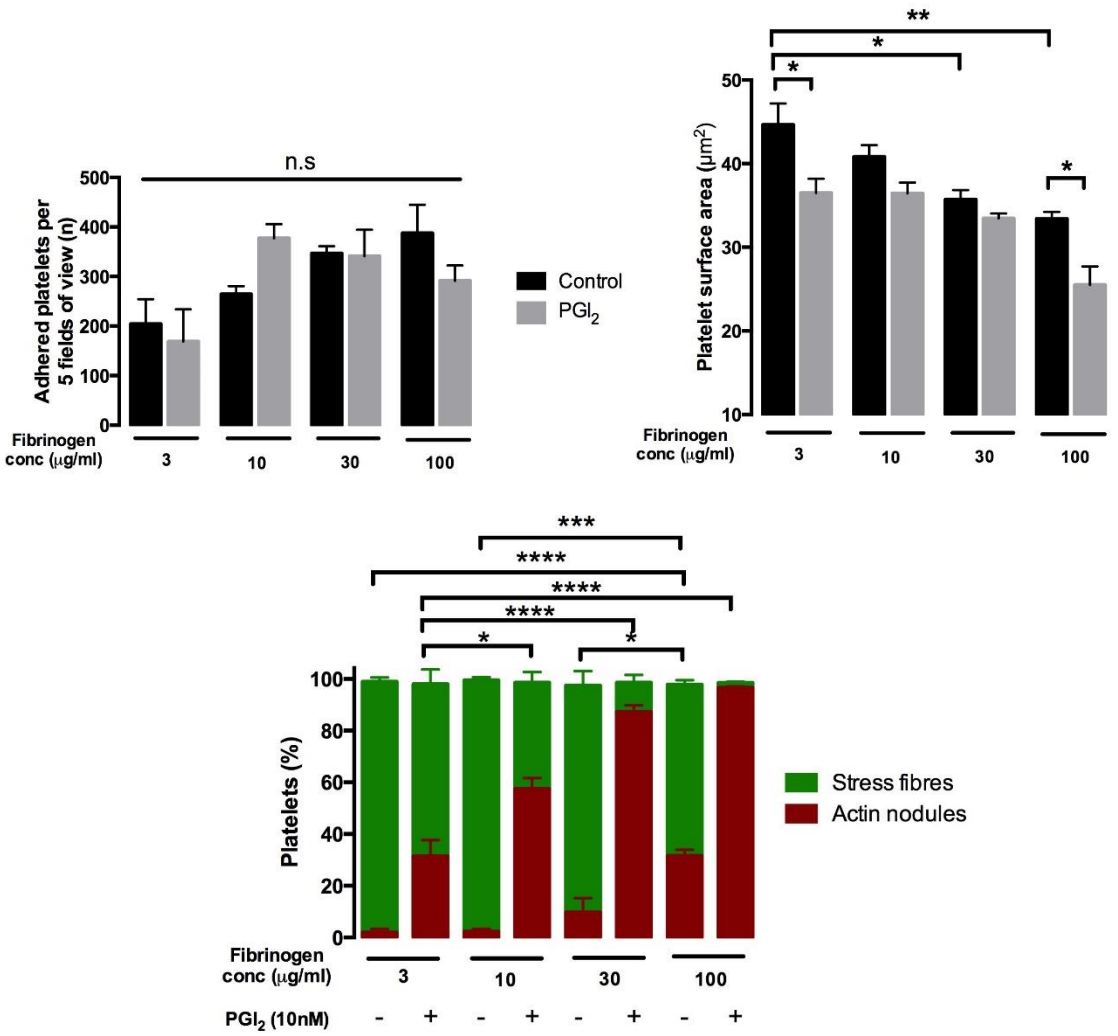

Figure 5.6. Data analysis of images acquired from the investigation of the effect of PGI_2 on platelets spread on different fibrinogen densities. A) *Average numbers of adhered platelets per five fields of view,* ***B)*** *mean platelet surface area of 100 platelets per repeat and condition,* ***C)*** *percentage of platelets per condition positive for actin nodules or stress fibres. Data representative of three individual repeat experiments. Data was statistically analysed via two-way ANOVA with Tukey post-hoc analysis. Actin structures data was arcsine transformed prior to analysis, however percentage data is displayed. Statistical significance was defined as p ≤ 0.05 (*≤0.05, **≤0.01***≤0.001, ****≤0.0001).*

5.2.6. Effect of Cyclic nucleotides on the characteristics of actin nodules in fibrinogen spread platelets

The above analysis has shown that, PGI_2 treatment of spread platelets significantly reduced the number of platelets positive for stress fibres, with a concomitant increase in the number of platelets positive for actin nodules, indicating a reversal of platelet stress fibres and a hypothesised loss of contractility. Interestingly, there appeared to be a difference in both the size and number of the nodules formed in PGI_2 treated platelets compared to nodules formed in control platelets. Therefore, further analysis of the images obtained in 5.1 and 5.3 was performed to quantify both the size and number of nodules within these platelets. A minimum of 100 nodules were measured for size per experimental condition and a minimum of 50 nodule-positive platelets were used for platelet number counting. As shown in figure 5.5 and table 5.1, control nodule-positive platelets appear to have a lower average nodule number than those treated with PGI_2, however this difference was only with 10µg/ml coatings. Treatment with PGI_2 resulted in a significant reduction in nodule size only on 100µg/ml coatings, however, the size of nodules formed on 3µg/ml were significantly larger than those formed on 100µg/ml when both were treated with PGI_2. With a lack of sufficient nodules formed in untreated platelets spread on 3µg/ml, a comparison to 100µg/ml could not be performed.

Table 5.1. **Numerical data from the analysis of the characteristics of nodules formed on varying fibrinogen concentrations in the presence or absence of PGI_2.**

Fibrinogen density (µg/ml)	Treatment	Nodule number (n)	Nodule size (nm^2)
3	Control	n/a	n/a
	PGI_2	8.125 ± 0.67	166 ± 33.53
10	Control	4.361 ± 0.82	182.7 ± 27.79
	PGI_2	9.23 ± 0.71	127.6 ± 15.04
30	Control	6.31 ± 1.43	96.45 ± 9.05
	PGI_2	8.167 ± 0.88	87.86 ± 27.11
100	Control	6.628 ± 0.42	92.3 ± 14.33
	PGI_2	9.376 ± 0.75	51.47 ± 4.34

* Data represented as means ± S.E.M.

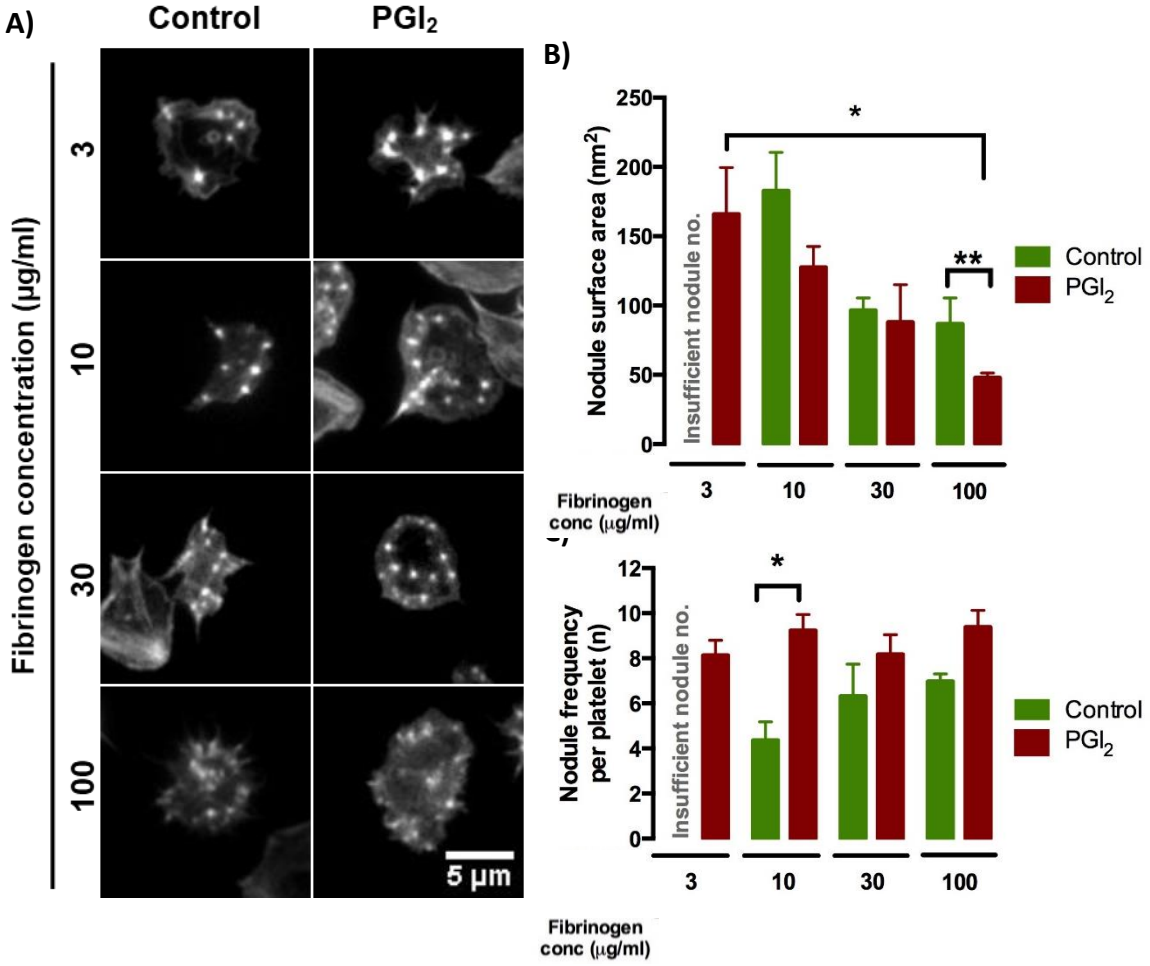

Figure 5.7. Fibrinogen matrix density dramatically affects nodule characteristics. *Platelets ($2x10^7$) were spread for 25 minutes on 3,10,30 or 100µg/ml fibrinogen-coated coverslips prior to treatment with 10nM PGI_2 for 20 minutes* ***A)*** *Representative images of platelet platelets positive for actin nodules per condition.* ***B)*** *Average nodule surface area (nm^2). 100 nodules per condition, per repeat were measured through the Fiji software package.* ***C)*** *Average nodule number per platelet deemed nodule positive. 50 individual platelets per condition and repeat were randomly selected for nodule counting. Data represented as means with S.E.M and is representative of three independent repeat experiments, with significance defined as p ≤ 0.05 (*≤ 0.05). Scale bar represents 5µm.*

5.2.7. cAMP levels in platelets spread on LDF and HDF in the presence or absence of PGI_2

The reduced numbers of platelets undergoing stress fibre reversal on LDF when compared to HDF when treated with PGI_2 suggests that these platelets have somehow acquired resistance. As IP receptor activation causes the production of cAMP through AC activation, intraplatelet cAMP was next investigated. It was hypothesised that LDF spread platelets would have lower cAMP levels in response to PGI_2 stimulation than HDF spread counterparts. To generate lysates for cAMP ELISA analysis, $2x10^8$/ml platelets were spread on 100µg/ml or 3µg/ml fibrinogen prior to treatment with 10nM PGI_2 for a further 2 or 20 minutes. Platelets were then lysed in kit-specific lysis buffer and stored immediately at -20^oC for further batches to use in the assay.

As shown in figure 5.8, control platelets spread on HDF and LDF for 20 + 2 minutes have similarly low average cAMP levels of 30.98fmol ± and 65.22fmol ± 34.53, respectively. However, upon treatment with 10nM PGI_2 for 2 minutes, cAMP levels in HDF spread platelets significantly increased to 490.6fmol ± 137.2. Conversely, platelets spread on LDF have no significant difference in cAMP levels in response to PGI_2 treatment (169.6fmol ± 100.1). When platelets spread on 3µg/ml were treated with PGI_2 for 20 minutes, no significant difference was seen in either group compared to control platelets. Additionally, although seemingly increased, cAMP levels in 100µg/ml spread platelets treated with PGI_2 were not significantly different from their control counterparts. Further experimental repeats could clarify this.

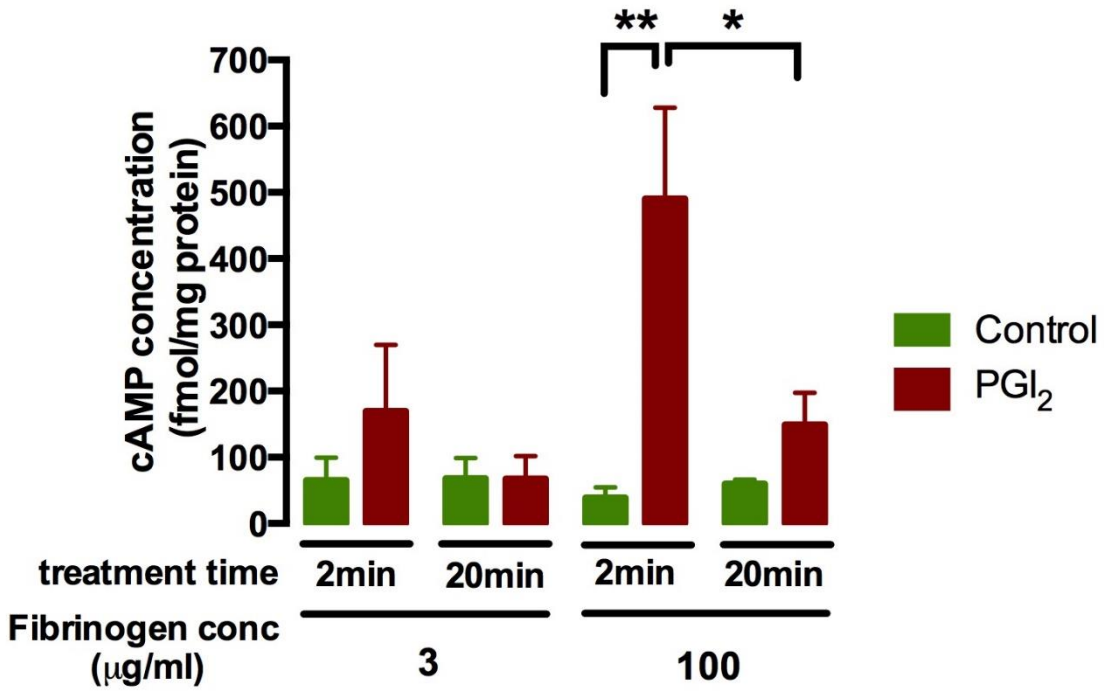

Figure 5.8. Effect of PGI_2 treatment on cAMP levels in platelets spread on HDF and LDF. *Washed platelets ($2x10^8$/ml) were spread on 3μg/ml and 100μg/ml fibrinogen prior to treatment with 10nM PGI_2 or a vehicle control (0.005% ethanol) for both 2 and 20 minutes. After incubation, spread platelets were lysed in kit-specific lysis buffer and analysed for cAMP concentration through a colorimetric cAMP ELISA assay. Protein concentration was determined for each lysate, with this being used to equalise raw data with protein loading (femptomoles per mg). Data represented as means with S.E.M and are representative of three independent experiments, with significance defined as p≤0.05 (*≤0.05, **≤0.01).*

5.2.8. PGI_2 insensitivity of platelets spread on LDF is likely regulated through adenylyl cyclase activity

After showing that a) PGI_2 can cause differential stress fibre reversal in platelets and b) actin nodule characteristics are dependent on the density of underlying matrix protein, we next sought to uncover how this phenomenon occurs with regards to components within the cAMP:PKA pathway. Production of the cAMP secondary messenger is through activation of membrane-bound AC, which rapidly synthesises cAMP upon G_s activation through IP agonism. At the same time cAMP signals have been shown to be degraded by PDE3 in platelets. To investigate this, the direct AC activator, forskolin, or the PDE3 inhibitor, milrinone, was incubated on spread platelets. It was hypothesised that if platelets spread on LDF reversed stress fibres to forskolin, then a loss of AC function would likely be the cause of PGI_2 resistance. Conversely, if LDF spread platelets reversed in response to milrinone treatment, PGI_2 resistance would likely be through enhanced activation of PDE3.

Platelets were spread on either 3µg/ml or 100µg/ml fibrinogen for 25 minutes prior to treatment with or without milrinone (10µM) or forskolin (1µM) for a further 20 minutes. As shown in figures 5.9 and 5.10, platelet surface area in LDF was significantly higher than in HDF, which was in agreement with previous findings (247). Platelet adhesion was also consistent and was similar on either density of fibrinogen and remain unchanged irrespective of treatment. Interestingly, when treated with milrinone, platelets spread on LDF were resistant to this treatment, indicating that an increase of PDE3 activity in platelets spread on LDF is unlikely. However, there was high variation in these milrinone treated platelets, which may suggest that some donors may respond to PDE3 inhibition and others may not on LDF. This may reflect the basal levels of cAMP production in response to being spread on LDF in different donors. For example, if an individual has a relatively high level of basal cAMP production, then inhibition of the PDE3 would allow this to accrue further, leading to platelet actin cytoskeletal reversal and potentially a reduction in spread platelet surface area. Conversely, if another donor's platelets were to have low to no levels of basal cAMP production when spread on LDF, then these platelets would accrue very little cAMP, if any, in response to PDE3 inhibition. Direct activation of AC with forskolion on either LDF or HDF spread platelets caused significant stress fibre reversal compared to controls. Platelet surface area in both conditions seems to be reduced, however this effect was only significant in platelets spread on LDF. These initial findings suggest that, like in collagen-spread platelets,

there appears to be a resistance in LDF spread platelets to PGI_2, and that this is seemingly mediated through regulation of AC function, as when activated with the potent AC activator, forskolin, platelets spread on LDF, like HDF, readily reverse their formed actin stress fibres into actin nodules.

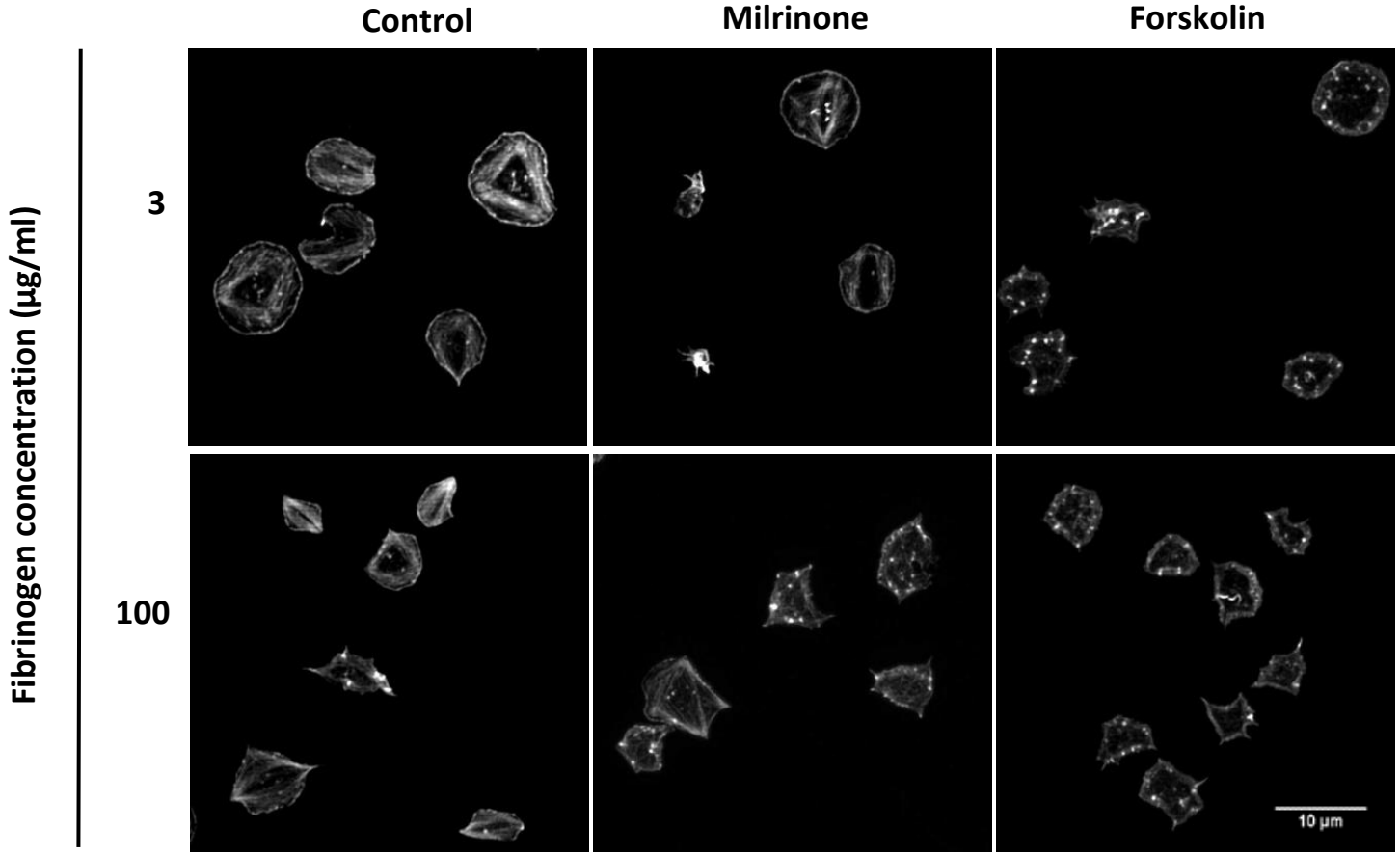

Figure 5.9. Effect of cAMP elevating agents on platelets spread on low- and high-density fibrinogen. *Platelets ($2x10^7$) were spread on fibrinogen (3 and 100µg/ml) for 25 minutes prior to treatment with vehicle (0.005% ethanol), milrinone (10µM) or forskolin (1µM) for a further 20 minutes. Platelets were then fixed in 4% formaldehyde and permeabilised in 0.1% Triton x-100 before being stained in rhodamine-B phalloidin. Images are representative of 3 individual experiments. Scale bar represents 10µm.*

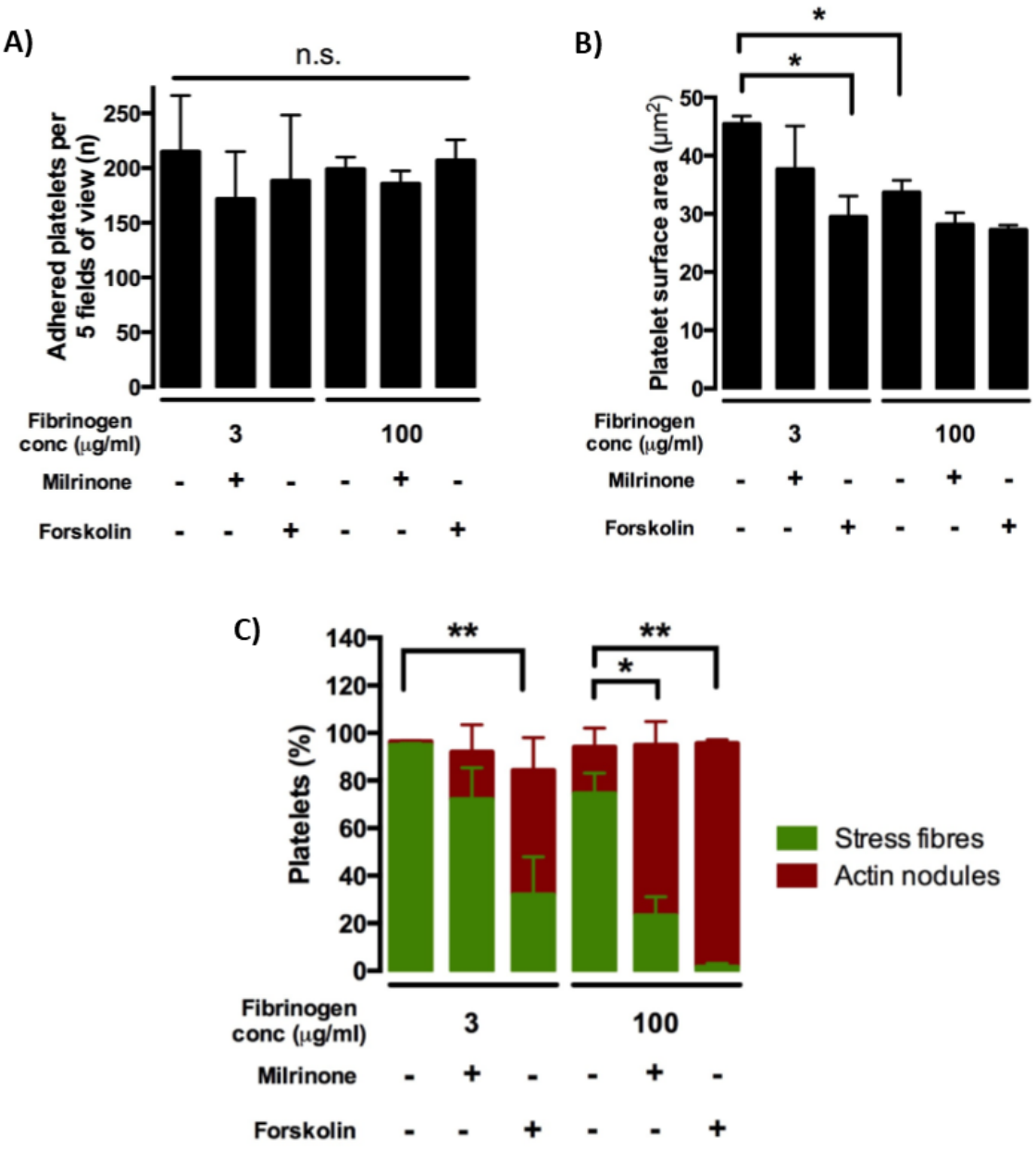

Figure 5.10. Analysis of the effect of cAMP elevating agents on platelets spread on low- and high-density fibrinogen. A) *Average numbers of adhered platelets per five fields of view,* ***B)*** *mean platelet surface area of 100 platelets per repeat and condition,* ***C)*** *percentage of platelets per condition positive for actin nodules or stress fibres. Data representative of three independent repeat experiments. Significance was defined as p≤0.05 (*≤0.05, **≤0.01, ***≤0.001, ****≤0.0001).*

5.2.9. Nodule characteristics in LDF and HDF spread platelets upon treatment with cAMP elevating agents

Next, nodule analysis was performed to determine the effect of mirlinone and forskolin on nodules formed on either fibrinogen density (shown in figure 5.11.). Due to the lack of nodule positive platelets on LDF, no measurements or analysis was performed. In response to milrinone treatment, there were sufficient nodule positive platelets to analyse. These nodules were significantly larger in size than those formed due to foskolin treatment. This suggests that direct AC activation can lead to reduction in nodule size, as seen with HDF spread platelets treated with PGI_2 (figure 5.5 and 5.6.). Oddly, on HDF, there were no significant differences in nodule size or number with any treatment, which may be a result of comparatively reduced cAMP formation in these platelets compared to PGI_2, which has been shown previously (327).

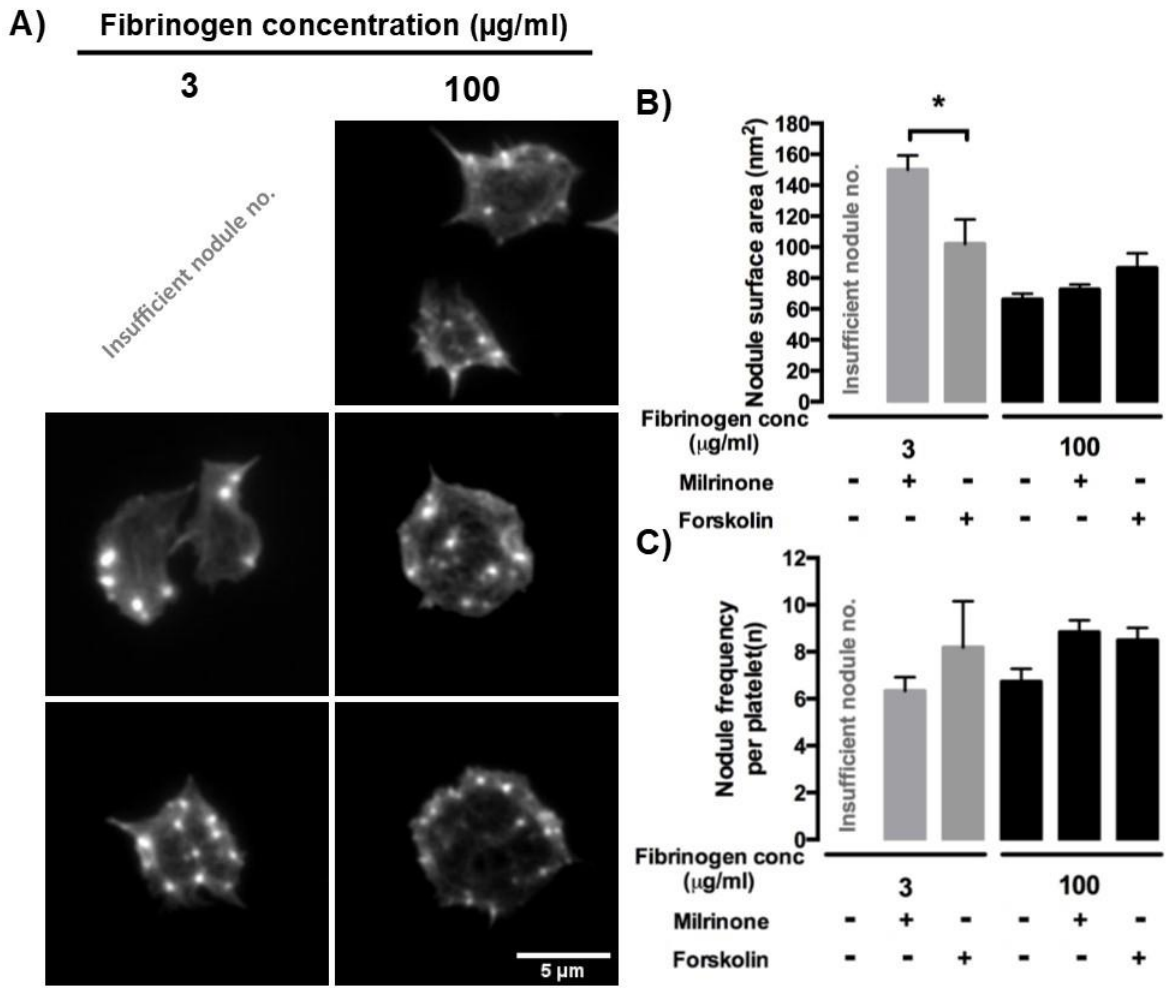

Figure 5.11. Analysis of the effect of fibrinogen density and PGI_2 treatment on nodule characteristics. *Platelets ($2x10^7$) were spread on fibrinogen (3 and 100µg/ml) for 25 minutes prior to treatment with vehicle (0.005% ethanol), milrinone (10µM) or forskolin (1µM) for a further 20 minutes.* ***A)*** *Representative images of platelet platelets positive for actin nodules per condition.* ***B)*** *Average nodule surface area (nm^2). 100 nodules per condition, per repeat were measured through the Fiji software package.* ***C)*** *Average nodule number per platelet deemed nodule positive. 50 individual platelets per condition and repeat were randomly selected for nodule counting. Data represented as means with S.E.M and is representative of three independent repeat experiments, with significance defined as $p \leq 0.05$ (*≤ 0.05). Scale bar represents 5µm.*

5.2.10. Characterisation of actin nodules in platelets adhered to fibrinogen under flow in the presence or absence of PGI_2

As the formation of nodules under flow has been shown to be critical for stable thrombus formation in WAS patients, nodule analysis was performed on the fibrinogen flow microscopy images acquired in chapter 4 (figure 4.15) in the form of nodule size and number. Analysis of these images indicated that nodules formed in PGI_2 treated platelets were more numerous and have a decreased surface area (figure 5.12). These findings mirror those from spread platelets treated with PGI_2 under static conditions, however due to the limited number of repeats (n=2), no statistical analysis could be performed. Additionally, the distribution of these nodules appears different from those formed under static adhesion assays. Nodules formed under flow seem to be localised close to the membrane.

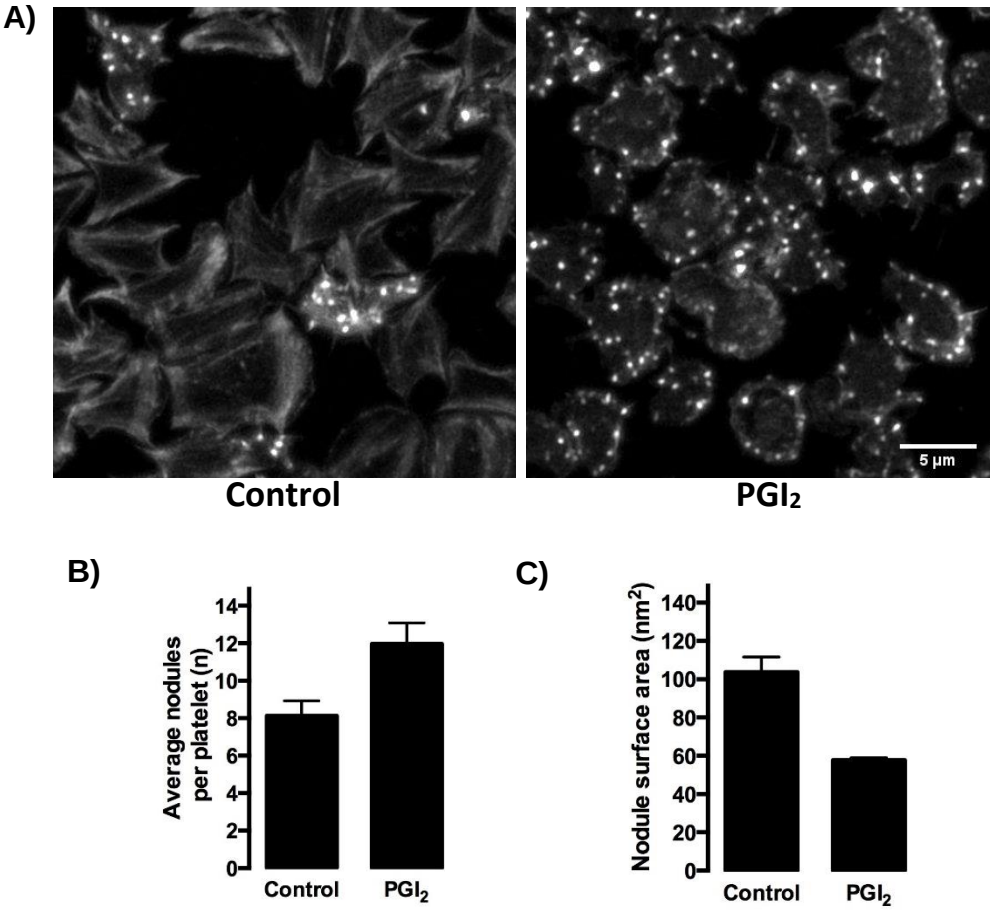

Figure 5.12. Actin nodule characteristics in platelets adhered to fibrinogen under flow in the presence or absence of PGI_2. A) *Average nodules per nodule-positive platelet. 50 platelets per experimental condition were analysed for nodule number via manual counting of nodular actin staining.* ***B)*** *Mean platelet nodule surface area. 100 nodules were manually analysed for surface coverage through the Fiji software package. Data is representative of two independent repeats (SD). Scale bar represents 5µm.*

5.3. Discussion

This chapter reports the investigations into the effect of fibrinogen matrix density on platelet sensitivity to PGI_2 and actin nodule characteristics. Firstly, the validation of previous findings reported from the lab was performed and resulted in data in agreement with this (figure 5.1). Fibrinogen spread platelets that were treated with PGI_2 completely reverse their stress fibres and form actin nodules (301), possibly resulting in a loss of contractility. It was also found that actin nodule characteristics, in the form of size and number, were altered in response to PGI_2.

The effect of NO on actin nodule characteristics was next analysed using imaged obtained in chapter 3 (figure 3.1). This was done to determine whether the effect seen with PGI_2 was novel, or shared with NO, which also was shown to regulate the same cytoskeletal signalling (273,301). NO treatment was found to also cause a significant increase in the number of actin nodules and a reduction in nodule size (shown in figure 5.2), thereby demonstrating that both PGI_2 and NO can both alter nodule properties. This may be a due to the regulation of similar targets of NO and PGI_2 signalling, such as RhoA, and suggests that there may be a synergistic effect of these two inhibitors on nodule dynamics.

The temporal formation of actin nodules in response to PGI_2 was next investigated. This was to ensure nodules form in real time and were not an artefact of fixing and staining platelets, and to uncover their dynamics during the 20 minute treatment window with PGI_2. This was performed using LifeAct mouse platelets, which were spread to form stress fibres, upon which PGI_2 was added and resulting actin cytoskeletal responses recorded. These were measured against nodules which were formed during platelet spreading to compare dynamics in nodules formed during spreading against those formed after spreading and PGI_2 stimulation. Consistent with previously data reported in this thesis and elsewhere, stress fibres dismantle in response to PGI_2, with subsequent formation of actin nodules. This validated the static stress fibre-actin nodule percentage readouts that have been used and demonstrated their reciprocal relationship. It was found that individual nodule lifetimes were similar between control condition nodules and those formed in response to PGI_2. This was true when represented as either mean or median lifetime, therefore, PGI_2 does not appear to increase nodule turnover rates. This may be due to the limited resolving power of the microscope used for videocapture, which Poulter et *al.* showed to be unfavourable in the imaging of platelet actin

nodules (229). Perhaps structured illumination or total internal reflection approaches would provide better video quality and reduce the noise seen in epifluorescence imaging. Nodule incidence using this method, however, did increase with PGI_2 treatment and was significantly higher than in the control, indicating that PGI_2 causes enhanced nodule formation. In these mouse platelets PGI_2-induced stress fibre reversal appeared to diminish around 20 minutes, by which time nodules began to diminish and stress fibres began to reform. This is an interesting finding, and demonstrates in real time that platelets are refractory to PGI_2 inhibition, and should be studied further. Perhaps platelets are refractory to many 'rounds' of PGI_2 stimulation, which platelets may encounter at sites of increased shear within the vasculature (328,329). One potential caveat of this methodology could be the differences in nodule structure and dynamics in murine platelets. A full comparison should be made between murine and human platelets regarding the size, number and incidence of actin nodules in response to PGI_2

There have been several reports of differing fibrinogen matrix concentrations affecting spreading dynamics and contractility in platelets through altered signalling (247,330,331). It was therefore hypothesised that platelets spread on varying fibrinogen densities would have different sensitivities to PGI_2. This was to be investigated by using increasing concentrations of fibrinogen to coat glass coverslips for platelet spreading. However, first a validation of the relationship between initial fibrinogen concentration for coatings and the resulting fibrinogen density was performed. This was done using high- (100µg/ml) and a low (3µg/ml) concentrations for coverslip coating (figure 5.2). It was found that 100µg/ml coatings had a significantly higher MFI than 3µg/ml and BSA controls, indicating that the two coating concentrations led to significantly different levels of fibrinogen deposition to the coverslip surface. Measurement of the topology of these surfaces through atomic force microscopy could also highlight their stiffness'. This would be important as it was previously shown that different concentrations of immobilised fibrinogen oriented themselves differently onto glass coverslips (332). Increasing matrix stiffness causes increased platelet signalling and spreading, which could confer PGI_2 resistance (305)

Having validated the difference in fibrinogen adsorption using high and low fibrinogen concentrations for coating, the effect of fibrinogen density on platelet actin dynamics and sensitivity to PGI_2 was investigated (figure 5.3). A dose response

curve using 3, 10 and 30 and 100µg/ml fibrinogen was used for platelet spreading and resulted in a significantly lower spreading surface area in 30µg/ml and 100µg/ml coatings compared to 3µg/ml, which was in agreement with data from Jirouskova *et al*. who also demonstrated that LDF caused increased platelet spreading (247). Interestingly, in control conditions, actin nodule formation seemed to increase the higher the matrix concentration, and was significant between higher and lower densities. This would suggest that a significant proportion on platelets interacting with high-density fibrinogen are slower spreading than those on lower densities. Surprisingly, in response to PGI_2 treatment, there was a dose-dependent increase in stress fibre reversal and accompanying actin nodule formation with higher density coatings. There was no significant difference in stress fibre reversal between 30µg/ml and 100µg/ml coatings, due to almost complete reversal. These findings although seemingly counterintuitive, agree with the literature regarding fibrinogen and its ability to inhibit platelet function. Owagnat *et al*. have shown that the deposition of fibrinogen onto formed thrombi *in vitro* prevents further thrombus growth when additional platelets are perfused (333). A small number of platelets initially attached to the shell of the thrombus, however no further aggregation of platelets occurred thereafter. These authors also visualised the deposition of fibrinogen within and on *in vitro* formed thrombi and found higher levels within the shell of the thrombus. The inhibitory capacity of fibrinogen has also been reported by another group, who demonstrated that higher fibrinogen concentrations prevented platelet adhesion to biomaterials used in prosthetics and cardiovascular stents (334). Additionally, low density fibrinogen also caused an increase in platelet adhesion on these coatings, which was stronger, suggesting that at this density, fibrinogen immobilised on such devices can become prothrombotic by modulating platelet contractility. The data obtained in figure 5.6 may also be applicable, as this increase in presumed contractility may not be able to be regulated by endothelial-derived PGI_2 also, which may further exacerbate platelet adhesion and thrombus formation *in vivo*. Further investigation into platelet contractility should be investigated using the matrix concentrations used in figure 5.5, including any resulting changes in contractility in response to PGI_2 treatment. In response to PGI_2, actin nodule numbers significantly increased in 10µg/ml coatings only. Due to the insufficient number of nodules formed on 3µg/ml, no reliable comparison could be made between control and PGI_2 treatment without trying to seek nodule positive platelets during microscopy, which would of introduced bias into the data. With PGI_2

treatment, there was a significant difference between the size of nodules formed on 3µg/ml and 100µg/ml coatings, indicating that nodule size could be determined by matrix density. More experimental repeats which could capture actin nodule positive platelets on 3µg/ml fibrinogen should be performed to determine the true effect of ligand density on nodule formation, as using PGI_2 data as a proxy is not desirable.

The diminished cytoskeletal effects of PGI_2 treatment seen in platelets spread on LDF compared to HDF suggested that they were somehow resistant to PGI_2. This could have been a result of either diminished downstream signalling from the IP-receptor, or an inability for active PKA to target the actin cytoskeleton. To address this this question, the intracellular levels of cAMP in spread platelets in response to PGI_2 treatment were analysed using an ELISA assay. This was performed on HDF and LDF spread platelets at two PGI_2 treatment time points (2min and 20min). cAMP levels in platelets spread on either density were not significantly different at either time point, indicating that basal cAMP synthesis was low in both conditions. In response to 2 minutes of PGI_2 treatment, LDF led to a small increase in cAMP levels, however this was not significant. Conversely, platelets spread on HDF significantly increased intracellular cAMP content when treated. This increase was also significantly higher than cAMP levels in platelets spread on LDF, indicating that matrix density dramatically affects cAMP concentrations. cAMP levels at 20 minutes of PGI_2 treatment remained similar to basal levels in LDF spread platelets, suggesting that they remained resistant to PGI_2-induced cAMP synthesis. Interestingly, cAMP levels in HDF spread platelets returned to cAMP levels after 20 minutes of treatment, which suggests cAMP hydrolysis through PDE activity. These findings, along with the spreading data shown in figures 5.1 and 5.3 show that fibrinogen density can regulate PGI_2 sensitivity in spread platelets. These data also agree with the aforementioned inhibitory abilities of fibrinogen on platelets attaching to thrombi (333,334). Increased sensitivity to PGI_2, according to the data presented here, would result in increased rates of stress fibre reversal and a diminished ability for platelets to remain attached to the thrombus.

Next the source of PGI_2 resistance was investigated. Due to the low levels of cAMP in response to PGI_2 stimulation in platelet spread on LDF, it was hypothesised that this was a result of either AC inhibition or enhanced PDE3 activity. This was investigated using milrinone and forskolin, to block PDE3 or activate AC, respectively, in spread platelets on 3µg/ml of 100µg/ml fibrinogen coatings.

Consistent with previous data for our lab, no treatment caused a significant reduction in platelet adhesion, further demonstrating that PKA activity cannot cause platelet embolisation under static conditions. Changes in platelet surface area was found to be only significant between the 3µg/ml control and 3µg/ml forskolin treatment. Although it has been shown that milrinone and forskolin cause a reduction in spread platelet surface area previously, this was not shown in the platelets used for this experiment. It was found that in response to milrinone, platelets on HDF significantly reversed their stress fibres and formed actin nodules, whereas those spread on LDF did not. This suggested that HDF spread platelets had higher PDE3 activity at 20 minutes, which corresponds to the reduction in cAMP concentration measured by ELISA. There was noticeable variation in the amount to stress fibres and actin nodules after milrinone treatment in LDF, which may be a result of donor variability in PDE activity on this density of matrix. In response to AC activation, platelets spread on either density of matrix significantly reversed their formed stress fibres into actin nodules. Considering the lack of cAMP upon PGI_2 treatment in LDF and the lack of response to PDE3 inhibition, it appears that LDF causes inhibition of AC function in platelets.

This data indicates that there may be an integral mechanism in platelets that controls AC function depending on fibrinogen density. This, paired with findings from Owagnat *et al.* demonstrating that plasma fibrinogen inhibits thrombus formation, could result in a situation where plasma fibrinogen bound to active $\alpha_{IIb}\beta_3$ causes increased sensitivity to PGI_2 (333). This may also put into context the reports of low plasma fibrinogen levels and incidence of thrombosis (335). Further work to uncover this possibility would involve cAMP measurement of platelets in the presence or absence of PGI_2 and soluble fibrinogen at varying concentrations. Additionally, downstream markers of PKA activity such as $pVASP^{ser157}$ and pPKA should be probed for. A possible detrimental effect of LDF-induced AC inhibition could be the lack of PGI_2 response in platelets attached to biomaterials such as stents. The adhesion of platelets to these materials was shown to occur mostly at low 1-3µg/ml fibrinogen densities (334), which according to the data presented in this chapter, would become insensitive to PGI_2 also, which may then permit further platelet activation and potential thrombus formation through sustained stress fibre formation.

The source of AC inhibition in LDF spread platelets could be through several mechanisms. As previously reported by Jirouskova *et al*. intraplatelet Ca^{2+} levels in platelets spreading on LDF are both elevated and sustained, whereas HDF are not (247). AC5/6 are inhibited by low, physiologically relevant micromolar levels of Ca^{2+} (318), which could mean that LDF AC5 or AC6 could be inhibited by high Ca^{2+} levels induced by LDF. To initially test this hypothesis, exogenous Ca^{2+} could be added to both LDF and HDF spread platelets prior to PGI_2 stimulation. If correct, Ca^{2+} would cause AC inhibition in platelets spread on HDF, subsequent PGI_2 resistance and lack of stress fibre reversal.

Stress fibre reversal in response to PGI_2 has been shown in figure 4.15 in chapter 4 and may explain the embolisation of platelets from thrombi formed on collagen, which platelets have been shown to do when actin-myosin interactions are inhibited (195,336). Actin nodules are a critical factor in thrombus stability (229), and are also a result of stress fibre reversal under both static and shear stress conditions in response to PGI_2 (figure 4.15, chapter 4). Like static conditions, there was a noticeable difference in the number and size of actin nodules in the presence or absence of PGI_2. Therefore, further nodule analysis was performed on images obtained from figure 4.15, which appear to show an increase in the amount of nodules (per nodule positive platelet), and a reduction in their surface area (figure 5.10). Unfortunately, no statistical analysis could be performed due to insufficient data sets, which should be addressed with further experimental repeats. The distribution of nodules after PGI_2 perfusion was drastically different from control platelets. PGI_2 stimulation cause nodules to form at the periphery of the platelet, which may indicate their requirement for platelet adhesion prior to stress fibre formation by anchoring the periphery to the matrix, thereby preventing flowing plasma from lifting the platelet away from the underlying matrix. As this fibrinogen presented in the flow channel is likely to be very stiff, this keeps the platelets in place, whereas a softer presentation of fibrinogen on the outside of the thrombus would cause embolisation through diminished shear-induced signalling.

Although in its infancy, preliminary research into the purpose of the actin nodule has emphasised their requirement for stable platelet adhesion and thrombus formation under flow (229). This may highlight a role for actin nodules in the intermediate stages of platelet spreading and stress fibre formation under flow, as platelets from WAS patients still formed stress fibres in static adhesion assays (229). Real time

actin nodule data obtained in figure 5.7 demonstrated an increase in the number of cumulative actin nodules over time, which could mean an increase in cAMP-induced nodule dynamics. This suggests that platelets may require PKA for nodule formation and may explain why LDF results in so few nodule positive platelets. A time course of platelet spreading on LDF could clarify if they do form nodules before fully spreading. This could also be done using the PKA biosensor mice previously used by Hiratsuka *et al*. to visualise PKA activity during nodule formation (302).

5.4. Conclusion

This chapter has uncovered the role of fibrinogen matrix density in the regulation of PGI_2 sensitivity and actin nodule characteristics. PGI_2 insensitivity was shown to be a result of AC inhibition on LDF, which was not seen using HDF. Additionally, LDF resulted in almost no actin nodules compared to HDF. This difference was also seen in nodules formed in response to PGI_2, where LDF nodules were significantly larger than those formed on HDF. Under flow, nodules appear to be smaller and more numerous in response to PGI_2 and may be a result of increased nodule dynamics.

Chapter 6. Discussion

6.0. Summary

This thesis has investigated the effect of cyclic nucleotides on the regulation of the spread platelet actin cytoskeleton and its effects on thrombus stability. During this investigation, I have demonstrated the importance of matrix type and concentration in the susceptibility of interacting platelets to cyclic nucleotide-mediated reversal of stress fibres. Taking with previous findings highlighting the need for platelet contractility, the findings presented here shed further light onto the critical nature of platelet stress fibre formation and sustenance during and after thrombus formation. It is clear that different matrices prevent or permit cyclic nucleotide-mediated actin cytoskeleton rearrangement, which may be a result of defined areas within the thrombus where PKG and PKA activity may or may not be required to limit thrombus formation.

6.1. Matrix deposition dramatically effects platelet sensitivity to endothelial derived inhibitors: laying the bricks that determine thrombus structure

There is a growing consensus that thrombi have distinct areas of contractility, where there is limited perfusion of plasma and retention of soluble agonists, including thrombin, ADP and TXA_2, which leads to distinct areas of solute retention within the thrombus due to platelet packing (76,78,337). Currently, the distribution of matrices within and around the thrombus and its impact on thrombus formation has not been investigated. Uncovering this would be of great benefit for our deeper understanding of thrombus formation. It has been well documented that thrombi can take many forms, with some being red clots, which are red blood cell rich and platelet poor, or white clots, that are predominantly platelets and fibrin (338). Perhaps the distribution of exposed matrices upon vascular injury, among other factors, can lay out the blueprints for thrombus structure.

Platelets are traditionally thought to be kept in check by NO and PGI_2 prior to matrix adhesion and thrombus formation, with little importance stressed on the ongoing regulation of thrombus structure by these inhibitors. In this thesis, I have demonstrated that platelets, depending on the matrix protein that they are interacting with and its concentration, can reverse their formed stress fibres, leading to a reduction in platelet surface area and thrombus height under flow. These findings suggest that the upper-most layers of the thrombus are more sensitive to CN inhibition, whereas platelets within the lower levels towards the thrombus ‘core’ are not. In line with the previous thrombus structure findings, platelet contractility

within the developing thrombus may lead to distinct areas of PGI_2 and NO permeation. In the upper layers of the thrombus, where contractility is lowest and spaces between platelets are larger, plasma may perfuse through and 'bathe' the platelets in inhibitory, CN-generating signals. This would then keep platelets attached to the outside of the thrombus in a semi-quiescent state, thereby limiting further platelet secretion and subsequent platelet binding. Additionally, platelets on the outside of the thrombus would be exposed to higher shear than those deeper within, which would lead to the controlled embolisation of these outer-most platelets if their activity level and was below that required to meet the challenge of these inhibitory signals. Failure to do so would lead to insufficient actin-myosin contractility to remain bound to the thrombus. The balance between activation and inhibition at the outer-most shell of the thrombus appears to be on a knife-edge, and factors swaying this balance could be the determining factor between occlusive and non-occlusive thrombi.

6.2. Nitric oxide in the regulation of thrombus size

In chapter 3 I have demonstrated that NO and its subsequent activation of cGMP synthesis and PKG activation leads to the reversal of formed stress fibres on fibrinogen-coated matrices. This ultimately led to a reduction in the height of preformed thrombi on collagen-coated surfaces under flow. There are several implications of these findings. Normally, vascular endothelial cells produce NO, and due to platelet size and laminar flow, platelets are pushed towards the endothelium and are thought to be constantly 'bathed' in NO. However, in disease states such as diabetes, hypocholesterolaemia and hypertension there are numerous reports of reduced endothelial production or platelet responsiveness to NO (339–342). This loss of NO production in the endothelium or platelet NO sensitivity would mean an increased level of stress fibre sustenance during and after thrombus formation, where NO helps define the boundaries of the thrombus by establishing a threshold between activatory and inhibitory signals to the actin cytoskeleton. NO can directly react with haemoglobin on the red cell membrane which would otherwise absorb the produced NO, diminishing the vascular endothelium's ability to inhibit platelets and prevent excessive thrombus growth. Free haem has previously been experimentally used to absorb NO and diminish platelet inhibition (343). Radomski *et al*. also used haem to block the effect of NO to demonstrate the synergistic effect of picomolar and nanomolar levels of PGI_2 and NO, respectively (177). The findings of NO and PGI_2 synergism observed here support this, and further work involving this

synergism should be undertaken. It would be useful to understand the importance of free haem in the post-perfusion of NO in our flow microscopy assays, as conditions causing haemolysis may lead to a diminished ability for NO to inhibit platelet contractility (343,344).

Shear stress encountered by platelets during thrombus formation contributes to the structure of the thrombus (345,346). Conversely, there has recently been a report of shear-induced cGMP generation in platelets at the outer-most edge of thrombi (298). Loss of cGMP-sGC signalling led to a significant increase in thrombosis, and more pertinently, a decrease in thrombus dissolution after formation compared to WT controls. This finding demonstrates NO-mediated thrombus consolidation, in agreement with collagen flow findings presented in chapter 3. Therefore, it is likely that this autoregulatory brake in thrombosis is modulating platelet contractility through inhibition of RhoA. This is an attractive concept, in which a growing thrombus is exposed to increasing shear rate as the thrombus grows and stenoses the blood vessel. By increasing susceptibility to NO, platelets ensure that excessive thrombus formation is impeded and blood flow to vital tissues, such as the myocardium, is maintained. This hypothesis is supported by the increased incidence of MI in families with hereditary loss of function mutations in the α-subunit of sGC, *GUCY1A3* (200). Investigation into *ex vivo* thrombus formation with these individual's platelets, their response to NO and any stress fibre reversibility would be an effective way to demonstrate any effect of NO on stress fibres.

Although often thought of as redundant partners, NO and PGI_2, are likely synergistic in their regulation of the platelet cytoskeleton. Seminal work from Salvador Moncada's group in the late eighties showed that at low, non-effective concentration, NO and PGI_2 could synergise to inhibit platelet aggregation (347). Since then, there has been little clarification of this effect. Using the same concentrations of these inhibitors, I have shown that NO and PGI_2 alone did not affect the spread platelet actin cytoskeleton. However, when used together, they cause significant reversal of formed stress fibres. This synergistic relationship is further indicated by the seemingly different mechanisms that they use for inhibiting RhoA, with PGI_2 causing phosphorylation of $RhoA^{ser188}$, and NO causing inhibition of by some other, potentially novel mechanism. These findings place emphasis on the relationship of NO and PGI_2 and puts into context the disparity between their estimated plasma concentrations and those used experimentally.

6.3. Collagen-mediated resistance to PGI_2 in spreading and spread platelets: the foundation in the thrombus blueprint?

Our group has previously shown that collagen spread platelets are resistant to PGI_2, unlike those that have spread on fibrinogen, which readily reverse their formed stress fibres in response to PGI_2 treatment. Here in chapter 4, I have recapitulated this result and have shown that at the same concentration of PGI_2, there was no effect when preincubating platelets. This demonstrates that immobilised collagen is a powerful mechanism that platelets can become PGI_2 resistant. The importance of this phenomenon requires further investigation. This could be a mechanism that platelets utilise to form uninterrupted seeding of the thrombus. Platelet contractility is required for stable thrombus formation (195). This is a RhoA-dependent process, which our group and others, have shown to be potently regulated by PGI_2 (272,273). The impact of impaired actin-myosin contractility has been highlighted using and the ROCK inhibitor, Y27632, *in vivo*, which drastically inhibits thrombus formation (195). This effect could also be a contributor to occlusive thrombi in stenosed atherosclerotic vessels. Upon plaque rupture, collagens are exposed to oncoming platelets, however in this scenario, the seeding of the thrombus begins much further into the vessel. As the blueprinted process of thrombus formation begins, brought about by the subendothelial collagen foundation, the thrombus may likely become occlusive, as it's 'core' of thrombin-activated and granule-secreted platelets are highly contractile and limit plasma, thus PGI_2, perfusion (76,78,79) (Figure 6.1.).

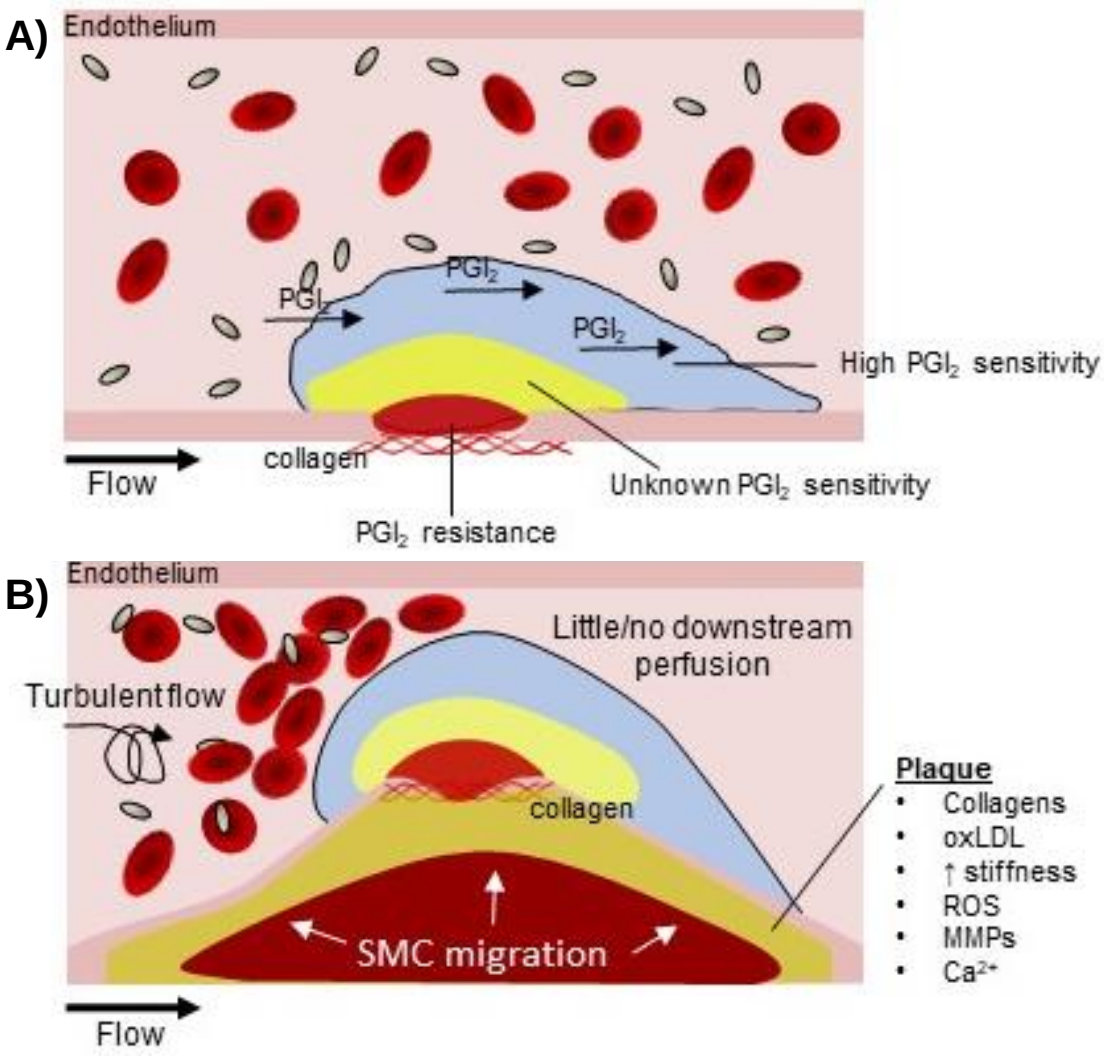

Figure 6.1. Proposed effect of collagen mediated PGI_2 insensitivity during thrombus formation and in atherosclerosis. A) *Under normal physiological conditions, collagen is retained within the subendothelium far from the opposing luminal wall. Upon endothelial damage, collagen becomes exposed to oncoming platelets in laminar flowing blood, which then bind to collagen via GPO and GFOGER peptide sequences and are resistant to PGI_2 exposure. Subsequent bulking of the aggregate leads to areas of defined solute retention, brought about by platelet contractility, with areas deeper down towards the core (red and yellow) having limited plasma permeability likely resulting in a lack of PGI_2 exposure, which allows further unimpeded platelet contraction through RhoA function. The outside 'shell' of the thrombus has increased permeability due to a concentration gradient of generated thrombin, ADP, TXA_2 and other agonists that permeates from the core and the middle zone (yellow). This permits the perfusion of PGI_2 throughout the shell and the maintenance of these platelets' semi-quiescent state and perfusion of blood to downstream sites.* ***B)*** *Collagen-mediated occlusion of vasculature in a stenosed atherosclerotic vessel. Due to increased collagen synthesis, SMC migration into the vessel lumen and other proactivatory factors within the atheroma, collagen is presented further into the lumen than in healthy vessels. Upon plaque rupture, platelets begin the concerted process of thrombus formation, firstly with PGI_2-resistance brought about by collagen interaction. Aggregate bulking then begins with thrombin generation and secondary mediator release, leading to a thrombus that can occlude the vessel and cause downstream ischemia. Additionally, a growing thrombus seeded further into the lumen could cause turbulent flow, thereby disrupting the 'bathing' of oncoming platelets in inhibitory signals.*

6.4. Molecular mechanisms causing collagen mediated PGI_2 resistance

There are several findings from the data presented in chapter 4 that seem counterintuitive yet were consistent. Therefore, there must be one or several processes that occur in collagen spread platelets that lead to PGI_2 resistance through diminished cAMP synthesis, whilst also causing concurrent PKA activity.

Initially, it was hypothesised that ADP release was causing AC inhibition. ADP signalling has been shown to inhibit AC function in platelets through activation of $G\alpha_i$ via P2Y12 activation (165,348). However, this was discounted as a factor due to the lack of re-establishment of PGI_2 sensitivity in collagen spread platelets in the presence of apyrase. Regulators of G protein signalling (RGS) proteins are another potential mechanism of AC inhibition. They act as GAPs, thereby encouraging the intrinsic GTPase activity of G-proteins, which leads to their inhibition (349). The isoform RGS2 has been identified as a selective G_s inhibitor and prevents to synthesis of cAMP by AC. This was later implicated in ADP-independent regulation of AC function in platelets by Noe *et al*. and showed that patients with a heterozygous RGS2 mutation had significantly diminished cAMP generation due to increased AC binding (350). Furthermore, RGS2 has been shown to inhibit AC5 (also expressed in platelets) function in HEK293 cells in a $G\alpha_i$-independent manner (220,351). Currently, there have been no investigations into the effect of GPVI activation on the function of RGS proteins in platelets. The hypothesis of this effect is illustrated in figure 6.2. However, this hypothesis does not account for the increase in markers of PKA, although there could be several processes underway during collagen-mediated platelet spreading.

The role of PKA in platelets is very different to its effect on nucleated cells. This could potentially be explained by differences in isoform expression and available substrates in each cell type. More recently, there has been increasing interest in the spatiotemporal regulation of PKA activity through AKAPs. These anchoring proteins localise PKA isoforms with many substrates depending on the AKAP conformation and add yet another layer of complexity to the PKA signalling pathway. However, only a select few have been isolated and identified in platelets, including small molecular AKAP (smAKAP) and moesin (228,352). Interestingly, Margarucci *et al.* observed the assembly of PKA anchoring proteins, notably AKAP9 and AKAP2 to the plasma membrane upon GPVI stimulation in platelets along with the two α and β catalytic subunits of PKA, suggesting that PKA activity may be primed upon

collagen stimulation (353). Conversely, the purpose of this AKAP:PKA-Cα/β binding may be to prevent cAMP formation and obscuring PKA catalytic subunits from being activated. Unfortunately, AC enrichment within these AKAPs was not analysed and requires further investigation. Also requiring exploration is the full screening of AKAPs in platelets and identifying which AKAPs associate with AC isoforms upon collagen and fibrinogen activation.

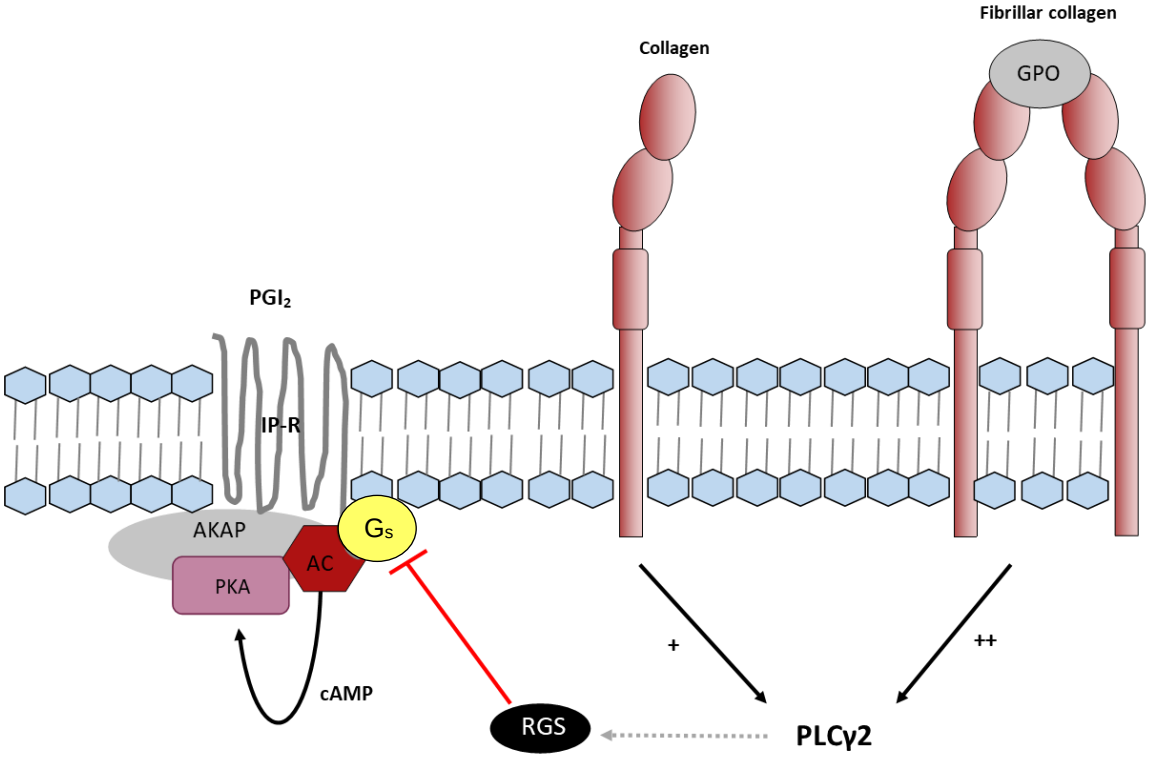

Figure 6.2. Proposed mechanism of G_s and downstream AC inhibition through collagen-mediated activation of RGS proteins. *Activation of the GPVI receptor (red) with fibrillar or monomeric collagen via GPO sequences leads to varying levels of downstream PLCγ2 activation and subsequent activation of RGS isoforms. Activated RGS can inhibit the function of G_s signalling downstream of the IP receptor, leading to a lack of cAMP synthesis in response to PGI_2 stimulation.*

The unexplained increase in PKA substrate and VASP phosphorylation could be a result of non-specificity of the antibodies used, which may be binding to other substrates which may be phosphorylated by kinases, or promiscuity of the targeted phosphorylation site to other kinases. Wentworth *et al*. have previously demonstrated that pVASP can be phosphorylated at ser157 in a PKC-dependent manner in response to thrombin (310). It has yet to be investigated if collagen shares

this similar effect. An experiment to be performed carrying forward would be the inhibition of PKC and its respective isoforms when spreading on Horm collagen or CRP, where there should be no significant increase in the levels of pPKA substrate or pVASPser157. If the elevated phosphorylation pattern persists, this would suggest that PKA is indeed activated upon GPVI activation and would refute both that a) the current consensus that PKA signalling leads to platelet inhibition, and b) PKA is only activated in platelets with elevated cAMP levels.

One potential mechanism that neatly brings together the disparate cAMP and PKA findings is collagen-mediated release of sphingosine-1-monophosphate (S1P). S1P release has been shown in platelets in response to PAR and GPVI stimulation (354). This release could result in autocrine and paracrine activation of $G\alpha_i$ through the S1P receptor reportedly expressed by platelets and lead to the inhibition of AC in an identical manner to ADP signalling. Importantly, sphingosine has been shown to increase PKA activity in a cAMP-independent manner in COS cells (312). In activated platelets, S1P has also been shown to be dephosphorylated into sphingosine by S1P phosphorylase, which could then go on to activate PKA (317). This would be a fitting explanation for the conflicting data. This may shed doubt onto the notion of PKA playing an exclusive inhibitory role in platelets, unless the PKA activity observed in collagen spread platelets is autoinhibitory. An illustration of this hypothesis is shown in figure 6.3. As this mechanism fits the current set of data detailed in chapter 5, the existence of this mechanism in collagen-spread platelets should be studied as a priority. Perhaps the effect of PKA is dependent on the activation method, with cAMP imparting an inhibitory role and sphingosine as an activatory role, alongside specific compartmentalisation with AKAPs.

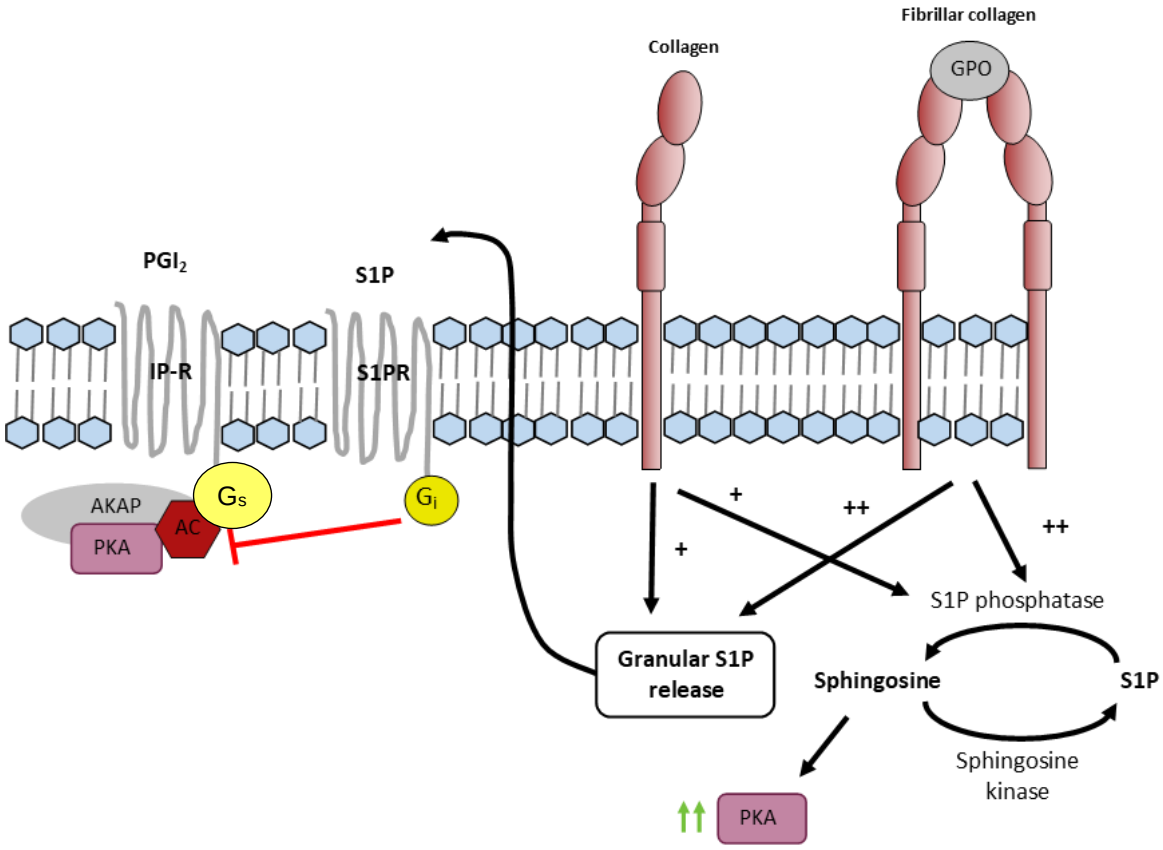

Figure 6.3. Proposed mechanism of collagen-mediated inhibition of AC function and cAMP-independent activation of PKA via S1P autocrine and paracrine signalling. *Activation of dimeric or monomeric GPVI by collagen caused increased release and/or synthesis or S1P in platelets. S1P then binds to the S1P receptor shown to be expressed on the platelet plasma membrane, leading to activation of the G_i α-protein. Activated G_i, as seen with P2Y12 agonism, inhibits AC function, leading to reduced cAMP formation and decreased cAMP dependent PKA activation. Platelet activation has been shown to cause the dephosphorylation of synthesised intracellular, non-granule S1P into sphingosine through activation of S1P phosphatase. Sphingosine can then activate PKA in a cAMP-independent manner, potentially leading to different effects within the cell.*

6.5. Fibrinogen density determines PGI_2 sensitivity and nodule characteristics: implications for thrombus formation?

In chapter 5, I have highlighted the ability of fibrinogen matrix coating density to impart varying levels of PGI_2 sensitivity in platelets. This was found to be in a similar mechanism to collagen-spread platelets, with stress fibre reversal only occurring when AC was activated with forskolin, and not when PDE3 was inhibited by milrinone. This, like collagen spread platelets, indicated that levels of AC activity when in LDF spread platelets was much lower than in those spread on HDF. In agreement with this, cAMP levels in LDF spread platelets were significantly lower than those on HDF when treated with PGI_2. The key question to address with this novel data is whether this effect is physiologically relevant and how this may impact thrombus formation in health and disease.

Fibrinogen in suspension has been shown to inhibit platelet activity (355). In agreement with this, there are reported cases of thrombotic events in individuals with afibrinogenaemia (335). The importance of fibrinogen immobilisation as a requirement for platelet reactivity is well known. Qiu *et al.* have used 3µg/ml fibrinogen solutions to coat slides of varying polyacrylamide stiffnesses and showed that as stiffness increases, so does platelet spreading (305). Although not used in the study, one can speculate as to why the standard 100µg/ml fibrinogen coating was not used, considering the findings presented in chapter 5 and those previously reported by Jirouskova *et al*. (247). It is likely that platelets are mechanosensing HDF coatings as low-stiffness and are not activating as robustly as those spread on LDF coatings, which may be sensed as high-stiffness. The downstream signalling of platelet mechanosensing has been poorly investigated, with only one report into the mechanosensing protein, vinculin, in platelet function and thrombus formation (356). In this study, the authors demonstrate that vinculin knockout in mice causes no difference in aggregation, adhesion and spreading to several agonists, although there was a significant prolongation of tail bleeding times. These investigators however did not study the role of matrix stiffness or density on these knockout platelets and should be a topic for further investigation. At the time of writing this manuscript, new findings reported from Macwan *et al* indicate that when partially stimulated over a prolonged time, platelets show hallmarks of PKA activation, such as $pVASP^{ser157}$, indicating that both their intrinsic PKA pathway increases, as does their sensitivity to PGI_2 (357). This agrees with findings in chapter 5 of this thesis and suggests that if platelets spread on HDF signal weaker than those on LDF, then

PGI_2 sensitivity may increase in the former and decrease in the latter due this autoregulation.

I have generated data that demonstrates a relationship between fibrinogen matrix density and actin nodule dynamics in platelets. As density decreases, nodule size increases and *vice versa*. However, in control conditions, formation of actin nodules is extremely low on LDF compared to HDF and suggests a different signalling mechanism is taking place. This may be a result of Rac1-mediated spreading as shown previously on LDF compared to HDF, leading to enhanced lamellipodia and stress fibre formation (247). There is still work underway to determine the role of actin nodules prior to, during and after thrombus formation and currently there has only been a handful of reports. Actin nodules bear striking resemblance to podosomes found in other cell types. They contain F-actin, the Arp2/3 complex and WASP, talin, vinculin, and are rich in phosphotyrosine (pTyr), which indicate that both nodules and podosomes have similar purposes in sensing underlying matrices to determine changes in cell behaviour accordingly (103). Poulter *et al*. have reported findings using WAS patient platelets that are devoid of WASP, and thus have diminished Arp2/3 function (229). Platelets from these individuals fail to form actin nodules and struggle to form stable adhesions under flow, indicating the importance of actin nodules in thrombus formation. The presence of vinculin further increases the likelihood that nodules are mechanosensing structures. This supports the increase in nodule size in LDF spread platelets and suggests that as fibrinogen density decreases, stiffness increases, leading to larger nodules. The changes in the quantities of pTyr in these nodules compared to HDF nodules should be analysed through simple immunofluorescence microscopy. A higher intensity of pTyr staining in LDF nodules would agree with the previous findings from Jirouskova *et al*., who showed its elevation in LDF spread platelets, indicating increased platelet activity (247).

Zhang *et al*. have shown an inverse relationship between $\alpha_{IIb}\beta_3$ tension during platelet spreading and PS exposure (358). As platelets degranulate, integrin tension diminishes by over 60%. This was shown to occur after approximately 20 minutes of spreading, a time at which stress fibres become prevalent in human platelets that spread on fibrinogen (273). Considering that the actin nodule is densely surrounded by $\alpha_{IIb}\beta_3$ and is critical for thrombus formation, it is likely that nodules allow directed degranulation, providing the necessary secondary mediators and adhesive proteins

required for firm attachment at sites of injury. Fibronectin release from granule stores is a mechanism by which platelets can 'fill in the gaps' in pre-existing matrices and then begin to spread over (57). Possibly nodules may be directing granule secretion and adhesion protein deposition during platelet spreading, and the increased nodule size in LDF spread platelets may be a marker of this, whereas the smaller nodules seen in HDF reflect their constant probing of high-density matrices which would not require matrix deposition. To test this hypothesis, the presence of membrane fusion proteins and regulators of granule release at actin nodules should be investigated. The role of actin nodules in sensing underlying matrix properties should also be studied. The limited data available here and published elsewhere implicates nodules as key platelet components during thrombus formation, likely through sensing of the mechanical and proteinaceous properties of the underlying matrix.

6.6. The matrix responsible for PGI_2 sensitivity in spread platelets: Collagen or fibrinogen?

I have shown that collagen can inhibit AC function in spread platelets and high-density fibrinogen can cause sensitivity to PGI_2. This raises the question of if it is primarily one of these matrix proteins or their respective receptors that is the sole cause of these findings. I have also shown that platelets spread on fibronectin are sensitive to PGI_2 stress fibre reversal, which could suggest that the effect of insensitivity on collagen is due to GPVI activation. However, fibronectin itself can bind with and signal through $\alpha_{IIb}\beta_3$ via its RGD sequences. This could potentially mean that the activation of $\alpha_{IIb}\beta_3$ is what imparts PGI_2 sensitivity in spread platelets. Areas throughout the thrombus that are lacking $\alpha_{IIb}\beta_3$ activity could therefore be resistant and maintain their position though RhoA-mediated contractility. This hypothesis should be tested using the $\alpha_{IIb}\beta_3$ blocking peptide, eptifibatide in platelet spreading on a number of different matrices prior to treatment with PGI_2. If αIIbβ3 is the cause of sensitivity, its inhibition could impart PGI2 resistance. Conversely, the hypothesis that insensitivity is derived from GPVI activity could be tested by spreading platelets on collagen in the presence of a human GPVI blocking antibody, or the Fc-based Revacept. If GPVI is the cause of resistance, there would be no observable change in cytoskeletal phenotype upon PGI_2 treatment. Recently, the ability of D-domain recognition by GPVI in platelets has been highlighted by Induruwa *et al*., which was shown to facilitate platelet adhesion to fibrinogen at low shear rate (359). Interestingly, fibrinogen D-domains have been shown to be

exposed in low-density coatings and causes stain on the fibrinogen monomer by laying horizontally (360). Considering these studies, it appears that GPVI is the central player in determining PGI_2 resistance.

6.7. Can platelets autonomously use PKA activity to finely control actin dynamics?

The temporal action of PGI_2 on spread platelets appears to be maximal at around 20 minutes, as indicated by the return to a stress fibre positive phenotype using real time F-actin visualisation with LifeAct mice. This suggests that platelets are refractory to PGI_2 stimulation and downstream PKA activation. This makes sense, as platelets in the vasculature are likely exposed to varying concentrations of PGI_2 throughout the body and are required to overcome this during clot formation. The recently reported findings from Macwan *et al*. also demonstrates the platelet's ability to activate PKA irrespective of PGI_2 treatment, as shown indicated here in collagen-spread platelets (357). This could indicate that platelets under the correct experimental and physiological conditions can switch off and on PKA to regulate platelet function during changes within the thrombus. It is widely accepted that after establishing a thrombus, it is subsequently consolidated and loses most of its bulk through embolisation of platelets from the thrombus and increased contractility in the remaining platelets. As discussed previously, I propose that PGI_2 perfusion through the outer shell of the thrombus may be a major contributor to this controlled embolisation. However, PKA may also be utilised in platelets as a mechanism to locally regulate actin dynamics. This is not a new phenomenon within cellular biology and has been shown to occur in migratory cells at the lamellipodial edge, resulting in the inhibition of RhoA and the setting of migratory pace. This system could be in place in platelets to control cell spreading and contractility depending on the underlying matrix, its concentration and the level of shear stress present.

6.8. The therapeutic benefit of targeting PGI_2 sensitivity in platelets

Experimental inhibition of platelet actin dynamics significantly diminishes the formation and stability of thrombi. However, inhibition of actin dynamics in platelets as a therapy is not possible due to the ubiquitous nature of the actin cytoskeleton and its regulators. This would be a highly effective therapy if targeted correctly with a platelet-specific delivery method like Gp1b-linked nanoparticles or vesicles, however these methods are far from therapeutic use. Therefore, a more subtle approach must be made that targets the interlinking of pathways within the platelet

and allows the limiting of thrombus size whilst ensuring sufficient haemostasis; a common caveat with current antiplatelet therapies. Data shown in chapters 4 and 5 demonstrate that matrix type and density can have a dramatic effect on PGI_2 sensitivity. Modifying the underlying signalling leading to this could allow the reestablishment of PGI_2 sensitivity. For example, a correctly dosed S1P-R inhibitor or inhibitors of RGS proteins that are in higher abundance in platelets. However, these factors require thorough investigation to clarify their effect on PGI_2 insensitivity in response to varying matrix types and concentrations. In those with vascular endothelial dysfunction where PGI_2 synthesis could be diminished, the PGI_2 analog, iloprost, could be used to increase basal IP-R agonism and act as a two-pronged approach. The enhanced sensitivity of platelets to PGI_2 has been experimentally shown using P2Y12 antagonists, which prevent downstream activation of G_i and allow continued AC activity (308,361).

Currently, the antiplatelet Fc drug, Revacept, is in stage II clinical trial and inhibits platelet interactions with collagen by binding to and obscuring GPO sites for GPVI (www.clinicaltrials.gov/ct2/show/NCT01645306). With the collagen data presented here, the use of this drug may at least prevent PGI_2 insensitivity in platelets attaching to sites of vascular injury where GPVI activity predominates. This is especially desirable in stenosed atherosclerotic vessels, where the subendothelium is presented further into the lumen. By forcing PGI_2 sensitivity platelets attaching to collagen, thrombus bulk could be diminished, and vessel occlusion prevented.

6.9. Limitations of this work

Although due care was taken in planning the experiments performed in this body of work with the resources at hand, there are limitations of these findings which require further work to address.

1. *Spreading experiments were performed on washed platelets, which have been stripped of any plasma components*.

This was required for the investigation of the effect of NO and PGI_2 because there may be residual metabolites of PGI_2 or NO which may affect individuals results due to non-platelet factors, such as increased synthesis of these inhibitors between donors. Additionally, there may also be plasma components which may interact with NO and PGI_2 and therefore cause differential levels of their breakdown, which would add further variation to the findings not related to the platelets themselves.

Circumventing this problem with NO is problematic due its high reactivity and resulting millisecond half-life in the plasma. It is hypothesised that the predominant action of NO on platelets is due to laminar flow within the blood vessel which pushes platelets closest to the endothelial wall where NO and PGI_2 is released (11). Therefore, in a static spreading assay, this effect is not present, which may result in the soaking up of released NO with plasma proteins.

2. *Spreading and flow experiments were performed on 2-dimensional (2D) glass-adsorbed matrices that were ultra-stiff.*

The stiffness of glass coverslips is much stiffer than any structure which the platelet may interact with in the human body and limits the physiological relevance of the findings obtained, as platelets may not form the typical stress fibres seen in platelet spreading assays. The 2D nature of the platelet spreading assay is also unlikely to be seen in the body. Thrombus formation is a swift process, and it is unlikely that platelets within the thrombus will be spreading only in the XY plane. These limitations notwithstanding, the analysis of stress fibre sustenance was valuable as a readout for platelet contractility.

3. *The sensitivity of spread platelets to PGI_2 and NO were tested on isolated matrix proteins.*

Endothelial damage causes the exposure of a multitude of matrix proteins, including collagens, fibronectin, vitronectin and laminin (362). Additionally, vWF exposure from damaged endothelium and chemical interactions between matrix types further adds complexity to the area of injury (363,364). Therefore, areas of vascular damage are heterogeneous, and will result in a spectrum of platelet responses and thrombus characteristics. Further investigation into the role of GPVI-mediated platelet cAMP inhibition in mixtures of matrices should be performed. Potentially, the presence of collagen at sites of vascular damage can shut down cAMP formation in platelets irrespective of any other matrix protein that the platelet is interacting with. Findings from such research may further shed light on the criticality of GPVI signalling in thrombus formation.

6.10. Future directions

1. *Visualising in situ thrombi to determine matrix protein deposition*

The findings presented here show that platelet sensitivity to PGI_2 is dependent on the type and concentration of matrix proteins that the platelet has been exposed to. In figure 6.1 I have taken these findings to hypothesise the effect of this phenomenon during and after thrombus formation. To further these findings, the visualisation and quantification of matrices within a thrombus should be performed. Although it is known that collagen resides within the subendothelium, the deposition and concentration of fibrinogen within a formed thrombus has not been investigated. In order to investigate this, thrombi will be formed within WT mice, preferably through laser induced injury, which imitates mechanical injury more accurately than ferric chloride method. This thrombus would then be fixed and stained for matrix proteins, including collagens, fibrinogen and fibrin. Using proatherogenic mouse models such as ApoE knockout mice (365), the influence of vessel stiffening, increased collagen synthesis and stenosis on thrombus formation could also be explored and compared to WT counterparts.

2. *Visualising real-time in vivo thrombus formation and sustenance in response to PGI_2 and NO*

Individuals with hereditary mutations in NO or PGI_2 signalling are at a higher risk of myocardial infarction and stroke (200,366), highlighting the impact of these inhibitors in the prevention of occlusive thrombus formation. The direct mechanism of NO and PGI_2 action in *in vivo* thrombosis should be uncovered. This could be undertaken using mice lacking functional PKA or sGC function in *in vivo* thrombus formation assays. There have been reports of the use of such mice previously, which importantly don't spontaneously thrombose (189,367). Only upon vascular damage do these mice form occlusive thrombi, suggesting that NO and PGI_2 have little influence in the regulation of unstimulated platelets. This work and previous work from our lab has implicated cyclic nucleotide signalling in the controlled embolisation of platelet from preformed thrombi *in vitro* (273,301). By uncovering the *in vivo* effects of NO and PGI_2 during and after thrombus formation, we may be able to demonstrate physiological relevance of our findings. To make this finding more specific to platelet contractility, inhibitors of actin-myosin interactions should be used, such as the ROCK inhibitor Y27632, and the MLCK inhibitor, ML7.

3. *Do people with dysfunctional platelet GPVI signalling have an increased thrombus susceptibility to PGI_2?*

There have been several reports of dysfunctional GPVI signalling, either as a result of homozygous mutations, or generated anti-GPVI autoantibodies, resulting in varying levels of bleeding phenotypes (368,369). Additionally, oral administration of inhibitors of downstream Bruton tyrosine kinase (Btk) causes inadvertent GPVI dysfunction in platelets and excessive bleeding episodes upon injury (370,371). Perhaps platelets from these individuals have an increased susceptibility to PGI_2 inhibition *in vivo* through a lack of GPVI signalling. Due to the rarity of GPVI mutations, it would be more appropriate to investigate the effect of Btk inhibition on platelet PGI_2 sensitivity in CLL patients, considering the widespread use of these inhibitors as chemotherapy agents. This would consist of *in vitro* platelet spreading and thrombus formation on several matrices in the presence or absence of cAMP elevating agents. Findings from such a study could highlight both the role of GPVI in PGI_2 resistance and a novel mechanism by which Btk antagonism causes bleeding

4. *Effect of matrix stiffness on platelet cyclic nucleotide sensitivity*

Due to the theorised mechanosensing capabilities of actin nodules brought about by vinculin enrichment within them, an investigation into the effect of different matrix stiffness on PGI_2/NO sensitivity should be undertaken. Our data surrounding matrix density coatings suggest that the stiffness of matrices may also influence this, as increasing matrix density correlates with a decrease in stiffness. Investigations from the Shattil group in the University of California have shown little effect of vinculin deficiency in murine platelets (356). However, this work did not involve investigation into full platelet spreading on platelet agonists, nor their respective concentrations or stiffnesses. There have been several reports of the ability of platelets to mechanosense underlying matrices, leading to enhanced contractility and spreading through small RhoGTPase signaling (305,358). To investigate the role of matrix stiffness in PKA/PKG sensitivity in platelets, a similar approach to Qiu *et al.*, would be used (305). In short, polyacrylamide gels of varying stiffnesses would be fabricated and fibrinogen absorbed over the gel. Unlike the previous authors, platelet actin dynamics would be visualised to assess stress fibre formation on different stiffnesses. Platelet lysates would also be made to uncover underlying platelet signalling, including markers of platelet contractility and PKA/PKG activity upon PGI_2 and NO treatment, respectively.

6. *Measurement of platelet contractility within the thrombus*

Although we have shown stress fibre formation and reversion back into an actin nodule phenotype upon CN signalling, this has been performed in static conditions and do not reflect the impact of platelet-platelet interactions on the stiffness of the thrombus. Although I have observed this reversal in platelets adhered and spread on fibrinogen at arterial shear, the direct interaction with the stiff polymer of flow channels is not representative of formed thrombi. Perhaps under flow, platelets do not form stress fibres in the upper layers of the thrombus due to a reduction in substrate stiffness and so are less contractile than platelets within the thrombus core. Chen *et al*. have recently reported a method of measuring platelet contractility within a forming thrombus (372). Called microfluidic-integrated microclot-array-elastometry (clotMAT), this method involves the fabrication of flexible PDMS micropillars on a stretchable membrane base, allowing the measurement of thrombus contractility and stiffness. Using this method, these authors found that inhibition of myosin and αIIbβ3 activity through blebbistatin and abciximab, respectively, abolished platelet contractility using this method. This method could be used in the study of CN signalling on thrombi, especially considering that our findings indicate that fibrinogen spread platelets are sensitive to CN signalling, which leads to the reduction of platelet contractility through RhoA inhibition (273,301).

7. *Does shear rate affect platelet susceptibility to CN signalling?*

As of yet, the effect of PGI_2/NO on formed thrombi under different shear rates has not been investigated. It would be reasonable to hypothesise that high shear leads to increased resistance of platelets to PGI_2/NO, as integrin signalling would be increased as a result. However, the findings in chapter 5 suggest that increased integrin binding causes and increase in PGI_2 sensitivity. Findings from recent work by Wen *et al*. have uncovered a role of shear stress in the induction of NO sensitivity and subsequent PKG activation to nanomolar concentrations of DEANONOate (298). Additionally, this work demonstrated that cGMP, in the absence of exogenous NO, is most active in platelets on the outer shell of the thrombus. To clarify this effect, *in vitro* thrombus formation assays should be performed to establish platelet-rich thrombi. PGI_2 and/or NO should then further be perfused at different shear rates through the thrombus, with measurements of thrombus height/volume and surface coverage. Stress fibre sustenance could also be analysed in platelets spread on

fibrinogen in response to PGI_2/NO treatment. Ideally, this experiment could be performed using the method outlined by Wen *et al* for real time cGMP formation, and the transgenic mouse model used by Hiratsuka *et al.* for real time PKA activity (302).

6.11. Concluding remarks

In this thesis I have investigated the actin cytoskeletal effects of PGI_2 and NO on platelets that have been spread on differing matrices. I have identified a number of novel effects, including; 1) NO causes stress fibre reversal by inhibiting RhoA in a phosphorylation-independent manner, leading to a reduction in thrombus high in treated thrombi; 2) Immobilised collagen imparts PGI_2 resistance in platelets and prevents stress fibre reversal likely through inhibition of cAMP synthesis; 3) Fibrinogen density affects PGI_2 sensitivity in a dose-dependent manner by reducing cAMP levels; and 4) fibrinogen density modulates actin nodule size in spread platelets. These findings indicate that platelets can regulate their sensitivity to CN-elevating agents and protect themselves from loss of contractility in the form of stress fibre reversal. Possible therapeutic targets from further investigations into the underlying signalling during these processes could lead to nuanced antiplatelet agents with limited off-target effects.

Chapter 7. References

1. Naghavi M, Wang H, Lozano R, Davis A, Liang X, Zhou M, et al. Global, regional, and national age-sex specific all-cause and cause-specific mortality for 240 causes of death, 1990-2013: A systematic analysis for the Global Burden of Disease Study 2013. *The Lancet*. 2015;**385**(**9963**):117–71.

2. Haley WE, Roth DL, Hovater M, Clay OJ. Long-term impact of stroke on family caregiver well-being: a population-based case-control study. *Neurology* [Internet]. 2015 Mar 31 [cited 2019 Jun 19];**84**(**13**):1323–9. Available from: http://www.ncbi.nlm.nih.gov/pubmed/25740862

3. Trialists A. Collaborative meta-analysis of randomised trials of antiplatelet therapy for prevention of death, myocardial infarction, and stroke in high risk patients. *Bmj*. 2002;**324**.

4. Bhatnagar P, Wickramasinghe K, Wilkins E, Townsend N. Trends in the epidemiology of cardiovascular disease in the UK [Internet]. Vol. 102, Heart. 2016 [cited 2019 Jun 19]. p. 1945–52. Available from: http://dx.doi.org/10.1136/heartjnl-2016-309573

5. Belch J, MacCuish A, Campbell I, Cobbe S, Taylor R, Prescott R, et al. The prevention of progression of arterial disease and diabetes (POPADAD) trial: factorial randomised placebo controlled trial of aspirin and antioxidants in patients with diabetes and asymptomatic peripheral arterial disease. *BMJ (Clinical research ed)*. 2008;**337**.

6. Fowkes FGR, Price JF, Stewart MCW, Butcher I, Leng GC, Pell ACH, et al. Aspirin for prevention of cardiovascular events in a general population screened for a low ankle brachial index: A randomized controlled trial. *JAMA - Journal of the American Medical Association*. 2010;**303**(**9**):841–8.

7. Goh C, Churilov L, Mitchell P, Dowling R, Yan B. Clopidogrel hyper-response and bleeding risk in neurointerventional procedures. *American Journal of Neuroradiology*. 2013;**34**(**4**):721–6.

8. Ittaman S V, VanWormer JJ, Rezkalla SH. The role of aspirin in the prevention of cardiovascular disease. *Clinical medicine & research* [Internet]. 2014 Dec [cited 2017 Jun 8];**12**(**3**–**4**):147–54. Available from: http://www.ncbi.nlm.nih.gov/pubmed/24573704

9. Roquer J, Rodríguez Campello A, Gomis M, Ois A, Puente V, Munteis E. Previous antiplatelet therapy is an independent predictor of 30-day mortality after spontaneous

supratentorial intracerebral hemorrhage. *Journal of neurology* [Internet]. 2005 Apr [cited 2019 Aug 5];**252**(**4**):412–6. Available from: http://www.ncbi.nlm.nih.gov/pubmed/15739042

10. Zaninetti C, Biino G, Noris P, Melazzini F, Civaschi E, Balduini CL. Personalized reference intervals for platelet count reduce the number of subjects with unexplained thrombocytopenia. *Haematologica* [Internet]. 2015 Sep [cited 2019 Jul 16];**100**(**9**):e338-40. Available from: http://www.ncbi.nlm.nih.gov/pubmed/25957395

11. Aarts PA, van den Broek SA, Prins GW, Kuiken GD, Sixma JJ, Heethaar RM. Blood platelets are concentrated near the wall and red blood cells, in the center in flowing blood. *Arteriosclerosis: An Official Journal of the American Heart Association, Inc*. 1988;

12. Walton BL, Lehmann M, Skorczewski T, Holle LA, Beckman JD, Cribb JA, et al. Elevated hematocrit enhances platelet accumulation following vascular injury. *Blood*. 2017;**129**(**18**):2537–46.

13. Li J, Yang C, Xia Y, Bertino A, Glaspy J, Roberts M, et al. Thrombocytopenia caused by the development of antibodies to thrombopoietin. *Blood* [Internet]. 2001 Dec 1 [cited 2019 Aug 5];**98**(**12**):3241–8. Available from: http://www.ncbi.nlm.nih.gov/pubmed/11719360

14. Neunert CE, Buchanan GR, Imbach P, Bolton-Maggs PHB, Bennett CM, Neufeld E, et al. Bleeding manifestations and management of children with persistent and chronic immune thrombocytopenia: Data from the Intercontinental Cooperative ITP Study Group (ICIS). *Blood*. 2013;**121**(**22**):4457–62.

15. Ang L, Palakodeti V, Khalid A, Tsimikas S, Idrees Z, Tran P, et al. Elevated Plasma Fibrinogen and Diabetes Mellitus Are Associated With Lower Inhibition of Platelet Reactivity With Clopidogrel. *Journal of the American College of Cardiology*. 2008;**52**(**13**):1052–9.

16. Jurasz P, Alonso-Escolano D, Radomski MW. Platelet-cancer interactions: Mechanisms and pharmacology of tumour cell-induced platelet aggregation. Vol. 143, British Journal of Pharmacology. 2004. p. 819–26.

17. Wraith KS, Magwenzi S, Aburima A, Wen Y, Leake D, Naseem KM. Oxidized low-density lipoproteins induce rapid platelet activation and shape change through tyrosine kinase and Rho kinase-signaling pathways. *Blood* [Internet]. 2013 Jul 25 [cited 2018 Oct 1];**122**(**4**):580–9. Available from: http://www.ncbi.nlm.nih.gov/pubmed/23699602

18. Wilson PW, D'Agostino RB, Levy D, Belanger AM, Silbershatz H, Kannel WB. Prediction of coronary heart disease using risk factor categories. *Circulation* [Internet]. 1998 May 12

[cited 2019 Jun 19];**97**(**18**):1837–47. Available from: http://www.ncbi.nlm.nih.gov/pubmed/9603539

19. Bettache N, Baisamy L, Baghdiguian S, Payrastre B, Mangeat P, Bienvenue A. Mechanical constraint imposed on plasma membrane through transverse phospholipid imbalance induces reversible actin polymerization via phosphoinositide 3-kinase activation. *Journal of cell science* [Internet]. 2003 Jun 1 [cited 2019 Aug 5];**116**(**Pt 11**):2277–84. Available from: http://www.ncbi.nlm.nih.gov/pubmed/12697835

20. Lefrançais E, Ortiz-Muñoz G, Caudrillier A, Mallavia B, Liu F, Sayah DM, et al. The lung is a site of platelet biogenesis and a reservoir for haematopoietic progenitors. *Nature* [Internet]. 2017 [cited 2019 Aug 5];**544**(**7648**):105–9. Available from: http://www.ncbi.nlm.nih.gov/pubmed/28329764

21. Kong Z, Qin P, Xiao S, Zhou H, Li H, Yang R, et al. A novel recombinant human thrombopoietin therapy for the management of immune thrombocytopenia in pregnancy. *Blood* [Internet]. 2017 Aug 31 [cited 2019 Jun 18];**130**(**9**):1097–103. Available from: http://www.ncbi.nlm.nih.gov/pubmed/28630121

22. Siegal D, Crowther M, Cuker A. Thrombopoietin Receptor Agonists in Primary Immune Thrombocytopenia. *Seminars in Hematology*. 2013;**50**(**SUPPL.1**).

23. Vitrat N, Cohen-Solal K, Pique C, Le Couedic JP, Norol F, Larsen AK, et al. Endomitosis of human megakaryocytes are due to abortive mitosis. *Blood* [Internet]. 1998;**91**(**10**):3711–23. Available from: www.bloodjournal.org

24. Handagama P, Scarborough RM, Shuman MA, Bainton DF. Endocytosis of fibrinogen into megakaryocyte and platelet alpha-granules is mediated by alpha IIb beta 3 (glycoprotein IIb-IIIa). *Blood* [Internet]. 1993 Jul 1 [cited 2019 Aug 5];**82**(**1**):135–8. Available from: http://www.ncbi.nlm.nih.gov/pubmed/8391871

25. Schulze H, Korpal M, Hurov J, Kim S-W, Zhang J, Cantley LC, et al. Characterization of the megakaryocyte demarcation membrane system and its role in thrombopoiesis. *Blood* [Internet]. 2006 May 15 [cited 2019 Jun 18];**107**(**10**):3868–75. Available from: http://www.ncbi.nlm.nih.gov/pubmed/16434494

26. Italiano JE, Lecine P, Shivdasani RA, Hartwig JH. Blood Platelets Are Assembled Principally at the Ends of Proplatelet Processes Produced by Differentiated Megakaryocytes. *The Journal of Cell Biology* [Internet]. 1999 Dec 13 [cited 2019 Aug 5];**147**(**6**):1299–312. Available from: http://www.ncbi.nlm.nih.gov/pubmed/10601342

27. Bender M, Stritt S, Nurden P, van Eeuwijk JMM, Zieger B, Kentouche K, et al. Megakaryocyte-specific Profilin1-deficiency alters microtubule stability and causes a Wiskott–Aldrich syndrome-like platelet defect. *Nature Communications* [Internet]. 2014 Dec 4 [cited 2019 Jun 18];**5**(**1**):4746. Available from: http://www.nature.com/articles/ncomms5746

28. Kunishima S, Kobayashi R, Itoh TJ, Hamaguchi M, Saito H. Mutation of the beta1-tubulin gene associated with congenital macrothrombocytopenia affecting microtubule assembly. *Blood* [Internet]. 2009 Oct 2 [cited 2019 Aug 5];**113**(**2**):458–61. Available from: http://www.ncbi.nlm.nih.gov/pubmed/18849486

29. Richardson JL, Shivdasani RA, Boers C, Hartwig JH, Italiano JE. Mechanisms of organelle transport and capture along proplatelets during platelet production. *Blood* [Internet]. 2005 Dec 15 [cited 2019 Aug 5];**106**(**13**):4066–75. Available from: http://www.ncbi.nlm.nih.gov/pubmed/16118320

30. Schwer HD, Lecine P, Tiwari S, Italiano JE, Hartwig JH, Shivdasani RA. A lineage-restricted and divergent beta-tubulin isoform is essential for the biogenesis, structure and function of blood platelets. *Current biology : CB* [Internet]. 2001 Apr 17 [cited 2019 Aug 5];**11**(**8**):579–86. Available from: http://www.ncbi.nlm.nih.gov/pubmed/11369202

31. Diagouraga B, Grichine A, Fertin A, Wang J, Khochbin S, Sadoul K. Motor-driven marginal band coiling promotes cell shape change during platelet activation. *The Journal of cell biology* [Internet]. 2014 Jan 20 [cited 2019 Aug 5];**204**(**2**):177–85. Available from: http://www.ncbi.nlm.nih.gov/pubmed/24421335

32. Lievens D, Zernecke A, Seijkens T, Soehnlein O, Beckers L, Munnix ICA, et al. Platelet CD40L mediates thrombotic and inflammatory processes in atherosclerosis. *Blood*. 2010;**116**(**20**):4317–27.

33. Machlus KR, Johnson KE, Kulenthirarajan R, Forward JA, Tippy MD, Soussou TS, et al. CCL5 derived from platelets increases megakaryocyte proplatelet formation. *Blood*. 2016;**127**(**7**):921–6.

34. Gaertner F, Ahmad Z, Rosenberger G, Fan S, Nicolai L, Busch B, et al. Migrating Platelets Are Mechano-scavengers that Collect and Bundle Bacteria. *Cell* [Internet]. 2017 Nov 30 [cited 2019 Aug 5];**171**(**6**):1368-1382.e23. Available from: http://www.ncbi.nlm.nih.gov/pubmed/29195076

35. Silverstein RL. Type 2 scavenger receptor CD36 in platelet activation: the role of

hyperlipemia and oxidative stress. *Clinical lipidology* [Internet]. 2009 Dec [cited 2019 Aug 5];**4**(**6**):767. Available from: http://www.ncbi.nlm.nih.gov/pubmed/20161667

36. Escolar G, White JG. The platelet open canalicular system: a final common pathway. *Blood cells* [Internet]. 1991 [cited 2019 Aug 5];**17**(**3**):467–85; discussion 486-95. Available from: http://www.ncbi.nlm.nih.gov/pubmed/1760557

37. Nakashima S, Suganuma A, Matsui A, Hattori H, Sato M, Takenaka A, et al. Primary role of calcium ions in arachidonic acid release from rat platelet membranes. Comparison with human platelet membranes. *Biochemical Journal* [Internet]. 1989 Apr 1 [cited 2019 Aug 5];**259**(**1**):139–44. Available from: http://www.biochemj.org/cgi/doi/10.1042/bj2590139

38. O'Donnell VB, Murphy RC, Watson SP. Platelet lipidomics: Modern day perspective on lipid discovery and characterization in platelets. Vol. 114, Circulation Research. 2014. p. 1185–203.

39. Obergfell A, Eto K, Mocsai A, Buensuceso C, Moores SL, Brugge JS, et al. Coordinate interactions of Csk, Src, and Syk kinases with αIIbβ3 initiate integrin signaling to the cytoskeleton. *The Journal of Cell Biology* [Internet]. 2002 Apr 15 [cited 2019 May 31];**157**(**2**):265–75. Available from: http://www.jcb.org/lookup/doi/10.1083/jcb.200112113

40. Petrich BG, Marchese P, Ruggeri ZM, Spiess S, Weichert RAM, Ye F, et al. Talin is required for integrin-mediated platelet function in hemostasis and thrombosis. *The Journal of experimental medicine* [Internet]. 2007 Dec 24 [cited 2019 May 31];**204**(**13**):3103–11. Available from: http://www.ncbi.nlm.nih.gov/pubmed/18086863

41. Leo L, Paola J Di, Judd BA, Koretzky GA, Lentz SR. Role of the adapter protein SLP-76 in GPVI-dependent platelet procoagulant responses to collagen. *Blood*. 2002;**100**(**8**):2839–44.

42. Guidetti GF, Canobbio I, Torti M. PI3K/Akt in platelet integrin signaling and implications in thrombosis. *Advances in Biological Regulation* [Internet]. 2015 Sep [cited 2019 Aug 5];**59**:36–52. Available from: https://linkinghub.elsevier.com/retrieve/pii/S2212492615300051

43. White JG. Platelet glycosomes. *Platelets*. 1999;**10**(**4**):242–6.

44. Boudreau LH, Duchez AC, Cloutier N, Soulet D, Martin N, Bollinger J, et al. Platelets release mitochondria serving as substrate for bactericidal group IIA-secreted phospholipase a to promote inflammation. *Blood*. 2014;**124**(**14**):2173–83.

45. Aibibula M, Naseem KM, Sturmey RG. Glucose metabolism and metabolic flexibility in blood platelets. *Journal of Thrombosis and Haemostasis* [Internet]. 2018 Nov [cited 2019 Aug 5];**16**(**11**):2300–14. Available from: http://www.ncbi.nlm.nih.gov/pubmed/30151891

46. Hayward CPM, Furmaniak-Kazmierczak E, Cieutat AM, Moore JC, Bainton DF, Nesheim ME, et al. Factor V is complexed with multimerin in resting platelet lysates and colocalizes with multimerin in platelet α-granules. *Journal of Biological Chemistry*. 1995;**270**(**33**):19217–24.

47. Quinton TM, Murugappan S, Kim S, Jin J, Kunapuli SP. Different G protein-coupled signaling pathways are involved in alpha granule release from human platelets. *Journal of Thrombosis and Haemostasis* [Internet]. 2004 Jun [cited 2019 Aug 5];**2**(**6**):978–84. Available from: http://www.ncbi.nlm.nih.gov/pubmed/15140134

48. Abou-Saleh H, Théorêt JF, Yacoub D, Merhi Y. Neutrophil P-selectin-glycoprotein-ligand-I binding to platelet P-selectin enhances metalloproteinase 2 secretion and platelet-neutrophil aggregation. *Thrombosis and Haemostasis*. 2005;**94**(**6**):1230–5.

49. White J. Use of the Electron Microscope for Diagnosis of Platelet Disorders. *Seminars in Thrombosis and Hemostasis* [Internet]. 1998 Apr 6 [cited 2019 Aug 5];**24**(**02**):163–8. Available from: http://www.thieme-connect.de/DOI/DOI?10.1055/s-2007-995836

50. Merten M, Thiagarajan P. P-Selectin Expression on Platelets Determines Size and Stability of Platelet Aggregates. *Circulation* [Internet]. 2000 Oct 17 [cited 2019 Jul 19];**102**(**16**):1931–6. Available from: https://www.ahajournals.org/doi/10.1161/01.CIR.102.16.1931

51. Morel A, Rywaniak J, Bijak M, Miller E, Niwald M, Saluk J. Flow cytometric analysis reveals the high levels of platelet activation parameters in circulation of multiple sclerosis patients. *Molecular and Cellular Biochemistry* [Internet]. 2017 Jun 16 [cited 2019 Jul 19];**430**(**1**–**2**):69–80. Available from: http://link.springer.com/10.1007/s11010-017-2955-7

52. Diacovo T, Roth S, Buccola J, Bainton D, Springer T. Neutrophil rolling, arrest, and transmigration across activated, surface-adherent platelets via sequential action of P-selectin and the beta 2-integrin CD11b/CD18. *Blood* [Internet]. 1996 [cited 2019 Jul 19];**88**(**1**). Available from: http://www.bloodjournal.org/content/88/1/146?ijkey=276c209611d69088ea4d6ef1439f2913a8883885&keytype2=tf_ipsecsha

53. Polanowska-Grabowska R, Wallace K, Field JJ, Chen L, Marshall MA, Figler R, et al. P-Selectin–Mediated Platelet-Neutrophil Aggregate Formation Activates Neutrophils in

Mouse and Human Sickle Cell Disease. *Arteriosclerosis, Thrombosis, and Vascular Biology* [Internet]. 2010 Dec [cited 2019 Jul 19];**30**(**12**):2392–9. Available from: http://www.ncbi.nlm.nih.gov/pubmed/21071696

54. Wagner C, Mascelli M, Neblock D, Weisman H, Coller B, Jordan R. Analysis of GPIIb/IIIa receptor number by quantification of 7E3 binding to human platelets. *Blood* [Internet]. 1996 [cited 2019 Jul 20];**88**(**3**). Available from: http://www.bloodjournal.org/content/88/3/907?ijkey=29a1867d9211cf053688b186dbcae5d81959169c&keytype2=tf_ipsecsha&sso-checked=true

55. Woods V., Wolff L., Keller D. Resting platelets contain a substantial centrally located pool of glycoprotein IIb-IIIa complex which may be accessible to some but not other extracellular proteins. *Journal of Biological Chemistry*. 1986;**261**(**32**):15242–51.

56. Leung LL. Role of thrombospondin in platelet aggregation. *Journal of Clinical Investigation* [Internet]. 1984 Nov 1 [cited 2019 Jul 20];**74**(**5**):1764–72. Available from: http://www.jci.org/articles/view/111595

57. Sakurai Y, Fitch-Tewfik JL, Qiu Y, Ahn B, Myers DR, Tran R, et al. Platelet geometry sensing spatially regulates α-granule secretion to enable matrix self-deposition. *Blood* [Internet]. 2015 Jul 23 [cited 2019 Jun 14];**126**(**4**):531–8. Available from: http://www.bloodjournal.org/cgi/doi/10.1182/blood-2014-11-607614

58. Heijnen HF, Debili N, Vainchencker W, Breton-Gorius J, Geuze HJ, Sixma JJ. Multivesicular bodies are an intermediate stage in the formation of platelet alpha-granules. *Blood* [Internet]. 1998 Apr 1 [cited 2019 Aug 5];**91**(**7**):2313–25. Available from: http://www.ncbi.nlm.nih.gov/pubmed/9516129

59. Alberio L, Safa O, Clemetson KJ, Esmon CT, Dale GL. Surface expression and functional characterization of alpha-granule factor V in human platelets: effects of ionophore A23187, thrombin, collagen, and convulxin. *Blood* [Internet]. 2000 Mar 1 [cited 2019 Jul 20];**95**(**5**):1694–702. Available from: http://www.ncbi.nlm.nih.gov/pubmed/10688826

60. Piersma SR, Broxterman HJ, Kapci M, de Haas RR, Hoekman K, Verheul HMW, et al. Proteomics of the TRAP-induced platelet releasate. *Journal of Proteomics* [Internet]. 2009 Feb 15 [cited 2019 Jul 20];**72**(**1**):91–109. Available from: http://www.ncbi.nlm.nih.gov/pubmed/19049909

61. Nurden AT, Nurden P. The gray platelet syndrome: Clinical spectrum of the disease. *Blood Reviews* [Internet]. 2007 Jan [cited 2019 Aug 5];**21**(**1**):21–36. Available from:

http://www.ncbi.nlm.nih.gov/pubmed/16442192

62. Urban D, Pluthero FG, Christensen H, Baidya S, Rand ML, Das A, et al. Decreased numbers of dense granules in fetal and neonatal platelets. *Haematologica* [Internet]. 2017 [cited 2019 Jul 21];**102**(**2**):e36–8. Available from: http://www.ncbi.nlm.nih.gov/pubmed/27810994

63. Polasek J. Platelet secretory granules or secretory lysosomes? [Internet]. Vol. 16, Platelets. 2005 [cited 2019 Jul 21]. p. 500–1. Available from: https://www.tandfonline.com/action/journalInformation?journalCode=iplt20

64. Zhong C, Ling Y, Ding J, Yu Z, Fujimoto K, Ogawa K. The Intracellular Calcium Store Function of Platelet Granules. *Acta Histochemica et Cytochemica* [Internet]. 1997 [cited 2019 Aug 5];**30**(**5/6**):439–44. Available from: http://joi.jlc.jst.go.jp/JST.Journalarchive/ahc1968/30.439?from=CrossRef

65. Lages B, Weiss HJ. Secreted dense granule adenine nucleotides promote calcium influx and the maintenance of elevated cytosolic calcium levels in stimulated human platelets. *Thrombosis and haemostasis* [Internet]. 1999 Feb [cited 2019 Aug 5];**81**(**2**):286–92. Available from: http://www.ncbi.nlm.nih.gov/pubmed/10064008

66. Abraham SM, Boayue K, Ahmed I. Platelet Delta Storage Pool Deficiency In Children : A Case Series. *Blood* [Internet]. 2013 [cited 2019 Jul 19];**122**(**21**). Available from: http://www.bloodjournal.org/content/122/21/4747

67. Masliah-Planchon J, Darnige L, Bellucci S. Molecular determinants of platelet delta storage pool deficiencies: an update. *British journal of haematology* [Internet]. 2013 Jan [cited 2019 Jul 19];**160**(**1**):5–11. Available from: http://doi.wiley.com/10.1111/bjh.12064

68. Cloutier N, Allaeys I, Marcoux G, Machlus KR, Mailhot B, Zufferey A, et al. Platelets release pathogenic serotonin and return to circulation after immune complex-mediated sequestration. *Proceedings of the National Academy of Sciences* [Internet]. 2018 Feb 13 [cited 2019 Aug 5];**115**(**7**):E1550–9. Available from: http://www.ncbi.nlm.nih.gov/pubmed/29386381

69. Ikeda Y, Handa M, Kawano K, Kamata T, Murata M, Araki Y, et al. The role of von Willebrand factor and fibrinogen in platelet aggregation under varying shear stress. *Journal of Clinical Investigation* [Internet]. 1991 Apr 1 [cited 2019 Jun 13];**87**(**4**):1234–40. Available from: http://www.jci.org/articles/view/115124

70. Siediecki C, Lestini B, Kottke-Marchant K, Eppell S, Wilson D, Marchant R. Shear-dependent

changes in the three-dimensional structure of human von Willebrand factor. *Blood* [Internet]. 1996 [cited 2019 Jun 13];**88**(**8**). Available from: http://www.bloodjournal.org/content/88/8/2939.short?sso-checked=true

71. Yago T, Lou J, Wu T, Yang J, Miner JJ, Coburn L, et al. Platelet glycoprotein Ibα forms catch bonds with human WT vWF but not with type 2B von Willebrand disease vWF. *The Journal of Clinical Investigation* [Internet]. 2008 [cited 2019 Jun 13];**118**. Available from: http://www.jci.org

72. Schoenwaelder SM, Yuan Y, Josefsson EC, White MJ, Yao Y, Mason KD, et al. Two distinct pathways regulate platelet phosphatidylserine exposure and procoagulant function. *Blood* [Internet]. 2009 Jul 16 [cited 2019 Jun 13];**114**(**3**):663–6. Available from: http://www.bloodjournal.org/cgi/doi/10.1182/blood-2009-01-200345

73. Osdoit S, Rosa J-P. Fibrin clot retraction by human platelets correlates with alpha(IIb)beta(3) integrin-dependent protein tyrosine dephosphorylation. *Journal of Biological Chemistry* [Internet]. 2001 Mar 2 [cited 2019 Aug 5];**276**(**9**):6703–10. Available from: http://www.ncbi.nlm.nih.gov/pubmed/11084040

74. Alshehri OM, Hughes CE, Montague S, Watson SK, Frampton J, Bender M, et al. Fibrin activates GPVI in human and mouse platelets. *Blood* [Internet]. 2015 Sep 24 [cited 2018 Nov 1];**126**(**13**):1601–8. Available from: http://www.ncbi.nlm.nih.gov/pubmed/26282541

75. Lam WA, Chaudhuri O, Crow A, Webster KD, Li T-D, Kita A, et al. Mechanics and contraction dynamics of single platelets and implications for clot stiffening. *Nature Materials* [Internet]. 2011 Jan 5 [cited 2019 Jun 13];**10**(**1**):61–6. Available from: http://www.nature.com/articles/nmat2903

76. Welsh JD, Stalker TJ, Voronov R, Muthard RW, Tomaiuolo M, Diamond SL, et al. A systems approach to hemostasis: 1. The interdependence of thrombus architecture and agonist movements in the gaps between platelets. *Blood* [Internet]. 2014 Sep 11 [cited 2017 Mar 2];**124**(**11**):1808–15. Available from: http://www.ncbi.nlm.nih.gov/pubmed/24951424

77. Tomaiuolo M, Stalker TJ, Welsh JD, Diamond SL, Sinno T, Brass LF. A systems approach to hemostasis: 2. Computational analysis of molecular transport in the thrombus microenvironment. *Blood* [Internet]. 2014 Sep 11 [cited 2017 Mar 2];**124**(**11**):1816–23. Available from: http://www.ncbi.nlm.nih.gov/pubmed/24951425

78. Stalker TJ, Welsh JD, Tomaiuolo M, Wu J, Colace T V., Diamond SL, et al. A systems approach to hemostasis: 3. Thrombus consolidation regulates intrathrombus solute

transport and local thrombin activity. *Blood* [Internet]. 2014 Sep 11 [cited 2017 Mar 2];**124**(**11**):1824–31. Available from: http://www.ncbi.nlm.nih.gov/pubmed/24951426

79. Welsh JD, Muthard RW, Stalker TJ, Taliaferro JP, Diamond SL, Brass LF. A systems approach to hemostasis: 4. How hemostatic thrombi limit the loss of plasma-borne molecules from the microvasculature. *Blood* [Internet]. 2016 Mar 24 [cited 2019 Aug 5];**127**(**12**):1598–605. Available from: http://www.ncbi.nlm.nih.gov/pubmed/26738537

80. Salsmann A, Schaffner-reckinger E, Kabile F, Kieffer N. A New Functional Role of the Fibrinogen RGD Motif as the Molecular Switch That Selectively Triggers Integrin □ IIb □ 3-dependent RhoA Activation during Cell Spreading *. 2005;**280**(**39**):33610–9.

81. Blombäck B, Hessel B, Hogg D. Disulfide bridges in nh2 -terminal part of human fibrinogen. *Thrombosis research* [Internet]. 1976 May [cited 2019 May 28];**8**(**5**):639–58. Available from: http://www.ncbi.nlm.nih.gov/pubmed/936108

82. Kollman JM, Pandi L, Sawaya MR, Riley M, Doolittle RF. Crystal Structure of Human Fibrinogen. *Biochemistry* [Internet]. 2009 May 12 [cited 2019 May 28];**48**(**18**):3877–86. Available from: https://pubs.acs.org/doi/10.1021/bi802205g

83. Yamazumi K, Shimura K, Terukina S, Takahashi N, Matsuda M. A gamma methionine-310 to threonine substitution and consequent N-glycosylation at gamma asparagine-308 identified in a congenital dysfibrinogenemia associated with posttraumatic bleeding, fibrinogen Asahi. *Journal of Clinical Investigation* [Internet]. 1989 May 1 [cited 2019 May 28];**83**(**5**):1590–7. Available from: http://www.ncbi.nlm.nih.gov/pubmed/2496144

84. Pizzo S V, Schwartz ML, Hill RL, McKee PA. The effect of plasmin on the subunit structure of human fibrin. *The Journal of biological chemistry* [Internet]. 1973 Jul 10 [cited 2019 Aug 5];**248**(**13**):4574–83. Available from: http://www.ncbi.nlm.nih.gov/pubmed/4268861

85. Nurden AT, Didry D, Kieffer N, McEver RP. Residual amounts of glycoproteins IIb and IIIa may be present in the platelets of most patients with Glanzmann's thrombasthenia. *Blood* [Internet]. 1985 Apr [cited 2019 May 28];**65**(**4**):1021–4. Available from: http://www.ncbi.nlm.nih.gov/pubmed/3156640

86. Newman PJ, Seligsohn U, Lyman S, Coller BS. The molecular genetic basis of Glanzmann thrombasthenia in the Iraqi-Jewish and Arab populations in Israel. *Proceedings of the National Academy of Sciences* [Internet]. 1991 Apr 15 [cited 2019 May 29];**88**(**8**):3160–4. Available from: http://www.ncbi.nlm.nih.gov/pubmed/2014236

87. Caen JP, Castaldi PA, Leclerc JC, Inceman S, Larrieu MJ, Probst M, et al. Congenital bleeding

disorders with long bleeding time and normal platelet count: I. Glanzmann's thrombasthenia (report of fifteen patients). *The American Journal of Medicine* [Internet]. 1966 Jul 1 [cited 2019 May 28];**41**(**1**):4–26. Available from: https://www.sciencedirect.com/science/article/pii/0002934366900039

88. Adair BD, Yeager M. Three-dimensional model of the human platelet integrin alpha IIbbeta 3 based on electron cryomicroscopy and x-ray crystallography. *Proceedings of the National Academy of Sciences of the United States of America* [Internet]. 2002 Oct 29 [cited 2019 May 30];**99**(**22**):14059–64. Available from: http://www.pnas.org/cgi/doi/10.1073/pnas.212498199

89. Sasaki M, Kleinman HK, Huber H, Deutzmann R, Yamada Y. Laminin, a multidomain protein. The A chain has a unique globular domain and homology with the basement membrane proteoglycan and the laminin B chains. *The Journal of biological chemistry* [Internet]. 1988 Nov 15 [cited 2019 Jul 22];**263**(**32**):16536–44. Available from: http://www.ncbi.nlm.nih.gov/pubmed/3182802

90. Farrell DH, Thiagarajant P, Chung DW, Davie EW. Role of fibrinogen a and y chain sites in platelet aggregation [Internet]. Vol. 89, Biochemistry. 1992 [cited 2019 May 30]. Available from: https://www.pnas.org/content/pnas/89/22/10729.full.pdf

91. Li F, Redick SD, Erickson HP, Moy VT. Force measurements of the alpha5beta1 integrin-fibronectin interaction. *Biophysical journal* [Internet]. 2003 Feb [cited 2019 Jul 22];**84**(**2 Pt 1**):1252–62. Available from: http://www.ncbi.nlm.nih.gov/pubmed/12547805

92. Springer TA, Zhu J, Xiao T. Structural basis for distinctive recognition of fibrinogen gammaC peptide by the platelet integrin alphaIIbbeta3. *The Journal of cell biology* [Internet]. 2008 Aug 25 [cited 2019 May 30];**182**(**4**):791–800. Available from: http://www.ncbi.nlm.nih.gov/pubmed/18710925

93. Xiao T, Takagi J, Coller BS, Wang J-H, Springer TA. Structural basis for allostery in integrins and binding to fibrinogen-mimetic therapeutics. *Nature* [Internet]. 2004 Nov 19 [cited 2019 Aug 5];**432**(**7013**):59–67. Available from: http://www.ncbi.nlm.nih.gov/pubmed/15378069

94. Sharda A, Kim SH, Jasuja R, Gopal S, Flaumenhaft R, Furie BC, et al. Defective PDI release from platelets and endothelial cells impairs thrombus formation in Hermansky-Pudlak syndrome. *Blood* [Internet]. 2015 Mar 5 [cited 2019 May 30];**125**(**10**):1633–42. Available from: http://www.ncbi.nlm.nih.gov/pubmed/25593336

95. O'Toole T, Mandelman D, Forsyth J, Shattil S, Plow E, Ginsberg M. Modulation of the affinity of integrin alpha IIb beta 3 (GPIIb-IIIa) by the cytoplasmic domain of alpha IIb. *Science* [Internet]. 1991 Nov 8 [cited 2019 May 30];**254**(**5033**):845–7. Available from: http://www.sciencemag.org/cgi/doi/10.1126/science.1948065

96. Li Z, Delaney MK, O'Brien KA, Du X. Signaling During Platelet Adhesion and Activation. *Arteriosclerosis, Thrombosis, and Vascular Biology* [Internet]. 2010 Dec [cited 2019 May 30];**30**(**12**):2341–9. Available from: https://www.ahajournals.org/doi/10.1161/ATVBAHA.110.207522

97. Gilmore AP, Burridge K. Regulation of vinculin binding to talin and actin by phosphatidyl-inositol-4-5-bisphosphate. *Nature* [Internet]. 1996 Jun [cited 2019 May 31];**381**(**6582**):531–5. Available from: http://www.nature.com/articles/381531a0

98. Ma Y-Q, Qin J, Plow EF. Platelet integrin alpha(IIb)beta(3) : activation mechanisms. *Journal of Thrombosis and Haemostasis* [Internet]. 2007 Jul [cited 2019 May 28];**5**(**7**):1345–52. Available from: http://www.ncbi.nlm.nih.gov/pubmed/17635696

99. Law DA, DeGuzman FR, Heiser P, Ministri-Madrid K, Killeen N, Phillips DR. Integrin cytoplasmic tyrosine motif is required for outside-in αIIbβ3 signalling and platelet function. *Nature* [Internet]. 1999 Oct 21 [cited 2019 May 30];**401**(**6755**):808–11. Available from: http://www.ncbi.nlm.nih.gov/pubmed/10548108

100. Arias-Salgado EG, Lizano S, Sarkar S, Brugge JS, Ginsberg MH, Shattil SJ. Src kinase activation by direct interaction with the integrin cytoplasmic domain. *Proceedings of the National Academy of Sciences* [Internet]. 2003 Nov 11 [cited 2019 May 31];**100**(**23**):13298–302. Available from: http://www.pnas.org/cgi/doi/10.1073/pnas.2336149100

101. Miao B, Skidan I, Yang J, Lugovskoy A, Reibarkh M, Long K, et al. Small molecule inhibition of phosphatidylinositol-3,4,5-triphosphate (PIP3) binding to pleckstrin homology domains. *Proceedings of the National Academy of Sciences of the United States of America* [Internet]. 2010 Nov 16 [cited 2019 Aug 5];**107**(**46**):20126–31. Available from: http://www.ncbi.nlm.nih.gov/pubmed/21041639

102. Wonerow P, Pearce AC, Vaux DJ, Watson SP. A Critical Role for Phospholipase Cγ2 in $\alpha_{IIb}\beta_3$-mediated Platelet Spreading. *Journal of Biological Chemistry* [Internet]. 2003 Sep 26 [cited 2019 May 26];**278**(**39**):37520–9. Available from: http://www.jbc.org/lookup/doi/10.1074/jbc.M305077200

103. Calaminus SDJ, Thomas SG, Mccarty OJT, Machesky LM, Watson SP. Identification of a

novel, actin-rich structure, the actin nodule, in the early stages of platelet spreading. *Journal of Thrombosis and Haemostasis* [Internet]. 2008 Nov [cited 2017 Apr 23];**6**(**11**):1944–52. Available from: http://www.ncbi.nlm.nih.gov/pubmed/18761725

104. Yin H, Stojanovic A, Hay N, Du X. The role of Akt in the signaling pathway of the glycoprotein Ib-IX induced platelet activation. *Blood* [Internet]. 2008 Jan 15 [cited 2019 May 31];**111**(**2**):658–65. Available from: http://www.bloodjournal.org/cgi/doi/10.1182/blood-2007-04-085514

105. Falasca M. Activation of phospholipase Cgamma by PI 3-kinase-induced PH domain-mediated membrane targeting. *The EMBO Journal* [Internet]. 1998 Jan 15 [cited 2019 May 31];**17**(**2**):414–22. Available from: http://emboj.embopress.org/cgi/doi/10.1093/emboj/17.2.414

106. Kassouf N, Ambily A, Watson S, Hassock S, Authi HS, Srivastava S, et al. Phosphatidylinositol-3,4,5-trisphosphate stimulates Ca 2 + elevation and Akt phosphorylation to constitute a major mechanism of thromboxane A 2 formation in human platelets. *Cellular Signalling* [Internet]. 2015 [cited 2019 May 31];**27**:1488–98. Available from: http://dx.doi.org/10.1016/j.cellsig.2015.03.008

107. Soriani A, Moiran B, De Virgilio M, Kawakami T, Altman A, Lowell C, et al. A role for PKCtheta in outside-in alphaIIbbeta3 signaling. *Journal of Thrombosis and Haemostasis* [Internet]. 2006 Mar 1 [cited 2019 May 27];**4**(**3**):648–55. Available from: http://doi.wiley.com/10.1111/j.1538-7836.2006.01806.x

108. Hathaway DR, Adelstein RS. Human platelet myosin light chain kinase requires the calcium-binding protein calmodulin for activity. *Proceedings of the National Academy of Sciences* [Internet]. 1979 Apr 1 [cited 2019 May 31];**76**(**4**):1653–7. Available from: http://www.ncbi.nlm.nih.gov/pubmed/156362

109. Nishikawa M, Tanaka T, Hidaka H. Ca2+ -calmodulin-dependent phosphorylation and platelet secretion. *Nature* [Internet]. 1980 Oct [cited 2019 May 31];**287**(**5785**):863–5. Available from: http://www.nature.com/articles/287863a0

110. Buensuceso CS, Obergfell A, Soriani A, Eto K, Kiosses WB, Arias-Salgado EG, et al. Regulation of outside-in signaling in platelets by integrin-associated protein kinase C beta. *The Journal of biological chemistry* [Internet]. 2005 Jan 7 [cited 2019 May 31];**280**(**1**):644–53. Available from: http://www.ncbi.nlm.nih.gov/pubmed/15536078

111. Burke GL, Evans GW, Riley WA, Sharrett AR, Howard G, Barnes RW, et al. Arterial wall

thickness is associated with prevalent cardiovascular disease in middle-aged adults. The Atherosclerosis Risk in Communities (ARIC) Study. *Stroke* [Internet]. 1995 Mar [cited 2019 Jun 5];**26**(**3**):386–91. Available from: http://www.ncbi.nlm.nih.gov/pubmed/7886711

112. Andreeva ER, Pugach IM, Orekhov AN. Collagen-synthesizing cells in initial and advanced atherosclerotic lesions of human aorta. *Atherosclerosis*. 1997;**130**(**1**–**2**):133–42.

113. North KN, Whiteman DAH, Pepin MG, Byers PH. Cerebrovascular complications in Ehlers-Danlos syndrome type IV. *Annals of Neurology* [Internet]. 1995 Dec [cited 2019 Jun 5];**38**(**6**):960–4. Available from: http://doi.wiley.com/10.1002/ana.410380620

114. Eagleton MJ. Arterial complications of vascular Ehlers-Danlos syndrome. *Journal of Vascular Surgery* [Internet]. 2016 Dec 1 [cited 2019 Jun 5];**64**(**6**):1869–80. Available from: https://www.sciencedirect.com/science/article/pii/S074152141630876X?via%3Dihub

115. Henrita Van Zanten G, De Graaf S, Slootweg PJ, Heijnen HFG, Connolly TM, De Groot PG, et al. Increased Platelet Deposition on Atherosclerotic Coronary Arteries [Internet]. Vol. 93. 1994 [cited 2019 May 30]. Available from: https://www.ncbi.nlm.nih.gov/pmc/articles/PMC293885/pdf/jcinvest00031-0167.pdf

116. Smethurst PA, Onley DJ, Jarvis GE, O'Connor MN, Knight CG, Herr AB, et al. Structural basis for the platelet-collagen interaction: the smallest motif within collagen that recognizes and activates platelet Glycoprotein VI contains two glycine-proline-hydroxyproline triplets. *The Journal of biological chemistry* [Internet]. 2007 Jan 12 [cited 2019 Jun 7];**282**(**2**):1296–304. Available from: http://www.jbc.org/lookup/doi/10.1074/jbc.M606479200

117. Bella J. Collagen structure: new tricks from a very old dog. *Biochemical Journal* [Internet]. 2016 Apr 15 [cited 2019 Aug 5];**473**(**8**):1001–25. Available from: http://www.ncbi.nlm.nih.gov/pubmed/27060106

118. Knight CG, Morton LF, Peachey AR, Tuckwell DS, Farndale RW, Barnes MJ. The collagen-binding A-domains of integrins alpha(1)beta(1) and alpha(2)beta(1) recognize the same specific amino acid sequence, GFOGER, in native (triple-helical) collagens. *The Journal of biological chemistry* [Internet]. 2000 Jan 7 [cited 2019 Jun 7];**275**(**1**):35–40. Available from: http://www.jbc.org/lookup/doi/10.1074/jbc.275.1.35

119. Buehler MJ. Nature designs tough collagen: Explaining the nanostructure of collagen fibrils. *Proceedings of the National Academy of Sciences* [Internet]. 2006 Aug 15 [cited 2019 Aug 5];**103**(**33**):12285–90. Available from: https://www.pnas.org/content/103/33/12285

120. Chen H, Locke D, Liu Y, Liu C, Kahn ML. The Platelet Receptor GPVI Mediates Both

Adhesion and Signaling Responses to Collagen in a Receptor Density-dependent Fashion* Downloaded from. *THE JOURNAL OF BIOLOGICAL CHEMISTRY* [Internet]. 2002 [cited 2019 May 30];**277**(**4**):3011–9. Available from: http://www.jbc.org/

121. Massberg S, Gawaz M, Grüner S, Schulte V, Konrad I, Zohlnhöfer D, et al. A Crucial Role of Glycoprotein VI for Platelet Recruitment to the Injured Arterial Wall In Vivo. *The Journal of Experimental Medicine J Exp Med The* [Internet]. 2003 [cited 2019 May 30];**197**(**1**):41–9. Available from: http://www.jem.org/cgi/doi/10.1084/jem.20020945

122. Dubois C, Panicot-Dubois L, Merrill-Skoloff G, Furie B, Furie BC. Glycoprotein VI-dependent and -independent pathways of thrombus formation in vivo. *Blood* [Internet]. 2006 [cited 2019 May 30];**107**(**10**):3902–6. Available from: www.bloodjournal.org

123. Bender M, May F, Lorenz V, Thielmann I, Hagedorn I, Finney BA, et al. Combined In Vivo Depletion of Glycoprotein VI and C-Type Lectin-Like Receptor 2 Severely Compromises Hemostasis and Abrogates Arterial Thrombosis in Mice. *Arteriosclerosis, Thrombosis, and Vascular Biology* [Internet]. 2013 May [cited 2019 May 30];**33**(**5**):926–34. Available from: https://www.ahajournals.org/doi/10.1161/ATVBAHA.112.300672

124. Moroi M, Jung SM. Platelet glycoprotein VI: its structure and function. *Thrombosis Research* [Internet]. 2004 Jan [cited 2019 Jun 7];**114**(**4**):221–33. Available from: https://linkinghub.elsevier.com/retrieve/pii/S0049384804003780

125. Ezumi Y, Shindoh K, Tsuji M, Takayama H. Physical and Functional Association of the Src Family Kinases Fyn and Lyn with the Collagen Receptor Glycoprotein VI-Fc Receptor Chain Complex on Human Platelets. *J Exp Med* [Internet]. 1998 [cited 2019 Jun 7];**188**(**2**):267–76. Available from: http://www.jem.org

126. Suzuki-Inoue K, Tulasne D, Shen Y, Bori-Sanz T, Inoue O, Jung SM, et al. Association of Fyn and Lyn with the Proline-rich Domain of Glycoprotein VI Regulates Intracellular Signaling. *Journal of Biological Chemistry* [Internet]. 2002 Jun 14 [cited 2019 Aug 5];**277**(**24**):21561–6. Available from: http://www.ncbi.nlm.nih.gov/pubmed/11943772

127. Loyau S, Dumont B, Ollivier V, Boulaftali Y, Feldman L, Ajzenberg N, et al. Platelet Glycoprotein VI Dimerization, an Active Process Inducing Receptor Competence, Is an Indicator of Platelet Reactivity. *Arteriosclerosis, Thrombosis, and Vascular Biology* [Internet]. 2012 Mar [cited 2019 Jun 7];**32**(**3**):778–85. Available from: https://www.ahajournals.org/doi/10.1161/ATVBAHA.111.241067

128. Poulter NS, Pollitt AY, Owen DM, Gardiner EE, Andrews RK, Shimizu H, et al. Clustering of

glycoprotein VI (GPVI) dimers upon adhesion to collagen as a mechanism to regulate GPVI signaling in platelets. *Journal of Thrombosis and Haemostasis* [Internet]. 2017 Mar [cited 2019 Aug 5];**15**(**3**):549–64. Available from: http://www.ncbi.nlm.nih.gov/pubmed/28058806

129. Tsuji M, Ezumi Y, Arai M, Takayama H. A Novel Association of Fc Receptor γ-Chain with Glycoprotein VI and Their Co-expression as a Collagen Receptor in Human Platelets. *Journal of Biological Chemistry* [Internet]. 1997 Sep 19 [cited 2019 Jun 7];**272**(**38**):23528–31. Available from: http://www.jbc.org/lookup/doi/10.1074/jbc.272.38.23528

130. Clemetson JM, Polgar J, Magnenat E, Wells TNC, Clemetson KJ. The Platelet Collagen Receptor Glycoprotein VI Is a Member of the Immunoglobulin Superfamily Closely Related to FcαR and the Natural Killer Receptors. *Journal of Biological Chemistry* [Internet]. 1999 Oct 8 [cited 2019 Jun 2];**274**(**41**):29019–24. Available from: http://www.jbc.org/lookup/doi/10.1074/jbc.274.41.29019

131. Nieswandt B, Bergmeier W, Schulte V, Rackebrandt K, Gessner JE, Zirngibl H. Expression and function of the mouse collagen receptor glycoprotein VI is strictly dependent on its association with the FcRgamma chain. *The Journal of biological chemistry* [Internet]. 2000 Aug 4 [cited 2019 Aug 5];**275**(**31**):23998–4002. Available from: http://www.ncbi.nlm.nih.gov/pubmed/10825177

132. Gibbins J, Asselin J, Farndale R, Barnes M, Law CL, Watson SP. Tyrosine phosphorylation of the Fc receptor γ-chain in collagen- stimulated platelets. *Journal of Biological Chemistry* [Internet]. 1996 [cited 2019 Jun 7];**271**(**30**):18095–9. Available from: http://www.jbc.org/

133. Rayes J, Watson SP, Nieswandt B. Functional significance of the platelet immune receptors GPVI and CLEC-2. *Journal of Clinical Investigation*. 2019;**129**(**1**):12–23.

134. Poole A, Gibbins JM, Turner M, van Vugt MJ, van de Winkel JGJ, Saito T, et al. The Fc receptor γ-chain and the tyrosine kinase Syk are essential for activation of mouse platelets by collagen. *The EMBO Journal* [Internet]. 1997 May 1 [cited 2019 Jun 7];**16**(**9**):2333–41. Available from: http://emboj.embopress.org/cgi/doi/10.1093/emboj/16.9.2333

135. Pasquet JM, Gross B, Quek L, Asazuma N, Zhang W, Sommers CL, et al. LAT is required for tyrosine phosphorylation of phospholipase cgamma2 and platelet activation by the collagen receptor GPVI. *Molecular and cellular biology* [Internet]. 1999 Dec [cited 2019 Jun 7];**19**(**12**):8326–34. Available from: http://www.ncbi.nlm.nih.gov/pubmed/10567557

136. Atkinson BT. Tec regulates platelet activation by GPVI in the absence of Btk. *Blood*

[Internet]. 2003 Jul 31 [cited 2019 Jun 3];**102**(**10**):3592–9. Available from: http://www.bloodjournal.org/cgi/doi/10.1182/blood-2003-04-1142

137. Pearce AC, Senis YA, Billadeau DD, Turner M, Watson SP, Vigorito E. Vav1 and vav3 have critical but redundant roles in mediating platelet activation by collagen. *The Journal of biological chemistry* [Internet]. 2004 Dec 24 [cited 2019 Jun 3];**279**(**52**):53955–62. Available from: http://www.ncbi.nlm.nih.gov/pubmed/15456756

138. Hughes CE, Auger JM, McGlade J, Eble JA, Pearce AC, Watson SP. Differential roles for the adapters Gads and LAT in platelet activation by GPVI and CLEC-2. *Journal of thrombosis and haemostasis : JTH* [Internet]. 2008 Dec [cited 2019 Jun 3];**6**(**12**):2152–9. Available from: http://www.ncbi.nlm.nih.gov/pubmed/18826392

139. Ungerer M, Rosport K, Bültmann A, Piechatzek R, Uhland K, Schlieper P, et al. Novel Antiplatelet Drug Revacept (Dimeric Glycoprotein VI-Fc) Specifically and Efficiently Inhibited Collagen-Induced Platelet Aggregation Without Affecting General Hemostasis in Humans. *Circulation* [Internet]. 2011 May 3 [cited 2019 Feb 22];**123**(**17**):1891–9. Available from: https://www.ahajournals.org/doi/10.1161/CIRCULATIONAHA.110.980623

140. Michelson AD. Platelets. 3rd ed. Elsevier; 2013. 1353 p.

141. Kunicki TJ, Orchekowski R, Annis D, Honda Y. Variability of integrin alpha 2 beta 1 activity on human platelets. *Blood* [Internet]. 1993 [cited 2019 Jun 7];**82**(**9**):2693–2693703. Available from: www.bloodjournal.org

142. Kritzik M, Savage B, Nugent DJ, Santoso S, Ruggeri ZM, Kunicki TJ. Nucleotide polymorphisms in the alpha2 gene define multiple alleles that are associated with differences in platelet alpha2 beta1 density. *Blood* [Internet]. 1998 Oct 1 [cited 2019 Aug 5];**92**(**7**):2382–8. Available from: http://www.ncbi.nlm.nih.gov/pubmed/9746778

143. Van de Walle GR, Schoolmeester A, Iserbyt BF, Cosemans JMEM, Heemskerk JWM, Hoylaerts MF, et al. Activation of alphaIIbbeta3 is a sufficient but also an imperative prerequisite for activation of alpha2beta1 on platelets. *Blood* [Internet]. 2007 [cited 2019 Aug 5];**109**(**2**):595–602. Available from: https://www.semanticscholar.org/paper/Activation-of-alphaIIbbeta3-is-a-sufficient-but-an-Walle-Schoolmeester/98d69d95659faac492d9a8689d9a53b427dff2e5

144. Tuckwell D, Calderwood DA, Green LJ, Humphries MJ. Integrin alpha 2 I-domain is a binding site for collagens. *Journal of cell science* [Internet]. 1995 Apr [cited 2019 Aug 5];**108 (Pt 4)**:1629–37. Available from: http://www.ncbi.nlm.nih.gov/pubmed/7615681

145. Bazzoni G, Ma L, Blue M-L, Hemler ME. Divalent Cations and Ligands Induce Conformational Changes That Are Highly Divergent among beta 1 Integrins. *Journal of Biological Chemistry* [Internet]. 1998 Mar 20 [cited 2019 Jun 8];**273**(**12**):6670–8. Available from: http://www.ncbi.nlm.nih.gov/pubmed/9506964

146. Lahav J, Wijnen EM, Hess O, Hamaia SW, Griffiths D, Makris M, et al. Enzymatically catalyzed disulfide exchange is required for platelet adhesion to collagen via integrin alpha 2 beta 1. *Blood* [Internet]. 2003 Sep 15 [cited 2019 Jun 8];**102**(**6**):2085–92. Available from: http://www.ncbi.nlm.nih.gov/pubmed/12791669

147. Nieswandt B, Brakebusch C, Bergmeier W, Schulte V, Bouvard D, Mokhtari-Nejad R, et al. Glycoprotein VI but not alpha2beta1 integrin is essential for platelet interaction with collagen. *The EMBO journal* [Internet]. 2001 May 1 [cited 2019 Jun 8];**20**(**9**):2120–30. Available from: http://www.ncbi.nlm.nih.gov/pubmed/11331578

148. Holtkötter O, Nieswandt B, Smyth N, Müller W, Hafner M, Schulte V, et al. Integrin alpha 2-deficient mice develop normally, are fertile, but display partially defective platelet interaction with collagen. *The Journal of biological chemistry* [Internet]. 2002 Mar 29 [cited 2019 Jun 8];**277**(**13**):10789–94. Available from: http://www.ncbi.nlm.nih.gov/pubmed/11788609

149. Sarratt KL, Chen H, Zutter MM, Santoro SA, Hammer DA, Kahn ML. GPVI and alpha2beta1 play independent critical roles during platelet adhesion and aggregate formation to collagen under flow. *Blood* [Internet]. 2005 Aug 15 [cited 2019 Aug 6];**106**(**4**):1268–77. Available from: http://www.ncbi.nlm.nih.gov/pubmed/15886326

150. Inoue O, Suzuki-Inoue K, McCarty OJT, Moroi M, Ruggeri ZM, Kunicki TJ, et al. Laminin stimulates spreading of platelets through integrin 6beta1-dependent activation of GPVI. *Blood* [Internet]. 2006 Feb 15 [cited 2019 Aug 6];**107**(**4**):1405–12. Available from: http://www.ncbi.nlm.nih.gov/pubmed/16219796

151. Schaff M, Tang C, Maurer E, Bourdon C, Receveur N, Eckly A, et al. Integrin alpha6beta1 Is the Main Receptor for Vascular Laminins and Plays a Role in Platelet Adhesion, Activation, and Arterial Thrombosis. *Circulation* [Internet]. 2013 Jul 30 [cited 2019 Aug 6];**128**(**5**):541–52. Available from: http://www.ncbi.nlm.nih.gov/pubmed/23797810

152. Olorundare OE, Peyruchaud O, Albrecht RM, Mosher DF. Assembly of a fibronectin matrix by adherent platelets stimulated by lysophosphatidic acid and other agonists. *Blood* [Internet]. 2001 Jul 1 [cited 2019 Aug 6];**98**(**1**):117–24. Available from: http://www.ncbi.nlm.nih.gov/pubmed/11418470

153. Cho J, Mosher DF. Role of fibronectin assembly in platelet thrombus formation. *Journal of Thrombosis and Haemostasis* [Internet]. 2006 Jul [cited 2017 Jul 18];**4**(**7**):1461–9. Available from: http://www.ncbi.nlm.nih.gov/pubmed/16839338

154. Savoia A, Pastore A, De Rocco D, Civaschi E, Di Stazio M, Bottega R, et al. Clinical and genetic aspects of Bernard-Soulier syndrome: searching for genotype/phenotype correlations. *Haematologica* [Internet]. 2011 Mar 1 [cited 2019 Jun 15];**96**(**3**):417–23. Available from: http://www.haematologica.org/cgi/doi/10.3324/haematol.2010.032631

155. Levy GG, Nichols WC, Lian EC, Foroud T, McClintick JN, McGee BM, et al. Mutations in a member of the ADAMTS gene family cause thrombotic thrombocytopenic purpura. *Nature* [Internet]. 2001 Oct [cited 2019 Jun 15];**413**(**6855**):488–94. Available from: http://www.nature.com/articles/35097008

156. Sadler JE. Von Willebrand factor, ADAMTS13, and thrombotic thrombocytopenic purpura Clinical features of idiopathic TTP. *Blood* [Internet]. 2008 [cited 2019 Jun 15];**112**:11–8. Available from: www.bloodjournal.org

157. Vu TK, Hung DT, Wheaton VI, Coughlin SR. Molecular cloning of a functional thrombin receptor reveals a novel proteolytic mechanism of receptor activation. *Cell* [Internet]. 1991 Mar 22 [cited 2019 Jun 9];**64**(**6**):1057–68. Available from: http://www.ncbi.nlm.nih.gov/pubmed/1672265

158. Monroe DM, Hoffman M, Roberts HR. Platelets and thrombin generation [Internet]. Vol. 22, Arteriosclerosis, Thrombosis, and Vascular Biology. 2002 [cited 2019 Jun 9]. p. 1381–9. Available from: http://www.atvbaha.org

159. Klages B, Brandt U, Simon MI, Schultz G, Offermanns S. Activation of G G12/G13 Results in Shape Change and Rho/Rho-Kinase–mediated Myosin Light Chain Phosphorylation in Mouse Platelets. *The Journal of Cell Biology* [Internet]. 1999 Feb 22 [cited 2019 Jun 9];**144**(**4**):745–54. Available from: http://www.ncbi.nlm.nih.gov/pubmed/10037795

160. Offermanns S, Toombs CF, Hu Y-H, Simon MI. Defective platelet activation in Gαq-deficient mice. *Nature* [Internet]. 1997 Sep 11 [cited 2018 Nov 1];**389**(**6647**):183–6. Available from: http://www.ncbi.nlm.nih.gov/pubmed/9296496

161. Banno Y, Asano T, Nozawa Y. Stimulation by G protein betagamma subunits of phospholipase C beta isoforms in human platelets. *Thrombosis and haemostasis* [Internet]. 1998 May [cited 2019 Jun 9];**79**(**5**):1008–13. Available from: http://www.ncbi.nlm.nih.gov/pubmed/9609238

162. Zhang W, Colman RW. Thrombin regulates intracellular cyclic AMP concentration in human platelets through phosphorylation/activation of phosphodiesterase 3A. *Blood* [Internet]. 2007 Sep 1 [cited 2019 Aug 6];**110**(**5**):1475–82. Available from: http://www.ncbi.nlm.nih.gov/pubmed/17392505

163. Vandendries ER, Hamilton JR, Coughlin SR, Furie B, Furie BC. Par4 is required for platelet thrombus propagation but not fibrin generation in a mouse model of thrombosis. *Proceedings of the National Academy of Sciences of the United States of America* [Internet]. 2007 Jan 2 [cited 2019 Aug 6];**104**(**1**):288–92. Available from: http://www.ncbi.nlm.nih.gov/pubmed/17190826

164. Vinholt PJ, Nielsen C, Söderström AC, Brandes A, Nybo M. Dabigatran reduces thrombin-induced platelet aggregation and activation in a dose-dependent manner. *Journal of Thrombosis and Thrombolysis* [Internet]. 2017 Aug 3 [cited 2019 Jun 8];**44**(**2**):216–22. Available from: http://link.springer.com/10.1007/s11239-017-1512-2

165. Cooper DMF, Rodbell M. ADP is a potent inhibitor of human platelet plasma membrane adenylate cyclase. *Nature 1979 282:5738* [Internet]. 1979 [cited 2019 Jun 8];**282**(**5738**):517. Available from: https://www.nature.com/articles/282517a0

166. Dessauer CW, Chen-Goodspeed M, Chen J. Mechanism of Galpha i-mediated inhibition of type V adenylyl cyclase. *The Journal of biological chemistry* [Internet]. 2002 Aug 9 [cited 2019 Jun 9];**277**(**32**):28823–9. Available from: http://www.jbc.org/lookup/doi/10.1074/jbc.M203962200

167. Foster CJ, Prosser DM, Agans JM, Zhai Y, Smith MD, Lachowicz JE, et al. Molecular identification and characterization of the platelet ADP receptor targeted by thienopyridine antithrombotic drugs. *The Journal of clinical investigation* [Internet]. 2001 Jun [cited 2019 Jun 8];**107**(**12**):1591–8. Available from: http://www.ncbi.nlm.nih.gov/pubmed/11413167

168. Hollopeter G, Jantzen H-M, Vincent D, Li G, England L, Ramakrishnan V, et al. Identification of the platelet ADP receptor targeted by antithrombotic drugs. *Nature* [Internet]. 2001 Jan 11 [cited 2017 Apr 19];**409**(**6817**):202–7. Available from: http://www.ncbi.nlm.nih.gov/pubmed/11196645

169. Cattaneo M, Zighetti ML, Lombardi R, Martinez C, Lecchi A, Conley PB, et al. Molecular bases of defective signal transduction in the platelet P2Y12 receptor of a patient with congenital bleeding. *Proceedings of the National Academy of Sciences of the United States of America* [Internet]. 2003 Feb 18 [cited 2019 Jun 8];**100**(**4**):1978–83. Available from: http://www.ncbi.nlm.nih.gov/pubmed/12578987

170. Becker RC, Bassand JP, Budaj A, Wojdyla DM, James SK, Cornel JH, et al. Bleeding complications with the P2Y12 receptor antagonists clopidogrel and ticagrelor in the PLATelet inhibition and patient outcomes (PLATO) trial. *European Heart Journal*. 2011;**32**(**23**):2933–44.

171. Hammarstrom S, Falardeau P. Resolution of prostaglandin endoperoxide synthase and thromboxane synthase of human platelets [Internet]. Vol. 74, Biochemistry. 1977 [cited 2019 Jun 9]. Available from: https://www.pnas.org/content/pnas/74/9/3691.full.pdf

172. Moers A, Nieswandt B, Massberg S, Wettschureck N, Grüner S, Konrad I, et al. G13 is an essential mediator of platelet activation in hemostasis and thrombosis. *Nature Medicine* [Internet]. 2003 Nov 5 [cited 2019 Jun 14];**9**(**11**):1418–22. Available from: http://www.nature.com/articles/nm943

173. Baigent, C; Sudlow, C; Collins R; Peto R. Collaborative meta-analysis of randomised trials of antiplatelet therapy for prevention of death, myocardial infarction, and stroke in high risk patients. *BMJ* [Internet]. 2002 Jan 12 [cited 2019 Jun 9];**324**(**7329**):71–86. Available from: http://www.ncbi.nlm.nih.gov/pubmed/11786451

174. Rothwell PM, Cook NR, Gaziano JM, Price JF, Belch JFF, Roncaglioni MC, et al. Effects of aspirin on risks of vascular events and cancer according to bodyweight and dose: analysis of individual patient data from randomised trials. *The Lancet*. 2018;**392**(**10145**):387–99.

175. Furchgott RF, Zawadzki J V. The obligatory role of endothelial cells in the relaxation of arterial smooth muscle by acetylcholine. *Nature* [Internet]. 1980 Nov [cited 2019 Jun 17];**288**(**5789**):373–6. Available from: http://www.nature.com/articles/288373a0

176. Palmer RMJ, Ferrige AG, Moncada S. Nitric oxide release accounts for the biological activity of endothelium-derived relaxing factor. *Nature* [Internet]. 1987 Jun [cited 2019 Jun 17];**327**(**6122**):524–6. Available from: http://www.nature.com/articles/327524a0

177. Radomski M., Palmer RM., Moncada S. ENDOGENOUS NITRIC OXIDE INHIBITS HUMAN PLATELET ADHESION TO VASCULAR ENDOTHELIUM. *The Lancet* [Internet]. 1987 Nov [cited 2019 Jun 17];**330**(**8567**):1057–8. Available from: https://linkinghub.elsevier.com/retrieve/pii/S0140673687914814

178. Freedman JE, Sauter R, Battinelli EM, Ault K, Knowles C, Huang PL, et al. Deficient platelet-derived nitric oxide and enhanced hemostasis in mice lacking the NOSIII gene. *Circulation research* [Internet]. 1999 Jun 25 [cited 2019 Jun 17];**84**(**12**):1416–21. Available from: http://www.ncbi.nlm.nih.gov/pubmed/10381894

179. Özüyaman B, Gödecke A, Küsters S, Kirchhoff E, Scharf R, Schrader J. Endothelial nitric oxide synthase plays a minor role in inhibition of arterial thrombus formation. *Thrombosis and Haemostasis* [Internet]. 2005 Dec 11 [cited 2019 Jun 17];**93**(**06**):1161–7. Available from: http://www.ncbi.nlm.nih.gov/pubmed/15968403

180. Iafrati MD, Vitseva O, Tanriverdi K, Blair P, Rex S, Chakrabarti S, et al. Compensatory mechanisms influence hemostasis in setting of eNOS deficiency. *Am J Physiol Heart Circ Physiol* [Internet]. 2005 [cited 2019 Jun 17];**288**:1627–32. Available from: www.ajpheart.org

181. de Frutos, Sánchez de Miguel L, Farré J, Gómez J, Romero J, Marcos-Alberca P, et al. Expression of an endothelial-type nitric oxide synthase isoform in human neutrophils: modification by tumor necrosis factor-alpha and during acute myocardial infarction. *Journal of the American College of Cardiology* [Internet]. 2001 Mar 1 [cited 2019 Jun 17];**37**(**3**):800–7. Available from: http://www.ncbi.nlm.nih.gov/pubmed/11693755

182. Freedman JE, Loscalzo J, Barnard MR, Alpert C, Keaney JF, Michelson AD. Nitric oxide released from activated platelets inhibits platelet recruitment. *Journal of Clinical Investigation* [Internet]. 1997 Jul 15 [cited 2019 Jun 17];**100**(**2**):350–6. Available from: http://www.jci.org/articles/view/119540

183. Cozzi MR, Guglielmini G, Battiston M, Momi S, Lombardi E, Miller EC, et al. Visualization of nitric oxide production by individual platelets during adhesion in flowing blood. *Blood* [Internet]. 2015 [cited 2017 Apr 19];**125**(**4**). Available from: http://www.bloodjournal.org/content/125/4/697

184. Cozzi MR, Guglielmini G, Battiston M, Momi S, Lombardi E, Miller EC, et al. Visualization of nitric oxide production by individual platelets during adhesion in flowing blood. *Blood* [Internet]. 2015 Jan 22 [cited 2019 Jun 17];**125**(**4**):697–705. Available from: http://www.ncbi.nlm.nih.gov/pubmed/25480660

185. Fleming I, Schulz C, Fichtlscherer B, Kemp B, Fisslthaler B, Busse R. AMP-activated protein kinase (AMPK) regulates the insulin-induced activation of the nitric oxide synthase in human platelets. *Thrombosis and Haemostasis* [Internet]. 2003 Dec 5 [cited 2019 Jun 17];**90**(**11**):863–71. Available from: http://www.thieme-connect.de/DOI/DOI?10.1160/TH03-04-0228

186. Carrizzo A, Di Pardo A, Maglione V, Damato A, Amico E, Formisano L, et al. Nitric Oxide Dysregulation in Platelets from Patients with Advanced Huntington Disease. Scavone C, editor. *PLoS ONE* [Internet]. 2014 Feb 25 [cited 2019 Jun 17];**9**(**2**):e89745. Available from:

https://dx.plos.org/10.1371/journal.pone.0089745

187. Barnett SD, Buxton ILO. The role of S-nitrosoglutathione reductase (GSNOR) in human disease and therapy. Vol. 52, Critical Reviews in Biochemistry and Molecular Biology. 2017. p. 340–54.

188. Xiao F, Gordge MP. Cell surface thiol isomerases may explain the platelet-selective action of S-nitrosoglutathione. *Nitric Oxide - Biology and Chemistry*. 2011;**25**(**3**):303–8.

189. Dangel O, Mergia E, Karlisch K, Groneberg D, Koesling D, Friebe A. Nitric oxide-sensitive guanylyl cyclase is the only nitric oxide receptor mediating platelet inhibition. *Journal of Thrombosis and Haemostasis* [Internet]. 2010 Jun 7 [cited 2017 Apr 19];**8**(**6**):1343–52. Available from: http://www.ncbi.nlm.nih.gov/pubmed/20149081

190. Friebe A, Koesling D. Mechanism of YC-1-Induced Activation of Soluble Guanylyl Cyclase. *Molecular Pharmacology* [Internet]. 1998 Jan 1 [cited 2019 Jun 17];**53**(**1**):123–7. Available from: http://www.ncbi.nlm.nih.gov/pubmed/9443939

191. Massberg S, Sausbier M, Klatt P, Bauer M, Pfeifer A, Siess W, et al. Increased Adhesion and Aggregation of Platelets Lacking Cyclic Guanosine 3',5'-Monophosphate Kinase I. *The Journal of Experimental Medicine*. 1999;**189**(**8**):1255–64.

192. Goldstein I, Burnett AL, Rosen RC, Park PW, Stecher VJ. The Serendipitous Story of Sildenafil: An Unexpected Oral Therapy for Erectile Dysfunction. *Sexual medicine reviews* [Internet]. 2019 [cited 2019 Aug 6];**7**(**1**):115–28. Available from: http://www.ncbi.nlm.nih.gov/pubmed/30301707

193. Wilson LS, Elbatarny HS, Crawley SW, Bennett BM, Maurice DH. Compartmentation and compartment-specific regulation of PDE5 by protein kinase G allows selective cGMP-mediated regulation of platelet functions. *Proceedings of the National Academy of Sciences of the United States of America* [Internet]. 2008 Sep 9 [cited 2017 Mar 28];**105**(**36**):13650–5. Available from: http://www.ncbi.nlm.nih.gov/pubmed/18757735

194. Nesbitt WS, Giuliano S, Kulkarni S, Dopheide SM, Harper IS, Jackson SP. Intercellular calcium communication regulates platelet aggregation and thrombus growth. *The Journal of cell biology* [Internet]. 2003 Mar 31 [cited 2019 Jun 17];**160**(**7**):1151–61. Available from: http://www.ncbi.nlm.nih.gov/pubmed/12668663

195. Calaminus SDJ, Auger JM, McCarty OJT, Wakelam MJO, Machesky LM, Watson SP. MyosinIIa contractility is required for maintenance of platelet structure during spreading on collagen and contributes to thrombus stability. *Journal of Thrombosis and Haemostasis*

[Internet]. 2007 Oct [cited 2017 Apr 23];**5**(**10**):2136–45. Available from: http://doi.wiley.com/10.1111/j.1538-7836.2007.02696.x

196. Paul BZS, Daniel JL, Kunapuli SP. Platelet shape change is mediated by both calcium-dependent and - independent signaling pathways. Role of p160 Rho-associated coiled-coil-containing protein kinase in platelet shape change. *Journal of Biological Chemistry*. 1999;**274**(**40**):28293–300.

197. Antl M, von Brühl M-L, Eiglsperger C, Werner M, Konrad I, Kocher T, et al. IRAG mediates NO/cGMP-dependent inhibition of platelet aggregation and thrombus formation. *Blood* [Internet]. 2007 [cited 2017 Mar 28];**109**(**2**). Available from: http://www.bloodjournal.org/content/109/2/552.long?sso-checked=true

198. Chrzanowska-Wodnicka M, Smyth SS, Schoenwaelder SM, Fischer TH, White GC. Rap1b is required for normal platelet function and hemostasis in mice. *Journal of Clinical Investigation*. 2005;**115**(**3**):680–7.

199. Aburima A, Walladbegi K, Wake JD, Naseem KM. cGMP signaling inhibits platelet shape change through regulation of the RhoA-Rho Kinase-MLC phosphatase signaling pathway. *Journal of thrombosis and haemostasis : JTH* [Internet]. 2017 [cited 2019 Aug 6];**15**(**8**):1668–78. Available from: http://www.ncbi.nlm.nih.gov/pubmed/28509344

200. Erdmann J, Stark K, Esslinger UB, Rumpf PM, Koesling D, de Wit C, et al. Dysfunctional nitric oxide signalling increases risk of myocardial infarction. *Nature* [Internet]. 2013 Nov 10 [cited 2017 Mar 3];**504**(**7480**):432–6. Available from: http://www.ncbi.nlm.nih.gov/pubmed/24213632

201. Smolenski A. Novel roles of cAMP/cGMP-dependent signaling in platelets. *Journal of thrombosis and haemostasis : JTH* [Internet]. 2012 Feb [cited 2019 Aug 6];**10**(**2**):167–76. Available from: http://www.ncbi.nlm.nih.gov/pubmed/22136590

202. Murray AJ. Pharmacological PKA inhibition: All may not be what it seems. Vol. 1, Science Signaling. 2008.

203. Johnston AS, Lehnart SE, Burgoyne JR. Ca(2+) signaling in the myocardium by (redox) regulation of PKA/CaMKII. *Frontiers in pharmacology* [Internet]. 2015 Aug 10 [cited 2019 May 23];**6**:166. Available from: http://journal.frontiersin.org/Article/10.3389/fphar.2015.00166/abstract

204. Smith FD, Esseltine JL, Langeberg LK, Scott JD, Reichow SL, Shi D, et al. Intrinsic disorder within an AKAP-protein kinase A complex guides local substrate phosphorylation. *eLife*.

2013;**2013**(**2**).

205. Butt E, Abel K, Krieger M, Palm D, Hoppe V, Hoppe J, et al. cAMP- and cGMP-dependent protein kinase phosphorylation sites of the focal adhesion vasodilator-stimulated phosphoprotein (VASP) in vitro and in intact human platelets. *The Journal of biological chemistry* [Internet]. 1994 May 20 [cited 2019 May 22];**269**(**20**):14509–17. Available from: http://www.ncbi.nlm.nih.gov/pubmed/8182057

206. Benz PM, Laban H, Zink J, Günther L, Walter U, Gambaryan S, et al. Vasodilator-Stimulated Phosphoprotein (VASP)-dependent and -independent pathways regulate thrombin-induced activation of Rap1b in platelets. *Cell communication and signaling : CCS* [Internet]. 2016 [cited 2019 May 22];**14**(**1**):21. Available from: http://www.ncbi.nlm.nih.gov/pubmed/27620165

207. Hofmann T, Obukhov AG, Schaefer M, Harteneck C, Gudermann T, Schultz G. Direct activation of human TRPC6 and TRPC3 channels by diacylglycerol. *Nature*. 1999;**397**(**6716**):259–63.

208. Hassock SR, Zhu MX, Trost C, Flockerzi V, Authi KS. Expression and role of TRPC proteins in human platelets: Evidence that TRPC6 forms the store-independent calcium entry channel. *Blood*. 2002;**100**(**8**):2801–11.

209. Brock TG, McNish RW, Peters-Golden M. Arachidonic Acid Is Preferentially Metabolized by Cyclooxygenase-2 to Prostacyclin and Prostaglandin E $_2$. *Journal of Biological Chemistry* [Internet]. 1999 Apr 23 [cited 2019 May 23];**274**(**17**):11660–6. Available from: http://www.ncbi.nlm.nih.gov/pubmed/10206978

210. Moncada S, Gryglewski R, Bunting S, Vane JR. An enzyme isolated from arteries transforms prostaglandin endoperoxides to an unstable substance that inhibits platelet aggregation. *Nature* [Internet]. 1976 Oct 21 [cited 2018 Jul 27];**263**(**5579**):663–5. Available from: http://www.ncbi.nlm.nih.gov/pubmed/802670

211. Moncada S, Herman AG, Higgs EA, Vane JR. Differential formation of prostacyclin (PGX or PGI2) by layers of the arterial wall. An explanation for the anti-thrombotic properties of vascular endothelium. *Thrombosis Research* [Internet]. 1977 Sep [cited 2018 Jul 29];**11**(**3**):323–44. Available from: http://linkinghub.elsevier.com/retrieve/pii/0049384877901852

212. Rosenkranz B, Fischer C, Weimer KE, Froelich JC. Metabolism of prostacyclin and 6-keto-prostaglandin F1α in man. *Journal of Biological Chemistry* [Internet]. 1980 [cited 2019 May

24];**255**(**21**):10194–8. Available from: http://www.jbc.org/content/255/21/10194.full.pdf

213. FitzGerald GA, Brash AR, Falardeau P, Oates JA. Estimated rate of prostacyclin secretion into the circulation of normal man. *The Journal of clinical investigation* [Internet]. 1981 Nov [cited 2018 Jul 29];**68**(**5**):1272–6. Available from: http://www.ncbi.nlm.nih.gov/pubmed/7028786

214. Haslam RJ, McClenaghan MD. Measurement of circulating prostacyclin. *Nature* [Internet]. 1981 [cited 2019 May 24];**292**(**5821**):364–6. Available from: https://www.nature.com/articles/292364a0.pdf

215. Frangos JA, Eskin SG, McIntire L V, Ives CL. Flow effects on prostacyclin production by cultured human endothelial cells. *Science (New York, NY)* [Internet]. 1985 Mar 22 [cited 2019 May 24];**227**(**4693**):1477–9. Available from: http://www.ncbi.nlm.nih.gov/pubmed/3883488

216. Hanada T, Hashimoto M, Nosaka S, Sasaki T, Nakayama K, Masumura S, et al. Shear stress enhances prostacyclin release from endocardial endothelial cells. *Life sciences* [Internet]. 2000 [cited 2019 May 24];**66**(**3**):215–20. Available from: http://www.ncbi.nlm.nih.gov/pubmed/10665996

217. Jüni P, Nartey L, Reichenbach S, Sterchi R, Dieppe PA, Egger M. Risk of cardiovascular events and rofecoxib: cumulative meta-analysis. *The Lancet* [Internet]. 2004 Dec [cited 2019 May 21];**364**(**9450**):2021–9. Available from: https://linkinghub.elsevier.com/retrieve/pii/S0140673604175144

218. Dutta-Roy AK, Sinha AK. Purification and properties of prostaglandin E1/prostacyclin receptor of human blood platelets. *The Journal of biological chemistry* [Internet]. 1987 Sep 15 [cited 2019 Aug 6];**262**(**26**):12685–91. Available from: http://www.ncbi.nlm.nih.gov/pubmed/2887571

219. Katsel PL, Tagliente TM, Schwarz TE, Craddock-Royal BD, Patel ND, Maayani S. Molecular and biochemical evidence for the presence of type III adenylyl cyclase in human platelets. *Platelets* [Internet]. 2003 Feb [cited 2019 May 21];**14**(**1**):21–33. Available from: http://www.ncbi.nlm.nih.gov/pubmed/12623444

220. Burkhart JM, Vaudel M, Gambaryan S, Radau S, Walter U, Martens L, et al. The first comprehensive and quantitative analysis of human platelet protein composition allows the comparative analysis of structural and functional pathways. *Blood* [Internet]. 2012 Oct 11 [cited 2019 Aug 6];**120**(**15**):e73-82. Available from:

http://www.ncbi.nlm.nih.gov/pubmed/22869793

221. Cooper DMF. Regulation and organization of adenylyl cyclases and cAMP. *Biochemical Journal*. 2003;**375**(**3**):517–29.

222. Lai L, Yan L, Gao S, Hu C-L, Ge H, Davidow A, et al. Type 5 adenylyl cyclase increases oxidative stress by transcriptional regulation of manganese superoxide dismutase via the SIRT1/FoxO3a pathway. *Circulation* [Internet]. 2013 Apr 23 [cited 2019 May 21];**127**(**16**):1692–701. Available from: http://www.ncbi.nlm.nih.gov/pubmed/23536361

223. Hidaka H, Asano T. Human blood platelet 3': 5'-cyclic nucleotide phosphodiesterase. Isolation of low-Km and high-Km phosphodiesterase. *Biochimica et biophysica acta* [Internet]. 1976 Apr 8 [cited 2019 May 24];**429**(**2**):485–97. Available from: http://www.ncbi.nlm.nih.gov/pubmed/177073

224. Grant PG, Mannarino AF, Colman RW. Purification and characterization of a cyclic GMP-stimulated cyclic nucleotide phosphodiesterase from the cytosol of human platelets. *Thrombosis research* [Internet]. 1990 Jul 1 [cited 2019 May 24];**59**(**1**):105–19. Available from: http://www.ncbi.nlm.nih.gov/pubmed/2169075

225. Manns JM, Brenna KJ, Colman RW, Sheth SB. Differential regulation of human platelet responses by cGMP inhibited and stimulated cAMP phosphodiesterases. *Thrombosis and haemostasis* [Internet]. 2002 May [cited 2019 May 24];**87**(**5**):873–9. Available from: http://www.ncbi.nlm.nih.gov/pubmed/12038792

226. Feijge MA., Ansink K, Vanschoonbeek K, Heemskerk JW. Control of platelet activation by cyclic AMP turnover and cyclic nucleotide phosphodiesterase type-3. *Biochemical Pharmacology* [Internet]. 2004 Apr 15 [cited 2019 May 23];**67**(**8**):1559–67. Available from: https://www.sciencedirect.com/science/article/pii/S0006295204000280?via%3Dihub

227. Esseltine JL, Scott JD. AKAP signaling complexes: pointing towards the next generation of therapeutic targets? *Trends in pharmacological sciences* [Internet]. 2013 [cited 2019 May 25];**34**(**12**). Available from: https://www.ncbi.nlm.nih.gov/pmc/articles/PMC3879114/

228. Raslan Z, Magwenzi S, Aburima A, Taskén K, Naseem KM. Targeting of type I protein kinase A to lipid rafts is required for platelet inhibition by the 3',5'-cyclic adenosine monophosphate-signaling pathway. *Journal of Thrombosis and Haemostasis*. 2015;**13**(**9**):1721–34.

229. Poulter NS, Pollitt AY, Davies A, Malinova D, Nash GB, Hannon MJ, et al. Platelet actin nodules are podosome-like structures dependent on Wiskott–Aldrich syndrome protein

and ARP2/3 complex. *Nature Communications* [Internet]. 2015 Jun 1 [cited 2017 Apr 23];**6**:7254. Available from: http://www.ncbi.nlm.nih.gov/pubmed/26028144

230. Bearer EL, Prakash JM, Li Z. Actin Dynamics in Platelets. *International Review of Cytology* [Internet]. 2002 [cited 2019 Jun 10];**217**:137. Available from: https://www.ncbi.nlm.nih.gov/pmc/articles/PMC3376087/

231. Flaumenhaft R, Dilks JR, Rozenvayn N, Monahan-Earley RA, Feng D, Dvorak AM. The actin cytoskeleton differentially regulates platelet α-granule and dense-granule secretion. *Blood* [Internet]. 2005 [cited 2019 Jun 10];**105**(**10**):3879–87. Available from: www.bloodjournal.org

232. Fox JEB, Phillips DR. Inhibition of actin polymerization in blood platelets by cytochalasins. *Nature*. 1981;**292**(**5824**):650–2.

233. Svitkina TM, Borisy GG. Arp2/3 complex and actin depolymerizing factor/cofilin in dendritic organization and treadmilling of actin filament array in lamellipodia. *The Journal of cell biology* [Internet]. 1999 May 31 [cited 2019 Aug 6];**145**(**5**):1009–26. Available from: http://www.ncbi.nlm.nih.gov/pubmed/10352018

234. Arber S, Barbayannis FA, Hanser H, Schneider C, Stanyon CA, Bernard O, et al. Regulation of actin dynamics through phosphorylation of cofilin by LIM-kinase. *Nature* [Internet]. 1998 Jun [cited 2019 Jun 14];**393**(**6687**):805–9. Available from: http://www.nature.com/articles/31729

235. Watanabe N. p140mDia, a mammalian homolog of Drosophila diaphanous, is a target protein for Rho small GTPase and is a ligand for profilin. *The EMBO Journal* [Internet]. 1997 Jun 1 [cited 2019 Jun 14];**16**(**11**):3044–56. Available from: http://emboj.embopress.org/cgi/doi/10.1093/emboj/16.11.3044

236. Goldschmidt-Clermont PJ, Machesky LM, Doberstein SK, Pollard TD. Mechanism of the interaction of human platelet profilin with actin. *The Journal of cell biology* [Internet]. 1991 Jun [cited 2019 Aug 6];**113**(**5**):1081–9. Available from: http://www.ncbi.nlm.nih.gov/pubmed/1645736

237. Machesky LM, Insall RH. Scar1 and the related Wiskott-Aldrich syndrome protein, WASP, regulate the actin cytoskeleton through the Arp2/3 complex. *Current Biology* [Internet]. 1998 [cited 2019 Aug 6];**8**(**25**):1347–56. Available from: http://www.ncbi.nlm.nih.gov/pubmed/9889097

238. Mullins RD, Heuser JA, Pollard TD. The interaction of Arp2/3 complex with actin:

nucleation, high affinity pointed end capping, and formation of branching networks of filaments. *Proceedings of the National Academy of Sciences of the United States of America* [Internet]. 1998 May 26 [cited 2019 Aug 6];**95**(**11**):6181–6. Available from: http://www.ncbi.nlm.nih.gov/pubmed/9600938

239. McCarty OJT, Larson MK, Auger JM, Kalia N, Atkinson BT, Pearce AC, et al. Rac1 is essential for platelet lamellipodia formation and aggregate stability under flow. *The Journal of biological chemistry* [Internet]. 2005 Nov 25 [cited 2017 Apr 21];**280**(**47**):39474–84. Available from: http://www.ncbi.nlm.nih.gov/pubmed/16195235

240. Pruyne D. Role of Formins in Actin Assembly: Nucleation and Barbed-End Association. *Science* [Internet]. 2002 Jul 26 [cited 2019 Jun 14];**297**(**5581**):612–5. Available from: http://www.sciencemag.org/cgi/doi/10.1126/science.1072309

241. Nakamura F, Stossel TP, Hartwig JH. The filamins: Organizers of cell structure and function. Vol. 5, Cell Adhesion and Migration. 2011. p. 160–9.

242. Barkalow K, Witke W, Kwiatkowski DJ, Hartwig JH. Coordinated regulation of platelet actin filament barbed ends by gelsolin and capping protein. *Journal of Cell Biology* [Internet]. 1996 [cited 2019 Jun 10];**134**(**2**):389–99. Available from: http://doi.org/10.1083/jcb.134.2.389

243. Nachmias VT, Golla R, Casella JF, Barron-Casella E. Cap Z, a calcium insensitive capping protein in resting and activated platelets. *FEBS Letters*. 1996;**378**(**3**):258–62.

244. Aspenström P, Lindberg U, Hall A. Two GTPases, Cdc42 and Rac, bind directly to a protein implicated in the immunodeficiency disorder Wiskott-Aldrich syndrome. *Current biology : CB* [Internet]. 1996 Jan 1 [cited 2019 Oct 17];**6**(**1**):70–5. Available from: http://www.ncbi.nlm.nih.gov/pubmed/8805223

245. Akbar H, Shang X, Perveen R, Berryman M, Funk K, Johnson JF, et al. Gene targeting implicates Cdc42 GTPase in GPVI and non-GPVI mediated platelet filopodia formation, secretion and aggregation. *PLoS ONE*. 2011;**6**(**7**).

246. Pleines I, Eckly A, Elvers M, Hagedorn I, Eliautou S, Bender M, et al. Multiple alterations of platelet functions dominated by increased secretion in mice lacking Cdc42 in platelets. 2017;**115**(**16**):3364–74.

247. Jiroušková M, Jaiswal JK, Coller BS. Ligand density dramatically affects integrin ??IIb??3-mediated platelet signaling and spreading. *Blood*. 2007;**109**(**12**):5260–9.

248. Ellis S, Mellor H. The novel Rho-family GTPase rif regulates coordinated actin-based membrane rearrangements. *Current biology : CB* [Internet]. 2000 Nov 2 [cited 2019 Oct 17];**10**(**21**):1387–90. Available from: http://www.ncbi.nlm.nih.gov/pubmed/11084341

249. Goh WI, Sudhaharan T, Lim KB, Sem KP, Lau CL, Ahmed S. Rif-mDia1 interaction is involved in filopodium formation independent of Cdc42 and rac effectors. *Journal of Biological Chemistry*. 2011 Apr 15;**286**(**15**):13681–94.

250. Pellegrin S, Mellor H. The Rho family GTPase Rif induces filopodia through mDia2. *Current biology : CB* [Internet]. 2005 Jan 26 [cited 2019 Oct 17];**15**(**2**):129–33. Available from: http://www.ncbi.nlm.nih.gov/pubmed/15668168

251. Goggs R, Savage JS, Mellor H, Poole AW. The Small GTPase Rif Is Dispensable for Platelet Filopodia Generation in Mice. 2013;**8**(**1**).

252. Martin K, Reimann A, Fritz RD, Ryu H, Jeon NL, Pertz O. Spatio-temporal co-ordination of RhoA , Rac1 and Cdc42 activation during prototypical edge protrusion and retraction dynamics. *Nature Publishing Group* [Internet]. 2016;(**October 2015**):1–14. Available from: http://dx.doi.org/10.1038/srep21901

253. Pandey D, Goyal P, Dwivedi S, Siess W. Unraveling a novel Rac1-mediated signaling pathway that regulates cofilin dephosphorylation and secretion in thrombin-stimulated platelets. *Blood* [Internet]. 2009 Jul 9 [cited 2019 Jun 12];**114**(**2**):415–24. Available from: http://www.ncbi.nlm.nih.gov/pubmed/19429871

254. Dwivedi S, Pandey D, Khandoga AL, Brandl R, Siess W. Rac1-mediated signaling plays a central role in secretion-dependent platelet aggregation in human blood stimulated by atherosclerotic plaque. *Journal of Translational Medicine*. 2010;

255. Marei H, Malliri A. GEFs: Dual regulation of Rac1 signaling [Internet]. Vol. 8, Small GTPases. Taylor & Francis; 2017. p. 90–9. Available from: http://dx.doi.org/10.1080/21541248.2016.1202635

256. Aslan JE, Tormoen GW, Loren CP, Pang J, McCarty OJT. S6K1 and mTOR regulate Rac1-driven platelet activation and aggregation. *Blood* [Internet]. 2011 Sep 15 [cited 2017 Dec 5];**118**(**11**):3129–36. Available from: http://www.ncbi.nlm.nih.gov/pubmed/21757621

257. Qian F, Le Breton GC, Chen J, Deng J, Christman JW, Wu D, et al. Role for the guanine nucleotide exchange factor phosphatidylinositol-3,4,5-trisphosphate-dependent rac exchanger 1 in platelet secretion and aggregation. *Arteriosclerosis, thrombosis, and vascular biology* [Internet]. 2012 Mar [cited 2017 Dec 5];**32**(**3**):768–77. Available from:

http://www.ncbi.nlm.nih.gov/pubmed/22207728

258. Hartwig JH. Mechanisms of actin rearrangements mediating platelet activation. *Journal of Cell Biology*. 1992;**118**(**6**):1421–41.

259. Wonerow P, Pearce AC, Vaux DJ, Watson SP. A Critical Role for Phospholipase Cγ2 in αIIbβ3-mediated Platelet Spreading. *Journal of Biological Chemistry* [Internet]. 2003 Sep 26 [cited 2019 Jun 14];**278**(**39**):37520–9. Available from: http://www.jbc.org/content/278/39/37520.full

260. Gratacap MP, Payrastre B, Nieswandt B, Offermanns S. Differential regulation of Rho and Rac through heterotrimeric G-proteins and cyclic nucleotides. *The Journal of biological chemistry* [Internet]. 2001 Dec 21 [cited 2019 May 2];**276**(**51**):47906–13. Available from: http://www.ncbi.nlm.nih.gov/pubmed/11560922

261. Miki H, Suetsugu S, Takenawa T. WAVE, a novel WASP-family protein involved in actin reorganization induced by Rac. *The EMBO journal* [Internet]. 1998 Dec 1 [cited 2019 Aug 6];**17**(**23**):6932–41. Available from: http://www.ncbi.nlm.nih.gov/pubmed/9843499

262. Machesky LM, Mullins RD, Higgs HN, Kaiser DA, Blanchoin L, May RC, et al. Scar, a WASp-related protein, activates nucleation of actin filaments by the Arp2/3 complex. *Proceedings of the National Academy of Sciences of the United States of America* [Internet]. 1999 Mar 30 [cited 2019 Aug 6];**96**(**7**):3739–44. Available from: http://www.ncbi.nlm.nih.gov/pubmed/10097107

263. Zhu Q, Watanabe C, Liu T, Hollenbaugh D, Blaese RM, Kanner SB, et al. Wiskott-Aldrich syndrome/X-linked thrombocytopenia: WASP gene mutations, protein expression, and phenotype. *Blood* [Internet]. 1997 Oct 1 [cited 2019 Jun 14];**90**(**7**):2680–9. Available from: http://www.ncbi.nlm.nih.gov/pubmed/9326235

264. Feghhi S, Tooley WW, Sniadecki NJ. Nonmuscle Myosin IIA Regulates Platelet Contractile Forces Through Rho Kinase and Myosin Light-Chain Kinase. *Journal of Biomechanical Engineering*. 2016;**138**(**10**):104506.

265. Riddick N, Ohtani K-I, Surks HK. Targeting by myosin phosphatase-RhoA interacting protein mediates RhoA/ROCK regulation of myosin phosphatase. *Journal of cellular biochemistry* [Internet]. 2008 Mar 1 [cited 2019 Aug 6];**103**(**4**):1158–70. Available from: http://www.ncbi.nlm.nih.gov/pubmed/17661354

266. Gong H, Shen B, Flevaris P, Chow C, Lam SCT, Voyno-Yasenetskaya TA, et al. G protein subunit Gα13 binds to integrin αIIbβ3 and mediates integrin "outside-in" signaling. *Science*.

2010;**327**(**5963**):340–3.

267. Pleines I, Hagedorn I, Gupta S, May F, Chakarova L, van Hengel J, et al. Megakaryocyte-specific RhoA deficiency causes macrothrombocytopenia and defective platelet activation in hemostasis and thrombosis. *Blood* [Internet]. 2012 Jan 26 [cited 2019 Aug 6];**119**(**4**):1054–63. Available from: http://www.ncbi.nlm.nih.gov/pubmed/22045984

268. Egot M, Kauskot A, Lasne D, Gaussem P, Bachelot-Loza C. Biphasic myosin II light chain activation during clot retraction. *Thrombosis and haemostasis* [Internet]. 2013 Dec [cited 2019 Aug 6];**110**(**6**):1215–22. Available from: http://www.ncbi.nlm.nih.gov/pubmed/23965920

269. Huang J-S, Dong L, Kozasa T, Le Breton GC. Signaling through G(alpha)13 switch region I is essential for protease-activated receptor 1-mediated human platelet shape change, aggregation, and secretion. *The Journal of biological chemistry* [Internet]. 2007 Apr 6 [cited 2019 Aug 6];**282**(**14**):10210–22. Available from: http://www.ncbi.nlm.nih.gov/pubmed/17298951

270. Arthur WT, Burridge K. RhoA inactivation by p190RhoGAP regulates cell spreading and migration by promoting membrane protrusion and polarity. *Molecular biology of the cell* [Internet]. 2001 Sep [cited 2019 Aug 6];**12**(**9**):2711–20. Available from: http://www.ncbi.nlm.nih.gov/pubmed/11553710

271. Dib K, Melander F, Andersson T. Role of p190RhoGAP in β 2 Integrin Regulation of RhoA in Human Neutrophils. *The Journal of Immunology*. 2001;**166**(**10**):6311–22.

272. Aburima A, Wraith KS, Raslan Z, Law R, Magwenzi S, Naseem KM. cAMP signaling regulates platelet myosin light chain (MLC) phosphorylation and shape change through targeting the RhoA-Rho kinase-MLC phosphatase signaling pathway. *Blood* [Internet]. 2013 Nov 14 [cited 2017 Apr 24];**122**(**20**):3533–45. Available from: http://www.ncbi.nlm.nih.gov/pubmed/24100445

273. Yusuf MZ, Raslan Z, Atkinson L, Aburima A, Thomas SG, Naseem KM, et al. Prostacyclin reverses platelet stress fibre formation causing platelet aggregate instability. *Scientific Reports* [Internet]. 2017 Dec 17 [cited 2018 Jan 21];**7**(**1**):5582. Available from: http://www.ncbi.nlm.nih.gov/pubmed/28717253

274. Tamma G, Klussmann E, Procino G, Svelto M, Rosenthal W, Valenti G, et al. cAMP-induced AQP2 translocation is associated with RhoA inhibition through RhoA phosphorylation and interaction with RhoGDI. *Journal of cell science* [Internet]. 2003 Apr 15 [cited 2019 Jun

14];**116**(**Pt 8**):1519–25. Available from: http://www.ncbi.nlm.nih.gov/pubmed/10806109

275. Schindelin J, Arganda-Carreras I, Frise E, Kaynig V, Longair M, Pietzsch T, et al. Fiji: an open-source platform for biological-image analysis. *Nature Methods* [Internet]. 2012 Jul 28 [cited 2019 Jul 15];**9**(**7**):676–82. Available from: http://www.nature.com/articles/nmeth.2019

276. Pellegrin S, Mellor H. Rho GTPase Activation Assays. *Current Protocols in Cell Biology* [Internet]. 2008 Mar 1 [cited 2019 Oct 15];**38**(**1**):14.8.1-14.8.19. Available from: http://doi.wiley.com/10.1002/0471143030.cb1408s38

277. Riedl J, Crevenna AH, Kessenbrock K, Yu JH, Neukirchen D, Bista M, et al. Lifeact: a versatile marker to visualize F-actin. *Nature methods* [Internet]. 2008 Jul [cited 2019 Jun 20];**5**(**7**):605–7. Available from: http://www.ncbi.nlm.nih.gov/pubmed/18536722

278. Kehrel B, Wierwille S, Clemetson KJ, Anders O, Steiner M, Knight CG, et al. Glycoprotein VI is a major collagen receptor for platelet activation: it recognizes the platelet-activating quaternary structure of collagen, whereas CD36, glycoprotein IIb/IIIa, and von Willebrand factor do not. *Blood* [Internet]. 1998 Jan 15 [cited 2019 Jul 28];**91**(**2**):491–9. Available from: http://www.ncbi.nlm.nih.gov/pubmed/9427702

279. Mccarty OJT, Zhao Y, Andrew N, Machesky LM, Staunton D, Frampton J, et al. Evaluation of the role of platelet integrins in fibronectin-dependent spreading and adhesion. *Journal of Thrombosis and Haemostasis* [Internet]. 2004 Oct [cited 2019 Jul 28];**2**(**10**):1823–33. Available from: http://www.ncbi.nlm.nih.gov/pubmed/15456495

280. Pleines I, Hagedorn I, Gupta S, May F, Chakarova L, Hengel J Van, et al. Megakaryocyte-specific RhoA deficiency causes macrothrombocytopenia and defective platelet activation in hemostasis and thrombosis. 2017;**119**(**4**):1054–64.

281. Roberts W, Michno A, Aburima A, Naseem KM. Nitric oxide inhibits von Willebrand factor-mediated platelet adhesion and spreading through regulation of integrin Î± IIb Î² 3 and myosin light chain. *Journal of Thrombosis and Haemostasis* [Internet]. 2009 Dec [cited 2017 Mar 21];**7**(**12**):2106–15. Available from: http://www.ncbi.nlm.nih.gov/pubmed/19765213

282. Antl M, von Bruhl M-L, Eiglsperger C, Werner M, Konrad I, Kocher T, et al. IRAG mediates NO/cGMP-dependent inhibition of platelet aggregation and thrombus formation. *Blood* [Internet]. 2007 Jan 15 [cited 2017 Apr 19];**109**(**2**):552–9. Available from: http://www.ncbi.nlm.nih.gov/pubmed/16990611

283. Ting LH, Feghhi S, Taparia N, Smith AO, Karchin A, Lim E, et al. Contractile forces in platelet aggregates under microfluidic shear gradients reflect platelet inhibition and bleeding risk. *Nature Communications*. 2019;**10**(**1**).

284. Yusuf MZ, Raslan Z, Atkinson L, Aburima A, Thomas SG, Naseem KM, et al. Prostacyclin reverses platelet stress fibre formation causing platelet aggregate instability. *Scientific Reports* [Internet]. 2017;**7**(**1**):5582. Available from: http://www.nature.com/articles/s41598-017-05817-9

285. Gent M. A randomised, blinded, trial of clopidogrel versus aspirin in patients at risk of ischaemic events (CAPRIE). *Lancet*. 1996;**348**(**9038**):1329–39.

286. Wallentin L, Becker RC, Budaj A, Cannon CP, Emanuelsson H, Held C, et al. Ticagrelor versus Clopidogrel in Patients with Acute Coronary Syndromes. *New England Journal of Medicine* [Internet]. 2009 Sep 10 [cited 2019 Jul 28];**361**(**11**):1045–57. Available from: http://www.nejm.org/doi/abs/10.1056/NEJMoa0904327

287. Radomski MW, Palmer RMJ, Moncada S. The anti-aggregating properties of vascular endothelium: interactions between prostacyclin and nitric oxide. *British Journal of Pharmacology*. 1987;**92**(**3**):639–46.

288. Goto S, Tamura N, Ishida H. Ability of anti-glycoprotein IIb/IIIa agents to dissolve platelet thrombi formed on a collagen surface under blood flow conditions. *Journal of the American College of Cardiology* [Internet]. 2004 Jul 21 [cited 2019 Jul 30];**44**(**2**):316–23. Available from: https://linkinghub.elsevier.com/retrieve/pii/S0735109704008472

289. Feng W, Valiyaveettil M, Dudiki T, Mahabeleshwar GH, Andre P, Podrez EA, et al. β3 phosphorylation of platelet αIIbβ3 is crucial for stability of arterial thrombus and microparticle formation in vivo. *Thrombosis Journal* [Internet]. 2017 Dec 30 [cited 2019 Jul 30];**15**(**1**):22. Available from: http://thrombosisjournal.biomedcentral.com/articles/10.1186/s12959-017-0145-1

290. Li Q, Lancaster JR. Calibration of nitric oxide flux generation from diazeniumdiolate Å NO donors. *Nitric Oxide*. 2009;**21**:69–75.

291. Yoon Y, Song J, Hong SH, Kim JQ. Plasma nitric oxide concentrations and nitric oxide synthase gene polymorphisms in coronary artery disease. *Clinical chemistry* [Internet]. 2000 Oct [cited 2019 Aug 6];**46**(**10**):1626–30. Available from: http://www.ncbi.nlm.nih.gov/pubmed/11017941

292. Bryan NS, Grisham MB. Methods to detect nitric oxide and its metabolites in biological

samples. Vol. 43, Free Radical Biology and Medicine. 2007. p. 645–57.

293. Neishi Y, Mochizuki S, Miyasaka T, Kawamoto T, Kume T, Sukmawan R, et al. Evaluation of bioavailability of nitric oxide in coronary circulation by direct measurement of plasma nitric oxide concentration [Internet]. Vol. 102. 2005 [cited 2019 Jul 29]. Available from: www.pnas.orgcgidoi10.1073pnas.0501392102

294. Fitzgerald GA, Brash AR, Falardeau P, Oates JA. Estimated rate of prostacyclin secretion into the circulation of normal man. *Journal of Clinical Investigation* [Internet]. 1981 [cited 2019 Jul 28];**68**(**5**):1272–6. Available from: https://pdfs.semanticscholar.org/6022/20a845ee9a739d497cb470ca11448748c656.pdf

295. Cavalca V, Rocca B, Squellerio I, Dragani A, Veglia F, Pagliaccia F, et al. In vivo prostacyclin biosynthesis and effects of different aspirin regimens in patients with essential thrombocythaemia. *Thrombosis and Haemostasis* [Internet]. 2014 [cited 2019 Jul 28];**112**(**1**):118–27. Available from: http://dx.doi.org/10.1160/TH13-10-0844

296. Nagy Z, Wynne K, von Kriegsheim A, Gambaryan S, Smolenski A. Cyclic Nucleotide-dependent Protein Kinases Target ARHGAP17 and ARHGEF6 Complexes in Platelets. *Journal of Biological Chemistry* [Internet]. 2015 Dec 11 [cited 2017 Apr 19];**290**(**50**):29974–83. Available from: http://www.ncbi.nlm.nih.gov/pubmed/26507661

297. Haushalter KJ, Casteel DE, Raffeiner A, Stefan E, Patel HH, Taylor SS. Phosphorylation of protein kinase A (PKA) regulatory subunit RIα by protein kinase G (PKG) primes PKA for catalytic activity in cells. *Journal of Biological Chemistry* [Internet]. 2018 Mar 23 [cited 2019 Jul 25];**293**(**12**):4411–21. Available from: http://www.jbc.org/lookup/doi/10.1074/jbc.M117.809988

298. Wen L, Feil S, Wolters M, Thunemann M, Regler F, Schmidt K, et al. A shear-dependent NO-cGMP-cGKI cascade in platelets acts as an auto-regulatory brake of thrombosis. *Nature communications* [Internet]. 2018 [cited 2019 Apr 2];**9**(**1**):4301. Available from: http://www.ncbi.nlm.nih.gov/pubmed/30327468

299. Onselaer M-B, Hardy AT, Wilson C, Sanchez X, Babar AK, Miller JLC, et al. Fibrin and D-dimer bind to monomeric GPVI. *Blood advances* [Internet]. 2017 Aug 22 [cited 2019 May 11];**1**(**19**):1495–504. Available from: http://www.ncbi.nlm.nih.gov/pubmed/29296791

300. Lickert S, Sorrentino S, Studt JD, Medalia O, Vogel V, Schoen I. Morphometric analysis of spread platelets identifies integrin α iIb β 3 -specific contractile phenotype. *Scientific Reports*. 2018;**8**(**1**).

301. Atkinson L, Yusuf MZ, Aburima A, Ahmed Y, Thomas SG, Naseem KM, et al. Reversal of stress fibre formation by Nitric Oxide mediated RhoA inhibition leads to reduction in the height of preformed thrombi. *Scientific Reports* [Internet]. 2018 Dec 14 [cited 2018 Jul 2];**8**(**1**):3032. Available from: http://www.ncbi.nlm.nih.gov/pubmed/29445102

302. Hiratsuka T, Sano T, Kato H, Komatsu N, Imajo M, Kamioka Y, et al. Live imaging of extracellular signal-regulated kinase and protein kinase A activities during thrombus formation in mice expressing biosensors based on Förster resonance energy transfer. *Journal of Thrombosis and Haemostasis* [Internet]. 2017 Jul [cited 2017 Jul 19];**15**(**7**):1487–99. Available from: http://www.ncbi.nlm.nih.gov/pubmed/28453888

303. Holme PA, Ørvim U, Hamers MJAG, Solum NO, Brosstad FR, Barstad RM, et al. Shear-induced platelet activation and platelet microparticle formation at blood flow conditions as in arteries with a severe stenosis. *Arteriosclerosis, Thrombosis, and Vascular Biology*. 1997;

304. Reininger AJ, Bernlochner I, Penz SM, Ravanat C, Smethurst P, Farndale RW, et al. A 2-Step Mechanism of Arterial Thrombus Formation Induced by Human Atherosclerotic Plaques. *Journal of the American College of Cardiology*. 2010;**55**(**11**):1147–58.

305. Qiu Y, Brown AC, Myers DR, Sakurai Y, Mannino RG, Tran R, et al. Platelet mechanosensing of substrate stiffness during clot formation mediates adhesion, spreading, and activation. *Proceedings of the National Academy of Sciences of the United States of America* [Internet]. 2014;**111**(**40**):14430–5. Available from: http://www.pubmedcentral.nih.gov/articlerender.fcgi?artid=4210024&tool=pmcentrez&rendertype=abstract

306. Clark JC, Kavanagh DM, Watson S, Pike JA, Andrews RK, Gardiner EE, et al. Adenosine and Forskolin Inhibit Platelet Aggregation by Collagen but not the Proximal Signalling Events. *Thrombosis and haemostasis* [Internet]. 2019 Jul [cited 2019 Aug 9];**119**(**7**):1124–37. Available from: http://www.ncbi.nlm.nih.gov/pubmed/31129912

307. Li Z, Ajdic J, Eigenthaler M, Du X. A predominant role for cAMP-dependent protein kinase in the cGMP-induced phosphorylation of vasodilator-stimulated phosphoprotein and platelet inhibition in humans. *Blood*. 2003;**101**(**11**):4423–9.

308. Cattaneo M, Lecchi A. Inhibition of the platelet P2Y12 receptor for adenosine diphosphate potentiates the antiplatelet effect of prostacyclin. *Journal of thrombosis and haemostasis : JTH* [Internet]. 2007 Mar [cited 2019 Jul 26];**5**(**3**):577–82. Available from: http://www.ncbi.nlm.nih.gov/pubmed/17155953

309. Gong H, Shen B, Flevaris P, Chow C, Lam SC-T, Voyno-Yasenetskaya TA, et al. G protein subunit Galpha13 binds to integrin alphaIIbbeta3 and mediates integrin "outside-in" signaling. *Science (New York, NY)* [Internet]. 2010 Jan 15 [cited 2019 Jun 14];**327**(**5963**):340–3. Available from: http://www.ncbi.nlm.nih.gov/pubmed/20075254

310. Wentworth JKT, Pula G, Poole AW. Vasodilator-stimulated phosphoprotein (VASP) is phosphorylated on Ser157 by protein kinase C-dependent and -independent mechanisms in thrombin-stimulated human platelets. *The Biochemical journal* [Internet]. 2006 Jan 15 [cited 2019 Aug 9];**393**(**Pt 2**):555–64. Available from: http://www.ncbi.nlm.nih.gov/pubmed/16197368

311. Dulin NO, Niu J, Browning DD, Ye RD, Voyno-Yasenetskaya T. Cyclic AMP-independent activation of protein kinase A by vasoactive peptides. *The Journal of biological chemistry* [Internet]. 2001 Jun 15 [cited 2019 Jul 10];**276**(**24**):20827–30. Available from: http://www.ncbi.nlm.nih.gov/pubmed/11331270

312. Ma Y, Pitson S, Hercus T, Murphy J, Lopez A, Woodcock J. Sphingosine Activates Protein Kinase A Type II by a Novel cAMP-independent Mechanism. *Journal of Biological Chemistry* [Internet]. 2005 Jul 15 [cited 2019 Jul 26];**280**(**28**):26011–7. Available from: http://www.jbc.org/lookup/doi/10.1074/jbc.M409081200

313. Li Z, Xi X, Gu M, Feil R, Ye RD, Eigenthaler M, et al. A stimulatory role for cGMP-dependent protein kinase in platelet activation. Vol. 112, Cell. 2003. p. 77–86.

314. Heemskerk JW, Vuist WM, Feijge MA, Reutelingsperger CP, Lindhout T. Collagen but not fibrinogen surfaces induce bleb formation, exposure of phosphatidylserine, and procoagulant activity of adherent platelets: evidence for regulation by protein tyrosine kinase-dependent Ca2+ responses. *Blood* [Internet]. 1997 [cited 2019 Aug 9];**90**(**7**):2615–25. Available from: http://www.ncbi.nlm.nih.gov/pubmed/9326228

315. Ma Y, Pitson S, Hercus T, Murphy J, Lopez A, Woodcock J. Sphingosine Activates Protein Kinase A Type II by a Novel cAMP-independent Mechanism. *Journal of Biological Chemistry* [Internet]. 2005 Jul 15 [cited 2019 Jul 10];**280**(**28**):26011–7. Available from: http://www.ncbi.nlm.nih.gov/pubmed/15883165

316. Badawy SMM, Okada T, Kajimoto T, Hirase M, Matovelo SA, Nakamura S, et al. Extracellular α-synuclein drives sphingosine 1-phosphate receptor subtype 1 out of lipid rafts, leading to impaired inhibitory G-protein signaling. *The Journal of biological chemistry* [Internet]. 2018 [cited 2019 Aug 9];**293**(**21**):8208–16. Available from: http://www.ncbi.nlm.nih.gov/pubmed/29632069

317. Yatomi Y, Ruan F, Hakomori S, Igarashi Y. Sphingosine-1-phosphate: a platelet-activating sphingolipid released from agonist-stimulated human platelets. *Blood*. 1995;**86**(**1**).

318. Guillou JL, Nakata H, Cooper DMF. Inhibition by calcium of mammalian adenylyl cyclases. *Journal of Biological Chemistry*. 1999;**274**(**50**):35539–45.

319. Tang T, Gao MH, Lai NC, Firth AL, Takahashi T, Guo T, et al. Adenylyl cyclase type 6 deletion decreases left ventricular function via impaired calcium handling. *Circulation*. 2008;**117**(**1**):61–9.

320. Willoughby D, Ong HL, De Souza LB, Wachten S, Ambudkar IS, Cooper DMF. TRPC1 contributes to the Ca 2+ -dependent regulation of adenylate cyclases. *Biochemical Journal*. 2014;**464**(**1**):73–84.

321. El-Daher SS, Patel Y, Siddiqua A, Hassock S, Edmunds S, Maddison B, et al. Distinct localization and function of (1,4,5)IP(3) receptor subtypes and the (1,3,4,5)IP(4) receptor GAP1(IP4BP) in highly purified human platelet membranes. *Blood* [Internet]. 2000 Jun 1 [cited 2019 May 17];**95**(**11**):3412–22. Available from: http://www.ncbi.nlm.nih.gov/pubmed/10828023

322. Siljander P, Farndale RW, Feijge MAH, Comfurius P, Kos S, Bevers EM, et al. Platelet Adhesion Enhances the Glycoprotein VI–Dependent Procoagulant Response. *Arteriosclerosis, Thrombosis, and Vascular Biology* [Internet]. 2001;**21**(**4**):618–27. Available from: http://www.atvbaha.org

323. Inoue O, Suzuki-Inoue K, Dean WL, Frampton J, Watson SP. Integrin alpha2beta1 mediates outside-in regulation of platelet spreading on collagen through activation of Src kinases and PLCgamma2. *The Journal of cell biology* [Internet]. 2003 Mar 3 [cited 2019 Aug 9];**160**(**5**):769–80. Available from: http://www.ncbi.nlm.nih.gov/pubmed/12615912

324. Calderwood DA, Shattil SJ, Ginsberg MH. Integrins and actin filaments: reciprocal regulation of cell adhesion and signaling. *The Journal of biological chemistry* [Internet]. 2000 Jul 28 [cited 2019 Aug 9];**275**(**30**):22607–10. Available from: http://www.ncbi.nlm.nih.gov/pubmed/10801899

325. Schachtner H, Calaminus SDJ, Sinclair A, Monypenny J, Blundell MP, Leon C, et al. Megakaryocytes assemble podosomes that degrade matrix and protrude through basement membrane. *Blood* [Internet]. 2013 Mar 28 [cited 2019 Jan 27];**121**(**13**):2542–52. Available from: http://www.ncbi.nlm.nih.gov/pubmed/23305739

326. Qiu Y, Brown AC, Myers DR, Sakurai Y, Mannino RG, Tran R, et al. Platelet mechanosensing

of substrate stiffness during clot formation mediates adhesion, spreading, and activation. *Proceedings of the National Academy of Sciences of the United States of America* [Internet]. 2014 Oct 7 [cited 2019 Jan 27];**111**(**40**):14430–5. Available from: http://www.ncbi.nlm.nih.gov/pubmed/25246564

327. Signarvic RS, Cierniewska A, Stalker TJ, Fong KP, Chatterjee MS, Hess PR, et al. RGS/Gi2 interactions modulate platelet accumulation and thrombus formation at sites of vascular injury. *Blood* [Internet]. 2010 Dec 23 [cited 2019 Aug 12];**116**(**26**):6092–100. Available from: http://www.ncbi.nlm.nih.gov/pubmed/20852125

328. Grabowski EF, Jaffe EA, Weksler BB. Prostacyclin production by cultured endothelial cell monolayers exposed to step increases in shear stress. *The Journal of laboratory and clinical medicine*. 1985;

329. Koller A, Sun D, Kaley G. Role of shear stress and endothelial prostaglandins in flow- and viscosity-induced dilation of arterioles in vitro. *Circulation Research*. 1993;

330. Lee D, Fong KP, King MR, Brass LF, Hammer DA. Differential dynamics of platelet contact and spreading. *Biophysical journal* [Internet]. 2012 Feb 8 [cited 2018 Oct 1];**102**(**3**):472–82. Available from: http://www.ncbi.nlm.nih.gov/pubmed/22325269

331. Zarka R, Horev MB, Volberg T, Neubauer S, Kessler H, Spatz JP, et al. Differential Modulation of Platelet Adhesion and Spreading by Adhesive Ligand Density. *Nano letters* [Internet]. 2019 [cited 2019 Aug 9];**19**(**3**):1418–27. Available from: http://www.ncbi.nlm.nih.gov/pubmed/30649888

332. Dyr J., Tichý I, Jiroušková M, Tobiška P, Slavík R, Homola J, et al. Molecular arrangement of adsorbed fibrinogen molecules characterized by specific monoclonal antibodies and a surface plasmon resonance sensor. *Sensors and Actuators B: Chemical* [Internet]. 1998 Aug 31 [cited 2019 May 11];**51**(**1**–**3**):268–72. Available from: https://www.sciencedirect.com/science/article/pii/S0925400598002044

333. Owaynat H, Yermolenko IS, Turaga R, Lishko VK, Sheller MR, Ugarova TP. Deposition of fibrinogen on the surface of in vitro thrombi prevents platelet adhesion. *Thrombosis research* [Internet]. 2015 Dec [cited 2019 Aug 3];**136**(**6**):1231–9. Available from: http://www.ncbi.nlm.nih.gov/pubmed/26482763

334. Safiullin R, Christenson W, Owaynat H, Yermolenko IS, Kadirov MK, Ros R, et al. Fibrinogen matrix deposited on the surface of biomaterials acts as a natural anti-adhesive coating. *Biomaterials* [Internet]. 2015 Oct [cited 2019 Aug 3];**67**:151–9. Available from:

http://www.ncbi.nlm.nih.gov/pubmed/26210181

335. Lak M, Keihani M, Elahi F, Peyvandi F, Mannucci PM. Bleeding and thrombosis in 55 patients with inherited afibrinogenaemia. *British journal of haematology* [Internet]. 1999 Oct [cited 2019 Aug 11];**107**(**1**):204–6. Available from: http://www.ncbi.nlm.nih.gov/pubmed/10520042

336. Ono A, Westein E, Hsiao S, Nesbitt WS, Hamilton JR, Schoenwaelder SM, et al. Identification of a fibrin-independent platelet contractile mechanism regulating primary hemostasis and thrombus growth. *Blood*. 2008;

337. Tomaiuolo M, Matzko CN, Poventud-Fuentes I, Weisel JW, Brass LF, Stalker TJ. Interrelationships between structure and function during the hemostatic response to injury. *Proceedings of the National Academy of Sciences* [Internet]. 2019 Feb 5 [cited 2019 Jul 23];**116**(**6**):2243–52. Available from: http://www.pnas.org/lookup/doi/10.1073/pnas.1813642116

338. Ahn SH, Hong R, Choo IS, Heo JH, Nam HS, Kang HG, et al. Histologic features of acute thrombi retrieved from stroke patients during mechanical reperfusion therapy. *International Journal of Stroke* [Internet]. 2016 Dec 9 [cited 2019 Jul 26];**11**(**9**):1036–44. Available from: http://journals.sagepub.com/doi/10.1177/1747493016641965

339. Buga GM, Gold ME, Fukuto JM, Ignarro LJ. Shear stress-induced release of nitric oxide from endothelial cells grown on beads. *Hypertension* [Internet]. 1991 [cited 2019 May 6];**17**(**2**):187–93. Available from: http://ahajournals.org

340. Uematsu M, Ohara Y, Navas JP, Nishida K, Murphy TJ, Alexander RW, et al. Regulation of endothelial cell nitric oxide synthase mRNA expression by shear stress. *American Journal of Physiology-Cell Physiology* [Internet]. 2017 [cited 2019 May 6];**269**(**6**):C1371–8. Available from: www.physiology.org/journal/ajpcell

341. Magwenzi S, Woodward C, Wraith KS, Aburima A, Raslan Z, Jones H, et al. Oxidized LDL activates blood platelets through CD36 / NOX2 – mediated inhibition of the cGMP / protein kinase G signaling cascade. *Platelets and Thrombopoiesis*. 2015;**125**(**17**):2693–704.

342. Assmann TS, Brondani LA, Bouças AP, Rheinheimer J, de Souza BM, Canani LH, et al. Nitric oxide levels in patients with diabetes mellitus: A systematic review and meta-analysis. *Nitric Oxide* [Internet]. 2016 Dec 30 [cited 2019 May 6];**61**:1–9. Available from: http://www.ncbi.nlm.nih.gov/pubmed/27677584

343. Villagra J, Shiva S, Hunter LA, Machado RF, Gladwin MT, Kato GJ. Platelet activation in

patients with sickle disease, hemolysis-associated pulmonary hypertension, and nitric oxide scavenging by cell-free hemoglobin. *Blood* [Internet]. 2007 Sep 15 [cited 2019 Jul 26];**110**(**6**):2166–72. Available from: http://www.ncbi.nlm.nih.gov/pubmed/17536019

344. Donadee C, Raat NJH, Kanias T, Tejero J, Lee JS, Kelley EE, et al. Nitric Oxide Scavenging by Red Blood Cell Microparticles and Cell-Free Hemoglobin as a Mechanism for the Red Cell Storage Lesion. *Circulation* [Internet]. 2011 Jul 26 [cited 2019 Jul 26];**124**(**4**):465–76. Available from: http://www.ncbi.nlm.nih.gov/pubmed/21747051

345. Feng S, Lu X, Reséndiz JC, Kroll MH. Pathological shear stress directly regulates platelet $\alpha_{IIb}\beta_3$ signaling. *American Journal of Physiology-Cell Physiology* [Internet]. 2006 Dec [cited 2019 Jul 26];**291**(**6**):C1346–54. Available from: http://www.physiology.org/doi/10.1152/ajpcell.00559.2005

346. Kasirer-Friede A, Ruggeri ZM, Shattil SJ. Role for ADAP in shear flow-induced platelet mechanotransduction. *Blood* [Internet]. 2010 Mar 18 [cited 2019 Aug 10];**115**(**11**):2274–82. Available from: http://www.ncbi.nlm.nih.gov/pubmed/19996090

347. Radomski MW, Palmer RM, Moncada S. The anti-aggregating properties of vascular endothelium: interactions between prostacyclin and nitric oxide. *British journal of pharmacology* [Internet]. 1987 Nov [cited 2019 Jun 17];**92**(**3**):639–46. Available from: http://www.ncbi.nlm.nih.gov/pubmed/3322462

348. Iyú D, Glenn JR, White AE, Fox SC, Dovlatova N, Heptinstall S. $P2Y_{12}$ and EP3 antagonists promote the inhibitory effects of natural modulators of platelet aggregation that act via cAMP. *Platelets* [Internet]. 2011 Nov 12 [cited 2019 May 12];**22**(**7**):504–15. Available from: http://www.tandfonline.com/doi/full/10.3109/09537104.2011.576284

349. Abramow-Newerly M, Roy AA, Nunn C, Chidiac P. RGS proteins have a signalling complex: Interactions between RGS proteins and GPCRs, effectors, and auxiliary proteins. *Cellular Signalling* [Internet]. 2006 May [cited 2019 May 12];**18**(**5**):579–91. Available from: https://linkinghub.elsevier.com/retrieve/pii/S0898656805002305

350. Noé L, Di Michele M, Giets E, Thys C, Wittevrongel C, De Vos R, et al. Platelet Gs hypofunction and abnormal morphology resulting from a heterozygous RGS2 mutation. *Journal of Thrombosis and Haemostasis* [Internet]. 2010 Apr 16 [cited 2019 May 9];**8**(**7**):1594–603. Available from: http://www.ncbi.nlm.nih.gov/pubmed/20403096

351. Salim S, Sinnarajah S, Kehrl JH, Dessauer CW. Identification of RGS2 and Type V Adenylyl Cyclase Interaction Sites. *Journal of Biological Chemistry* [Internet]. 2003 May 2 [cited 2019

May 9];**278**(**18**):15842–9. Available from: http://www.ncbi.nlm.nih.gov/pubmed/12604604

352. Burgers PP, Ma Y, Margarucci L, Mackey M, van der Heyden MAG, Ellisman M, et al. A Small Novel A-Kinase Anchoring Protein (AKAP) That Localizes Specifically Protein Kinase A-Regulatory Subunit I (PKA-RI) to the Plasma Membrane. *Journal of Biological Chemistry* [Internet]. 2012 Dec 21 [cited 2019 May 10];**287**(**52**):43789–97. Available from: http://www.ncbi.nlm.nih.gov/pubmed/23115245

353. Margarucci L, Roest M, Preisinger C, Bleijerveld OB, van Holten TC, Heck AJR, et al. Collagen stimulation of platelets induces a rapid spatial response of cAMP and cGMP signaling scaffolds. *Molecular BioSystems* [Internet]. 2011 Jul [cited 2017 Jul 14];**7**(**7**):2311. Available from: http://www.ncbi.nlm.nih.gov/pubmed/21597619

354. Jonnalagadda D, Sunkara M, Morris AJ, Whiteheart SW. Granule-mediated release of sphingosine-1-phosphate by activated platelets. *Biochimica et Biophysica Acta (BBA) - Molecular and Cell Biology of Lipids* [Internet]. 2014 Nov [cited 2019 Jul 26];**1841**(**11**):1581–9. Available from: https://linkinghub.elsevier.com/retrieve/pii/S1388198114001681

355. Endenburg SC, Lindeboom-Blokzijl L, Zwaginga JJ, Sixma JJ, de Groot PG. Plasma Fibrinogen Inhibits Platelet Adhesion in Flowing Blood to Immobilized Fibrinogen. *Arteriosclerosis, Thrombosis, and Vascular Biology* [Internet]. 1996 May [cited 2019 Jul 25];**16**(**5**):633–8. Available from: https://www.ahajournals.org/doi/10.1161/01.ATV.16.5.633

356. Mitsios J V, Prevost N, Kasirer-Friede A, Gutierrez E, Groisman A, Abrams CS, et al. What is vinculin needed for in platelets? *Journal of thrombosis and haemostasis : JTH* [Internet]. 2010 Oct [cited 2019 Aug 11];**8**(**10**):2294–304. Available from: http://www.ncbi.nlm.nih.gov/pubmed/20670372

357. Macwan AS, Boknäs N, Ntzouni MP, Ramström S, Gibbins JM, Faxälv L, et al. Gradient-dependent inhibition of stimulatory signaling from platelet G protein-coupled receptors. *Haematologica* [Internet]. 2019 Jul [cited 2019 Jul 23];**104**(**7**):1482–92. Available from: http://www.haematologica.org/lookup/doi/10.3324/haematol.2018.205815

358. Zhang Y, Qiu Y, Blanchard AT, Chang Y, Brockman JM, Ma VP-Y, et al. Platelet integrins exhibit anisotropic mechanosensing and harness piconewton forces to mediate platelet aggregation. *Proceedings of the National Academy of Sciences of the United States of America* [Internet]. 2018 [cited 2019 Aug 11];**115**(**2**):325–30. Available from: http://www.ncbi.nlm.nih.gov/pubmed/29269394

359. Induruwa I, Moroi M, Bonna A, Malcor JD, Howes JM, Warburton EA, et al. Platelet collagen receptor Glycoprotein VI-dimer recognizes fibrinogen and fibrin through their D-domains, contributing to platelet adhesion and activation during thrombus formation. *Journal of Thrombosis and Haemostasis*. 2018 Feb 1;**16**(**2**):389–404.

360. Moskowitz KA, Kudryk B, Coller BS. Fibrinogen coating density affects the conformation of immobilized fibrinogen: implications for platelet adhesion and spreading. *Thrombosis and haemostasis* [Internet]. 1998 Apr [cited 2018 Oct 1];**79**(**4**):824–31. Available from: http://www.ncbi.nlm.nih.gov/pubmed/9569199

361. Chan M V., Knowles RBM, Lundberg MH, Tucker AT, Mohamed NA, Kirkby NS, et al. P2Y $_{12}$ receptor blockade synergizes strongly with nitric oxide and prostacyclin to inhibit platelet activation. *British Journal of Clinical Pharmacology* [Internet]. 2016 Apr [cited 2019 Jul 26];**81**(**4**):621–33. Available from: http://www.ncbi.nlm.nih.gov/pubmed/26561399

362. Xu J, Shi G-P. Vascular wall extracellular matrix proteins and vascular diseases. *Biochimica et Biophysica Acta (BBA) - Molecular Basis of Disease* [Internet]. 2014 Nov 1 [cited 2019 Jul 26];**1842**(**11**):2106–19. Available from: https://www.sciencedirect.com/science/article/pii/S0925443914002191

363. Huck V, Schneider MF, Gorzelanny C, Schneider SW. The various states of von Willebrand factor and their function in physiology and pathophysiology. *Thrombosis and haemostasis* [Internet]. 2014 Apr 1 [cited 2019 Aug 11];**111**(**4**):598–609. Available from: http://www.ncbi.nlm.nih.gov/pubmed/24573248

364. Collighan RJ, Griffin M. Transglutaminase 2 cross-linking of matrix proteins: Biological significance and medical applications. Amino Acids. 2009.

365. Véniant MM, Withycombe S, Young SG. Lipoprotein size and atherosclerosis susceptibility in Apoe -/- and Ldlr -/- mice. Vol. 21, Arteriosclerosis, Thrombosis, and Vascular Biology. 2001. p. 1567–70.

366. Arehart E, Stitham J, Asselbergs FW, Douville K, MacKenzie T, Fetalvero KM, et al. Acceleration of Cardiovascular Disease by a Dysfunctional Prostacyclin Receptor Mutation. *Circulation Research* [Internet]. 2008 [cited 2017 Apr 18];**102**(**8**). Available from: http://circres.ahajournals.org/content/102/8/986.short

367. Zhao L, Liu J, He C, Yan R, Zhou K, Cui Q, et al. Protein kinase A determines platelet life span and survival by regulating apoptosis. *Journal of Clinical Investigation*. 2017;**127**(**12**):4338–51.

368. Kojima H, Moroi M, Jung SM, Goto S, Tamura N, Kozuma Y, et al. Characterization of a patient with glycoprotein (GP) VI deficiency possessing neither anti-GPVI autoantibody nor genetic aberration. *Journal of thrombosis and haemostasis : JTH* [Internet]. 2006 Nov [cited 2019 Aug 11];**4**(**11**):2433–42. Available from: http://www.ncbi.nlm.nih.gov/pubmed/17059472

369. Hermans C, Wittevrongel C, Thys C, Smethurst PA, Van Geet C, Freson K. A compound heterozygous mutation in glycoprotein VI in a patient with a bleeding disorder. *Journal of thrombosis and haemostasis : JTH* [Internet]. 2009 Aug [cited 2019 Aug 11];**7**(**8**):1356–63. Available from: http://www.ncbi.nlm.nih.gov/pubmed/19552682

370. Rigg RA, Aslan JE, Healy LD, Wallisch M, Thierheimer MLD, Loren CP, et al. Oral administration of Bruton's tyrosine kinase inhibitors impairs GPVI-mediated platelet function. *American Journal of Physiology - Cell Physiology* [Internet]. 2016 [cited 2019 May 12];**310**(**5**):C373. Available from: https://www.ncbi.nlm.nih.gov/pmc/articles/PMC4971826/

371. Shatzel JJ, Olson SR, Tao DL, McCarty OJT, Danilov A V., DeLoughery TG. Ibrutinib-associated bleeding: pathogenesis, management and risk reduction strategies. Vol. 15, Journal of Thrombosis and Haemostasis. 2017. p. 835–47.

372. Chen Z, Lu J, Zhang C, Hsia I, Yu X, Marecki L, et al. Microclot array elastometry for integrated measurement of thrombus formation and clot biomechanics under fluid shear. *Nature Communications* [Internet]. 2019 [cited 2019 May 7];**10**(**1**). Available from: https://doi.org/10.1038/s41467-019-10067-6

373. Machlus KR, Italiano JE. The incredible journey: From megakaryocyte development to platelet formation. *The Journal of cell biology* [Internet]. 2013 Jun 10 [cited 2019 Aug 5];**201**(**6**):785–96. Available from: http://www.ncbi.nlm.nih.gov/pubmed/23751492

374. Isogai T, van der Kammen R, Leyton-Puig D, Kedziora KM, Jalink K, Innocenti M. Initiation of lamellipodia and ruffles involves cooperation between mDia1 and the Arp2/3 complex. *Journal of Cell Science*. 2015;**128**(**20**):3796–810.